THE MINISTRY OF NATIONAL INFRASTRUCTURES
GEOLOGICAL SURVEY OF ISRAEL

Benthic paleoecology and taphonomy of marine high-productivity settings: Cretaceous Mishash Formation and a modern analog

*Yael Edelman-Furstenberg

* Department of Geophysical Sciences, University of Chicago, USA and Geological Survey of Israel, Jerusalem, Israel

This thesis was submitted for the degree "Doctor of Philosophy"
to the senate of the The University of Chicago, USA

The study was carried out under the supervision of:
Prof. Susan M. Kidwell, Department of Geophysical Sciences, University of Chicago, USA
Dr. Ahuva Almogi-Labin and Dr. Zeev Lewy, Geological Survey of Israel

Report GSI/10/04
Jerusalem, October 2004

TABLE OF CONTENTS

LIST OF TABLES

LIST OF FIGURES

ACKNOWLEDGMENTS

These past six years of learning, working and writing my dissertation would not have been as productive as they were without the help of many.

Special thanks are due to Ahuva Almogi-Labin, who has been my special "guardian" throughout this project, was the one who introduced me to Zeev Lewy (Zebra) and followed me throughout the project with any assistance I needed. Zebra was generous enough to take me to the field of his study and introduce me to the Upper Cretaceous varied fossil assemblages. Working with Zebra in the field sharpened my skills of "fossil hunting" as I was trying desperately to find them first…

Thanks to my advisor, Susan Kidwell and committee members, Dave Jablonski, Dave Archer, Mike LaBarbabra and Fred Ziegler, of the University of Chicago, who throughout this duration, have always made time for me and encouraged me in such a productive way.

Fieldwork would have been the same without the technician staff of the Survey. Moshe Arnon, Yaakov Mizrachi, David Sidi and Shlomo Ashkenazi who did not hesitate to help/climb/run to/run back from with anything. Thanks to the Bat-Sheva Cohen and Chana Netzer-Cohen for feeding me and for their endless help in formatting and graphic improvement of the dissertation.

I would like to thank the University of Cape Town members John Compton and John Rogers who helped me dive into the Namibian upwelling samples and guide

me through the hundreds of green buckets, and also John Pether from De Beers Marine who so generously made a reference collection for my use.

Financial support for these years was greatly appreciated. Grants were from the United States-Israel Binational Sciene Foundation, the Petroleum Research Foundation of the United States and the Ministry of National Infrastructures of Israel.

Lastly but most importantly I would like to thank my husband Ariel and our two daughters Roni and Na'ama. Each had an important, although reverse, impact on the duration of this dissertation…

ABSTRACT

Factors governing the deposition of sediments rich in silica, organic carbon, and phosphorite in high-productivity (upwelling) marine settings are complex, and the high degree of organic rain to the seafloor and associated anoxia has resulted in these regions being regarded as "benthic dead zones". However, contrary to this stereotype, the Upper Campanian Mishash Formation of Israel, which is one of the most intensive and geographically extensive high-productivity regions in the geologic record, contains abundant and diverse benthic macrofauna. I examined both this ancient record and macrobenthos death assemblages from the modern Benguela system (SW Africa) to explore gradients in community structure and taphonomic conditions across upwelling seafloors, and to use these features to infer seafloor conditions, especially bottom oxygen levels.

Five sections of the Mishash Formation from southern Israel were described. The lower Phosphatic-Carbonate unit of the Formation contains a series of 1-9 meters thick cycles composed of micritic organic-rich carbonates, cherts and porcelanites and diagenetically obliterated carbonate layers; each cycle is capped by a phosphate-bearing shell bed. An upward trend of overall coarsening grain size, increasing fossil abundance and shell packing in each cycle is interpreted as reflecting an increase in bottom oxygen and water energy levels, from quasi-aerobic (below storm wave base) to fully aerobic (above fair-weather wave base). Faunal analysis indicate decreasing species richness, body size and abundance of

deposit-feeding bivalves along an inferred increasing oxygen gradient, associated to closer proximity to upwelling center.

For Benguelan death assemblages, an increase in species richness, epifaunal-infaunal ratio, disarticulation of shells, and decrease deposit-feeding bivalve abundance and in body size of chemosymbiotic bivalves is observed with increasing distance from the upwelling center, from opal and organic-rich oozes towards phosphate-rich sands. This corresponds to an onshore-offshore gradient of increasing oxygen reported for northern Benguela waters by others.

This study demonstrates the local abundance and diversity of macrobenthos in upwelling systems, as well as their sensitivity to seafloor conditions. Modern Benguela and Cretaceous Mishash systems are both characterized by highly dynamic and patchy seafloors, including the co-occurrence of anaerobic to fully aerobic conditions even within the upwelling center.

INTRODUCTION TO DISSERTATION

Factors governing the deposition of sediments rich in silica, organic carbon, and phosphorite in high-productivity (upwelling) marine settings are complex, and remain unclear for both modern and ancient examples. The high degree of organic rain to the seafloor and associated anoxia resulted in these regions has caused them to be regarded as "benthic dead zones" with no macrofauna living, or characterized by frequent mass mortalities (e.g., Brongersma-Sander, 1957). However, field observations by Zeev Lewy (Geological Survey of Israel) on the Upper Cretaceous Mishash Formation in southern Israel revealed abundant and diverse macrobenthos throughout this record. The Mishash Formation was always regarded as a high-productivity setting characterized by anoxic or low-oxygen conditions (Reiss, 1962; Bein et al., 1990; Almogi-Labin et al., 1993).

Macroinvertebrates have been shown to be sensitive recorders of seafloor oxygen conditions, water energy and sediment mass properties based on studies in modern systems (e.g., Rhoads and Boyer, 1982), and have a rich fossil record via their skeletal remains and sedimentary traces. Macrofaunal skeletal remains can also provide paleoenvironmental information owing to their post-mortem chemical reactivity and distinctive hydrodynamic behaviors as sedimentary grains (e.g., Fürsich, 1978; Brett and Baird, 1986; Kidwell and Bosence, 1991). Surprisingly, macroinvertebrate death and fossil assemblages of upwelling regions have not been

studied in detail, probably due to this stereotypic view of benthic "dead zones".

The primary aim of my dissertation was to determine the nature of macrobenthos across an upwelling tract and, if present, infer seafloor conditions, especially bottom oxygen levels. The strategy I employed was to look for macrofaunal community structure variations and taphonomic gradients across an ancient (chapters 1 and 2) and modern (chapter 3) upwelling environment and achieve yet a better understanding of these systems by comparison of these two examples.

Presented here is the first investigation of the ecological and taphonomic nature of macrobenthic invertebrate assemblages under upwelling conditions. The Upper Cretaceous (Campanian) Mishash Fm. of Israel provides an excellent ancient example from the southern Tethys, capturing a ~9 my-long record of organic-rich carbonates, cherts, porcelanites and phosphorites within one of the most extensive high-productivity complexes in the stratigraphic record. As a counterpart, the Benguela upwelling tract off SW Africa is one of the major eastern boundary upwelling systems of today's oceans, and on a relatively broad shelf from a passive margin, is similar in physiography and tectonic setting to the Cretaceous Mishash, which lay along the southern margin of the Tethys.

In Chapter one I establish a regional paleoenvironmental reconstruction by describing and sampling a paleohigh, paleolow and three paleointermediate

sections of the Upper Campanian Mishash Formation of southern Israel, three of them in great detail. Each of the sections was measured and described for sedimentologic composition, bed thicknesses, macrofaunal content, and bioclastic fabric of any included skeletal material. During this work I discovered a fine-scale cyclicity of one to nine meters thick para-cycles that constitute the Phosphatic-Carbonate unit (sensu Soudry et al., 1985) of the Phosphate Member of the Mishash Formation. Fossil-rich beds are stratigraphicaly positioned at the boundaries of the para-cycles. An upward trend of coarsening grain size, increasing abundance of fossil remains and higher degree of shell packing was detected along such a cycle. This is associated to a change in the environmental settings, specifically an inferred increase in bottom oxygen content and bottom water energy from anaerobic-dysaerobic to fully aerobic seafloors.

Stratigraphic data from the different locations demonstrate the geographic patchiness of these systems during accumulation of the Mishash. The proximity to the center of the ancient high productivity center as well as the nature of the topographic barriers on the seafloor is represented by two end-member basins. The fossiliferous Qazra sub-basin demonstrates the full variability of the system, including laminated layers barren of trace or body fossils, uo to densely-packed shell beds. On the other end, the Zin sub-basin lacks shelly intervals but contains abundant burrowed and bioturbated intervals, providing clear evidence of past macrobenthic life in this setting, despite up to 25% weight of organic carbon in

core samples (Almogi-Labin et al., 1990).

In addition, quantitative macrofaunal analysis was conducted for the ancient and modern upwelling environments (chapters two and three, respectively). In chapter two, I describe and document, for the first time, the composition of macrobenthos (specifically bivalves and gastropods) in an Upper Cretaceous high-productivity tract based on material collected from each of the main lithologies, namely micritic organic-rich carbonate, thin porcelanite and chert beds, massive biomicrite carbonate layers, and loosely to densely packed shell beds. Diagenesis resulted in obliteration of skeletal remains in the carbonate layers and concretions, where only "ghosts" of skeletal remains were detected. Thus these layers were excluded from the macrobenthic quantitative analysis. A total of twenty one samples were examined from three locations in the Qazra sub-basin.

The different facies of the Mishash contain benthic assemblages with different taxonomic compositions, trophic structures, body sizes, species richnesses and evenness, and are consistent with independent ichnologic and sedimentologic evidence of seafloor conditions during the deposition of the Mishash Formation (described in chapter one).

Facies 1 is characterized by mostly laminated layers (ichnofabric index – ii1-2 of Droser and Bottjer, 1986) and, when present, mostly articulated sparsely-

distributed shells. This corresponds to a quasi-aerobic to dysaerobic seafloor (following inferred oxygen levels of Bottjer and Savrda, 1987, 1991). Low oxygen levels are consistent with the macrofauna evidence for facies 1, which contains a low number of infaunal deposit feeding mollusks (dominantly *Mesosaccella* species). The less abundant corbulid species show smaller body sizes than their counterparts in more aerated locations, in facies 3 (P-value of 0.0001).

Facies 2 is characterized by *Planolites* burrows (ii2-4), layers of sparsely to loosely-packed shells with a mixed state of articulation and orientation, and correspond to a dysaerobic seafloor. The chert and porcelanite beds of facies 2 comprise of a range of trophic levels and seem to represent a highly variable set of samples that range between seafloor conditions that abut facies 1 and overlap with facies 3.

Facies 3 is characterized by shell beds with a lower contact of *Thalassinoides* burrows (ii3-4), shells are mostly densely-packed, disarticulated and of disturbed orientation and correspond to an aerobic seafloor. This aerobic environment is also suggested by the shell beds comprised of a variety of species rather than a single dominant one (significantly higher species richness). These assemblages are comprised mainly of infaunal suspension feeders (*Mesocallista andersoni* and *"Meretrix"* species) but epifaunal species are also present.

Thus, each facies is characterized by a specific shelly macrofaunal assemblage

and community structure, as well as distinctive lithotype and also by ichnofabric and taphonomic features. The fossil record captures the patterns one would expect to see based on modern studies in low-oxygen and high-organic systems outside of upwelling zones (e.g., Rhoads and Morse, 1971; Savrda et al., 1984; Tyson and Pearson, 1991; Clarke and Warwick, 1994). Contrary to stereotypes that upwelling zones are barren of macrobenthos, variations in species richness, trophic groups and body size are detected along an inferred increasing distance from the upwelling center, from the organic-rich facies towards the shell beds.

In chapter three, I describe and document in much of the same fashion the composition of macrobenthos death assemblages across the full breadth of the Benguela upwelling shelf, which includes three main lithologies, namely opal and organic-rich oozes, carbonate-rich oozes and phosphate-rich sands. Two deeper-water carbonate-rich samples were also examined and are interpreted as representing the more "normal" marine environment, farther from the upwelling effects. A total of 16 samples were examined, but only 13 showed any presence of skeletal material.

On the northern Benguela shelf, I observe a gradient in macrobenthic death assemblage structure from low species richness and high abundance of deep-burrowing deposit-feeding or large chemosymbiotic bivalves, to significantly higher richness and decreased levels of deep-burrowing deposit-feeding and chemosymbiotic bivalves, in accordance with the upwelling facies-gradient from

diatomaceous ooze in areas of maximum upwelling intensity outward to the aerated but food-abundant carbonate oozes and spatially coexisting phosphorite concentrations.

Discrete taphofacies could be recognized across the upwelling region. Facies 1 (opal-organic rich) has a very low damage profile with high frequency of shell articulation and rare edge modification, indicating the rarity to absence of predators, grazers and significant bioturbators. Facies 2 (carbonate-rich) is characterized by an intermediate taphonomic profile and thus moderate abundances of predators and boring organisms, while facies 3 (phosphate-rich) is characterized by the highest damage profile, having relatively elevated numbers of rounded, fragmented and bored shells as well as very little associated sedimentary matrix. In summary, it seems that with increasing distance from the upwelling cells there is an increase in both predators and micro-boring animal abundance, which fosters post-mortem shell destruction. Alternatively, the higher frequency of damage in facies 3 might instead indicate taphonomic conditions similar to the carbonate facies but with more prolonged time-averaging, and thus an older average or maximum age of shells in the assemblage with greater time to accrue damage on surviving shells.

A comparison between Benguela and Mishash macrofaunal evidence (chapter 4) shows an overall increase in species richness, epifaunal-infaunal ratio, and disarticulation of shells, along with a decrease in body size of chemosymbiotic bivalves and change in trophic groups with increasing distance from the inferred (in

the ancient case) upwelling center, from the siliceous facies (i.e., barren porcelanite layers in Porcelanite unit of Misahsh Formation and opal and organic-rich samples of Benguela) towards the shell beds and phosphorite facies. This is parallel to an increasing oxygen gradient reported for northern Benguela (Bailey, 1991).

In conclusion, this study demonstrates the abundance and diversity of macrobenthos in upwelling systems, as well as their sensitivity to seafloor conditions across strong gradients in bottom oxygen and organic matter supply, and especially the value of macrobenthos in differentiating and more fully understanding the seafloor mosaic under upwelling systems (as in the case of the chert and porcelanite layers in the Mishash Formation). Modern Benguela and Cretaceous Mishash systems are both characterized by highly dynamic and patchy seafloors, including the co-occurrence of anaerobic to fully aerobic conditions even within the upwelling zone itself.

CHAPTER 1

CYCLIC UPWELLING FACIES ALONG THE LATE CRETACEOUS SOUTHERN TETHYS: BENTHIC ECOLOGICAL EVIDENCE OF A HIGH-PRODUCTIVITY MOSAIC, ISRAEL

INTRODUCTION

Post-Paleozoic marine high-productivity settings are associated with deposits rich in silica, organic-rich carbonates, and phosphate. High nutrient levels, usually supplied by upwelling, drive high productivity of the water column and the resulting microplankton "blooms". The dead remains settle to the seafloor where they produce organically enriched sediments (Parrish and Curtis, 1982; Suess and Thiede, 1983; Thiede and Suess, 1983; Summerhayes et al., 1992; Wilkerson et al., 2000; Parrish et al., 2001; but see Glenn and Arthur, 1990). The rate of decomposition and burial of organic matter, together with phosphogenesis and taphonomic processes such as dissolution and lateral transport of remains, will determine the ultimate composition of these deposits on the seafloor. Their stratigraphic records are further subject to modification by compaction and other diagenesis.

High-productivity settings, both modern and ancient, have been studied in considerable detail because of their association with economically important deposits (oil and phosphates), their role in global chemical cycling (especially carbon burial), and their association with particular climatic and oceanographic

conditions (Parrish and Curtis, 1982; Suess and Thiede, 1983; Thiede and Suess, 1983; Summerhayes et al., 1992; Martinez et al., 2000). However, the levels of oxygenation in bottom waters during the accumulation of high-productivity deposits in these settings remain unclear.

Upwelling is known in modern systems to be spatially heterogeneous, with localized high-productivity cells along a single shelf, which vary in intensity seasonally according to wind intensity and direction (e.g. Shannon, 1985). We can thus expect a spatial and temporal mosaic of seafloor conditions to exist across high-productivity tracts over ecological and geologic time-scales, and expect to see this reflected in macrobenthic assemblage composition. Surprisingly, macrobenthic communities have received scant attention in either modern or ancient upwelling systems, probably because a stereotypic view of upwelling systems as “death zones” leads to the assumption that macrobenthos will be largely absent (but see Levin et al., 2000 for oxygen minimum zone environments). Macrobenthic invertebrates such as shelled mollusks, brachiopods, echinoderms, and crustaceans are sensitive recorders of seafloor oxygen levels, water energy and sediment mass properties in other modern systems, and leave a rich fossil record via their biomineralized skeletons. In addition to the ecological information that can be inferred from their morphology and taxonomic affinities to modern representatives, macrofaunal skeletal remains provide additional paleoenvironmental information owing to their post-mortem chemical reactivity and distinctive hydrodynamic

behaviors as sedimentary grains (Fürsich, 1978; Brett and Baird, 1986; Kidwell and Bosence, 1991, Behrensmeyer et al., 2000). The fossil record of these organisms, their composition and abundance as skeletons, and the traces of their burrowing and other activity in the seafloor, thus represents a potentially valuable new source of insight into paleoenvironmental conditions contemporaneous with sediment deposition, and with fewer difficulties than geochemical analysis in such diagenetically complex settings.

The present study was designed to determine the paleoecological and taphonomic utility of benthic fauna (skeletal plus trace fossil records of benthic macroinvertebrates), in an otherwise well-studied high-productivity setting of the Upper Cretaceous (Campanian) Mishash Formation of Israel. This formation is exceptionally exposed and part of one of the most extensive high-productivity complexes in the stratigraphic record. Organic-rich carbonate, siliceous (chert, porcelanite), and phosphate deposits are widely distributed along the southern margin of the former Tethys ocean in Israel. These deposits are part of an Upper Cretaceous-Eocene southern Tethys phosphate belt that extended from northern South America through North Africa to the Middle East (Notholt et al., 1989). Within this belt, the Mishash Fm. records the peak of a prolonged high-productivity regime of 9 m.y. maximum duration, within an overall 20 m.y. interval of phosphate-rich deposition (see Almogi-Labin et al., 1993).

The Mishash has already been extensively studied with regard to its economic potential (e.g., Nathan et al., 1979). As a consequence, there is an existing framework of lithostratigraphic (mapping) and biostratigraphic (time-correlation) units available (Reiss et al., 1985; Almogi-Labin et al., 1986; Gvirtzman et al., 1989; Lewy, 2001). Previous workers have investigated the geochemistry of its diverse biogenic sediments (Nathan et al., 1979; Shemesh and Kolodny, 1988; Bein et al., 1990; Kolodny and Garrison, 1994; Soudry et al., 2002), the role of microbial processes in phosphogenesis (Soudry and Champetier, 1983; Soudry, 2000; Soudry and Nathan, 2001), and have identified ecologically significant microfossil (Reiss, 1962, 1988; Almogi-Labin et al., 1993) and macrofossil assemblages (Chert Member of the Mishash Fm; see Chavan, 1947; Z. Lewy, unpub. obs.).

This study follows-on the controversy between the microfossil and macrofossil evidence for this Formation. The microfossil-foraminifera data indicate a near anoxic environment for these settings (e.g. Almogi-Labin et al., 1993), while the varied and diverse molluscan fauna observed by Z. Lewy (personal communication) point to an aerated marine environment. In addition this study focuses on the biogenic components present in the so-called "barren" layers intermittent with the coarse phosphorite layers described for the upper part of the Formation (Soudry, 1983; Soudry and Nathan, 2001).

GEOLOGICAL SETTINGS: MISHASH FORMATION

Israel was part of a stable carbonate platform along the southern margin of the Tethys Seaway from Late Albian to early Late Coniacian times. However, from the later Cretaceous into the Early Eocene, the broad shelf of this slowly subsiding passive margin underwent syndepositional folding and minor faulting associated with the Syrian Arc system (Krenkel, 1924). This deformation differentiated the outer part of the ramp-shelf (nearly 100 km wide) into sub-parallel NE-SW anticlinal ridges and synclinal basins, resulting in lateral changes in thickness and facies and producing a series of paleohighs whose flanks were sensitive to small-scale fluctuations in environmental conditions. The Campanian Mishash Formation comprises a shelf-wide tract of phosphate-rich, high-productivity facies that formed during the initial phase of syndepositional deformation.

The paleo-latitudinal position at 8-15° N, where easterly trade winds controlled the southern Tethys, strongly influenced the environmental extent of the different high-productivity Upper Cretaceous facies (Reiss, 1988). The Mishash Formation was originally defined in the northern Negev as a sequence of silica-, phosphate-, and carbonate beds, which lie above chalk of the Upper Coniacian-Lower Campanian Menuha Fm. and are overlain by organic-rich argillaceous chalk (“Oil Shale Member”) of the uppermost Campanian-Maastrichtian Ghareb Fm. (Reiss et al., 1985). Northwestward towards the ancient open ocean, the siliceous-phosphatic

rocks of the Mishash are replaced gradually by pelagic organic-rich chalk of the En-Zetim Fm. (Flexer, 1968).

For mapping purposes (lithostratigraphy), the Mishash Fm. has been divided into a lower Chert Member (well-bedded cherts, silicified carbonates, and porcelanites, overlain with beds of brecciated chert) and an upper Phosphate Member (Soudry et al., 1985), which has been the subject of most detailed study. The Phosphate Member comprises a distinct sedimentary cycle that ranges from 0 to 100 m in thickness when traced from anticline to syncline. It consists of interbedded silica, phosphate, and carbonate, and has a high organic content (up to 25% total organic carbon [TOC]) in subsurface sequences (Bein et al., 1990). Auto- and heterotrophic phytoplankton are rather common in these sediments and reflect high fertility of the waters (Eshet et al., 1994; Eshet and Almogi-Labin, 1996; Hoek et al., 1996). Although all three lithologies (phosphate, carbonate, porcelanite/chert) occur throughout the entire thickness of the Phosphate Member, up-section variation in the proportions of these components led Soudry et al. (1985) to distinguish three informal units within the Phosphate Member, namely the bottom Phosphatic-Carbonate, the middle Porcelanite, and the top Phosphorite units.

METHODS

This study focused on the excellent outcrops of the Phosphate Member of the Mishash Fm. in southern Israel. Five well-exposed locations were selected on the

basis of their disparate paleogeographic-paleotectonic positions and macrofaunal abundance. These 5 sections were measured and described in detail, with the aim of developing a physical framework for macrofaunal data and in order to extract as much paleoenvironmental information as possible from biogenic components and conventional sedimentologic features (Fig. 1.1).

Age control for correlation was based on ammonites (Lewy, 2001) and a peak in the abundance of a distinctively rich planktic foraminiferal assemblage, specifically the appearance of species of Globotruncanidae (Reiss, 1988; Almogi-Labin et al., 1993; Lewy and Odin, 2001). This latter feature occurred to different degrees but in the same lithostratigraphic position in most sections. Thus correlation was largely event-stratigraphic, relying heavily on the planktic foraminiferal peak since very few index fossils are present.

A paleohigh, paleolow and three paleointermediate sections of the Phosphate Member of the Mishash Formation were described and sampled to establish a regional paleoceanographic-paleoecological reconstruction. The five sections were described for lithologic/sedimentologic composition, bed thicknesses, macrofaunal content, ichnofabric and bioclastic fabric of any included skeletal material.

Droser and Bottjer's (1986) ichnofabric indices (ii) were used to categorize ichnofabric. In general, an increase in biological activity is associated with the

transition from laminated (category ii1) through burrowed/mottled (ii2-4) and to nearly (ii5) and completely homogenized layers (ii6). This corresponds to an increase in oxygen levels. However, because of the diagenetic reactivity of many facies within these highly productive regions, a massive-homogenized layer is not necessarily the product of extensive bioturbation but can be caused instead by post-depositional, chemical or physical obliteration of primary sedimentary features.

The description of skeletal accumulations included shell articulation, whether the molluscan fauna were in living position, shell condition (evidence of wear, fragmentation, boring, bio-encrustation), the density of shell packing (using Kidwell and Holland, 1991), and other aspects of bioclastic fabric associated with storm or high water energy events (e.g., distinctive patterns of shell stacking, mud sheltering by shells; Kidwell et al., 1986). In general, water energies above fair weather or storm wave base and higher oxygen levels permit shell modification and bioturbation by metazoans. Shells tend to be disarticulated, not in living position, bio-eroded and fragmented. High energy specifically produces finer material that is winnowed away, resulting in dense and in some instances distinctive, shell packing. At the other extreme, oxygenated conditions but low water energies (below storm wave base) retain in-habitat life position, shell articulation and finer-grained material (see Kidwell, 1991 and Kidwell and Bosence, 1991).

In addition, quantitative ecological data for macrofauna (specifically bivalves and gastropods) were collected from each of the main lithologies (i.e., organic-rich carbonates, cherts, porcelanites and coarse-phosphorite/shell beds) in each of the three locations of the Qazra sub-basin. The changes observed in the benthic community structure under a high-productivity regime were examined using species richness, species evenness, trophic modes and feeding types data (data presented in chapter 2).

Laboratory analysis of lithofacies composition

The original inclusion of large quantities of organic matter in carbonates and porcelanites made their identification in the field somewhat difficult, because of the tendency of the organic matter to oxidize during weathering, conveying similar “chalky” white appearances to both lithologies. Major-element chemical analysis (Appendix 1.1) and X-ray diffraction (XRD) of samples from different lithologies throughout the Phosphate Member was thus conducted to properly characterize and identify rock types. Results from geochemical analysis indicate a broad and continuous intergradation in composition with respect to the key carbonate, silicate, and phosphorite components (Appendix 1.1). End-member types that were readily distinguished in the field (chert, phosphatic grainstones, bioclastic limestones) did not require additional chemical analysis. Other lithologies such as "porcelanite" and "organic-rich carbonate" (the "organic-rich" characterization is based on TOC data from sub-surface cores, Bein et al., 1990) were best distinguished in outcrops

where color, laminations, and bioturbation had all been accentuated by favorable weathering. By combining the insights from geochemical analysis with these weathering features, the dominant component could be determined in the field.

BASIC FACIES TYPES

Four main litho-facies were identified throughout the high-productivity region: (1) laminated or mottled organic-rich carbonate mud; (2) porcelanite and chert; (3) micritic carbonate (layers or concretion-shaped); and (4) shell beds and/or coarse (sand to pebble sized) phosphorite layers (table 1). Each lithofacies is characterized by its distinctive combination of lithology, shelly macrofauna, ichnofabric and taphonomic features. Bottom conditions were then inferred from these characteristics, specifically dissolved oxygen concentration and water energy at the seafloor.

The oxygen levels inferred for the present reconstruction follow those of previous studies on oxygen-deficient benthic environments. Rhoads and Morse (1971), drawing on information from a relatively stable bathymetric gradient in oxygen in the Black Sea, characterized three ranges of inferred dissolved oxygen for benthic facies: **aerobic**, **dysaerobic** and **azoic/anaerobic**. This model has been refined and modified by further investigation on burrow structure and macrobenthos shells in the California continental borderland (Savrda et al., 1984). Savrda et al. (1984) differentiated between inferred dissolved oxygen levels in the overlying waters

(OW) and in the pore waters (PW), and characterized five dissolved oxygen zones (see also Savrda and Bottjer, 1987; 1991). These were: **anaerobic** (0 mlO_2/l in both OW and PW, characterized by laminated strata lacking both in-situ body fossils and microbioturbation); **quasi-aerobic** (<0.1 ml/l in OW, 0 ml/l in PW; laminated strata with slight microbioturbation, containing benthic microfossils but lacking macrobenthic ones); **exaerobic** (>0.1<1 ml/l in OW; 0 ml/l in PW; laminated strata, but containing in situ macro-epibenthic body fossils); **dysaerobic** (as exaerobic, but with some aeration of porewaters; bioturbated, low diversity of small macrobenthic body fossils, if any); and **aerobic** (>1.0 ml/l in OW and PW to some depth; thoroughly bioturbated, diverse assemblage of large, heavily calcified macrobenthic body fossils).

Bottom water energy levels were reconstructed for the Mishash Fm relying on the following:

(a)grain-size information, i.e., the better sorted the coarse sedimentary component, the higher the water energy. Maximum grain size itself was not a good energy index because most grains are biogenic and diagenetic in origin.

(b) shell orientation, i.e. whether distinctive storm-generated shell stacking or imbrication was present (an indication of high water energy).

(c)abundance of disarticulated shells and of shells out of life position. An increase in disarticulated shells may indicate higher water energy levels (see Kidwell and Bosence, 1991) and/or higher levels of bioturbation, which suggests higher oxygen

levels. Disarticulation per se was not considered a signal for high water energy, but rather taken into consideration as part of a larger set of potential water-energy indicators.

(d) extent of shell packing within a layer. Denser packing and winnowing of fine grains are taken to indicate higher water energy or more persistent reworking of the seafloor.

Water energies sufficient to generate densely-packed shell beds (or phosphorites) with shell stacking features, high disarticulation of shells and absence of fine mud matrix are attributed to seafloors above fair-weather wave base. Water energies sufficient to generate loosely to densely packed shell beds (or phosphorites) with shell-sheltered muds (meaning that not all finer grains were winnowed away) and mixed articulation states, indicate seafloors above storm wave base but below fair-weather wave base, i.e. within the transition zone. Finally, muddy (clay-silt grain size) facies with sparsely distributed shells and an absence of distinct shell beds indicate water energies below storm wave base (Kidwell, 1991; Kidwell and Bosence, 1991). Furthermore, relatively homogenized mud layers (Droser and Bottjer, 1986, ichnofabric index 4-5) are taken to indicate well-aerated conditions on the seafloor (>1 mlO_2/l). If layers are laminated (ii 1-2) then seafloor conditions are interpreted to have been anaerobic to quasi-aerobic, specifically dissolved oxygen levels of 0-1.0 ml/l (Savrda and Bottjer, 1986).

Table 1: Four main high-productivity facies observed in Mishash Fm, based on faunal assemblage, ichnofabric and taphonomic features. Facies are named after the

final form of lithology as observed in the field (i.e., at times the final lithology represents early diagenetic processes on the primary lithology).

FACIES	**Macrofauna:** key bivalves and trophic groups	**Ichnofabric:** Ichnofabric Index (ii) 1-5	**Bioclastic fabric:** Shell packing	Shell articulation	Shell orientation	**Inferred seafloor conditions:** oxygen =O_2 water energy =E
1- organic-rich carbonate mud	*Mesosaccella* (deposit-feeding infauna)	predominantly laminated (ii1-2)	barren to sparse	mostly articulated	many in life position	**O_2:** quasi-aerobic-dys-aerobic **E:** below storm wave base
2- porcelanites within organic-rich layers	mixed trophic groups	*Planolites* burrows (ii2-4)	sparse to loose	mixed	mixed orientation	**O_2:** dys-aerobic **E:** proximity of storm wave base
3- carbonate mud layers or concretion-shaped)	diagenetic obliteration	some mottling (diagenetic obliteration)	obliterated, loose	mixed	diagenetic obliteration	**O_2:** dys-aerobic **E:** within the transition zone
4- shell bed (at times topped with coarse phosphorite	*Nanonavis Mesocallista* (suspension-feeding epi- and infauna)	lower contact *Thalassinoides* burrows (ii3-4)	dense	mostly dis-articulated	all disturbed	**O_2:** aerobic **E:** above fair- weather wave base

Lithofacies 1

Lithofacies 1 consists mainly of laminated, organic-rich carbonate mud. Less common are mottled-burrowed intervals ranging from slightly burrowed (ii2) to ~50% disturbed (ii4). The burrows are mostly small diameter *Planolites*. This highly organic-rich lithofacies is commonly barren of macrofauna. However, in those layers containing macrofauna, the assemblage consists of very few species

(5-7) of bivalves, principally species of the deposit-feeding, infaunal genus *Mesosaccella* (no gastropods observed). The specimens are sparsely distributed and are dominantly articulated, silicified and with no apparent sign of fragmentation or abrasion. These organic-rich carbonate muds, which are in beds ranging from a few to tens of centimeters thick, are very common throughout the section and act as a "background" lithology for this highly productive system as a whole.

The lamination and shell articulation indicate a low-energy environment on the seafloor, i.e. below storm wave base. In addition, the very low number of species per bed found in this lithofacies as well as the faunal composition (typically dominated by a single species or couple of species of infaunal deposit feeders, mainly *Mesosaccella*), indicate an environmentally stressed seafloor. Infaunal deposit-feeding bivalves (as opposed to epifaunal or infaunal suspension-feeding species) are indicators of relatively high organic concentrations on the seafloor and together with *Planolites* (as opposed to the larger *Thalassinoides*) are indicators of nearly anaerobic to dysaerobic conditions. The few macrofauna would have colonized the seafloor during dysaerobic intervals. The low bottom-water energy and oxygen levels could be the result of a relatively deep basin with restricted water circulation due to a topographic barrier superimposed on proximity to the center of the high productivity cell.

Lithofacies 2

Lithofacies 2 is characterized by porcelanite and chert layers (ranging from a few to 40 cm thick). Mottled-burrowed intervals ranging from slightly burrowed (ii2) to ~50% disturbed (ii4), at times containing distinct *Planolites*, are typical in this lithofacies. The macrofaunal assemblage contains mixed trophic groups with both non-carnivore (*Eucyclomphalus* and *Turritella* species) and carnivore (*Gyrodes* and *Undiscala* species) gastropods along with mostly infaunal deposit-feeding bivalves, but also less common epifaunal suspension-feeding species (*Mesocallista* species and *Nanonavis* species, respectively). The species richness ranges from 7-16 species, with the most common taxon ranging in abundance from 20% (an evenly distributed assemblage) to 85% (assemblage highly dominated by one species) of the total assemblage (for details, see Edelman-Furstenberg, chapter 2). The shells, all silicified, are sparsely to loosely distributed within the layer and show almost no abrasion or fragmentation. Both articulated and disarticulated shells are present.

The mixed state of shell articulation and shell packing (sparse to loose rather than dense packing) point to a relatively low bottom-water energy, closer to storm wave-base levels than lithofacies 1. The intense diagenesis that characterizes these two lithologies (chert and porcelanite) makes it difficult to tease apart primary-initial siliceous phases from secondary chert and porcelanite (see Kolodny et al., 1965). This diagenesis is the reason for the relatively high variability within this lithofacies. In any case, when layers contain a slightly more diverse fauna (7-16

species per sample as opposed to 5-7 species in lithofacies 1) and small-diameter burrows (Savrda et al., 1984; Savrda and Bottjer, 1986) as well as loosely (rather than sparsely) packed shell accumulations, they are interpreted as a less stressed seafloor environment, though still low-oxygen, dysaerobic conditions.

The chert and porcelanite layers are inter-bedded within organic-rich carbonate mud. Lithofacies 1 and 2 are often in close proximity one to another. The assumption is that once upwelling increases, so do the algae (diatom) blooms. This increases the siliceous phase in the seafloor ooze, thereby resulting in porcelanite layers. Also, some of the less fossiliferous chert and porcelanites could be the replacements of carbonate mud (see Kolodny et al., 1965).

Lithofacies 3

Lithofacies 3 is characterized by micritic carbonate mud layers or "concretionary"-shaped layers. Carbonate layers are often regarded as the typical lithology expected in shallow-marine carbonate environments. The central portions of many of the concretionary-layers include macrofaunal remains or shell "ghosts". Diagenetic obliteration makes it difficult to recognize specimens with confidence. However, when recognition to major taxon is possible, the shells show both articulation and disarticulation and reflect a diverse macrofaunal assemblage. Both bivalves and gastropod species were recognized, though diagenesis made measurements difficult.

The diverse fauna and, when detectable, significant fabric mottling (comparable to ii4 of Droser and Bottjer, 1986), imply a less restricted seafloor than the former two facies, with dissolved oxygen levels closer to aerobic conditions. The mixed state of shell articulation and rare shell-stacking features imply bottom-water energies similar to those of the transition zone.

Lithofacies 4

Lithofacies 4 is characterized by molluscan shell beds (primarily bivalves and gastropods) or coarse (up to pebble size) phosphorite layers. *Thalassinoides* burrows mark the lower contact of these beds. These shell beds are composed of a diverse faunal assemblage with both bivalves and gastropods common. Species richness reaches as high as 22 species. The bivalves in the shell beds are mostly infaunal suspension or deposit feeders (*Mesocallista*, "Meretrix"and corbulid species and *Nucula* and *Mesosaccella*, respectively) but epifaunal species are also present (*Nanonavis*, *"Mytilus"* and *Plicatula* species). Shells are mostly disarticulated, fragmented and some are abraded. The shell beds are densely packed with almost all fine (silt-sand grain sizes) matrix winnowed away. In quite a few shell beds, storm-related shell stacking is apparent. Phosphatic granules and pebbles are commonly mixed with the shells, resulting in lithified phosphatic-shell bed layers. In some instances, the shelly phosphorite consists only of filled burrows of *Thalassinoides*.

The diverse faunal assemblage and trophic groups, together with large *Thalassinoides*, indicate an aerobic seafloor with high oxygen levels. The winnowing, storm-generated shell stacking and few abraded shells all point to high water-energy levels of local storms, probably above fair-weather wave base. This signifies a shallowing of water depth and/or little restriction of water circulation (i.e., deep topographic barrier).

LATERAL VARIABILITY IN LITHOLOGIC AND PALEONTOLOGIC COMPOSITION

The lithologically and faunally diverse Phosphate Member was examined across one sub-basin (informally denoted here the Qazra sub-basin) of the Mishash continental shelf in great detail, ranging from a syndepositional anticline to the adjacent syncline. The section at the paleolow location Nahal Ashosh totals 72 meters (top ~8 meters missing as compared to Soudry's 1983 description from a nearby outcrop). The Nahal Omer section (combined with the top ~10 meters of the adjacent Nahal Qazra section) is located in a paleointermediate position on the anticline flank, and is a total of 44 meters thick. Finally, the paleohigh section at Har Massa is a total of 14 meters thick. All sections are composed of the four key lithologies (or a combination of them): organic-rich carbonate mud; porcelanite and chert; carbonate layers; and phosphorite or shell beds. Each lithology varies in

relative abundance from anticline to syncline as well as upsection, as summarized below.

Soudry et al.'s (1985) three informal subdivisions of the Phosphate Member (the bottom Phosphatic-Carbonate unit, the middle Porcelanite unit, and the top Phosphorite unit) are readily recognized in most of the studied sections, mainly within the Qazra sub-basin.

Nahal Ashosh (paleolow)

Nahal Ashosh, the synclinal section, is the thickest section (Fig. 1.2). The bottom Phosphatic-Carbonate unit is 45 meters thick, the middle Porcelanite unit is 20 m thick and the top Phosphorite unit is 7 m thick.

The Phosphatic-Carbonate unit is dominated by organic-rich carbonate mud (51% of thickness) with porcelanite beds comprising only ~5% of the 45 meters. In general, this unit is characterized by many (20%) chert layers/lenses and by less frequent (15%) carbonate layers. Mottled, *Planolites*-rich layers as thick as 50 cm occur throughout. Within the lower 30 meters of the unit, thin (5-25 cm thick) shell accumulations are exhibited, while much thicker (almost meter thick), packed shell beds are found higher upsection (in the upper 15 m of the unit). Most of the shell beds have a basal *Thalassinoides* contact. The shell beds range from densely to loosely packed. The shell accumulations vary from being thin accumulations

strongly dominated by only a few species (the deposit-feeding bivalve *Mesosaccella* up to ~85% dominance, or the non-carnivorous gastropod *Eucyclomphalus* up to 72% dominance) to thick shell beds that are species-rich. The species-rich assemblages (up to 21 species) are far more common. Within the densely packed shell beds, individuals are relatively evenly distributed amongst the different species, with the highest abundance of one species reaching 35% of the assemblage (suspension-feeding corbulid bivalves). Bivalves (especially the shallow-burrower *Crassatella*) occur in both disarticulated and articulated states without a strong dominance of either. Gastropod species are not abundant in shell beds from this bottom unit.

Higher upsection, the Porcelanite unit is characterized by an increase in porcelanite layers relative to the underlying Phosphatic-Carbonate unit, and can be divided into two main parts. The lower 13 meters are characterized by approximately equal proportions of medium-bedded porcelanite layers (27%) and organic-rich carbonate muds (33%). Thick (1-2 m thick) *Thalassinoides*-burrowed phosphorite layers are present. Shell accumulations are fewer, and occur mainly in carbonate concretions where only ghosts of shells survive diagenesis (large *"Lucina"* shells). The upper 7 meters of the Porcelanite unit are dominantly (65%) massive layers of porcelanites, including carbonate-bearing porcelanite concretions up to 60 cm thick and rare shell pavements. Phosphorite-filled *Thalassinoides* burrows comprise 30% of the unit thickness.

The top Phosphorite unit is dominated by thick phosphorite layers with pebble and even cobble sized phosphate grains. Five 10-30 cm thick shell beds are present as well, with some dominated by articulated shells of the suspension-feeding bivalve "*Meretrix" rholfsi*, and others dominated by the deposit-feeding bivalve *Mesosaccella*.

Situated in the deepest part of the structural basin, the Nahal Ashosh paleolow is the thickest section examined. Notwithstanding the laminated intervals, a high abundance of *Planolites* (and some *Thalassinoides*, especially higher upsection) are present, suggesting moderate bottom oxygen levels. However, at times the levels were sufficiently well aerated (i.e., aerobic) to support the abundant and diverse (21 species in one assemblage) shelled faunal assemblage. Both articulated and disarticulated shells were recognized, suggesting that this location generally experienced a moderate water-energy regime, within the lower part of the transition zone. Note that disarticulation could be biogenic, which would indicate sufficient oxygen levels to support bioturbators. Thus, seafloor conditions in the paleolow were dynamic, ranging from exaerobic to fully aerobic conditions, as well as from low to relatively high bottom-water energy levels, below (laminated intervals) and above (dense packing of shells and winnowing of finer material) storm wave base, respectively. Overall, lithofacies 1 is the dominant type in the paleolow location.

Nahal Omer (paleointermediate)

Nahal Omer, situated on the flank of the Qazra sub-basin, is characterized by a more equitable distribution of lithologies (Fig. 1.3). The bottom Phosphatic-Carbonate unit is 20 meters thick, the middle Porcelanite unit is 17 meters and the top Phosphorite unit is 7 meters thick.

The Phosphatic-Carbonate unit comprises roughly equal thicknesses of organic-rich carbonate mud (30%), and siliceous layers of porcelanite and chert (20% and 10 %, respectively). Recurring shell beds (15%) and carbonate layers (8%) are also present, with less common phosphorites (up to granule grain size). The organic-rich carbonate muds range from laminated to highly bioturbated (Droser and Bottjer's ii 1-5). *Planolites* and subsidiary *Thalassinoides* occur throughout the section, especially at the basal contact of individual shell accumulations. Shell beds ranging from thin 5 cm shell accumulations to 30 cm thick shell beds are found in the lower half of the Phosphatic-Carbonate unit. Thicker shell beds between 20-80 cm are found in the upper half. The shell beds vary from loosely to densely packed and the bivalves are typically disarticulated (but articulated *Crassatella* species are also present), with bivalve and gastropod species equally common and the number of species within an assemblage as high as 22.

Higher upsection, the Porcelanite unit is characterized by increasing thickness of porcelanite layers and decreasing thickness of organic-rich carbonates. The lower

12 meters are characterized by thick sequences of medium-thickly bedded porcelanite layers (40%) and only minor organic-rich carbonates (3%). Thick (20-50 cm) mottled and *Thalassinoides* intervals occur throughout (thickness is difficult to estimate accurately due to rock debris that partially covers this unit). Six or seven (ambiguity due to patchiness) shell accumulations (20-40 cm thick) and coarse (granule grain size) phosphorite beds (10%) occur throughout the unit. A high abundance of just a few species characterize these shell assemblages, with articulated shells of the deposit-feeding taxa *Mesosaccella* together with the predatory gastropod *Gyrodes* comprising most of the assemblage or a dominance of large *"Lucina"* sp. The upper 5 meters of the Porcelanite unit are dominanted by massive layers of porcelanite, frequently lacking both macro- and microfossils. Thin sections taken from these rock layers are microfaunally-barren.

The top Phosphorite unit consists of 48% phosphorite beds ranging from sand to pebble size grains, fewer organic-rich carbonates (14%), few shell accumulations (mainly as thin, 5-15 cm pavements within or topping limestone concretions) and sporadic chert beds.

Structurally situated at an intermediate position on the flank of the basin, this location probably experienced similar or slightly more aerated and energetic conditions than the Nahal Ashosh paleolow location (i.e., relatively shallower basin water depths). Layers with distinct *Planolites* and *Thalassinoides* are present and

the increase in *Thalassinoides* abundance relative to that at Nahal Ashosh indicates an increase in bottom dissolved oxygen levels, close to aerobic (cf. Savrda et al., 1984; Savrda and Bottjer, 1986). This, together with the diverse and abundant shells (species richness as high as 22) suggest that seafloor conditions were well aerated, and even fully aerobic at times. Significant shell accumulations contain a higher percentage of disarticulated shells relative to the paleolow suggesting either higher bioturbation activity (indicating dysaerobic levels) and/or slightly higher water energy. Specifically, bottom-water energy corresponded to that of the transition zone, as in the paleolow location, although this location was probably in the intermediate, rather than the lower transition zone (abundance of dense packing was higher than that of the paleolow Nahal Ashosh location). This is also suggested by the slightly higher oxygen levels, which could be the result of higher frequency of local storm wave action.

Har Masa (paleohigh)

The paleohigh location, Har Massa, presents the thinnest section of the Phosphate Member (Fig. 1.4). The bottom Phosphatic-Carbonate unit is only 3 meters thick, the middle Porcelanite unit is 4 meters and the top Phosphorite unit is 7 meters thick.

The Phosphatic-Carbonate unit is dominated (75% of total thickness) by organic-rich carbonate mud, which contains up to 8.4% weight of phosphate (Appendix

1.1). These layers are frequently mottled (ii 4-5) or burrowed (*Planolites* and *Thalassinoides*) and only rarely laminated. Coarser material (granule-pebble grain size) is strewn within the layers. Only minor porcelanite and chert (7% and 4%, respectively) were identified and only one distinct shell bed was apparent. Note that one, more concretionary, shell accumulation, 20 cm higher upsection, is very patchy with an obscure boundary. Burrows, especially the ichnogenus *Thalassinoides*, are well-developed along the basal contacts of this shell bed. The shell bed contains a diverse macrofossil assemblage, with individuals relatively equally divided amongst the different species and a total species richness of 20. The shell bed is bioturbated, loosely-packed, with mostly disarticulated shells with both bivalves and gastropods common. Many shells are fragmented and abraded. The molluscan assemblage includes (though less common) epifaunal species that attach or cement themselves to the substratum, such as the shallow-water *Plicatula* species and the oyster *Rastellum*.

The Porcelanite unit is a combination of the different key lithologies, with no dominant one. The lower half of the Porcelanite unit consists of 40% organic-rich carbonates, 30% granule-pebble sized phosphorite layers and no porcelanite. Two patchily distributed shell beds (up to 20 cm thick) contain abundant, mostly articulated shells of *"Lucina"* (40% of individuals).

The top Phosphorite unit is composed mainly of thick phosphorite beds ranging from sand to pebble-sized grains. Micritic phosphate "rip-ups" are also present, and have been interpreted by Soudry (1987, 1994) as the product of microbial mats that were later fragmented under a high-energy regime.

The highest bottom-water energy levels of all five sections are found at this structurally high location. An increase in the percentage of *Thalassinoides* relative to the former locations, together with the rich (up to 20 species) and highly even distribution of individuals among species in the shell accumulation, suggest that seafloor conditions were often fully aerobic. Disarticulated shells, but especially the coarse material strewn throughout, and the "rip-ups" all point to a high-energy bottom-water regime. Bottom-water energy was similar to the upper transition zone and at times above fair-weather wave base. As in the case of the two former locations, small recurring storm events could produce the high-energy signatures (winnowing of fine material, dense packing of shells and storm generated features of shell stacking) and replenish seafloor oxygen to support the diverse fauna. In general, lithofacies 4 is typical of the paleohigh location.

In addition to the three locations within the Qazra sub-basin, two other stratigraphic sections from paleointermediate positions were described from the flanks of other Mishash sub-basins. These sections were chosen to provide a regional perspective of these special settings within the Mishash shelf. The Oron

location (specifically exposures in Nahal Talul in the Zin sub-basin) was studied in light of prior microfossil analysis done in the Oron region (Almogi-Labin et al., 1990, 1993; Bein et al., 1990; Eshet and Almogi-Labin, 1996). This sub-basin was examined in particular because of the low dissolved oxygen levels suggested by microfauna, and the extremely high organic carbon concentrations of up to 26% (Bein et al., 1990). Finally, in order to examine the transition of high-productivity facies with the open sea to the northwest, a section in the Judea Desert foothills was also measured. This location, situated on the inner flank of the sub-basin farthest from the paleoshore, was the best exposed section available for study.

Oron (paleointermediate)

The Oron section (~40 meters total), situated on the shoreward flank of the Zin sub-basin, is the poorest site with regard to macrofaunal remains (Fig. 1.5). The bottom Phosphatic-Carbonate unit is the best-exposed unit within the Phosphate Member, with the middle Porcelanite and top Phosphorite units quite poorly exposed. Thus, most of the focus was on the Phosphatic-Carbonate unit (specifically the lower, outcropping 18 meters).

The Phosphatic-Carbonate unit is dominated by organic-rich carbonate mud (65%). The siliceous layers of porcelanite and chert (11% and 9%, respectively), micritic carbonate layers - some concretion-shaped - (6%) and coarse grained (coarse sand to pebble) phosphorite horizons are less common. Only one loosely-

packed (0.5 m thick), monospecific (*Rastellum diluvianum*) shell bed is present. The organic-rich carbonates range from laminated intervals to more commonly highly bioturbated intervals (Droser and Bottjer ii 4-6). Distinct burrows of *Planolites* (but also *Thalassinoides*) are observed throughout the section. The bottom unit exhibits only a single loosely-packed shell bed with a basal burrowed contact. The epifaunal oyster *Rastellum diluvianum* is the sole species comprising this assemblage and is typically thin-shelled, fragmented and disarticulated. Only two other horizons contain skeletal macrofauna in this section: a 15 cm-thick sparsely packed bivalve layer and a 30 cm-thick coarser (granule-pebble size) phosphorite layer with bivalve fragments. The granule-size phosphorite fills the larger *Thalassinoides* burrows (only two events recorded), but the strata mostly exhibit silt-coarse sand layers.

The overlying Porcelanite unit and the Phosphorite unit are not exposed in this location, which is situated within a phosphate quarry and therefore lacks the top, excavated (economic) Phosphorite unit. The top unit is preserved rather poorly in an adjacent site (Givat Mador) and is characterized by recurring shell-bearing limestone concretions with loosely-packed, poorly preserved shells.

Without doubt this location represents the stereotypic expectation of high-productivity settings, and was by far the most restricted of the basins studied. Due to the scant outcropping of the middle and top units, the paleoenvironmental

interpretation is of the bottom Phosphatic-Carbonate unit alone. Notwithstanding the evidence for a very few high-oxygen events (and possibly high-energy) provided by the disarticulated *Rastellum diluvianum* shell bed and the one granule-size phosphate layer, the scarcity of shells, together with the largely laminated organic-rich carbonates, point to a very stressed environment with extremely low oxygen levels. On the other hand, the frequent mottled layers (at times nearly homogenized, ii5-6) that occur throughout are evidence of past unshelled but multicellular animal life. Thus, the oxygen levels probably fluctuated between a nearly anaerobic seafloor (lamination, absence of macrofauna) to dysaerobic seafloor conditions (per Savrda et al., 1984). The presence of quite a few fine-grained laminated intervals and only a few granule-size phosphate occurrences may indicate that bottom water energy was low at virtually all times, thus typically below storm wave base.

Judean Desert (paleointermediate)

The Phosphate Member in the Judean Desert section (measured in the western foothills of Wadi El Qilt) is 42 meters thick (Fig. 1.6). The bottom Phosphatic-Carbonate unit is 26 meters thick, the middle Porcelanite unit is 9.5 meters and the top Phosphorite unit is 6.5 meters thick.

The Phosphatic-Carbonate unit is strongly dominated by organic-rich carbonate mud (74%) with less frequent chert beds (12.5%), shell accumulations (7%),

carbonate layers – some concretion-shaped - (6%) and minor phosphorites (1.5%). Burrows are not as common as in the Oron section, although several burrowed contacts (at times as lower shell bed boundaries) are present. In general, the organic-rich carbonates are finely laminated with occasional mottled intervals. Several thin (5-20 cm thick) shell beds and a one meter-thick one are observed. These are either concentrated as shell pavements on concretions or in pods, or occur as loosely packed layers of fragmented, thin, fragile shells. The meter-thick shell bed exhibits disarticulation and scarce shell stacking, while another, thinner shell bed consists of finely and sharply fragmented shells (as produced by durophagous predation today). The diverse shell assemblages contain both bivalves and gastropods.

Higher upsection, the Porcelanite unit and the Phosphorite unit are largely covered by rock debris (probably due to the increase in the softer, porcelanite layers that are more prone to weathering). However, when exposed, the Porcelanite unit exhibits thick (40-50 cm) layers of chert and silicified carbonate concretions as well as a 60 cm thick layer of phosphorite (medium sand-pebble size).

The Phosphorite unit (when exposed) is characterized by thicker, 70-110 cm phosphorites with sand to pebble-sized nodules. Common fish and shark vertebrae as well as brown organic debris characterize these layers (referred to as bone phosphorites, e.g. Soudry, 1994).

Located closer to the deeper, open ocean, this section exhibits a pattern closer to the one expected in a normal shallow marine carbonate environment. Stereotypic high-productivity lithologies such as chert, porcelanite and phosphorite layers are in fact less abundant (or absent) in this location. The organic carbon content of the Judean Desert locality is estimated to be similar to that of the Shfela location (up to 15%, Bein et al., 1990) and not of the Zin sub-basin (up to 26%, Bein et al., 1990), thus less organic-rich than the Zin sub-basin. The lack of any coarsening of grains upsection indicates a consistently low water-energy regime, well below storm wave base. Furthermore, the loosely packed fragmented shell layers may show some disarticulation but are otherwise of ambiguous origin, generated either by small local storm events or by a bioturbating or scavenging organisms. Shell fragmentation alone is not sufficient to indicate high water energy in this case, since it could be of biogenic origin. This is further corroborated by the predator-nibbled shells observed within the thick shell bed. Water energy was only slightly higher than in the Zin sub-basin (some shell stacking) but still quite low, as suggested by the fine-grained strata. The mottling of layers together with the few but diverse shell accumulations suggest that oxygen was not a limiting factor in this location (it was characteristically aerobic). Oxygen was presumably replenished episodically from deeper, more oxygenated water layers offshore.

LITHOLOGIC CYCLICITY

Sediments are arranged in a series of recurring sedimentary cycles 1 to 9 meters thick in the Phosphatic-Carbonate unit and lower part of the Porcelanite unit at all three locations in the Qazra sub-basin. Given their physical scale, lithologic asymmetry, and utility for local (as opposed to regional) correlation, they are referred to as informal paracycles (syn. parasequences). Characteristically, the lowermost lithology in each cycle is an organic-rich carbonate, which is followed by alternating thin porcelanite and chert layers. These are followed by either a carbonate layer or concretion-shaped layer or a phosphate-bearing carbonate layer whose upper surface is strewn with coarse skeletal material, which in turn is overlain by a burrowed contact and a densely to loosely packed molluscan shell bed. In many instances the upper shell bed is capped by coarse phosphorite or is itself rich in phosphate grains.

Individual cycles can be well developed, showing the idealized full succession described above, or only partially developed, with only a subset of the complete lithologic succession. A typical paracycle characterizing the Phosphatic-Carbonate unit for each of the three locations within the Qazra sub-basin is shown in figures 1.7, 1.8 and 1.9 (paleohigh, paleointermediate and paleolow, respectively). The vertical distribution of para-sequences within the Phosphatic-Carbonate unit of the Qazra sub-basin is shown in figure 1.10, illustrating lateral variation in the number

of paracycles that can be recognized and characterized in the paleohigh, paleointermediate and paleolow locations.

The paleohigh location Har Massa preserves the thinnest section. Only a single paracycle 2.8 meters thick can be resolved within the lower Phosphatic-Carbonate unit, and this is capped with a 20 cm thick (sparsely to) loosely-packed shell bed (Fig. 1.7).

The paleointermediate location, Nahal Omer, is located on the synclinal flank of the basin. It exhibits a series of cycles throughout the lower part of the Phosphatic-Carbonate unit. The cycles constitute the lowermost 20 meters of the section. The first 3 cycles are the thickest and most complete (between 3.5-4.5 meters each); the next 4 cycles are each 1-1.5 m thick; and the uppermost cycle within the unit is 3 m thick. The phosphatic, loosely-densely packed shell beds that cap these cycles range from 20 to 70 cm thick. A typical cycle is plotted in figure 1.8.

The paleolow location, Nahal Ashosh, is the thickest section. It exhibits a series of cycles throughout the lowermost 45 meters (Phosphatic-Carbonate unit); a typical one is plotted in figure 1.9. Fluctuations in lithology are less striking in this thicker section, making the distinction of cycles less pronounced than in the paleointermediate location. In general, the succession of lithologies within cycles follows that observed at Omer, with the exception that the siliceous phase is

dominated by chert beds and only minor porcelanite layers. At Ashosh, paracycles are thickest in the lowest 20 meters of the section. The first three cycles are each 8-9 meters thick and can each be subdivided into sub-cycles of 1-2 meters thickness. They are followed by a 3m- and then a 2m-thick cycle. Higher upsection, five ~1 m thick cycles follow, and finally, the top cycle of this unit is 8.5 m thick. The loosely to densely packed shell beds that cap the paracycles are 20 to 90 cm thick, with the thicker shell beds in the upper part of the unit.

In both the Ashosh and Omer sections the organic-rich carbonate muds (lithofacies 1) are the most abundant strata, whereas in Massa the same is true but the organic-rich carbonates have a higher phosphate component. The siliceous phase within the Phosphatic-Carbonate unit is evident in all locations in the form of either chert or porcelanite. In the Ashosh section, however, porcelanites are very rare whereas cherts are abundant. In addition to the shell beds of the Phosphatic-Carbonate unit, several more shell beds occur in the higher, middle Porcelanite unit. Nonetheless, at all locations, the Phosphatic-Carbonate unit demonstrates the greatest number of shell beds, highest density of shell packing and the greatest bed-to-bed variation in lithology.

The paleointermediate section (Nahal Omer) of the Qazra sub-basin thus represents the highest degree of lithologic and paleontologic variability within the Phosphatic-Carbonate unit of the Phosphate Member and thus captures the basic

variability of the Mishash high-productivity complex. This section, which is located near the inflection point of a local basin (between a paleohigh and an adjacent paleolow), and thus is neither unusually thin nor unusually thick, is in the position of maximum sensitivity to environmental fluctuations (e.g. expansions and contractions of oxygen-minimum zone, food availability, substrate variability, relative changes in sea level, etc.). An “ideal sedimentological cycle” was configured relying on the detailed description of the different sections, but principally at Nahal Omer and is most characteristic of the lower part of the Phosphate Member. From one packed shell-bed or coarse phosphorite (Packstone A, Fig. 1.11) to the next (Packstone or coarse phosphorite B), a succession of lithologies from laminated organic-rich carbonates through thin porcelanite beds and carbonate concretions constitute the ideal paracycle.

The up-cycle trend of increasing bioturbation intensity, increasing faunal diversity and increasing abundance of the molluscan skeletal material observed within the Mishash paracycles is consistent with an increase in bottom oxygen levels and/or increase in the duration of individual aerated events, from low, nearly anaerobic levels to less hostile environments of fully aerobic conditions (Fig. 1.11). Moreover, going from the laminated or slightly burrowed organic-rich carbonates up-cycle to the capping shell bed/phosphorite layers, there is an increase from silt to pebble grain-sizes and from sparsely distributed shells to densely-packed

winnowed layers, which is consistent with an increase in bottom-water energy, from below storm wave base to above fair-weather wave base.

Variations in the dominant lithofacies among localities and upsection was probably controlled by relative proximity to the center of the upwelling/high-productivity cells and variations in intensity of the upwelling. That is, going upcycle from lithofacies 1 to lithofacies 4, one can infer a temporal decrease in upwelling intensity and/or an increase in distance from upwelling center as well as an upcycle trend in water energy (shallowing).

Larger spatial and stratigraphic patterns

In summary, looking at the small-scale trend, paracycles appear to be best developed in the intermediate, Nahal Omer section. The thinnest paleohigh section at Har Massa included only one fully recognizable cycle, with an incomplete cycle below and above it, whereas within the same time-period, eight cycles are evident at the intermediate Omer section, and 11 cycles in the Ashosh section from the deepest part of the basin (Fig. 1.10). An increase in cycle thickness is observed from anticline to syncline, with intermediate thickness in Omer. The duration of the Phosphate Member is ~7 m.y. long, between 79-72 m.y. (based on ammonite biostratigraphy, Lewy, 2001). However, based on the lithologic variations amongst the major components, Soudry et al. (1985) divided the Phosphate Member into three informal units and thus a finer (ammonite-) age correlation can be examined.

The bottom part of the section, the Phosphatic-Carbonate unit, encompasses the most pronounced paracycle cyclicity and records ~3.5 m.y. at maximum [based on a silicified phosphate marker bed at the top boundary of the Phosphatic-Carbonate unit (at ~75.4 m.y., Lewy, 2001), a planktic foraminiferal abundance peak (appearance of Globotruncanidae species at ~ 75.6 m.y., Reiss, 1988; Almogi-Labin et al., 1993; Lewy and Odin, 2001), as well as the first appearance of the ammonite *Didymoceras puebloense* (at ~75.5 m.y., Lewy, 2001, Omer section, personal observation)]. Assuming that the Ashosh section is 100% complete (11 cycles) each cycle there represents ~0.32 m.y. By comparison, the Omer section is only 73% complete (8 cycles) with each cycle representing at most ~0.44 m.y. and the Massa section (3 cycles) is approximately 27% complete with each cycle representing at most ~1.2 m.y. duration.

Within the time interval corresponding to the Phosphatic-Carbonate unit, the paleohigh section contains at least 3 cycles (i.e., one complete cycle and the beginnings of an earlier and later succession) contemporaneous to at least 8 and 11 paracycles in the paleointermediate and paleolow sections, respectively. In addition, farther from the crest of the paleo-anticline (specifically at the paleohigh locality, Har Massa) the single, complete, cycle opens up into two cycles, which suggests that a real condensation of the section takes place as one gets closer to the anticline ridge. This independent paracycle evidence for condensation is in

agreement with structural and sedimentologic evidence for condensation noted by previous studies (e.g., Soudry et al., 1985).

Cyclicity is absent at the Oron location, suggesting that a more continuous stressful environment persisted under the high-productivity regime in the Zin sub-basin, which hindered the development of the biological and lithological succession characterizing the environmentally more variable Qazra sub-basin. The Judean Desert foothill location (El Qilt sub-basin) illustrates rather rough cycles that do not exhibit all four key lithofacies (porcelanite is absent, and phosphorite layers and shell beds are minor). The oxygen levels at this location farthest from shore seem to be more stable than those of the Zin and Qazra sub-basins. These interpretations are supported by microfossil samples, which indicate continuous presence of foraminifera in the Judean Desert location, but show microfaunally barren intervals in the middle Porcelanite unit in the Qazra sub-basin (especially at Nahal Omer).

Superimposed on the pattern of small-scale paracycles within the Phosphate Member is a larger scale upsection trend in lithologic composition (as indicated by the unit names given by Soudry et al., 1985). Notwithstanding the densely packed shell beds, the lower Carbonate-Phosphate and Porcelanite units consist mainly of organic-rich carbonates (both laminated and mottled) and porcelanites with thick burrowed layers, whereas the overlying Phosphorite unit displays phosphate-

bearing-organic-rich carbonates, limestone concretions and few layered chert beds in its lower part and, in its upper part, a higher component of coarse material (bones, fish debris, fecal pellets) and phosphate pebbles. Thus the larger lithologic trend recapitulates an overall similar, though less detailed succession of lithologies seen upsection within individual paracycles (Fig. 1.12 - and compare to Figs 1.7-1.9), that is a shallowing-upwards trend and shift away from the upwelling center or overall decrease in upwelling intensity.

DISCUSSION

The results obtained from the different sub-basins in the present study demonstrate considerable variability within the system. The range of sub-environments within the high-productivity system is indicated by the two extremes, from the shelly and diverse Qazra sub-basin and to the faunally scant Zin sub-basin. The variation in lithologic dominance across the basins and the lithofacies changes along a single-paracycle succession also demonstrate the spatial and temporal heterogeneity of the high-productivity system.

Previous studies have focused on the sedimentologic and geochemical characteristics of the Mishash rather than on its fossil-rich sections, and these also demonstrate the complexity of the system (Soudry et al., 1985; Vengosh et al., 1987; Shemesh and Kolodny, 1988; Soudry, 2000; Soudry and Nathan, 2001, Soudry et al., 2002). Soudry described three main phosphate categories from the

Mishash: biodetrital phosphorite, massive peloidal phosphorite and laminated peloidal phosphorite. Biodetrital phosphorites occur mainly within the lower part of the Phosphate Member, principally in the lowermost Phosphatic–Carbonate unit (which was the focus of the present study), but also the middle Porcelanite unit. The massive peloidal phosphorites constitute the economically important phosphorite beds of the structurally high sections of the Mishash Fm, while the laminated peloidal phosphorites are present primarily in paleolows. Both the biodetrital and massive peloidal phosphorites are referred to as the "recycled facies", while the laminated peloidal phosphorites are referred to as the "pristine" facies (Soudry, 1992, 2000; Soudry and Nathan, 2001). The two facies imply very different depositional processes. The "pristine" facies are inferred to be remnants of microbial mat systems, whose microbes flourished after each high productivity event in the Mishash sea and formed the primary phosphate beds of the paleohighs. The "recycled" facies are interpreted as the products of syndepositional reworking of phosphate-productive mat deposits, especially storm reworking and mechanical concentration of phosphate from earlier, primary phosphates (Soudry, 1992, 2000; Soudry and Nathan, 2001). Soudry also refers to fluctuating bottom-water energies in association with the different phosphatic accumulations (Soudry, 1983, 1992, 2000).

The present macrofaunal/sedimentological study generally agrees with Soudry's insights while extending the detail in which the record can be interpreted,

especially the intervals that are relatively phosphate-poor (lithofacies 1; i.e., the "soft carbonates" of Soudry). Overall, Soudry (1983) interpreted the lower half of the Phosphatic-Carbonate unit as a low-energy interval, while the upper half of the unit was characterized by significantly more high-energy events, and therefore an overall higher water-energy regime. Macrofaunal analysis indicates the same trend, but reveals that many of the chert beds, carbonate concretionary-layers, and silicified phosphatic layers referred to by Soudry as low or relatively low bottom-water energy environments, were frequently capped by (storm-generated) shell pavements. These loosely to densely packed shell pavements are silicified, and some may be the residual of a former carbonate shell accumulation, with chertification obliterating most of the shelly remains except for the top and/or bottom boundaries, and ambiguous remains within layers. The shelly remnants in carbonate mud concretion-shaped layers and silicified phosphatic layers may be explained in a similar fashion: most show an obliterated interior layer of shell ghosts or a top pavement of shells as in the cherts. These shelly remains are commonly silicified as well. Thus, despite partial diagenesis and obliteration, ghosts or partial remains of molluscan shells are readily detected in the different lithologies and indicate a higher degree of seafloor oxygen and energy than previously recognized from sedimentology/geochemistry alone. Specifically, the macrofaunal remains suggest that seafloor oxygen levels were dysaerobic or higher and also that water energy levels were higher than previously recognized. Some of the thin (1-5 cm thick), densely packed shell pavements show storm-generated shell

stacking, signifying that intensity of seafloor disturbance was similar to that seen above storm wave base, but due to the obliteration of shells a more detailed interpretation is difficult.

There have been several micropaleontological studies of Mishash material from cores (Reiss, 1988; Almogi-Labin et al., 1993). Almogi-Labin et al. (1993) investigated the depositional environment of the Upper Campanian seafloor in two basins and recognized four benthic foraminiferal assemblage-types. The distribution patterns of the benthic foraminifera from both basins followed an oxygen gradient, with the Zin sub-basin interpreted as a low-oxygen (dysaerobic) environment in close proximity to a high-productivity center, and the more seaward Shefela sub-basin recording a more aerated marine environment (Almogi-Labin et al., 1993).

The results of the present macrofaunal analysis are consistent with the microfossil analysis of the Zin sub-basin. The low diversity of both benthic macrofaunal (molluscan) and microfaunal (foraminifera) assemblages reflects an oxygen-depleted (dysaerobic) seafloor in the Late Campanian. The depositional environment of the Judean Desert location of the present study is most similar to the Shefela location, although the seaward location of the present study is not actually within the paleo-open sea (it was the closest to an open-sea location that could be sampled). Both seaward locations exhibit the closest to normal-marine

conditions of the studied locations, and are considered to be marginal high-productivity facies. However, the complexity of the upwelling system that covered this region is not captured by single upwelling-representative locality. Examining the Zin-basin alone does not reveal the spatial patchiness or the temporal cyclicity typical of upwelling areas. Homogeneous diatomaceous mud characterizes the ooze beneath the center of upwelling cells. This is seen, for example, under the most permanent cell of the Benguela upwelling system, in the vicinity of Luderitz where the primary accumulation is diatomaceous (Shannon, 1985). However, the fairly homogeneous nature of the deposits (dominantly macrofossil- barren organic-rich carbonates) seen in the Zin sub-basin are not analogous to the depositional environment of the homogeneous diatomaceous ooze characterizing upwelling centers. Rather, the relatively uniform deposits of Zin are probably a consequence of the restricted water circulation in this basin in addition to the prevailing upwelling in the area. A high topographic barrier (high sill) for the Zin sub-basin would inhibit oxygen replenishment from either deeper or surface waters, which could result in stratification and oxygen depletion of bottom waters. It was under restricted water circulation within an upwelling regime that the expanded organic-rich sediments were deposited.

In conclusion, by examining additional locations a more detailed picture of seafloor conditions under high productivity systems unfolds. The varied nature of the upwelling regimes is evident from looking at the extremely different basins, the

Zin sub-basin (both molluscan and foraminiferal data) as opposed to the Qazra sub-basin and finally the ocean-ward localities (Judean Desert and Shefela sections). A patchy and varied mosaic of seafloor conditions prevailed under the high-productivity system and was not simply a low-oxygen, dysaerobic seafloor as suggested by previous microfaunal studies (Reiss, 1962, 1988; Almogi-Labin et al., 1993). Moreover, by examining the different localities one can re-organize and develop more accurately the spatial framework of the typical upwelling facies-belt. An upwelling facies-belt is a lithological gradient that corresponds to distance from the upwelling center, with siliceous oozes giving way to pelagic carbonates (e.g., Roger and Bremner, 1991). However, these facies-belts are each defined by a patchy mosaic composed of the four upwelling lithofacies; porcelanite/chert, organic-rich mud, phosphorite and carbonate. Upwelling in its nature consists of local cells within the overall high productivity area, thus creating a fundamental patchiness of sub-facies within the main parallel-to-shore facies-belt.

Macrofauna, both shelly and trace fossils, reflect oxygen levels of the seafloor and/or sediment-water interface. In some cases, bioturbation by macrofauna may be the only evidence for past aerobic life in macrofaunally barren intervals (e.g., Zin sub-basin). Moreover, because macrofauna are particularly sensitive to overlying waters it makes them an exceptional agent to understand the seafloor facies under upwelling environments. In addition, the hydrodynamic behavior of the shells as grain particles reveal the true complexity of the upwelling system, i.e., not only the

dysaerobic facies that the foraminifera see, but rather the full picture of the subsequent shallowing-up cycles. These are indicated by the winnowed and densely-packed macrofossil shell beds, with the dysaerobic facies winnowed away. Thus, by combining the present study's macrofaunal evidence with the microfossil data, an expanded oxygen profile of the Mishash seafloor is attained - specifically a vertical expression of the oxygen levels.

Both the ecologic and the taphonomic utility of macrobenthos are displayed as paleo-seafloor indicators of upwelling regions. Therefore, combining all the biogenic constituents observed along the facies tract with taphonomic and the more typical sedimentologic information provides a better tool for detailed reconstruction of past environment in high-productivity settings.

PALEOCEANOGRAPHIC SYNTHESIS: SEAFLOOR ENVIRONMENTAL MOSAIC

Although all five study locations are under the high-productivity regime, there are major differences from locality to locality. In general, the extent of mottling, burrowing and bioturbation increased upsection in all areas. The Oron location (Zin sub-basin) is very poor in macrofauna overall, and in fact the extensive mottled and burrowed intervals are the only solid evidence of macrobenthic life. This contrasts with the diverse and abundant body and trace fossils in all three locations of the Qazra sub-basin and also, but to a lesser degree, the Judean Desert location.

Superimposed on the unique hydrographic circulation of high-productivity regimes, structurally-induced morphologies of the basins contribute to explaining these differences.

Spatial reconstruction

A schematic ocean circulation reconstruction (Fig. 1.13) shows the different locations with respect to sill topography, relative distance from paleoshore and proximity to upwelling center.

The Qazra sub-basin, located on the side closer to the paleo-shore, was apparently controlled by the shallower water circulation and probably had a relatively deep sill, based on the evidence for higher bottom-water energies and oxygen concentrations. Accordingly, there was a greater replenishment by aerated surface waters since no significant barrier was present. Detailed examination of the structurally different sections within the Qazra sub-basin reveal large fluctuations in lithofacies dominance that are environmentally controlled. Highest water energies, above fair-weather wave base and highest oxygen levels (>>1 ml/l) existed on the high of the basin. Oxygen levels and water energy were significantly positive at times, even deep in the basin. In addition, the Qazra sub-basin was situated in close proximity to the upwelling center as seen by the high abundance of the siliceous phase (chert or porcelanite).

The Zin sub-basin also records a high abundance of the siliceous phase (though not as high as recorded for Qazra) and was, therefore, also situated in close proximity to the upwelling center. This is in accordance with the configuration of modern upwelling regions where the organic-rich facies overlaps strongly with areas of maximum opal content, as seen for example in the Benguela upwelling system, southwest Africa (Rogers and Bremner, 1991). The Zin sub-basin is characterized by frequent barren intervals with respect to shelly macrofauna and is associated with the low-oxygen "death-zone" that characterizes, in part, upwelling regions. This association with a dysaerobic seafloor is corroborated by microfaunal (foraminiferal) data (Almogi-Labin et al., 1993) as well as by macrofauna. This sub-basin seems to have been deep with a relatively sluggish, restricted water circulation (high sill) and thus a decrease in oxygenated water inflow, resulting in lower concentrations of dissolved oxygen on the seafloor. In addition, stratification of the water column acted to reduce the upwelling intensity. Moreover, a lower planktic-benthic foraminiferal ratio for the Zin sub-basin also suggests a more restricted water circulation than that of the Qazra sub-basin (personal observations).

Whereas both the Qazra and Zin sub-basins were situated in close proximity to the upwelling center, they each show a different sub-environment. The high organic matter associated with the upwelling center will clearly increase oxygen consumption and may promote the potential for anoxic conditions on the sea floor.

Tyson and Pearson (1991) pointed out that at any level of organic matter, the extent of oxygen depletion is a factor of: (a) the strength of the pycnocline; (b) the initial content of oxygen and volume of the bottom water; and (c) the duration of the stratified period (see also Stachowitsch, 1991). The sill level of these two basins played a major role in determining macrofaunal assemblages. The patchy and irregular pulses of upwelling resulted in less extreme conditions locally, which permitted the growth of abundant and diverse fauna in the Qazra sub-basin. In addition, the lowered sill may have permitted greater volumes of water to enter the basin. This could have potentially decreased the depth of the pycnocline and reduce stratification of the water column, increasing the oxygen content locally. The Zin sub-basin was also controlled by its sill. However, in contrast to the Qazra sub-basin, the high sill resulted in restricted water circulation and as a consequence lowered oxygen levels, inhibited biological activity in this sub-basin.

The Judean Desert locality is situated closest to the open paleo-ocean and is generally a fine-grained organic-rich carbonate environment, occasionally laminated, with relatively lower-diversity faunal assemblages than in the Qazra sub-basin, but much higher than that of the Zin sub-basin. These features indicate relatively low bottom water energies yet overall moderate oxygen levels, and suggest a ramp-like shelf morphology, since currents were apparently not focused there. The presence of macrobenthic fauna (trace and body fossils) within the section indicates that the most intense upwelling and low-oxygen conditions were

at a distance, and specifically located more onshore. Compared to the more organic-rich localities, the Judean Desert locality exhibits "nibbled" shells in some of the shell beds, linking fragmentation to higher oxygen levels, that is predator-prey interactions, rather than high water energies (see also Kidwell and Bosence, 1991). However, occasional seafloor modification by shell-stacking events in the Judean Desert area (that can be generated by local strong currents) point to water energies slightly higher than within the sill- controlled Zin sub-basin. The more pervasive body-fossil record suggests that bottom oxygen levels were also higher, presumably derived from the deeper, more oxygenated waters. The presence of laminated intervals, however, indicates that the Judean Desert seafloor did nonetheless experience episodes of low oxygen, sufficient to depress even burrowing soft-bodied forms episodically.

Recently, the onshore facies of the Mishash counterpart-formation in Jordan was investigated for its phosphorite accumulations (Pufahl et al., 2003). Bioclastic carbonates consisting of oyster banks were described for the Upper Campanian of Jordan and interpreted as a shallow-marine environment (Abed and Sadaqah, 1998). As explained for the shell bed data from the present study and in agreement with Soudry's previous phosphorite studies, the oyster beds from Jordon were interpreted to be storm generated events (Pufahl et al., 2003). This presents an additional, closer-to-paleoshore location within the onshore-offshore transect examined in the present study and gives a more inclusive regional picture.

Upwelling model

The spatial picture described above suggests three major depositional environments that existed under the upwelling regime of the southern Tethys. This is simulated in a schematic model shown in figure 1.14: **(a)** The typical mosaic of deposits that characterized the Mishash upwelling center, similar to those of Qazra sub-basin. This depositional environment characterizes a persistent but irregular upwelling regime with regards to upwelling frequency. The frequency of the upwelling pulses fluctuated both in space (increasing upwelling patchiness) and time (lithofacies cyclicity), with an increase in the frequency of upwelling pulses corresponding to an increase in abundance of the siliceous phase. The deposits record a range of seafloor oxygen levels and a range of energy environments. **(b)** Oxygen-deficient deposits that are characterized by some lamination, absence of macrofauna but burrowing and mottling of the layers, like the deposits of the Zin sub-basin. These deposits demonstrate the proximity to the upwelling center but, more importantly, the restricted nature of the water circulation and low oxygen concentrations due to a high sill. Finally, **(c)** normal marine deposits of a ramp-like configured sea, similar to the deposits of the Judean desert. Predator-prey interactions were the main influence on the taphonomic signature of the shells in the moderately diverse macrofaunal assemblages.

CONCLUSIONS

The extensive siliceous, phosphatic, and organic-rich carbonate rocks for which the Mishash Fm. is famous provide clear evidence that this was a high-productivity setting along the southern edge of the Late Cretaceous Tethyan Ocean. However, this new examination of these deposits indicates that, contrary to stereotypic thinking of such settings, abundant body and trace fossil evidence throughout the deposits signifies variable oxygen and water energy levels, and demonstrates the highly dynamic and spatially heterogeneous nature of this system. The geographic patchiness of these systems is demonstrated by the different locations. The effect of proximity to the center of the high productivity cells as well as the nature of the sill dynamics is represented by the two end-member basins. On the one hand the fossiliferous Qazra sub-basin demonstrates the variability of the system moving from laminated barren layers to densely shell-packed ones, and on the other hand, the Zin sub-basin that is burrowed and bioturbated and shows up to 25% weight of organic carbon in cores (Bein et al., 1990) but is lacking shelly intervals.

Climatic changes that affect the wind regime (Fenner, 2001 and refs within) were probably the cause for changes in the intensity and frequency of upwelling pulses over the region that resulted in the cyclic changes in environment. The folding and faulting that took place in the region affected the depth of the water source. Upwelled waters from deeper depths have different nutrient and oxygen

concentrations than those from shallower depth. The different water characteristics and sub-basin circulation affected the resultant benthic community.

Studies that incorporate macrofaunal data with outcropped sampled sections are rare in high productivity regions. The strong diagenetic overprint present in high-productivity deposits may be one reason for this. The scarcity of shelly-macrofaunal information from similar ancient (or modern) settings makes it difficult to determine and compare the extent to which these seafloors are actually death zones. The Mishash Formation proved to be a beneficial record to study. Not only can we better understand the environmental changes that occurred during the Upper Campanian Mishash, but rather expand this macrobenthic study to understanding high-productivity regions at large. The patchy nature and variety of sub-environments that characterize upwelling regions today are clearly seen in this Formation and demonstrate the need for more ancient/modern studies.

CHAPTER 2

MACROBENTHIC COMMUNITY STRUCTURE IN A HIGH-PRODUCTIVITY REGION: LATE CRETACEOUS MISHASH FORMATION (ISRAEL)

INTRODUCTION

Marine high-productivity settings are associated with sedimentary deposits rich in silica, organic-rich carbonates, and phosphate. High nutrient levels, usually supplied by upwelling, drive high productivity of the water column; after death algae, settle to the sea floor and may produce organically-enriched sediments (Parrish, 1982; Suess and Thiede, 1983; Thiede and Suess, 1983; Summerhayes et al., 1992; Wilkerson et al., 2000; Parrish et al., 2001; but see Glenn and Arthur, 1990). On the sea floor, the rate of decomposition and burial of organic matter together with phosphogenesis and taphonomic processes (such as grain dissolution and lateral transport) will determine the composition of these deposits, which will then be subject to further modification (e.g., chertification, carbonate dissolution and precipitation, etc.).

A spatially heterogeneous mosaic of environmental conditions and sediments characterizes seafloors of modern upwelling systems, with localized high-productivity cells along a single shelf (e.g., Shannon, 1985). We can thus expect a spatial and temporal mosaic of seafloor conditions to exist across ancient high-productivity tracts over both ecological and geologic time-scales, and expect to see this reflected in the composition of macrobenthic assemblages. Surprisingly, the

paleoecological significance of macroinvertebrates in these settings has been largely unexplored, probably due to a stereotypic view of upwelling systems as benthic “death zones”. However, distinct environmental gradients in the structure of macrobenthic communities (e.g., species richness, abundance, taxonomic composition, burrow diameter) have been found in modern ecological studies across regions of low oxygen and/or high organic matter (e.g., Rhoads and Morse, 1971; Savrda et al., 1984; Niermann et al., 1990; Arntz et al., 1991; Stachowitsch, 1991; Tyson and Pearson, 1991; Clarke and Warwick, 1994; Levin et al., 2000; Edelman-Furstenberg, Chapter 3). Moreover, macrobenthic invertebrates such as shelled mollusks, brachiopods, echinoderms, and crustaceans are sensitive recorders of seafloor oxygen levels, water energy and sediment mass properties, and leave a rich fossil record via their biomineralized skeletons. Investigating the fossil record of these organisms should thus provide a valuable new source of insight into paleoenvironmental conditions, one with fewer difficulties than geochemical analysis in such diagenetically complex settings.

Molluscan fossils from the Upper Campanian Mishash Formation of southern Israel were examined from an ecological perspective in order to determine the extent to which information on the composition and condition of macrobenthos assemblages can improve the inference of bottom-oxygen levels, food availability and other environmental gradients on high-productivity seafloors. This formation is exceptionally exposed and part of one of the most extensive high-productivity

complexes in the stratigraphic record. Organic-rich carbonate, siliceous (chert, porcelanite), and phosphate deposits are widely distributed along the southern margin of the former Tethys ocean in Israel. These deposits are part of an Upper Cretaceous-Eocene southern Tethys phosphate belt that extended from northern South America through North Africa to the Middle East (Notholt et al., 1989). Within this belt, the Mishash Fm. records the peak of a prolonged high-productivity regime of 9 m.y. maximum duration, within a phosphate-rich interval of 20 m.y. duration overall (see Almogi-Labin et al., 1993).

The Mishash has already been extensively studied with regard to its economic potential (e.g., Nathan et al., 1979). As a consequence, there is an existing framework of lithostratigraphic (mapping) and biostratigraphic (time-correlation) units available (Reiss et al., 1985; Almogi-Labin et al., 1986; Gvirtzman et al., 1989; Lewy, 2001). Also, previous workers have investigated the geochemistry of its diverse biogenic sediments (Nathan et al., 1979; Shemesh and Kolodny, 1988; Bein et al., 1990; Kolodny and Garrison, 1994; Soudry et al., 2002), the role of microbial processes in phosphogenesis (Soudry and Champetier, 1983; Soudry, 2000; Soudry and Nathan, 2001), and have identified ecologically significant microfossil (Reiss, 1962, 1988; Almogi-Labin et al., 1993) and macrofossil assemblages (Soudry and Lewy, 1988; Lewy, unpub. obs.). However, many questions regarding the environmental conditions remain unanswered, especially variations across the entire upwelling facies belt including the so-called "barren" intervals.

This study is a first attempt to investigate the paleoecological significance of macrobenthic invertebrate assemblages across an ancient high-productivity tract. Specifically, it explores macrobenthic evidence for bottom-water conditions across the Mishash upwelling tract of the southern Tethys, and the interplay of bottom oxygen levels and organic matter concentrations in dominating the benthic system. The research approach included basic descriptive measures of community-level ecological structure (diversity measures, life-habit types, etc.) rather than taxonomic composition alone, since ~75 million years separate the Mishash fauna from modern faunas. The state of preservation of skeletal remains (e.g., degree of articulation, fragmentation, orientation, etc. of shells) was also employed. Contrary to expectation, benthic community structure is highly variable within the high-productivity tract, and skeletal material in each of the different sub-environments carries a distinctive taphonomic and ecologic signature. Macrobenthos analysis modifies and expands the chemical (e.g., Kolodny, 1980; Soudry, 1987) and benthic microfossil (e.g., Reiss, 1988; Almogi-Labin et al., 1990) environmental interpretations of the Mishash and expands the range of bottom oxygen levels attributed to the Mishash seafloor.

GEOLOGICAL SETTING: MISHASH FORMATION

Israel was part of a stable carbonate platform along the southern margin of the Tethys Seaway from Late Albian to early Late Coniacian times. However, from the later Cretaceous into the Early Eocene, the broad shelf of this slowly subsiding passive margin experienced syndepositional folding and minor faulting associated with the Syrian Arc system (Krenkel, 1924). This deformation differentiated the outer part of the shelf (nearly 100 km wide) into sub-parallel NE-SW anticlinal ridges and synclinal basins, resulting in lateral changes in thickness and facies and producing a series of paleohighs whose flanks were sensitive to small-scale fluctuations in environmental conditions. The Campanian Mishash Formation comprises a shelf-wide tract of phosphate-rich, high-productivity facies that formed during the initial phase of syndepositional deformation.

The paleo-latitudinal position at 8-15° N of this part of the southern Tethys in the Upper Cretaceous would have put it under the influence of easterly trade winds, which would have had a major effect on the extent of high-productivity facies (Reiss, 1988). The Mishash Formation was originally defined in the northern Negev as a sequence of silica-, phosphate-, and organic-rich carbonate beds, which rest on chalk of the Upper Coniacian-Lower Campanian Menuha Fm. and are overlain by organic-rich argillaceous chalk (“Oil Shale Member”) of the uppermost Campanian-Maastrichtian Ghareb Fm. (Reiss et al., 1985). Northwestward towards the ancient open ocean, the siliceous-phosphatic rocks

of the Mishash are replaced gradually by pelagic organic-rich chalk of the Ein-Zetim Fm. (Flexer, 1968). Strata correlative to the upper Campanian Mishash Fm include the Duwi Formation of Egypt and Amman and Ruseifa Formations of Jordan.

For mapping purposes (lithostratigraphy), the Mishash Fm. was divided by Soudry et al. (1985) into a lower Chert Member (well-bedded cherts, silicified carbonates, and porcelanites, overlain with beds of brecciated chert) and an upper Phosphate Member, which has been the subject of most detailed study. The Phosphate Member comprises a distinct sedimentary cycle that ranges from 0 to 100 m in thickness when traced from anticlines to synclines across the fold belt. The member is quite heterogeneous lithologically, consisting of interbedded siliceous, phosphatic, and carbonate facies, and has a high organic content (up to 25% TOC) in subsurface samples (Bein et al., 1990). Both auto- and heterotrophic plankton are rather common in these sediments and reflect high fertility of the waters (Eshet et al., 1994; Eshet and Almogi-Labin, 1996; Hoek et al., 1996). Although all three lithologies (phosphate, carbonate, porcelanite/chert) occur throughout the entire thickness of the Phosphate Member, up-section variation in the proportions of these components led Soudry et al. (1985) to distinguish three informal units within the Phosphate Member, namely the lower Phosphatic-Carbonate, the middle Porcelanite, and the upper Phosphorite units.

Recurring sedimentary cycles of one to nine meters thickness characterize the lower Phosphatic-Carbonate unit of the Phosphate Member in both anticlinal and synclinal sections in many sections of the Mishash in southern Israel (Edelman-Furstenberg, Chapter 1). An “ideal sedimentological cycle” was configured relying on the detailed description of five different measured sections, and is most characteristic of the lower part of the Phosphate Member at Nahal Omer (see Edelman-Furstenberg, Chapter 1). From one densely packed shell-bed or, very rarely, a coarse phosphorite (Packstone A, Fig. 2.1) to the next (Packstone or coarse phosphorite B), lithologies succeed from laminated organic-rich carbonates through thin porcelanite and chert beds, to carbonate concretions or layers. These lithologies comprise the main building blocks of the high-productivity facies-mosaic across the Mishash seafloor.

METHODS

Field sampling of macrobenthic assemblages focused on three localities along an across-basin transect, using measured stratigraphic sections from paleohigh, paleointermediate and paleolow positions (respectively Har Massa, Nahal Omer and Nahal Ashosh in southern Israel, denoted as the Qazra sub-basin). Quantitative data for macrofaunal analysis (specifically benthic bivalves and gastropods) were collected from each of the main lithologies that comprised the three locations; i.e., organic-rich carbonates, thin porcelanite and chert beds, carbonate layers or concretions, and loosely to densely packed shell beds. For

sample locations within the sections see chapter 1, figures 1.2, 1.3 and 1.4. Coarse phosphorites were usually intermixed within the shell beds and rarely comprised a separate layer of significant thickness. Macrofaunal identification was difficult in these infrequent, lithified layers, with most fauna fragmented to a degree that prevented identification. Sampling concentrated mainly on the lower Phosphatic-carbonate unit of the Phosphate Member of the Mishash Formation where the lithological variation was greatest (Fig. 2.2).

As a first step, data for a cumulative sampling curve were collected while in the field. This served as a guide for establishing when data collection had been adequate for a given sample; i.e., the point when additional sets of specimens failed to yield new taxa. However, regardless of the sampling curve, a minimum of ~100 specimens were counted for each sample. Macrofaunal count-data for the Qazra sub-basin are given in Appendix 2.1.

Samples were examined for macrobenthic evidence for past seafloor conditions using methods that permitted comparison to modern systems. Other than several general reports on the Cretaceous fauna of the Middle-East (especially Picard, 1930 and Chavan, 1947), the macrofauna of the Mishash Fm has not been studied. Taxonomic and paleoecologic data for Upper Campanian species are thus scarce. Identification of many taxa for the present study was consequently limited to a generic rather than species level, and based on the species list and monographs for the

Phosphate Member taxa in Lewy and Edelman-Furstenberg (2003). Fortunately, even genus-level identification was sufficient for differentiating assemblages (with species within genera designated as a, b, etc.), and this was also sufficient to characterize community structure via such metrics as species richness and evenness. Bioclastic fabric was characterized primarily using bivalve shells that dominated the assemblages, focusing on shell orientation, close-packing, fragmentation, internal stratigraphy, and distinctive patterns of shell stacking (mostly using the criteria and terminology of Kidwell et al., 1986).

The oxygen levels inferred for the present reconstruction follow those of previous studies on oxygen-deficient benthic environments (Rhoads and Morse, 1971; Savrda et al., 1984; Savrda and Bottjer, 1987). Savrda et al. (1984) and Savrda and Bottjer (1987) investigated burrow structure and shelly macrobenthos in the California continental borderland and characterized five inferred dissolved oxygen zones [differentiating between inferred dissolved oxygen levels in the overlying waters (OW) and in the pore waters (PW)]. These were: **anaerobic** (0 mlO_2/l in both OW and PW, characterized by laminated strata lacking both in-situ body fossils and microbioturbation); **quasi-aerobic** (<0.1 ml/l in OW, 0 ml/l in PW; laminated strata with slight microbioturbation, containing benthic microfossils but lacking macrobenthic ones); **exaerobic** (>0.1<1 ml/l in OW; 0 ml/l in PW; laminated strata, but containing in situ macro-epibenthic body fossils); **dysaerobic** (as exaerobic, but with some aeration of porewaters; bioturbated, low diversity of small macrobenthic

body fossils, if any); and **aerobic** (>1.0 ml/l in OW and PW to some depth; thoroughly bioturbated, diverse assemblage of large, heavily calcified macrobenthic body fossils).

In order to find associations between samples and ecological variables, the data were organized into a matrix based on species abundance. Exact sample localities are shown in Chapter 1, figures 1.2, 1.3 and 1.4. The abundance data were standardized and expressed as percent abundance of each species. A cluster analysis (using Euclidean and Manhattan distance to construct a dissimilarity matrix) was employed to find associations between the samples. Both dissimilarity matrices clustered samples similarly, but the groups were visually more distinct using the Manhattan distances, and thus these are used to describe sample associations. The "R" Free Software (http://www.r-project.org/) was used to conduct the multivariate analysis using M. Foote's Q-mode clustering analysis program.

Variation in benthic community structure within this high-productivity system was examined using the following parameters:

Species richness is the total number of species per sample, whereas **species evenness** expresses how uniformly individuals are distributed among the different species and thus the extent to which the community is dominated by a small number of species. In modern ecological studies in oxygen-stressed environments, a

decrease in evenness usually reflects a shift to dominance by a few species of very abundant polychaetes (Niermann et al., 1990). In general a decrease in richness and in evenness correlates to increasing environmental stress (e.g., Rosenberg, 1976; Rhoads and Morse, 1971; Gray et al., 1988; Clarke and Warwick, 1994; Levin et al., 2002). As many authors have discussed (e.g., Clarke and Warwick, 1994), species richness is sample-size dependent: the larger the sample the more species are likely to be found. Thus, in order to compare between samples of different sizes, the number of species was counted from the sampling curves generated in the field, which were then plotted as cumulative abundance curves (figures 2.3-2.5). Evenness values were calculated using Hurlbert's evenness index PIE (1971), which is relatively insensitive to sample-size effects (e.g., Beisel et al., 2003) and is scaled from 0 (low evenness) to 1 (given in table 2.1) Note that the evenness index is defined logically only if a sample has one or more species. Samples having zero or one species are taken to have very low evenness.

Trophic groups: Assignment of species to trophic groups was based on the known ecology of living representatives of fossil genera and families. Pearson and Rosenberg (1978) showed, for example, that deposit feeders prefer organically-enriched areas; therefore, an increase in deposit-feeders (and chemo-autotrophs) is expected with increasing organic load/oxygen stress. Alternatively, an increase in suspension-feeders points to nutrient particles suspended in the water column rather than in the sediments. As oxygen levels at the seafloor decrease, the activity of

macrobenthos decreases, eventually leading to death. The following “death trend” among macrobenthos has been detected in modern marine and estuarine settings of rapid events leading to anoxia. First to die are the small-bodied and then the large-bodied epifaunal species; next, infauna begin to emerge from their burrows, with first the small-bodied and then the large-bodied infaunal species dying; finally, mortality of the entire benthic community occurs (Stachowitsch, 1991; Tyson and Pearson, 1991). The same trend is seen among burrowing infauna, which decrease in number along a decreasing oxygen gradient in the sediment (Bonsdorff et al., 1996).

Body size: This measure was collected for every specimen in the faunal counts, using maximum body length (apex to aperture for gastropods, anterior to posterior dimension for bivalves). All specimens were measured, but only whole shells were included in the size analysis. Body size at death has been shown to decrease as oxygen stress increases and is persistent in modern systems (Rhoads and Morse, 1971; Savrda et al., 1984; Diaz and Rosenberg, 1995).

RESULTS

The clustering derived from the Manhattan distance reveals three major biological associations that can be linked to different paleo-seafloor lithologies. The three associations (Fig. 2.6) are organic- rich carbonate muds (facies 1), thin cherts and porcelanites (facies 2) and shell beds (facies 3). Note that organic-rich carbonate sample 4 (i.e., YF O-5) clusters closer to samples from shell bed facies 3 than to the

other organic-rich samples. However, this sample was collected immediately below a shell bed and thus may not be representative of the organic-rich facies per se; its species richness is low (7) but individuals are evenly distributed among species (PIE of 0.8). Samples from thin cherts & porcelanites (facies 2) show a mixed faunal association intermediate to the two end-member facies 1 and 3 (Fig. 2.6). Notice that some samples from the cherts and porcelanites record a low species richness and evenness and high dominance of the bivalve *Mesosaccella* (samples 5, 7, 10) that is more similar to facies 1, whereas samples having higher species richnessess and evennesses and very low abundances of *Mesosaccella* (samples 9, 14) cluster more closely to samples from facies 3. Two samples from thin porcelanites and cherts (samples 6 and 11), from facies 2, contain exceptionally high abundances of gastropods and do not cluster with any of the above facies.

The main results of the study are presented in figures 2.3, 2.4, 2.5. The *x*-axes of these plots represent the ranking of species in decreasing order of abundance. The *y*-axes represent the cumulative abundance (normalized to percent-abundance) of each species within each sample, such that, when all species of a sample are plotted, the abundance reaches 100%. YF A-samples represent samples from the paleolow location Nahal Ashosh, samples YF O are from the paleointermediate Nahal Omer locality, and samples YF M are from the paleohigh Har Massa section.

Some samples were not included in the plots due to lack of macrofauna. The reasons for the lack of fauna could be: (a) the environment did not support fauna due to lack of oxygen (this might explain some faunally barren organic-rich carbonates); (b) diagenesis was particularly intense and obliterated faunal remains (this probably explains barren carbonate layers and concretions, and some thin cherts and porcelanites, where only unidentifiable ghosts of shells were present), or (c) exposure of the layers in the outcrop was inadequate for macrofaunal analysis (some lithified phosphorite layers and densely-packed shell beds). In total, benthic macrofauna counts were conducted for four organic-rich samples, five thin-chert and five thin-porcelanite beds, and seven shell beds (five densely-packed and two loosely-packed beds).

***Organic-rich carbonate facies-1:* area with strongest effects of upwelling**

Most organic-rich carbonate layers did not contain any observable macrofaunal remains. However, those organic-rich carbonate samples that did contain macrobenthic body fossils had a significantly low number of species for each sample ranging from 5 to 7 (median of 6, mean of 6 $\pm$ 0.81 standard deviation), with the most abundant taxon (*Mesosaccella* species) comprising 35 to 65% of individuals (Fig. 2.3) regardless of the location from which the samples were collected. Evenness values for fossiliferous samples from facies 1 range from intermediate to high (0.54-0.58, median of 0.56 and a mean of 0.56 $\pm$ 0.02).

Fossils are usually partially or completely silicified, rarely carbonate, and sometimes fragile. The percentage of shells preserved with articulated valves is the highest observed in any facies, with a maximum of 74% of shells articulated in one sample (median of 33%, mean of 42% $\pm$ 21%). Shells can be fragmented but no abrasion or rounding was observed. Shells are sparsely distributed within beds and are either flat-lying or at times preserved in life position. Benthic foraminifera are very abundant in facies 1 with one or two buliminid species dominating the assemblage, mainly *Praebulimina* spp.

The organic-rich facies-1 contains and is dominated by the highest observed proportion of infaunal (deep-burrowing) or deposit-feeding bivalve individuals observed in the Mishash (77% and 82%, respectively of all molluscan individuals, Fig. 2.7 and 2.8), with only 15.5% suspension feeders (e.g., corbulid spp. and *Mesocallista andersoni*). ANOVA testing shows significant differences between facies one and three for deep burrowers, $F(2,14) = 4.13$ (P-value = 0.043). Two-sample t test showed a significant decrease between facies 1 and 3 (P-value = 0.0065) and facies 2 and 3 in deep burrowing bivalves (P-value = 0.09) and between facies 1 and 3 for deposit feeding bivalves (P-value = 0.047). Feeding types and lifestyles for identified mollusks are given for the three facies in Appendix 2.2. Gastropods are present in biofacies 1, but only carnivorous ones. No epifaunal species were found except in a single sample immediately below a shellbed (YF O-5A), and thus might represent specimens mixed downward into the

organic-rich carbonate by bioturbation (this is the atypical sample 4 in Figure 2.6). The extremely high numbers of deposit-feeders suggest high loads of organic-matter and associated low oxygen levels in a stressed environment.

Chert & porcelanite facies-2: ***area with fluctuating effects of upwelling***

The thin-bedded and shelly chert and porcelanite layers in the Phosphatic-Carbonate unit constitute a highly variable set of samples that abut facies 1 and overlap with facies 3; they have species richness of 7 to16 (median of 10, mean of 11 $\pm$ 3) and medium evenness values that range between 0.24 to 0.79 (median of 0.7, mean of 0.66$\pm$ 0.19), with the most abundant species in these samples representing 20%-85% of individuals (Fig. 2.4).

Fossils are always silicified, usually dark brown and less commonly tan. Shell articulation reaches a maximum of 20% (median of 12%, mean of 14% $\pm$ 4%). Shells are sparsely to loosely packed within the layers, but usually occur in shell pavements on the top and/or bottom of the layer. Shells are often compressed and in a few instances deformed, suggesting that these pavements have been modified and perhaps generated by diagenesis (diagenetic concentrations sensu Kidwell et al., 1986). Associated foraminifera are mostly benthic (e.g., species of *Praebulimina*, *Nonionella*, *Gyroidinoides*), but a few planktic species are also present.

Assemblages from this facies vary considerably in trophic composition from one bed to another (Appendix 2.3), but range in composition between that of the other two (organic-rich carbonate and shell bed) facies of the system, suggesting that they capture a series of different community types of bottom seafloor conditions in terms of oxygen levels and organic matter content. There is no single dominant feeding type (Fig. 2.7) with an equal abundance of suspension feeding and deposit feeding bivalves (46% and 47%), and presence of both carnivorous and non-carnivorous gastropods within the facies. Thus an oxygenated (closer to "normal" marine) environment with predator-prey interactions is implied for samples of facies 2 that show a relatively high proportion of suspension feeding bivalves and gastropod species. Facies 2 is also characterized by low abundances of epifaunal and epi-to-shallow infaunal species, which together constitute 6% of the assemblage individuals (Fig. 2.8).

Shell Beds facies-3: ***area with reduced effects from upwelling (marginal to center)***

The shell bed samples (Fig. 2.5) are characterized by a higher species richness of 15-22 species (median of 20, mean of 19.14 $\pm$ 2.6) and by evenness values ranging from 0.64 to 0.78 (median of 0.74, mean of 0.72 $\pm$ 0.05), with the most abundant taxon comprising only 20 to 35% of individuals.

Fossils are preserved both as carbonate and as silicified shells (brown chert). Shells are rarely articulated, reaching a maximum of 8% in densely-packed shell beds and maximum of 36% in loosely-packed beds (median of 5%, mean of 10% ± 12%), may be fragmented and some show abraded surfaces. Shells are usually densely packed and form especially well lithified layers that are prominent in outcrop. This lithification made washing and sieving samples for foraminiferal analysis impractical.

The shell beds are composed of a variety of species rather than any single dominant one. These assemblages are comprised dominantly of shallow-burrower suspension-feeding species (74% and 76% of pooled individuals, respectively, Fig 2.7, 2.8), especially *Mesocallista andersoni, "Meretrix"* sp. and various corbulid species, and contains the lowest percent of deposit feeders (21% of pooled individuals, Fig 2.7). Epifaunal suspension feeders (such as *Nanonavis parallelus, Plicatula sp.* and *Pycnodonte vesicularis*) are also present as well as carnivorous and non-carnivorous gastropods. The species assemblage of facies 3 characterizes a more "normal marine" assemblage with predators and prey and, together with a dominance of suspension feeding bivalves, implies a less stressed environment.

Body size did not vary from facies to facies for most species (differences were not significant), but was observed among the more pervasive corbulid species (*Caestocorbula* sp.A), which have smaller maximum sizes and smaller size-range

in the organic-rich facies (range between 5-7 mm, mean 6.2 mm) than they do in the various shell beds, where they range in size from 3 to 18 mm (mean of 8.7). T-test between these two facies shows significant difference (P-value = 0.0001). Body size data refers to whole shells only and thus should be regarded as a minimum size. This trend may correspond to an increase in oxygen stress moving from the more aerated and higher water-energy shell bed facies, to the lower oxygen and lower water-energy organic-rich facies closer to the upwelling center.

Table 2. Characteristics and environmental associations for the three main high-productivity facies inferred by the community structure of the molluscan assemblages.

lithofacies features	Facies 1 - organic-rich carbonate	Facies 2 - thin chert & porcelanite	Facies 3 - shell beds
Richness (number of species per sample of 100 individuals)	0-7	7-16	15-22
Dominance (percent abundance of top taxon)	35-65%	20-85%	20-35%
Evenness index (PIE of Hurlburt 1971) Note: evenness values are <u>not</u> significantly different between the facies	undetermined zero (zero species) to 0.58 (excluding atypical YFO-5A sample with evenness of 0.8)	0.24-0.79	0.64-0.78
Key species (comprising>15% of all individuals in one or more samples)	*Mesosaccella spp., Nucula tenera,* corbulid spp.	*Mesosaccella spp., Nucula tenera,* corbulid spp. venerid spp., *"Lucina" blanckenhorni Nanonavis parallelus. Undiscala vicina, Turritella reyi, Eucyclomphalus* sp.	*Mesosaccella spp.,* corbulid spp., venerid spp., *"Lucina"-blanckenhorni*

	Facies 1 - organic-rich carbonate	Facies 2 - thin chert & porcelanite	Facies 3 - shell beds
Body size of selected species (significant differences between facies 1 and 3)	body size ranges for corbulid specimens – 5-7 mm (mean = 6.2 mm)	mixed sizes, ranging between those observed for facies 1 and 3 (mean = 7.3 mm)	body size ranges for corbulid specimens – 3-18 mm (mean = 8.7 mm)
Feeding mode B=bivalves [values given are % of individuals]	B=16% suspension feeders B=84% deposit feeders and chemosymbionts	B=46% suspension feeders B=54% deposit feeders and chemosymbionts	B=76% suspension feeders B=24% deposit feeders and chemosymbionts
Major Lifestyle (ratio of epifaunal:infaunal bivalve individuals)	0.012	0.1	0.3
Inferred environmental conditions	stressed, oxygen-deficient environment, with high food availability	Range from oxygen-stressed to environments with abundant oxygen	abundant oxygen, stable substrate, episodically high bottom water energy compared to other facies, environmentally condensed assemblage
Inferred bottom oxygen level	quasi-aerobic to dysaerobic	dysaerobic to aerobic	aerobic
Inferred upwelling category	area with strongest effects from upwelling (i.e., center of upwelling)	area with fluctuating effects from upwelling (ranging from center of upwelling – overlapping with facies 1- to adjacent to the center)	area with reduced effects from upwelling (i.e., marginal to the upwelling center)

DISCUSSION

Correlation of benthic community structure to environmental conditions

This study describes and documents, for the first time, composition of macrobenthos in an Upper Cretaceous high-productivity tract. The different facies of the Mishash contain benthic assemblages with different taxonomic compositions, trophic structures, species richnesses and evenness (Table 2.1), and are consistent with independent

ichnologic and sedimentologic evidence of seafloor conditions during the deposition of the Mishash Formation (see Edelman-Furstenberg, Chapter 1). Macrofaunal evidence argues that differences in seafloor oxygen concentration along with variable organic loads played major roles in structuring the fossil assemblages under the Tethys high-productivity system. Following previous studies on oxygen-deficient benthic environments (e.g., Rhoads and Morse, 1971; Savrda et al., 1984), a characterization of the bottom oxygen levels could be drawn from the faunal data.

Facies 1 is characterized by mostly laminated layers (ichnofabric index – ii1-2 of Droser and Bottjer, 1986) and, when present, mostly articulated sparsely-distributed shells. This corresponds to a quasi-aerobic to dysaerobic seafloor (Edelman-Furstenberg, Chapter 1). Low oxygen levels are consistent with the macrofauna evidence for facies 1, which contains a low number of infaunal deposit feeding mollusks (dominantly *Mesosaccella* species).

Facies 2 is characterized by *Planolites* burrows (ii2-4), layers of sparsely to loosely-packed shells with a mixed state of articulation and orientation, and correspond to a dysaerobic seafloor (Edelman-Furstenberg, Chapter 1). The chert and porcelanite beds of facies 2 comprise of a range of trophic levels and seem to represent an intermediate facies that ranges between seafloor conditions of facies 1 and 3.

Facies 3 is characterized by shell beds with a lower contact of *Thalassinoides* burrows (ii3-4), shells are mostly densely-packed, disarticulated and of disturbed orientation and correspond to an aerobic seafloor (Edelman-Furstenberg, Chapter 1). This aerobic environment is also suggested by the shell beds comprised of a variety of species rather than a single dominant one. These assemblages are comprised mainly of infaunal suspension feeders (*Mesocallista andersoni* and *"Meretrix"* species) but epifaunal species are also present. Thus, each facies is characterized by a specific shelly macrofaunal assemblage and community structure, as well as distinctive lithology and also by ichnofabric and taphonomic features.

Thus the fossil record captures the patterns one would expect to see based on modern studies in low-oxygen and high-organic systems outside of upwelling zones and, contrary to stereotypes that upwelling zones are barren of macrobenthos, variations in species richness and evenness are also detected along an increasing distance from the upwelling center, from the organic-rich facies towards the shell beds (Fig. 2.9).

The macrofaunally barren samples of facies 1 signify extreme upwelling conditions, where low oxygen levels were very persistent, resulting in no body fossils and rare trace fossils, whereas the fossiliferous samples of facies 1 represent somewhat less extreme conditions, but still in close proximity to the center of the upwelling cell such that oxygen levels are very low but not a limiting factor. This is implied by the very low species richness and relatively low evenness (high abundance of the dominant species).

The shell bed accumulations suggest the least extreme conditions of upwelling, with oxygen levels that can support a heterogeneous species assemblage with high species richness and relatively high evenness. The macrofaunal data extracted from the thin chert and porcelanite layers are highly variable from sample to sample (Fig. 2.9) and suffer from extensive diagenesis, namely silicification of originally carbonate shells (shells are identifiable only on bedding plane surfaces in the chert layers). However, surviving fossils can still reveal paleoenvironment. The chert/porcelanite samples that resemble the organic-rich samples (i.e., low species richness and evenness) are believed to be from similar facies, while the samples that follow the shell bed pattern with high species richness and evenness are believed to resemble the more oxygenated facies farther away from upwelling center. The silica required to silicify this fauna is assumed to have been contributed by the diatom-rich sediment derived from the large diatom blooms that characterize all known upwelling systems. Diatom remains were in fact detected in thin-sections taken from the Mishash by Moskovitz and others (1983) near the Qazra sub-basin.

The gradient across the facies and inferred oxygen-levels is comparable to that of modern upwelling systems, in which siliceous and organic-rich ooze forming under the centers of most intense upwelling, producing high organic-rain and low oxygen on the seafloor, give way laterally to pelagic carbonates and more normal (but still elevated) conditions toward the open ocean (e.g., the Benguela system of Namibia, SW Africa; Roger and Bremner, 1991). Edelman-Furstenberg (chapter 3) showed that this gradient

of facies in the Benguela system is associated with a distinct gradient in molluscan community structure, i.e. from assemblages of low diversity and evenness to assemblages of high diversity, evenness and variable trophic levels.

Whereas isotopic examination of high-productivity sediments yield information on the early and late stages of the ongoing diagenesis (e.g., Sass and Kolodny, 1972; Vengosh et al., 1987) that is so typical of upwelling regions, the macrofaunal evidence gives information of seafloor conditions regardless of the ongoing diagenesis and thus advances paleoenvironmental and environmental interpretations of seafloor conditions during deposition. Moreover, macrobenthos can give information on the water-energy regime during deposition comparable to information derived from sedimentary grains (see sedimentary interpretation, e.g., Soudry, 1987) due to their post-mortem hydrodynamic behaviour as grains (e.g., Fürsich, 1978; Kidwell and Bosence, 1991; Behrensmeyer et al., 2000), but especially in the case of bioturbated organic-rich carbonate layers and homogenized chert beds. In such homogeneous layers, environmental information like energy levels, oxygen levels and predator/prey interactions may still be reconstructed and interpreted using the macrobenthic “sedimentary grains” they contain. Finally, the advantage of studying macrobenthos alone or in addition to microbenthos, is by gaining a vertical aspect of seafloor conditions. Whereas, overall, the microfossils describe the pore-water condition of the sediment, the macrofauna represent the overlying water conditions.

Paleoecology of southern Tethys benthic fauna

Data concerning molluscan ecology and abundance from the Upper Cretaceous of the southern Tethys upwelling are scarce. Quantitative analysis for the present study largely corroborates the qualitative findings of earlier regional studies, but adds information on taxonomic composition and community structure by facies and increases the regional species list. Picard (1930) and Chavan (1947) gave a systematic description of the Mishash fauna they encountered. Reiss (1988) reported the general association of burrowing and suspension-feeding bivalves, gastropods and *Thalassinoides* in carbonate intercalations within the Misahsh Formation in southern Israel. He interpreted these as representing improved seafloor aeration at times of sealevel rise and decreased productivity (i.e., decreased upwelling) while, at times of restricted circulation and a stronger oxygen minimum with dysaerobic to anaerobic seafloor conditions, macrobenthos were absent. Almogi-Labin et al. (1993) examined core material from two locations in the Mishash and reported common prisms of the bivalve *Inoceramus*, occasional burrow molds, echinoid spines and ophiuroid ossicles and a low-diversity ostracod assemblage (maximum of four species). Thus, evidence of macrobenthic life was found in several locations within the Mishash. In the present study (21 samples), 64 molluscan species were identified for the Phosphate Member of the Mishash Formation of southern Israel, of which 44 were bivalves and 20 were gastropods (total faunal list for the Phosphate Member is given in Appendix 2.3).

The molluscan fauna of correlative sections to the Mishash show an overall similar species presence. Kassab and Mohamed (1996) reported 25 molluscan species for the Upper Campanian-Lower Maastrichtian Duwi Formation of Egypt, which are similar to the Mishash molluscan fauna at the genus level; however, most species are of Lower Maastrichtian distribution. In Jordan, Bandel et al. (1999) studied the silicified fauna of chert layer surfaces of the correlative Campanian Amman and Ruseifa Formations. They described these surfaces as rich in fauna, at times dominated by nuculid and solemyid bivalves and at other times by turritellid gastropods or scaphopods. Some of the chert beds showed a mixture of these. In the chalk, marly chalk, or chalky limestone there were no shells preserved, except large, calcitic and originally thick shells of oysters (Bandel et al., 1999). The abundance of the carnivorous naticids and scaphopods was interpreted by Bandel et al. to represent a well-oxygenated soft-bottom seafloor similar to the paleo-environment attributed to some of the chert beds from the Mishash Formation described in the present study that were based also on epifaunal abundance (e.g. samples YFM-2, YFO-7A and YFO-8). The chert beds that were dominated by a single species in Jordan, specifically nuculids, are similar to the species–poor and low evenness chert beds from the Mishash in the present study that indicate a dysaerobic and stressed paleo-seafloor (e.g., samples YFA-42 and YFA-36A). The epifaunal mytiloids that Bandel et al. found were small shells while the ones from the Mishash of the present study are large but found exclusively in the aerobic facies-3 (shell bed samples). Thus, the

chert samples from the Upper Campanian of Jordan exhibit a variety of paleoenvironments similar to the chert and porcelanite samples from the Upper Cretaceous of Israel and should be interpreted as such. In both cases, the chert layers represent the original carbonate environment that ranged the two extremes of the system (facies 1 and 3 of the present study) and imply differing degrees of proximity to the ancient upwelling center.

Oysters are present but not abundant within the shell beds of the Mishash (in facies 3 of the present study), indicating the harder substratum of these shellbeds. However, closer to the paleoshore in modern Jordan, oysters (families Ostreidae, Gryphaeidae and Palaeolophidae) were very abundant (Aqrabawi, 1993) and formed large colonies (Abed and Sadaqah, 1998; Bandel et al., 1999; Pufahl et al., 2003).

The key to understanding the variable and often contradicting environments exhibited by the silicified fauna of the chert layers in both the Mishash Formation of Israel (present study, facies 2) and the Ruseifa Formation of Jordan (Bandel et al., 1999) is to examine fauna across the full mosaic of upwelling facies. The differing community structures or absence and presence of specific fauna of the fossil assemblages across the upwelling tract is not attributed to diagenetic effects as Bandel et al. (1999) suggest, but rather represent the specific facies that was sampled within the range of seafloor conditions across the upwelling tract. Assemblages of Mishash fauna at the Qazra sub-basin showed a range of (a) micro- and

macrofaunally barren intervals; (b) sparse distribution of a high dominance of single species, usually infaunal, commonly articulated, bivalve shells along with total dominance of buliminid foraminifera; (c) infaunal and epifaunal bivalves and gastropods with varying degrees of shell packing, articulation and species richness and also a mixed assemblage of varying abundances of planktic and benthic foraminifera; and (d) densely-packed, diverse species of both epifaunal and infaunal bivalves as well as gastropods, often showing stacking orientation of the shells indicating high bottom water energy, due to local storms or currents (see also Edelman-Furstenberg, chapter 1). These assemblages correlate to an increasing bottom oxygen gradient and increasing bottom water energy levels, which are associated with proximity to the upwelling center along with increasing upwelling intensity. Thus, macrofaunal evidence indicates that anaerobic, dysaerobic and aerated conditions all prevailed under the southern Tethys of the Upper Campanian (facies 1-3 of present study) within the patchy framework of the upwelling seafloor.

Previous studies indicate that patterns in microfossil richness and taxonomic composition are consistent with the macrofaunal evidence, with diversity tracking oxygen levels, which are in turn mainly controlled by variations in the upwelling intensity. The ecology and distribution of benthic foraminifera species of the Mishash has been studied by Reiss (1962, 1988) and Almogi-Labin et al. (1990; 1993). The most common taxa in the more restricted basins, which were interpreted by them to represent locations closer to the upwelling center, were mainly

assemblages of a few species (mostly buliminids, *Praebulimina* and *Neobulimina* species) adapted to low oxygen levels. Almogi-Labin et al. (1993) described a more diverse foraminiferal assemblage ranging in composition and species richness from a low diversity assemblage of less than 10 species (buliminid dominated) to a diverse assemblage dominated by rotaliids with more than 20 species. The former assemblage was associated by them with an oxygen-deficient environment while the latter with a higher-oxygen, closer to a normal marine environment. In addition, the representative fauna (diatoms) of the upwelling cell are also reported to be of low diversity (and at times with high abundances) in the Mishash Formation and were interpreted by Soudry et al. (1981) and Moshkovitz et al. (1983) to indicate a restricted environment of high-productivity.

SUMMARY

In conclusion, it is striking how abundant and varied the macrobenthos are in these supposed “faunally barren” regions. The range of macrofaunal evidence from very few or none to abundant and diverse macrobenthic assemblages are characteristic of and describe more accurately the patchy and wide-ranging nature of the upwelling environment of the Upper Cretaceous. This range of environments in the ancient upwelling region compares to the mosaic of sub-facies that characterize modern upwelling facies-belts today (e.g., Benguela upwelling system).

The differences shown for the macrobenthic assemblage character and structure within the Mishash Formation high-productivity regime yield ecological implication, and correspond to proximity to the high-productivity center or to periods of intensified upwelling. The variable oxygen levels and organic load changes show how dynamic this setting really was. We see this expressed in the community structure and composition which ranges between two extremes: The **quasi-aerobic/dysaerobic, low oxygen** facies 1 is characterized by a smaller range in shell sizes, infaunal deposit feeders and low species richness, while the **aerobic, high oxygen** facies 3 is characterized by greater ranges in shell size, infaunal but also epifaunal suspension feeders and higher richness species.

The above ecological criteria may provide evidence of the original carbonate environment for the thin chert and porcelanite layers of facies 2, which is intermediate to the two above end-member facies. Chert or porcelanite layers containing a relatively even and rich assemblage of species (intermediate to the values of the two end-member facies) were most probably of the "normal" shallow-water carbonate marine environment farther from the upwelling center, whereas layers of chert and porcelanite recording very low species richness and evennesses (comparable or lower to those recorded for facies 1) describe primary depositional environments closer to the upwelling center.

CHAPTER 3

TAPHONOMY AND ECOLOGY OF MOLLUSCAN SKELETAL REMAINS ALONG AN UPWELLING TRACT: BENGUELA SYSTEM, SW AFRICA

INTRODUCTION

The Benguela system is one of the world's four major eastern boundary current systems. Off the coast of southwest Africa an intensive wind-induced coastal upwelling persists. In response to nutrient enrichment from deeper waters, the surface waters hold high abundances of diatoms (Schuette and Schrader, 1981) that, after death, settle to the seafloor, generating one of the most organic-rich sediments in today's oceans, up to 24.6% C_{org} by weight (Bremner, 1978; Bremner, 1983; Shannon, 1985; Rogers and Bremner, 1991). The continental shelf off Namibia (southwest Africa) is also one of the deepest and widest shelves in the word (Bremner, 1981) and is characterized by sediments rich in silica, organic matter and phosphate. The Benguela upwelling system has been the subject of a great deal of investigation regarding its physical oceanography (e.g., Shannon, 1985), chemical oceanography (e.g., Chapmen and Shannon, 1985) and geochemistry (e.g., Calvert and Price, 1983). A detailed review of the marine geological aspects of the underlying sediments was given by Rogers and Bremner (1991). They reported “molluscan sand and gravel” as a significant component of carbonate oozes on the Walvis middle shelf (up to 50% weight; Bremner 1983; Rogers and Bremner, 1991), especially in some samples shoreward of the 200 meter isobath. At least 52 mollusk species were recognized, though they reportedly

rarely comprised an important component of the shelf sediments (Bremner 1983; Rogers and Bremner, 1991). Various biogenic components of these upwelling deposits have been studied, amongst them planktic foraminifera (Rogers and Bremner, 1991 and references within; Giraudeau, 1993; Little et al., 1997) benthic foraminifera (Rogers and Bremner, 1991 and references within; Bruchert et al., 2000), ostracods (Dingle et al., 1989; Dingle, 1995) and general biodiversity patterns (Sakko, 1998). However, many of these studies have been based on only a few or single localities, and thus, many questions regarding the environmental deposition of the upwelling seafloor remain unanswered, especially variations across the full breadth of the upwelling facies belt including the continental shelf itself.

In particular, the macrofaunal invertebrate death assemblages of this and other major upwelling areas have never been examined in detail. The low-oxygen conditions that characterize these systems bring the assumption that they hold very low benthic invertebrate abundances and diversity. However, ecological studies in other regions of low oxygen and/or high organic-matter show that these kinds of settings are not devoid of macrofauna, but rather that the macrobenthic communities are highly variable. Distinct environmental gradients in the structure of macrobenthic communities (e.g., species richness, abundance, taxonomic composition, burrow diameter size) can typically be found across such areas (e.g., Rhoads and Morse, 1971; Savrda et al., 1984; Niermann et al., 1990; Arntz et al.,

1991; Stachowitsch, 1991; Tyson and Pearson, 1991; Clarke and Warwick, 1994; Levin et al., 2000). This environmental pattern, ranging from severely impacted to completely unaffected benthic communities, can be expected to be expresses spatially across seafloors experiencing different degrees of upwelling and high productivity.

In addition to the ecological information that can be inferred from the morphology and taxonomic composition of macrobenthic death assemblages, the state of preservation of the skeletal remains provides additional paleoenvironmental information owing to their post-mortem chemical reactivity and distinctive hydrodynamic behaviors as sedimentary grains (Fürsich, 1978; Brett and Baird, 1986; Kidwell and Bosence, 1991). Moreover, quantitative tests of "live-dead agreement" in modern environments indicate that molluscan skeletal death assemblages capture the composition and community structure of the local living community to a high degree (Aller, 1995; Kidwell, 2001; 2002a; 2002b), matching or even exceeding the quality of information acquired from any single biological census (Kidwell, 2003), due to the summing of seasonal and annual variations in time-averaged death assemblages (cf., Peterson 1977). In this way, ecological characterizations based on macrobenthic death assemblages can be considered as a more complete "modern" picture than information based on live censuses alone, and are particularly appropriate for comparisons with possible ancient analogs (where fossil assemblages are probably also time-averaged).

This study is a first attempt to investigate the taphonomic and paleoecological significance of macrobenthic invertebrate death assemblages accumulated under upwelling conditions. Specifically, it explores macrobenthic evidence for bottom-water conditions across the Benguela upwelling tract off the Namibian coast, SW Africa, and the role of bottom oxygen levels and/or organic matter concentrations in shaping the benthic system. Contrary to stereotypes, benthic community structure is highly variable across the high-productivity tract, and skeletal material in each of the different sub-environments carries a distinctive taphonomic signature.

Molluscan material sampled by previous researchers on the modern Namibian shelf during sedimentologic and geochemical surveys of this classic upwelling area (Birch, 1975; Rogers, 1977; Bremner, 1978) was analyzed in a taphonomic and ecological perspective, providing a point of comparison for a parallel study of an ancient, Cretaceous, upwelling system (see Chapter 2 for Cretaceous data). Modern Namibian sediments were re-examined in order to correlate composition and condition of benthic death assemblages with seafloor conditions, focusing on bottom oxygen levels, food availability and other environmental gradients. This is the area of Brongersma-Sanders' (1957) classic work on the role of upwelling in mass mortalities in the sea, making it a particularly interesting shelf for ecological and taphonomic evaluation of shelled benthos. In particular, how do the shelly

macroinvertebrate assemblages vary as a function of sediment composition; i.e., can we detect faunal differences between samples from siliceous ooze, organic-rich carbonate ooze, and phosphatic sands? How are differences in assemblage composition and post-mortem condition related, if at all, to bottom oxygen levels, photic-zone productivity or bottom water energy? To answer these questions, aspects of community-level ecological structure (diversity measurements, life-habit types, etc) were characterized in addition to taxonomic composition. The state of shell preservation was also examined, especially bioerosion, encrustation, other surface degradation, disarticulation, and fragmentation.

OCEANOGRAPHIC SETTINGS

Within the Atlantic continental shelf of Namibia, the Walvis Shelf is relatively wide (~140 km to the shelf-break), with both an inner and an outer shelf break at ~200 and ~400 m water depth, respectively (Shannon, 1985; Longhurst, 1998). The Walvis shelf is part of a passive margin, contrasting with the other well-studied modern upwelling areas of Peru, Baja California, and the southern California borderlands.

The modern Walvis shelf comprises a classic suite of high-productivity lithotypes (Rogers and Bremner, 1991). The inner shelf is a mosaic of diatomaceous ooze and organic-rich muds, and the remainder of the shelf and upper slope are dominated by foraminiferal ooze and patches of phosphorite that contain >20% phosphorite

grains by weight (figure 3.1). However, phosphorite is a variable but subsidiary component (usually <20 %) of all lithologies. Phosphorite-rich patches on the inner shelf are thought to be relict deposits from previous sea level lowstands (Bremner, 1978; 1983). However, the landward flank of the inner belt of diatomaceous ooze is one of the few sites in the world where concretionary phosphorites are presently forming (Bremner, 1980; Baturin, 1982; Rogers and Bremner, 1991).

The Walvis Shelf has experienced upwelling-related high productivity for the past 10 million years, with upwelling cells shifting in position and intensity through successive ten- and hundred-thousand year fluctuations in sea level (e.g., Shannon, 1985; Diester-Haass et al., 1992). The strongest upwelling occurs during austral winter, between April and November (Shannon, 1985). Strong southerly prevailing winds result in recurring Ekman transport and cool, nutrient-rich waters from medium depths of ~300 m (but from 150-200 m depth to the north, at 19° -24° S; Boyd (1987) cited in Boyer et al., 2000) come up to the surface. This establishes conditions for a highly productive ecosystem and results in an intense production of diatoms (Schuette and Schrader, 1981). These surface waters flow equatorward as far as 18° S and then deflect westwards near the Angola current (Fig. 3.2). A subsurface countercurrent flows poleward and is identified by its low oxygen concentration (Shannon and Nelson, 1996). Though the main upwelling cell is situated off Lüderitz (27° S), six cells are recognized along the western coast of Namibia and South Africa comprising the Benguela system. The northern boundary

of the Benguela system is the warm, saline Angola current, while to the south, at ~34° S, the warm Agulhas current predominates (Shannon, 1985; Shannon and Nelson, 1996).

The Benguela system can be divided to a northern and southern section just north of Lüderitz, where a pronounced (partial) divergence of the current occurs (Shannon, 1985; Shannon and Nelson, 1996). The northern Benguela coastline is bounded to the east by the arid Namib Desert, with the Kunene River to the north as its only constant supply of fresh water (e.g. Boyer et al., 2000). The width of upwelling ranges on average between 150-200 km from the coast and its intensity increases along narrow parts of the shelf and decreases along wider parts (Longhurst, 1998; Boyer et al., 2000 and references within). The northern Benguela is characterized by persistent, though less intense, upwelling as compared to the southern Benguela (e.g. Longhurst, 1998). Productivity is greatest in the north (Bremner, 1983), with typically lower seafloor oxygen levels (Shannon and Nelson, 1996; as low as <<0.5 ml/l).

MATERIAL AND METHODS

Box- and gravity-coring of the Walvis shelf in 1972-74 by G.F. Birch, J. Rogers and J.M. Bremner, while on the R.V. THOMAS B. DAVIE, revealed significant quantities of molluscan shell across the continental shelf and upper slope (Rogers and Bremner, 1991). The samples were taken approximately during the strongest

upwelling season, between mid-December and mid-March. Their sampling grid of 10 nautical miles extended from the shore at ~20 m to 2000 m water depth. The area investigated in the present study focused on samples from the northern half of the Benguela system (25°S-17°S, corresponding to Michael Bremner's Ph.D. field area, 1978), which holds the highest concentrations of organic matter within the Benguela system, as well as some of the lowest bottom-oxygen concentrations. The northern Benguela is not influenced by the large terrigenous input of the Orange River to the south. The samples appear to have been taken both from actively aggrading Holocene biogenic sediments and from older, possibly reworked transgressive lags (as encountered by Bremner, 1978; 1983). On average the samples are thought to represent only the past ~5000 or less years (Bremner, 1983).

Grab samples from the northern area were sub-sampled for the present study in two ways for taphonomic and ecologic analysis of molluscan death assemblages. (1) A random subset of samples (total 16) were taken from each end-member sediment type present on the shelf, based on lithologic information from the lithofacies maps of Bremner (1978) and Rogers and Bremner (1991). The end-member samples were taken from sediments containing maximum weight-percentages of opal, organic matter, $CaCO_3$ and phosphate that were 50-88%, 19-24%, >75% and >20%, respectively. The samples containing >7% weight organic-matter correspond to the opal-rich areas (as noted by Bremner, 1983), which are geographically parallel and adjacent to each other and aligned parallel to shore

(Fig. 3.1). (2) Ten samples were examined from an onshore-offshore transect located at approximately 25°S. This transect extended from shallow-offshore (38 meters) to slope depths (1500 meters) and was positioned to intersect with as many sediment types as possible. However, no single transect position would capture all the different upwelling lithofacies and thus, this series of samples is less inclusive than initially expected. The physical description for all twenty six samples is given in Table 3.1.

A random subset of fifteen samples was analyzed containing approximately three samples for each sediment-type, two of the samples from the opal-rich ooze were macrofaunally barren (TBD-3831 and TBD-4009-see footnote in table 3.1). Individual samples were weighed, sub-sampled to approximately 100 grams dry weight, and gently wet sieved through both a >1 mm and >2 mm sieve. The fractions were oven dried at 50°C. The >2 mm fraction was picked and counted for shelly macrofaunal remains. The >1<2 mm fraction was further surveyed for species not found in the coarser fraction; however, no additional species were encountered in this size fraction. This procedure was repeated for additional 100 gram sub-samples until no new species were added and at least 100 specimens were counted. In samples of low volume or low shell abundance, the entire sample was sieved and counted to maximize the number of counted individuals. Samples were also scanned for the presence of benthic foraminifera. The macrofaunal count-data for the analyzed samples are given in Appendix 3.1.

Table 3.1: Physical characters of the samples from northern Benguela.

sample no.	water depth (m)	lat-itude °N	long-itude °E	opal $	organic-matter $	phos-phate (raw) $$	carbonate $	sediment color #	% shelliness ##
TBD-3736	38	24 55.4	14 45.3	< trace	0-3.9	1.7 (raw)	2.2	light-olive grey	barren
TBD-3737	52	24 55.4	14 43.0	trace-4	4-6.9	4.3 (raw)	3.3	light-olive grey	< 5
TBD-3738	61	24 54.8	14 41.5	trace-4	4-6.9	8.9	4.3	light-olive grey	10
TBD-3739	76	24 54.8	14 39.0	5-49	7-11.9	6.6	9.2	light-olive grey	5
TBD-3740	83	24 54.8	14 37.4	5-49	7-11.9	8.6	7.3	olive black	< 5
TBD-4009	86	21 45.3	13 44.8	~56	12-18.9	0-4.9	0-4.9	dark-olive black	barren*
TBD-3955	96	20 07.0	12 45.7	~ 50	7-11.9	0-4.9	5-24.9	dark-olive black	10
TBD-3831	96	20 55.0	13 16.6	50-88	7-11.9	0-4.9	0-4.9	olive black	barren
TBD-3741	112	24 55.0	14 26.4	5-49	19-23.9	10.4	16.8	black	< 5
TBD-4033	129	22 25.5	13 41.6	trace-4	19-23.9	0-4.9	25-49.9	dark-olive black	10
TBD-3441	135	24 16.0	14 10.0	50-88	19-23.9	8.8	16.5	dark-olive	10
TBD-3519	138	22 56.0	13 53.3	~ 50	12-18.9	2.2	18.3	black olive	10
TBD-3800	147	21 35.0	13 14.0	< trace	4-6.9	0-4.9	> 75	olive	60
TBD-4018	154	22 04.6	13 28.6	< trace	0-3.9	0-4.9	> 75	olive	> 70
TBD-3414	154	24 36.0	14 08.0	trace-4	12-18.9	21.6	27.1	dark-olive black	15
TBD-3413	159	24 43.0	13 59.0	trace-4	4-6.9	44.8	22.1	grey black	60
TBD-3743	163	24 54.7	14 05.1	< trace	4-6.9	35	19.5	shells, no matrix	> 70 **
TBD-3770	169	22 15.0	13 27.0	trace-4	4-6.9	0-4.9	> 75	light olive	60
TBD-3710	181	19 22.0	12 07.2	< trace	0-3.9	> 20	25-49.9	dark-olive	> 70
TBD-3744	182	24 54.5	13 53.6	< trace	0-3.9	22.8	53.5	olive black	> 70
TBD-3563	321	24 35.9	13 46.5	< trace	4-6.9	48.6	27.3	dark-olive	> 70
TBD-4015	325	22 05.0	12 56.0	< trace	4-6.9	0-4.9	> 75	dark olive	15

sample no.	water depth (m)	lat-itude °N	long-itude °E	opal $	organic-matter $	phos-phate (raw) $$	carbonate $	sediment color #	% shelliness ##
TBD-3826	382	20 56.0	12 28.0	< trace	0-3.9	0-4.9	> 75	olive black	< 5
TBD-3524	475	22 56.0	12 58.0	< trace	0-3.9	2.6	70.5	dark olive	10
TBD-3746	673	24 55.0	13 31.0	< trace	7-11.9	3.5	60	dark-olive grey	barren
TBD-3748	1500	24 56.0	13 06.0	trace-4	4-6.9	1.1	73.9	light-olive grey	barren

$ Data from Bremner, 1978.
$$ Data given in weight percent, from Rogers and Bremner (1991) and Bremner (1992) unpublished description of the phosphorite deposit for the Geological Survey and FOSKOR managements.
Based on the Munsell color chart.
Shelliness defined as degree of close-packing, which is a visual estimation for percent-volume of shells in a rock or sample (Kidwell and Holland, 1991).
* = in sample TBD-4009 a total of 2 broken specimens were found in 300 g of sieved sediment.
** = sample TBD-3743 was very small (less than 50 g total sample) with species richness of 13 species for the sieved sample.

Sample evenness values were calculated using Hurlbert's evenness index (Probability of Interspecific Encounter PIE; 1971; Table 3.5). In order to find associations between samples and ecological variables, the data were organized into a matrix based on species abundance. Species abundance data were standardized and expressed as percent abundance of each species. A cluster analyses (using Euclidean distance to construct a dissimilarity matrix) was employed to find associations between the samples. The "R" Free Software package (http://www.r-project.org/) was used to conduct the multivariate analysis using M. Foote's Q-mode clustering analysis program.

Samples were examined for relationships between taxonomic composition, taphonomic condition of benthic death assemblages, and present-day seafloor conditions, including bottom oxygen levels using methods that permitted comparison to ancient systems (see Chapter 2). This included a determination of skeletal death assemblage diversity metrics (species richness and evenness), taxonomic composition, body sizes, life-habit types, feeding modes (gastropod feeding modes after Valentine et al., 2002), and state of shell preservation. Namibian taxa were identified to the lowest taxonomic level possible, usually genus or species, using published taxonomic monographs (e.g., Brown and Jarman, 1978; Kilburn and Rippey, 1982; Steyn and Lussi, 1998) and with the help of a sample reference collection assembled by John Pether, a molluscan expert at De Beers Marine (Pty) Limited. However, the focus of this work was on characterizing the community structure rather than taxonomic composition itself. In addition, the skeletal material of the bivalves from eleven of the analyzed samples was described for their state of preservation using table 3.2 below, from Kidwell et al., 2001). Following Kidwell et al. (2001), pristine conditions of these taphonomic variables (i.e., no damage recorded) were scored zero; low damage was scored 1; and high damage was scored 2. Damage to interior and exterior surfaces was scored separately and is tabulated in Appendix 3.2. The opal-rich sample, TBD-3741, was not scored for taphonomic analysis due to low number of specimens. One sample from the offshore, carbonate-rich samples was analyzed for shell damage (TBD

3524) and serves as an example of shell damage for the more "normal marine" conditions, less affected by the upwelling.

Table 3.2: Variables and damage states for bivalve shells in the present study. From Kidwell et al. (2001), as modified by Best and Kidwell (2000).

Variable	0 = No Damage	1 = Low Damage	2 = High Damage	Notes
Encrustation	None	Covering <10% shell area	Covering ≥10% shell area	Total coverage by all taxa
Boring	None	Affecting <10% shell area	Affecting ≥10% shell area	Non-predatory borings only
Fine-Scale Surface Alteration	None	Dull or chalky	Both chalky and pitted, or eroded	For shell interiors, area outside the pallial line only
Edge Modification	None	Chipped	Rounded	Commissural edge only
Fragmentation	Valve still articulated	Whole but disarticulated	Large or small fragment	

RESULTS

The clustering derived from the Euclidean distance reveals three major biological associations that can be linked to different seafloor lithologies and referred to as facies. The three facies are high opal- & organic- rich (facies 1), micritic shallow-water carbonates (147-169 m water depth, facies 2) and sand-sized phosphate (facies 3). The carbonate and phosphate samples, facies 2 and 3, are more similar to each other than to the opal-organic rich association - facies 1 (Fig. 3.3), while the two samples taken from locations with moderate organic-matter and opal concentrations (samples TBD-3519 and TBD-3955, numbers 4 and 5, respectively in figure 3.3) are more similar to the opal-and organic-rich facies 1 than to the other facies. Two offshore carbonate samples from water depth between 325-475 m

(TBD-4015 and TBD-3524, numbers 9 and 10, respectively in figure 3.3) are from locations more marginal to the upwelling center than the other facies and seem to reflect conditions that are closer to normal marine environments. Therefore, data obtained from these samples seem to diverge from the main upwelling pattern examined and obscure the picture.

The observed lithological gradient (Fig. 3.1) corresponds to distance from the upwelling center, with siliceous oozes giving way seaward to pelagic carbonates (Roger and Bremner, 1991). This also corresponds to an oxygen gradient, from areas under the major upwelling cells (areas with low bottom-water oxygen/high nutrient concentrations) to more open ocean settings (areas with higher levels of oxygen and lower nutrient enrichment).

Diversity metrics: Species richness and species evenness

Species richness is the number of species per sample**,** whereas **species evenness** expresses how uniformly individuals are distributed among the different species and thus the extent to which the community is dominated by a small number of species. Both indices usually decrease with increasing environmental stress (amongst others Rosenberg, 1976; Rhoads and Morse, 1971; Gray et al., 1988; Clarke and Warwick, 1994; Levin et al., 2002). Species richness in particular is sample-size dependent (the larger the sample the more species are likely to be found). Thus, in order to compare between samples in the present analysis, species

richness was counted and evenness calculated for a standard number of individuals (100) per sample (see Methods section above). The cumulative diversity curves for the three facies are given in figures 3.4-3.6 and the evenness indices and the numerical results are given in table 3.5.

On the shelf, the organic-rich areas physically overlap with areas of maximum opal content (see Fig 3.1) and both exhibit a very low species richness (Table 3.5, Fig. 3.4), with strong dominance by a single species (the most abundant taxon constitutes 97% to 100% of individuals in each of the opal- and organic rich samples, and 80% to 87% of individuals in samples of moderate levels of organic matter). Moreover, benthic foraminifera were commonly absent in the opal-rich samples (diatomaceous ooze). The shallow-water carbonate facies (Fig. 3.5) shows higher species richness, with the top taxon comprising 50-78% of the total assemblage. The phosphate facies (Fig. 3.6) is characterized by the highest species richness, with the most abundant species comprising only 17-40% of individuals.

Samples from the opal-organic rich facies always contain less than 10% shells (by volume). Samples with moderate levels of opal and organic matter (i.e., TBD 3519 and 3955 samples with 7-11.9% organic matter) do not contain more than 15% shells (Table. 3.1). Pearson's correlation shows that there is a negative relationship between shelliness and organic matter ($r = -0.44$, $t(24) = -2.39$, two-sided P-value = 0.025) such that shelliness decreases as organic matter increases in the sediment,

especially below a threshold organic content of 7% (Fig. 3.7). The most likely limiting factor under the upwelling system will probably be low oxygen concentrations, resulting from the high oxygen demand of the diatomaceous ooze, rather than food, which is unlikely to be limiting in these settings.

Taxonomic composition and rank order of species

The taxonomic composition of the macrobenthic death assemblages in the opal-organic rich facies are those expected for seafloors under upwelling cells. The chemoautotrophic infaunal bivalve *Lucinoma capensis* is essentially the only species occurring in the highly organic rich facies 1 (97-100% of individuals in opal and organic-rich samples), and dominates (80-87% of individuals) the samples of moderate levels of organic matter (e.g., TBD-3955, appendix 3.1). An internal septum (as described by Taylor and Glover, 1997) was detected in well-preserved shells of *Lucinoma*. This septum is part of a chemo-symbiont morphology that permits the bivalve to persist and even thrive under very low oxygen concentrations (Schweimanns and Felbeck, 1985; Cary et al., 1989; Hentschel et al., 1993). T-test statistics shows that the carbonate facies (facies 2) is characterized by the lowest abundance of this indicator taxon (2-4.8%, P-value = 0.0001), while the phosphate facies (facies 3) shows intermediate abundances of 1.2-21.9% (P-value = 0.0001).

As opposed to the essentially monospecific opal-organic rich facies, both the shallow carbonate and the phosphate facies contain a mixture of gastropods and

bivalves, with at least twice as many bivalve species as gastropods (Appendix 3.1). The carnivorous and detritivore genus *Nassarius* is the most abundant gastropod in both facies. The most abundant bivalves are mostly infauna but of mixed feeding types. They include species of *Carditella* (suspension feeder), *Tellina* (mixed feeder) and *Lucinoma* (chemoautotrophic). The phosphate facies includes additional species of the suspension-feeding bivalve genera *Dosinia*, *Mactra*, *Pitar*, *Trapezium* and *Limopsis* and the deposit feeders *Nucula* and *Nuculana*. Epifaunal suspension-feeding bivalves such as species from the Malleidae, Anomiidae and Mytilidae are also present in the carbonate and phosphate facies.

The highly shelly phosphate facies encompasses samples with a range of degrees of environmental condensation; i.e., assemblages that include fauna from different habitats or community states, time-averaged into a single assemblage (cf., Kidwell and Bosence, 1991 and references within). The relative abundance of *Lucinoma* may help identify the extent of environmental condensation. For example, *Lucinoma* is completely absent from the faunal assemblage of the phosphate-rich sample TBD-3743, but is the most abundant species in TBD-3563. The former sample had no muddy matrix, but rather seems to be a gravely shell-lag, whereas the latter is muddier and thus is more likely to reflect the present-day system. Therefore the abundance of this characteristic species of the opal-organic rich facies in a shelly phosphorite sample may be evidence for extent of environmental

condensation. The faunal assemblages that indicate a mixture of environments imply a longer time-averaging than samples comprising fauna from a single habitat.

Feeding types and lifestyles

Pearson and Rosenberg (1978) showed that deposit feeders prefer organically-enriched areas, and therefore a proportional increase in chemosymbionts and deposit-feeders in death assemblages is expected with increasing organic load/oxygen stress. Alternatively, an increase in suspension-feeders points to nutrient particles suspended in the water column rather than in the sediments. In general, infaunal species are capable of tolerating dysaerobic oxygen levels whereas epifauna are associated with higher oxygen levels (Rhoads and Morse, 1971; Tyson and Pearson, 1991) and having lower tolerance to decreased oxygen levels (Rabalais et al., 2002). However, these are only generalizations: some epifaunal and infaunal species have been observed to have identical sensitivity to decreasing oxygen levels (Diaz and Rosenberg, 1995), and in some areas decreased oxygen levels are characterized by a lower relative abundance of deep-burrowing bivalves and an absolute increase in short-lived surface-dwelling forms (Dauer et al., 1992).

In the Namibian shelf system, the opal-organic rich association (facies 1) is dominated entirely by the deep-burrowing chemoautotrophic bivalve *Lucinoma*. This contrasts to the carbonate facies 2, which is dominated by epifaunal-shallowly

burrowing suspension feeders (75% and 85%, respectively) and also to the phosphorite facies 3, which has no dominating life habitat but high abundances of suspension feeding bivalves (61%) and subsidiary epifaunal suspension feeders (Fig. 3.8 and Fig. 3.9). As expected, chemoautotrophic taxa dominate in the organically-enriched areas associated with the main upwelling cells. The increase in epifaunal and epifaunal-shallow burrowers in the latter two facies is associated with their distance from the main upwelling, where seafloor oxygen conditions are less extreme. The increase in epifaunal species (some byssate-attached, e.g. mytilids, malleiids, anomiids) can also indicates a decrease in seafloor soupiness/substrate stabilization. Gastropods are present in the carbonate and phosphate facies, with non-carnivorous species present only in the phosphate facies. The mixed trophic levels of gastropods and the higher abundance of deposit-feeding bivalves in the phosphate facies (Appendix 3.3) may point to relatively increased organic load (detritus matter) as compared to the carbonate facies.

Body size of key species

Body size at death was measured for every specimen in the faunal counts, using maximum body length (apex to aperture for gastropods, anterior to posterior dimension for bivalves). All specimens were measured, but only whole shells were included in the size analysis (with the exception of *Lucinoma* in TBD-3710, were all shells were fragmented). Among macrobenthos in other stressed systems, body

size at death has been observed to decrease as oxygen stress increases (Rhoads and Morse, 1971; Savrda et al., 1984; Diaz and Rosenberg, 1995).

The most pronounced size difference was seen in the individuals of the species *Lucinoma capensis*, which was present in all facies. Body size data refers to whole shells only and thus should be regarded as a minimum size. T-test shows significant body size differences for *Lucinoma* between facies 1 and facies 2 (P-value = 0.0001) and between facies 2 and 3 (P-value = 0.04). However, *Lucinoma* in facies 1 and 3 do not show a significant difference in size.

This body-size trend diverges from the expected trend of size decreasing along a decrease in oxygen levels, specifically body size also **increases** as oxygen level decreases. However, this is probably due to this taxon's chemosymbiotic adaptation to high organic load. Non-chemosymbiotic taxa such as *Dosinia*, *Tellina* and *Carditella* were present only in some of the samples and never in the opal-organic rich facies, and t-test statistics show no significant size differences among facies.

Taphonomic signatures

The state of preservation of bivalve shells was determined with respect to the degree of fragmentation, edge modification (commissural edge only), fine-scale surface alteration and degree of bioerosion; these variables were scored for both internal and external shell surfaces (Appendix 3.2). In general, the degree of damage on shells is expected to correlate with exposure time on the seafloor (e.g.,

Brett and Baird, 1986). However, it is possible for shells to acquire high damage early in their post-mortem history, and in fact the most commonly observed pattern is that “pristine” shells are generally young (recently dead), and poor condition shells are young to old (Meldahl and Flessa, 1990; and see Kidwell, 1997). Based on modern death assemblages from Panama, Best (2000) attributed a high degree of edge modification (rounded commissures) to bioerosion by microboring or grazing rather than physical abrasion (shown by SEM), and fragmentation and edge chipping to predation and scavenging rather than to high hydrodynamic energy (Zuschin et al., 2003). Fragmentation is now considered a poor indicator for high water energy (Davies et al., 1989; Best and Kidwell 2001; Zuschin et al., 2003 and references within), at least in modern systems, in contrast to earlier studies that associate fragmentation, especially of robust skeletons, to water energy rather than predation (e.g., Brett and Baird 1986).

Encrustation was scored for all shells, but was zero in all but one sample, and was thus omitted from the figures. For all other variables, the highest degree of damage (score 2) is presented with 95% binomial confidence intervals following Raup (1991) and using values calculated with S. Holland's "percentage error bars" computer program (University of Georgia, S. Holland's stratigraphy lab software). Overall, external shell surfaces scored the same or higher degrees of damage than internal surfaces in all variables across all samples with the exception of the opal-rich samples, which scored low damage levels for most variables (with 95%

significance, Fig. 3.10, Table 3.3). The trend of increasing overall damage from opal-organic rich facies to the phosphate facies corresponds to distance from the upwelling center and is presumably related to a decrease in organic load and increase in bottom oxygen concentrations. Samples with moderate opal and organic matter fit within this trend, showing a significantly higher degree of damage than assemblages from the opal-organic rich facies (except for fragmentation, which is the same), but lower damage than the phosphate facies. The offshore, deeper carbonate samples capture the taphonomic signature of a more normal-marine environment and less resemble that of an exceptionally productive one.

Table 3.3. Upper and lower confidence limits are given for the highest damage score (score 2) for the taphonomic variables in each of the different lithofacies. P = phosphate-rich samples, C = carbonate-rich samples, mO = samples with moderate levels of organic matter, O = opal- and organic rich, dC = deep carbonate-rich samples. EX = refers to external shell damage, and IN = internal shell damage.

lithofacies	score 2	lower error	upper error	**lithofacies**	score 2	lower error	upper error
P-fragmentation	51.3	45.4	57.2	C- fragmentation	14.5	11.4	17.7
P-edge modification	57.8	50.4	65.1	C-edge modification	22.5	18.5	26.6
P-EX-fine alteration	59.9	54.1	65.6	C-EX-fine alteration	11.9	9.1	14.9
P-IN-fine alteration	32.9	26.0	40.0	C-IN-fine alteration	7.1	4.7	9.9
P-EX-boring	41.9	36.1	47.7	C-EX-boring	15.7	12.5	19.0
P-IN-boring	34.7	27.7	41.9	C-IN-boring	8.8	6.1	11.6
mO- fragmentation	18.5	8.7	29.5	O- fragmentation	9.1	0.3	20.0
mO-edge modification	6.8	0.1	15.1	O-edge modification	0.0	0.0	0.0
mO-EX-fine alteration	5.6	0.1	12.5	O-EX-fine alteration	0.0	0.0	0.0
mO-IN-fine alteration	2.3	0.0	7.7	O-IN-fine alteration	0.0	0.0	0.0
mO-EX-boring	7.4	1.2	15.2	O-EX-boring	0.0	0.0	0.0
mO-IN-boring	2.3	0.0	7.7	O-IN-boring	0.0	0.0	0.0
dC-fragmentation	17.4	3.1	34.4				
dC-edge modification	0.0	0.0	0.0				
dC-EX-fine alteration	8.7	0.0	22.2				

dC-IN-fine alteration	0.0	0.0	0.0
dC-EX-boring	0.0	0.0	0.0
dC-IN-boring	0.0	0.0	0.0

Although levels of damage vary across this environmental gradient, there is an overall consistent pattern in the rank-order importance of damage types. Fragmentation is usually the highest-scoring damage type, and encrustation clearly the lowest scoring while edge modification, fine-scale surface modification and boring all lie in between.

Shell destruction may result from physical wave energy or bottom currents and may accompany biological processes of shell destruction. Bottom water energy may affect the degree of shell fragmentation and rounding of shell commissure, although SEM has shown that this is not always the case (see Best, 2000 and Zuschin et al., 2003 for general patterns in shell fragmentation). Only the phosphate facies shows a high degree of shell-edge modification (~50% of the shells in the facies are rounded, see figure 3.10). This may be attributed to physical abrasion in addition to biological activity, or simply to greater elapsed time of exposure on the seafloor, since these are also the samples where the taxonomic composition and lithology suggest environmental condensation of fauna. Except for the phosphate samples, where rounding is abundant as well as chipping, However, high percentages of edge chipping (see score number 1 in figure 3.10) as opposed to edge rounding in all the sub-environments, excluding phosphate-rich areas which also show rounding, points to predation and other biological attack rather

than physical abrasion as the most important factor (e.g., Zuschin et al., 2003). SEM will probably be required to accurately determine the nature of this damage.

Figure 3.11 contrasts shell damage for epifaunal versus infaunal species in facies 2 and 3 (carbonate and phosphorite facies, respectively. Facies 1, the opal-organic rich facies contains only infaunal *Lucinoma* specimens). The following trends are tentative due to the confinement of small number of shells suitable for this analysis. As observed in the total assemblage, higher damage levels are observed for both the epifaunal and infaunal individuals in the phosphate facies than the carbonate facies (confidence limits are given in Table 3.4). However, in contrast to expectation, the overall damage profile (with the exception of fragmentation) is actually lower or the same for epifaunal shells than for infaunal shells in both facies, which suggests a more hostile post-mortem environment within the sediment than on the seafloor. Specifically, damage from shell boring (boring polychaetes?) and, in the carbonate facies, fine-scale alteration (primarily from microbial attack) was more severe for infaunal taxa than for epifaunal ones.

Table 3.4. Upper and lower confidence limits are given for the highest damage score (score 2) for epifaunal shells and infaunal shells from the phosphate and carbonate facies (2 and 3) for all variables. P = phosphate-rich samples, C = carbonate-rich samples, EX = refers to external shell damage, and IN = internal shell damage.

P - epifauna	score=2	lower error	upper error	**C - epifauna**	score=2	lower error	upper error
fragmentation	57.1	38.4	75.4	fragmentation	71.4	36	100
EX-fine alteration	64.3	45.9	81.7	EX-fine alteration	0.0	0	0
IN-fine alteration	46.4	27.9	65.1	IN-fine alteration	0.0	0	0
EX- boring	21.4	7	37.4	EX- boring	0.0	0	0
IN-boring	14.3	2.5	28.7	IN-boring	0.0	0	0

P - infauna	score=2	lower error	upper error	**C - infauna**	score=2	lower error	upper error
fragmentation	50.4	41.9	58.9	fragmentation	37.0	24.3	50.2
EX-fine alteration	59.4	51	67.7	EX-fine alteration	16.7	7.3	27.2
IN-fine alteration	40.6	32.3	49	IN-fine alteration	13.0	4.7	22.7
EX- boring	33.1	25.2	41.2	EX- boring	20.4	10.2	31.7
IN-boring	30.1	22.4	38	IN-boring	16.7	7.3	27.2

It was commonly not possible to score epifaunal specimens for edge modification, internal fine alteration and internal shell boring, in broken or fragmented shells and so this variable was excluded from this epi-infaunal comparison. However, this reduced the sample size of scored epifaunal shells in the phosphate and carbonate samples to 28 and 7, respectively. Therefore the trends described for these associations are merely exploratory and do not show any significance differences among the groups. Larger sampling will be needed to test for robustness of these trends.

Contrary to taphonomic studies from other marine environments (e.g., Meldahl and Flessa, 1990; Allmon et al., 1995; Best and Kidwell, 2000; Kidwell et al., 2001; Lescinsky et al., 2002), biological encrustation in the Benguela upwelling system is extremely rare, being limited to only one internal and one external occurrence in a single sample (phosphate-rich TBD–3413). The absence of encrustation and the low to moderate boring of shells (from absence of boring in the opal-organic rich facies to 40% boring in the phosphorite facies), follows the

general pattern of low taphonomic damage in molluscan death assemblages from the main upwelling area, which is presumably related to limited macrofaunal activity in shaping the post-mortem signature of these settings. Nevertheless, it seems that the major force damaging the shells is indeed biological, including microbial attack to generate fine-scale alteration, with bottom-water energy only secondary. In summary, it seems that with increasing distance from the upwelling cells there is an increase in both predators and micro-boring animal abundance, which fosters post-mortem shell destruction.

Table 3.5: Characteristics and environmental associations for the three main upwelling facies inferred by the community structure of the molluscan death assemblages.

facies **features**	**Facies 1 -** Opal-Organic rich	**Facies 2 -** (shallow-water) Carbonate	**Facies 3 -** Phosphate	Offshore carbonate-rich samples
number of samples	5	3	3	2
Richness (number of species per sample of 100 individuals)	range = 0-3 median = 3 mean = 3.4 Sd = 2.5	range = 13-21 median = 16 mean = 17 Sd = 3.6	range = 20-27 median = 27 mean = 24.67 Sd = 4.0	range = 12-13 median = 12.5 mean = 12.5 Sd = 0.71
Dominance (percent abundance top taxon)	97.1-100%	49.7-77.5%	21.9-38.3%	20-26.5%
Evenness index (PIE of Hurlburt, 1971). Note - no significant difference between facies 1, 2, 3	undetermined zero (zero species) to 0.32	range=0.27-0.52 median = 0.52 mean = 0.43 Sd = 0.14	range=0.55-0.67 median = 0.64 mean = 0.62 Sd = 0.06	range=0.75-0.79 median = 0.77 mean = 0.77 Sd = 0.03
Key species (comprising>15% of all individuals in one or more samples)	*Lucinoma capensis*	*Carditella cf. capensis* *Carditella nimilis*	*Dosinia lupinus,* *Carditella nimilis,* *Lucinoma capensis,* *Tellina sp.* *[Trapezium sp.]*	Lutrarianae Mactridae *Tellina sp.* *Parvicardium sp.*
Minimum body size of key species (measured in mm)	*Lucinoma capensis* mean size=18.5	*Lucinoma capensis* mean size=7.7	*Lucinoma capensis* mean size=18.7	*Lucinoma capensis* mean size=7.0
Feeding mode (% bivalves for pooled individuals)	100% Chemo-symbionts	85% suspension feeders	61% suspension feeders	72% suspension feeders

facies features	**Facies 1 -** Opal-Organic rich	**Facies 2 -** (shallow-water) Carbonate	**Facies 3 -** Phosphate	Offshore carbonate-rich samples
Major Lifestyle (ratio of epifaunal species:infaunal species)	0 (Deep burrowers only)	0.56	0.91	0.43
Taphonomic signature [% score 0 = no damage] OI = overall score F = fragmentation EM = edge modification FA = fine-scale alteration of surface B = boring E = encrustation	OI=very low damage F=46 EM=91 External FA=88 Internal FA=79 External B=100 Internal B=94 External E=0 Internal E=0	OI= oderate damage F=3 EM=42 External FA=32 Internal FA=52 External B=67 Internal B=75 External E=0 Internal E=0	OI=high damage F=1 EM=4 External FA=3 Internal FA=12 External B=32 Internal B=33 External E=0.4 Internal E=0.6	OI=low damage F = 4 EM = 29 External FA = 78 Internal FA = 88 External B = 96 Internal B = 100 External E=0 Internal E=0
Environmental significance	stressed, oxygen-deficient environment, "soupy" sediment	abundant oxygen, moderately stabilized substrate, shell-rich due to local shell production.	abundant oxygen, stabilized substrate, increased bottom water energy, shell-rich due to low sedimentation rate, environmentally mixed assemblage	abundant oxygen, moderately "soupy" substrate, shell-richness due to local shell production.
Time averaging	generally a census assemblage	within-habitat time-averaged assemblage	within-habitat time-averaged to environmentally condensed assemblage	within-habitat time-averaged assemblage
Upwelling category	center of upwelling	marginal to the upwelling center	marginal to the upwelling center	"normal" marine environment (farther offshore than other facies yet adjacent to the upwelling system)

DISCUSSION

In modern ecological studies of stressed environments, community measurements are based on communities composed almost solely of polychaetes (see different

examples in Clarke and Warwick, 1994). These taxa are soft-bodied and are rarely preserved in the fossil record. Molluscs (bivalves and gastropods), on the other hand, have a high potential of preservation in the fossil record. This study has tried to describe and categorize the preservable, and thus predominantly molluscan, component of the macrofauna death assemblages of sub-environments within the Benguela upwelling system. This is especially important for assembling actualistic data that can later serve for identifying similar settings in the geological record.

Correlation of benthic community structure to environmental conditions

The center of the Namibian upwelling cells is reflected on seafloors by opaline-diatomaceous ooze and a high content of organic matter (facies 1). The margins of the upwelling cells correspond to seafloors with decreased organic matter and higher concentrations of carbonate and phosphate (facies 2 and 3). This trend is accompanied by an increase in species richness and general abundance of molluscan skeletal debris. In fact, each sub-environment within the mosaic of the upwelling system can be defined by a characteristic molluscan death-assemblage with distinct community structure and taphonomic profile (summarized in Table 3.5). Differences in seafloor oxygen concentration along with variable food availability played major roles in structuring the death assemblages under the Benguela system.

Similar to many upwelling areas both present and past (e.g., Parrish, 1998; Rogers and Bremner, 1991), the Benguela upwelling system is characterized by two facies belts aligned parallel to shore. The opal-rich and organic-rich areas overlap to form the main facies-belt, whereas immediately offshore of this belt is the marginal facies-belt comprised of interfingering carbonate-rich and phosphate-rich sediments (facies 2 and 3, respectively), together producing a mosaic of Opal-Carbonate-Phosphate facies diagnostic of upwelling as shown in figure 3.12. A similar pattern is observed from an upper Cretaceous upwelling-seafloor in Israel (see chapter 1). Farther offshore, and marginal to the system as a whole, sediments rich in carbonate dominate the outer shelf and upper slope, and represent seafloor conditions closer to normal-marine settings.

This spatial patchiness of carbonate mud and phosphate facies within a belt parallel to shore and offshore to siliceous, diatomaceous oozes can be explained by a combination of the following factors:

(a) Based on other studies, wind intensity and topographic layout of the coastline are major components that affect coastal upwelling (e.g., Shannon, 1985; Longhurst, 1998). Variability in the frequency and intensity of upwelling pulses determines nutrient replenishment to the photic zone, and is thus one of the main factors controlling the consequent ecological succession unique to upwelling regions (e.g., diatoms studied by Schuette and Schrader, 1981; Foraminifera

studied by Verheye, 2000). Spatial and temporal variability in these upwelling pulses should result in a patchy seafloor mosaic both in terms of sediment types and in terms of seafloor ecological conditions (food and oxygen availability), affecting benthic composition.

(b) The mosaic character of sediment types and faunal content is probably also affected by benthic population dynamics, which are shown to be temporally and spatially variable even in relatively stable environments (e.g., Sousa, 2001 and references within). The localized settlement of molluscan larvae or success of "pioneering" species (sensu Rhoads and Boyer, 1982) affect the mosaic of the resultant benthic assemblage. For example, opportunistic tellinid and mactrid bivalves are known to appear in high abundances in pioneering assemblages (Rhoads and Boyer, 1982 and references within) and are also found in high abundances in the phosphate facies and offshore carbonate samples of the Benguela system.

(c) Finally, a temporal dimension should be considered in understanding the patchy spatial distribution of the death assemblages along the upwelling tract (Fig.3.13). Based on their state of preservation, shell concentrations in the phosphate facies appear to be time-averaged to the greatest degree, representing multiple generations of shell accumulation from one or more habitats to successively occupy the sampled area (e.g., within-habitat time-averaging to

environmental condensation sensu Kidwell and Bosence, 1991 and references within). The taphonomic evidence for this is discussed below (section 5.2). However, faunal structure may capture part of this phenomenon as well. The most abundant taxa in the phosphate (facies 3) death assemblages are not limited to but include the most abundant taxa in both the opal-organic rich and shallow carbonate seafloors (facies 1 and 2), and so the total assemblage in the phosphate facies comprises species that range from oxygen-deficient to fully aerobic seafloors. Also, the highest abundance of epifaunal species and individuals are recorded for the phosphate facies; but, infaunal taxa are the most abundant, providing evidence for fluctuations in the stability or firmness of the substrate. This range of oxygen levels and life styles suggests a spectrum of environmental conditions that are captured over time and condensed into one death assemblage. Thus, the high species richness and >70% shelliness of the samples in the phosphate facies as contrasted with carbonate patches within the same belt is probably due to a lower rate of sedimentation in the phosphate patches rather than higher rates of shell production per se (see later discussion in section 5.3).

The relative abundance and size distribution of the key upwelling species, namely the chemoautotroph bivalve *Lucinoma capensis*, can be used to infer the nature of the initial community in the phosphate facies, and specifically, the proximity of the original assemblage to the upwelling center prior to post-mortem processes (Fig.3.12). *Lucinoma capensis* declines significantly in relative abundance from the

center of cells (opal-organic rich facies, 97-100% *Lucinoma*) outward to the seaward margin of the cells (i.e., the belt of interfingering carbonate and phosphate facies, as low as 1% *Lucinoma*). The abundance of *Lucinoma* rises back to 12% farther seaward from the upwelling center in the offshore carbonate-rich samples. Within the phosphate facies, a wide range of *Lucinoma* abundances are recorded (1.2-21%), with the implication that assemblages with the higher values were originally closest to the upwelling center. A 3.5-fold decrease in *Lucinoma* shell size across this facies tract, from upwelling center to carbonate facies (with no change farther away towards the deeper carbonate samples), provides further support for this idea. In contrast, essentially no size differences are measured for *Lucinoma* from the center of upwelling towards the phosphate margins implying that the *Lucinoma* shells of the phosphate facies-3 are from an upwelling-center origin.

Taphonomic gradients in damage and time-averaging

Discrete taphofacies could be recognized across the upwelling region (Fig. 3.14). Facies 1 (opal-organic rich) has a very low damage profile with high frequency of shell articulation and rare edge modification (see figure 3.10 and table 3.2), indicating the rarity to absence of predators, grazers and significant bioturbators. Facies 2 (carbonate-rich) is characterized by an intermediate taphonomic profile and thus moderate abundances of predators and boring organisms, while facies 3 (phosphate-rich) is characterized by the highest damage profile, having relatively

elevated numbers of rounded, fragmented and bored shells as well as very little associated sedimentary matrix. This latter set of features implies an even greater abundance of grazers, predators and boring organisms and possibly an increase in water energy (in the form of local currents that winnowed the finer sediment away in some of the samples or during marine transgression if these deposits are in part relictual – see later discussion). Alternatively, the higher frequency of damage might instead indicate taphonomic conditions similar to the carbonate facies but with more prolonged time-averaging, and thus an older average or maximum age of shells in the assemblage with greater time to accrue damage on surviving shells. The chipped and more degraded state of shell preservation in the phosphate facies might also result from the larger number of gastropods (i.e., predatory gastropods) found there than in the opal-organic facies, i.e. at the center of the zone of upwelling cells, where gastropods were entirely absent.

In general, the high levels of organic matter generated by upwelling regions can also, via **aerobic** microbial decomposition on or near the seafloor, contribute to high CO_2 concentrations in the porewaters of the relatively more aerated facies (cell margin facies). Dissolution of $CaCO_3$ is to be expected in these settings, which could then result in some of the relatively high levels of fragmentation (analogous to dissolution-caused fragmentation in microfossils (e.g., Johnson et al., 1977; Almogi-Labin et al., 1986) and, especially, fine-scale alteration of shell surfaces (from dissolution of mineral crystallites and/or microbial maceration of

microstructural organic matrix). Both fragmentation and fine-scale alteration occur at relatively high frequencies in the phosphate and carbonate facies. These conditions contrast with the more persistently anaerobic conditions of organic decomposition that would characterize the cell centers, where dominantly alkaline porewater conditions would arise, fostering shell preservation rather than shell destruction.

Finally, the samples from the offshore carbonates that represent normal shelf/slope marine seafloor are characterized by an overall low damage profile, despite abundant predatory gastropods. The high degree of chipping (~70%, fig. 3.10) of shells here as opposed to the opal-organic rich and moderate opal-organic rich seafloors, which also exhibit an overall low damage profile, further corroborate an aerobic and bioturbated seafloor for these offshore carbonates. Thus the overall low damage profile of the offshore carbonates probably reflects a relatively less time averaged assemblage, permitting little damage to accrue in the assemblage.

The various death assemblages from this upwelling system reflect within-habitat time-averaging (opal-organic rich facies, shallow-water carbonate facies, plus normal marine offshore carbonate samples). The shallow-water carbonate and phosphate facies are more complex, including assemblages that range from slightly time-averaged to considerable time-averaging and environmental condensation,

respectively, as indicated by the decrease in mud content and possibly by the increase in epifaunal:infaunal ratio (Fig. 3.14, note that this ratio is between the number of **species** present in each facies). These latter features also suggest a more stable or firm substrate in the phosphate facies, which would also result in greater exposure of shells to processes of post-mortem destruction. Thus, because of its time-averaged nature, the mosaic of facies under the upwelling region today is not a simple snap-shot product of the present-day upwelling regime proper, but should be a good analog of the ultimate facies-mosaic expected along such productivity trends elsewhere in the modern world and in the stratigraphic record.

It appears from this study that, in addition to taphonomic signature, the molluscan epifaunal species-infaunal species ratio may be a proxy for spatial trends in upwelling. However, the stressful seafloor conditions under upwelling areas yield relatively low number of molluscan species with low numbers of individuals, and thus statistical verification is difficult. In the future a larger sample-set might enable pooling of more samples to represent each facies and sufficient power to evaluate this trend more rigorously.

Ecology of the Benguela benthic fauna

Data concerning molluscan ecology and abundance from the Benguela upwelling area are scarce. Quantitative analysis for the present study largely corroborates the qualitative findings of earlier regional studies, but adds taxonomic composition by

facies and increases the regional species list. In the northern Benguela overall, Bremner (1978) reported 52 molluscan species from 84 samples. These species constituted a mixture of infaunal, epifaunal, suspension- and deposit-feeding bivalves and gastropods (e.g., *Dosinia, Lucinoma, Tellina, Limopsis, Ostrea, Nassarius, Turritella,* and *Natica*). In the present study (26 samples), 70 molluscan taxa were identified for the northern Benguela shelf, of which 51 were bivalves and 19 were gastropods.

The diatomaceous oozes of the Benguela are regarded as generally laminated and mollusc-poor (Rogers and Bremner, 1991 and references within). However, this "dead zone" is not completely barren, as evident from the abundant annelids and molluscs in other reports from the area (by Copenhagen, 1951, as cited in Rogers and Bremner, 1991). Moreover, as shown in this study of death assemblages, the diatomaceous ooze can apparently be inhabited by mono-specific assemblages of the chemoautotroph *Lucinoma capensis*. Distribution maps of the bivalves *Lucinoma* and *Dosinia* were given by Bremner (1978) for the same area investigated in the present study, and Bremner notes the similarity between the two species distributions patterns. However, if the whole upwelling tract is considered, as in the present study, *Lucinoma* occurs far more extensively than previously recorded. In fact, *Lucinoma* species are found across the entire upwelling region in the main upwelling cell facies-belt, in the marginal facies-belt and also in the deeper carbonate samples. *Dosinia* on the other hand is confined to the upwelling-

cell-margin facies-belt (carbonate and phosphate facies of this study). Thus, alone, *Dosinia* cannot be considered as useful an upwelling indicator species as *Lucinoma*.

The molluscan fauna of the southern Benguela appears to be quite different. Dredged samples from off Kleinzee, in the southern Benguela region (Fig. 3.2), were investigated by Pether (1993; 1994) who generated a list of 54 molluscan species. This molluscan fauna was sampled from a relictual sediment terrain from the Last Glacial maximum, and does not overlap completely with the species list generated in the present study, nor do the damage profiles of this material (as described by Pether) match the northern Benguela. Pether (1995, unpublished data) also identified 27 molluscan species in two cores off Hottentot Bay, Namibia, and noted that the material does not resemble the kind of shell accumulations seen along today's West-African beaches. Very little has been published regarding the molluscan fauna of Southwest Africa's beaches, notwithstanding the ongoing ecological observations being done by researchers at De Beers Marine and in local student projects. McLachlan (1985) and Donn and Cockcroft (1989) studied sandy beaches along the northern Benguela and report the bivalve *Donax* as the only molluscan taxon found. Both sandy and rocky beaches of the northern Benguela are characterized by lower species diversity as compared with other, more southern beaches of southern Benguela (McLachlan, 1985; Donn and Cockcroft, 1989; Sakko, 1998; Boyer et al., 2000). Overall, macrobenthic species diversity increases

across the northern Benguela shelf with depth (Donn and Cockcroft, 1989) and with substratum stability (McLachlan et al., 1984), as in many soft-sedimentary continental shelves. In general, the invertebrate fauna of those beaches is dominated by suspension feeders, which can exploit the high organic matter levels produced by offshore upwelling (principally diatoms). The infaunal bivalve *Donax serra* dominates the sandy beaches and the mussels *Perna perna, Semimytilus algosus and Mytilus galloprovincialis* the rocky beaches (Boyer et al., 2000).

Previous studies indicate that patterns in microfossil richness and taxonomic composition are consistent with the macrofaunal evidence, with diversity tracking oxygen levels, which are mainly controlled by variations in the upwelling intensity. The ecology and distribution of benthic foraminifera species of the Benguela system has been extensively studied (overview in Rogers and Bremner, 1991, p.41-61). The most common taxa for the northern Benguela are *Bolivina* sp., *Brizalina spathulatus*, *Ammonia becarrii* and *Uvigerina* sp, and these dominate a narrow to shelf-wide band adjacent to and seaward of the diatomaceous ooze (Bremner,1978; 1983). Benthic foraminifera are very abundant on the southern Africa shelf in general and increase in abundance with water depth. Increased upwelling intensity results in decreased diversity (Rogers, 1977; Bremner, 1978; Bruchert et al., 2000), in particular assemblages of a few species (mostly *Bolivina*) adapted to low oxygen levels. Ostracod assemblages exhibit the same pattern of upwelling intensity controlling distribution and composition (Dingle, 1995). In fact, ostracods do not

occur in the center of upwelling cells (Dingle et al., 1996), analogous to facies 1 of the present study.

Comparison to benthic ecology in other upwelling areas

Patterns found in molluscan fauna of the Benguela system are generally similar to those reported in other areas. Schneider and Wefer (1990) investigated molluscan shell layers in cores from the upwelling system off Peru and found that material was insufficient for a statistical analysis, with only 4 species reported, but this is an important attempt to document molluscan distribution under upwelling regimes. Schneider and Wefer (1990) found that shell layers were absent from cores generated under the most intense upwelling (laminated diatomaceous ooze), but were present in cores recording moderate upwelling (diatomaceous calcareous muds, bioturbation). It seems that the optimal environment for macrobenthic fauna in the upwelling region off Peru is at the upper boundary of the oxygen-minimum layer, which is on the outer shelf to upper slope environment and provides sufficient oxygen and food. However, although this trend in shell beds is consistent with the overall bio-facies trend of the Benguela shelf, caution is needed when comparing the two systems. Peruvian mollusks were obtained from 150-450 m water depth, in contrast to the largely <200 m water depths sampled in Namibia for this study. Moreover, Peruvian data were generated using a fine sieve size (300 μm), and thus the data include and are probably dominated numerically by larval and young juvenile individuals, in contrast to the 2mm mesh used for the Namibian

material. Arntz et al (1991) also report an extremely low macrobenthic density in the oxygen minimum zone (OMZ) of Peru (≥110 m water depth) for grab samples sieved in a 1 mm mesh, and 1-2 molluscan species in shallower depths of 40-79 m and 80-110 m, respectively.

Studies in other regions of low oxygen/high organic-matter have examined the correlation between the physical conditions and the structure of the macrobenthic community (for hypoxic-eutrificated environments see Pearson and Rosenberg, 1978; Warwick, 1988; Gray et al., 1990; Stachowitsch, 1991; Diaz and Rosenberg, 1995; for oxygen-minimum-zone regions see Tyson and Pearson, 1991; Levin et al., 2000; 2002). These workers find similar trends to that observed along the Benguela upwelling tract, namely decreasing diversity with increasing organic matter content (or decreasing bottom oxygen availability).

Especially interesting is the comparison with the seasonally upwelling area of the Arabian Sea. Levin and others (2000) examined macrobenthic community structure within and below the oxygen minimum zone (OMZ). The dysaerobic oxygen concentrations are comparable to the oxygen-deficient waters of the Benguela system (general oxygen levels reported in Shannon and Nelson, 1996) but the main difference is the total organic carbon (TOC) in each site. The Benguela exhibits a five-times higher organic matter content in the low oxygen sites compared to the Arabian Sea (19-24% as opposed to 4-5%, respectively). Furthermore, the Arabian

macrofauna investigated was the >300 μm size fraction and thus the species composition and relative abundance information reflects the inclusion of larval and juvenile mollusks rather than exclusively adults as in the Benguela samples. Nonetheless, some interesting similarities are present. Mollusca were practically absent in seafloors under the lowest oxygen levels, but increased to a maximum of 23% of the total macrofaunal assemblage in deeper water samples with >0.13 ml/l oxygen and available food (Levin et al., 2000). At the margins of the OMZ lucinid bivalves were observed (Levin et al., 2000). These similarities between the Benguela upwelling and the Arabian Sea OMZ raises interesting questions regarding the role of oxygen versus food availability in structuring the macrofaunal assemblages. It seems that the similar oxygen levels between the two examples, more so than the abundance of food (which is much higher under perennial upwelling areas, i.e., Benguela), is the major factor controlling the community structure. However future comparisons between shelly molluscan data rather than soft-bodied fauna needs to be done before a confident conclusion can be made.

Deep-sea benthic foraminiferal assemblages have also been shown to be controlled largely by the bottom oxygen and organic matter concentrations (Bernhard and Reimers, 1991; Jorrisen et al., 1995; De Stigter, 1996; Loubere, 1997; Kaiho, 1999). In addition to the Arabian Sea (Levin et al., 2000), other OMZ regions have also shown benthic foraminifera distribution patterns to be reflected by these two parameters (e.g. California continental borderlands -- Bernhard, 1992

and Sen Gupta and Machain-Castillo, 1993; Red Sea -- Edelman-Furstenberg, 2001; Peru margin -- Levin et al., 2002). As in the Benguela, *Bolivina* and *Bulimina* species are commonly the dominant fauna in very low oxygen and high organic matter levels (Bremner, 1978; Rogers and Bremner, 1991 references within; Bruchert et al., 2000).

Taphonomic studies across organic-enrichment gradients

Despite progress in research, a great degree of uncertainty remains for most modern environments on the impact of nutrient levels on rates and degree of damage for molluscan shells. A recent study on molluscan shell encrustation and bioerosion was conducted across eutrophic and mesotrophic reefs in the Java Sea (Lescinsky et al., 2002). The study showed that shells were bioeroded and encrusted to a greater degree in areas of higher productivity (up to 7.8% organic content, Lescinsky et al., 2002) than in low organic environments (2.3% TOC) and also showed greater damage in areas of lower sedimentation rates and harder substrates. This was attributed to the positive correlation between encrusters/borers and primary productivity on the one hand, while burial and soupy substrates prevents recruitment and settlement of encruster-organisms. The authors suggested that encrustation levels and shell bioerosion may be used to indicate paleoproductivity in the fossil record.

In contrast, under the Benguela upwelling system shell bioerosion is negatively correlated to increasing water productivity and encrustation is absent altogether in the highly productive facies (facies 1 of present study). This suggests that in settings with extremely high productivity (up to 24% organic matter in the Benguela system), encrusters and predators are inhibited rather than facilitated (see fig. 3.14), generating an opposite trend in taphonomic damage with respect to nutrients than found for reefs at the opposite end of the productivity spectrum.

Absolute sedimentation rates are not available for the Benguela system, and so it is not possible to test its effect on rates or degrees of post-mortem shell damage: the relatively good condition of shells in facies 1 and 2 is used in part to infer higher rates of sedimentation in these facies than in the phosphate facies 3, where shells are in overall poorer condition (Table 3.5). Shell damage does correlate with seafloor shelliness and firmness, as seen in other studies. Moreover, the phosphate-facies, shown in the present study to be associated with decreased productivity, also records the highest degree of shell damage and the only (although rare) evidence of encrustation across the high productivity region. Thus, under the Benguela system, burial or soupy substrate alone cannot be the reason for low encrustation of shells, as indicated by Lescinsky et al. (2002).

Thus levels of bioerosion and encrustation may be used as a proxy for paleo-productivity, but the relationship depends on the portion of the productivity

spectrum under consideration; damage levels are low at both the low and high extremes, and at a maximum in waters of intermediate productivity. Globally, high productivity in the marine realm is usually attributed to upwelling areas. The annual organic-matter supply rate for the diatomaceous mud belt off Walvis margin, NW Africa, is $2.3*10^6$ m^3 (Bremner, 1983). The stressful seafloor environment under upwelling regimes limits metazoan predators and borers, which in turn result in a distinctive and low profile of taphonomic damage. Moving outward into waters of lower but moderate productivity, oxygen levels increase and predators, bioeroders and encrusters are more abundant, promoting more kinds and greater intensity of shell damage.

The geological-ecological interpretation of the Benguela molluscan assemblages

The mixture of fairly fresh-looking fragile specimens (typical of quiet-water habitats) and robust disarticulated valves (typical of high-energy habitats) and their common association with pelletal phosphorite suggested to Bremner (1983) that surficial sediments from the northern Benguela shelf are an entirely relictual assemblage of shells and authigenic grains that have been mixed during the most recent transgression of the shelf. The phosphorites were inferred to be condensed and reworked by a two-phase evolution, with the phosphorites themselves associated with increased upwelling during a period of sea level rise and environmental condensation, and then later reworked and any organics oxidized

during subsequent marine regression (Compton et al., 1993; 2002). The main evidence for a relictual origin of the shell assemblages cited by Bremner (1978, 1983) were: (1) no living specimens were encountered; (2) shells typically occur in association with relictual phosphorite; and (3) all specimens were filled with ambient sediment.

The present study corroborates that the Benguela shelf record includes some relictual components. However, from a general perspective, the features listed above are somewhat ambiguous. For example, given the sparseness of living specimens that are generally collected in benthic ecologic surveys even in fully aerobic subtidal seafloors (especially at $\geq$ 2 mm mesh sizes), the lack of living specimens in the relatively small-volume sediment grabs might be attributed to insufficient sampling rather than actual absence of an indigenous living benthic community. The association of shells and relictual phosphorites does not necessarily mean they are the same age, as the shell assemblages could be from a later successional stage (colonists of an already inactive phosphorite seafloor). Finally, shells filled with ambient sediment are the norm in most depositional settings and across a range of time-averaging based on the stratigraphic record, and thus are not diagnostic of relictual shell lags (e.g., Fürsich ,1978; Kidwell and Bosence, 1991).

The diverse shelly accumulations examined in the present study are clearly associated with the highest percent of phosphate in the sediment, and their taphonomic and ecologic character suggest that the increased species richness of this phosphorite facies is probably due to low sedimentation rate rather than higher rates of shell production per se. This is consistent with previous descriptions of relictual sediments (Rogers, 1977) and relictual phosphate accumulations (Bremner, 1978; 1983) in the Benguela system. However, the extent of time averaging and condensation of environments within these shell assemblages varies within the phosphate facies, from various degrees of within-habitat time-averaging to environmentally condensed. Differences among samples in sediment type suggest the variable extent to which water energy (e.g., during marine transgression) affected these assemblages. Sample TBD-3743 (phosphate-rich), for example, had no fine material in the sediment and for that matter is the only sample across the tract that lacks the upwelling-indicator bivalve *Lucinoma capensis*. All the other samples across the variety of facies have some degree of fine-grained matrix. Sediments containing no, or little, matrix are most probably environmentally condensed and do not reflect the intensity of upwelling relative to the seafloor as it exists today. On the other hand, both the shallow- and offshore carbonate samples show differing degrees of damage and are time-averaged but probably within-habitat assemblages, and do reflect the present upwelling mosaic of habitats.

Death assemblages examined for the present study do not exhibit the same extent of damage as previously reported from the region by Pether (1993, 1994). Those relictual samples showed encrustation in addition to boring, fragmentation and abrasion and overall a higher degree of damage than do the death assemblages of the present study. Also death assemblages examined for the present study do not exhibit as high a proportion of **relictual species** as have been previously reported in this region. For example, Pether (1994) reported that 14% of bivalve species in his relictual assemblages apparently do not inhabit the western shelf today. This is not the case in the shelly material from the phosphate facies in the present study that record rare relictual species (based on the available macrofaunal data from Recent beaches in McLachlan, 1985; Donn and Cockcroft, 1989; Boyer et al., 2000 and from Kilburn and Rippey, 1982). In addition, the suggestion by Bremner (1983) that the similar distribution patterns of *Lucinoma* and *Dosinia* indicates mixing of the two species during an earlier Pleistocene transgression (the Flandrian transgression) is challenged on the basis of the different and expanded distribution patterns found for *Lucinoma* across the upwelling facies in the present study.

The new ecologic and taphonomic evidence thus supports the existence of a wider range of time averaging in the formation of molluscan sand and gravel samples in the northern Benguela than previously appreciated; these assemblages are not exclusively relictual, but reflect a spectrum of types, from within-habitat time-averaging of communities presently occupying the shelf (specifically in areas

directly under or marginal to active upwelling cells today), to various mixtures of shells from present-day and relictual (locally extinct) benthic communities (in phosphate-rich seafloors, which are offset from active cells). Thus by combining the biological evidence (e.g., presence-absence of indicative fauna, damage state of index-taxa) with the taphonomic signatures or states of shell damage for the different death assemblages across the Benguela upwelling, a proxy for the degree of "relictualness" and an indication for which post-mortem agents controlled the environment is attained. As a result a wider range of environments than proposed by previous workers (e.g., Bremner, 1978, 1983; Rogers, 1977; Pether, 1993, 1994) is to be attributed to these deposits, specifically from within-habitat assemblages to environmentally condensed.

CONCLUSIONS: AN ECOLOGIC AND TAPHONOMIC SEAFLOOR MOSAIC

Gradients observed in macrobenthos across upwelling systems are better regarded as patchy rather than a simple onshore-offshore gradient in environmental conditions. Water depth, substratum grain size, and habitable space are less important in these systems than is proximity to the upwelling centers, which determines organic rain and bottom oxygen levels. Upwelling regions prove to be a more complex system than the oxygen-poor and lifeless seafloors usually imagined. On the northern Benguela shelf, we observe a gradient in macrobenthic death assemblage structure from low species richness and high abundance of deep-

burrowing deposit-feeding or chemosymbiotic bivalves, to significantly higher richness and decreased levels of deep burrowing, deposit feeding and chemosymbiotic bivalves, in accordance with the upwelling facies-gradient from diatomaceous ooze in areas of maximum upwelling intensity outward to the aerated but food-abundant carbonate oozes and spatially coexisting phosphorite concentrations.

Both the taphofacies and ecologic data provide ways to distinguish between facies of low and high shell production along an increasing oxygen gradient, and also between assemblages with moderate and higher species richnesses associated with a temporal aspect of increasing time-averaging.

Previous research on macrobenthos from equivalent environments (i.e., high productivity and low oxygen environments) all focused on the dominating soft-bodied polychaetes and other annelids (e.g., Warwick, 1988; Levin et al., 2000). These characteristic fauna are rarely preserved in the fossil record and thus cannot be used as a representative assemblage for past reconstruction. The skeletal fauna $\geq$1 mm (at least) is practically the only comparable indicator for past records. Given the scarcity of information on macrobenthic ecology and taphonomy from modern high-productivity settings, these death assemblages can represent a "modern" analog and serve as a proxy for ancient upwelling environments.

CHAPTER 4

ANCIENT-MODERN COMPARISON OF MACROBENTHIC COMMUNITY STRUCTURE ON UPWELLING SEAFLOORS

INTRODUCTION

Factors governing the deposition of silica, organic carbon, and phosphate-rich sediments in high-productivity marine settings are complex. Fundamental questions regarding the mechanisms influencing the variations in levels of oxygenation in bottom waters during accumulation of high-productivity deposits remain unclear for both modern-upwelling and ancient examples.

Macrobenthic invertebrates are sensitive recorders of sea floor oxygen levels, water energy and sediment mass properties in modern systems, and can leave a strong fossil record via their biomineralized skeletons (e.g., Rhoads and Boyer, 1982). In addition to the ecological information that can be inferred from their morphology and taxonomy, macrofaunal skeletal remains can also provide paleoenvironmental information owing to their post-mortem chemical reactivity and distinctive hydrodynamic behaviors as sedimentary grains (e.g., Fürsich, 1978; Brett and Baird, 1986; Kidwell and Bosence, 1991). Surprisingly, macrobenthic communities have received scant attention in either modern or ancient upwelling systems, probably because a stereotypic view of upwelling systems as “death zones” leads to an assumption that macrobenthos will be largely absent. However, ecological studies in other regions of low oxygen and/or high organic-matter show

that these kinds of settings are not devoid of macrofauna, but rather that the macrobenthic communities are highly variable and diagnostic (e.g., Rhoads and Morse, 1971; Savrda et al., 1984; Tyson and Pearson, 1991; Levin et al., 2000). Moreover, macrobenthic evidence may permit paleoenvironmental interpretation with fewer of the pitfalls of geochemical analysis in such diagenetically complex settings.

Presented here is the first investigation of the ecological and taphonomic nature of macrobenthic invertebrate assemblages under upwelling conditions, using both modern and ancient settings to identify robust patterns. The Upper Cretaceous (Campanian) Mishash Fm. of Israel provides an excellent ancient example from the southern Tethys, capturing a ~9 my-long record of organic-rich carbonates, cherts, porcelanites and phosphorites within one of the most extensive high-productivity complexes in the stratigraphic record. As a counterpart, the Benguela upwelling tract off SW Africa is one of the major eastern boundary upwelling systems of today's oceans, and is similar in physiography and tectonic setting to the Mishash. Both systems have relatively wide shelves (~140 km for the Benguela versus ~250 km-wide for the Mishash shelf) and are part of a passive margin, contrasting with the narrow-shelved convergent plate boundaries of Peru, Baja California, and the southern California borderlands, which are some of the other well-studied modern upwelling areas. Overall, the northern Benguela and Mishash upwelling systems received negligible amounts of terrigenous sediment, notwithstanding some input

from the Kunene River to the north of the main Benguela upwelling system (e.g., Rogers and Bremner, 1991). In addition to being a perennial system, Benguela shelf sediments contain the highest organic matter contents known in modern upwelling areas (up to 24.6% weight; Bremner, 1978), similar to the ancient Mishash setting (up to 25% weight of total organic carbon; Bein et al., 1990). Seafloor oxygen levels are lowest for the northern Benguela and follow a gradient through the upwelling tract, ranging from O_2 < 0.5 ml/l near the coast to > 1 ml/l < 2 ml/l farther offshore (e.g., Bailey, 1991).

Although aspects of Benguela and Mishash upwelling deposits have been examined by previous workers, many of these studies have been based on only a single or few localities, and thus many questions regarding environmental conditions on the upwelling seafloor remain unanswered, especially variation across the full breadth of the upwelling system and continental shelf. Here, samples of benthic macrobenthos from both fossil and modern death assemblages were used to correlate faunal composition and post-mortem condition of molluscan skeletal remains with seafloor conditions, specifically bottom oxygen levels. This included a determination of species richness and evenness, life-habit types, body sizes and state of shell preservation. All taxa were identified to genus or species level, but because few taxa of genus rank were shared between the modern and the ~75 my-old Mishash Fm., the focus was on characterizing the community structure rather than taxonomic composition alone.

The relations between macrofaunal assemblage variations and seafloor composition are addressed in this study, i.e. can we detect any faunal differences across an upwelling zone? How do these patterns compare with ancient upwelling seafloor patterns? How are differences in faunal assemblage composition and post-mortem shell condition related to bottom oxygen levels? Contrary to stereotypes of barren seafloors, benthic communities are present but highly variable across these high-productivity tracts. These communities are characterized by distinctive community structures and taphonomic signatures. Both modern and ancient systems show consistent trends of increasing species richness and evenness with an increasing distance from the upwelling center, parallel to inferred increasing oxygen levels.

MATERIAL AND METHODS

Quantitative ecological data for benthic bivalves and gastropods were collected from each of the five main lithologies constituting the Upper Campanian Phosphate Member of the Mishash Formation in southern Israel (Fig. 4.1-a): (a) organic-rich carbonate mud; (b) thin-bedded, fossiliferous chert and porcelanite; (c) loosely to densely packed shell beds (skeletal calcirudites), some containing coarse sand-sized phosphorite (all three of these lithologies (a-c) occur in the lower part (i.e., Phosphatic-Carbonate unit) of the Phosphate Member, sensu Soudry et al., 1985); (d) massive, unfossiliferous porcelanite from the middle part of the Member

(Porcelanite unit of the Phosphate Member); and (e) loosely packed shell beds interbedded with these massive porcelanites (sampled specifically for body-size measurements of the chemosymbiotic bivalve *"Lucina" blankenhorni* Chavan).

Special attention was paid to variation in the abundance and maximum body size of lucinid bivalves in death assemblages, because of their diagnostic value. The bivalve *"Lucina"* is widely known to dominate sediments rich in organic matter (Schweimanns and Felbeck, 1985; Cary et al., 1989; Hentschel et al., 1993; Taylor and Glover, 1997). Lucinids are also known to grow to very large sizes under favorable conditions (Schweimanns and Felbeck, 1985).

Samples obtained from the modern southwestern African continental shelf in 1972-74 by G.F. Birch, J. Rogers and J.M. Bremner were re-sampled by the author, using the lithofacies maps of Bremner (1978) and Rogers and Bremner (1991) to ensure inclusion of samples from each end-member sediment type present on the shelf. Maximum weight-percentages of opal, organic matter, $CaCO_3$ and phosphate in samples were 50-88%, 19-24%, >75% and >20%, respectively (Bremner, 1978). All samples containing >7 weight-% organic-matter overlap with the opal-rich areas (as noted by Bremner, 1983), which are arrayed in belts adjacent to each other and parallel to shore (Fig. 4.1-b).

For faunal analysis, a minimum of ~100 specimens were counted from each sample from the Mishash Formation, and 100 gram sub-samples of Benguelan material were counted for macrofaunal remains until no new species were found and at least 100 specimens had been counted. In Benguela samples of small volume or low shell abundance, the entire sample was sieved (at 2 mm mesh) to maximize the number of counted individuals. Raw count data for Mishash and Benguelan samples are given in Appendix 4.1 and 4.2. Samples were also surveyed for the presence of benthic foraminifera.

Taxa were identified to species level. Margalef's index (*d*) was calculated, which provides a measure of species richness that takes sample size into consideration by standardizing the number of species encountered against the total number of individuals (e.g., Dodd and Stanton, 1990). Evenness was calculated using Hurlbert's index PIE (1971), which is relatively insensitive to sample-size effects (e.g., Beisel et al., 2003) and is scaled from 0 (low evenness) to 1. Body-size of key taxa were measured; trophic levels were assigned to each species according to modern family level information. Bioclastic fabric was characterized primarily using bivalve shells that dominated the assemblages, focusing on shell orientation, close-packing, fragmentation and presence of abraded and rounded shells (mostly using criteria of Kidwell et al., 1986 and Kidwell et al., 2001). Community structure data are summarized in Table 4.1.

Cluster analyses (using Euclidean and Manhattan distance to construct a dissimilarity matrix) were employed on each of the data sets to find associations among samples. A bivariate plot of evenness versus species richness (figure 4.2) permits a comparison of the ancient clustering associations to the modern clustered samples.

RESULTS

Samples from both ancient and modern seafloors group into four faunal associations based primarily on species richness (Fig. 4.2). ANOVA testing shows highly significant differences between the groups (P-value of 0.0001). Species richness and percent shelliness (a visual estimation for percent-volume of shells in a rock or sample, Kidwell and Holland, 1991) are significantly different among all groups (biofacies), while the percent of deposit feeding and chemosymbiotic bivalves were significantly different (P-value of 0.0001) between the pair of biofacies 1 and 2, and the pair of biofacies 3 and 4. Percent of epifaunal bivalves were not significantly different between the groups. A discriminative analysis conducted on this data for exploratory means shows four distinct groups (Fig. 4.3). Missing data (undefined zero evenness values) reduced samples to twenty eight. The four biofacies are discriminated along linear discriminant function 1 (LD1), which explains 90% of the variance. The analysis was done on species richness (d of Margalef), evenness (Hurlbert's PIE), percent deposit feeding and chemosymbiotic bivalves, percent epifaunal species, and percent shelliness in each

of the samples combining each biofacies. In both modern and ancient settings, these associations correspond to differences in seafloor lithology. This in turn corresponds to a gradient of decreasing oxygen and organic-enrichment (see general oxygen gradient for northern Benguela in Bailey, 1991 and Shannon and Nelson, 1996) that reflects increasing distance from the most intense centers of upwelling. This parallel between faunal association and modern ecological gradients are used to infer the (paleo)oxygen levels and upwelling mosaic of the ancient settings.

The community structure and taphonomic characteristics of these modern and fossil faunal associations differentiates the respective high-productivity/upwelling study areas into similar mosaics of sub-environments (Table 4.1).

Table 4.1: Combined ancient-modern community structure of the molluscan assemblages for the four main upwelling associations.

	Association 1 ancient / modern	**Association 2** ancient / modern	**Association 3** ancient / modern	**Association 4** ancient / modern
No. of samples	2 / 5	8 / 2	7 / 3	5 / 3
Sediment type	unfossiliferous porcelanites, laminated organic-rich carbonates / opal & organic rich oozes	organic-rich carbonates, cherts & porcelanites moderate levels of opal & organic mater oozes	loosely-packed carbonate shell beds, chert & porcelanites / carbonate-rich oozes	phosphate-bearing densely-packed carbonate shell beds / phosphate-rich samples
Richness *	0 / 0-1.1	2.2-4.4 / 2.5-2.6	4.5-7.4 / 6-8.1	8.8-10.1 / 8.7-11.9
Dominance ** (% top taxon)	barren / 99% *Lucinoma*	39% *Mesosaccella* / 83% *Lucinoma*	17% *Caestocorbula* / 59% *Carditella*	28% *Caestocorbula* / 25% *Dosinia*
Evenness index	0***/ 0***-0.14	0.4-0.71 / 0.19-0.32	0.7-0.84 / 0.27-0.52	0.64-0.77 / 0.55-0.67

	Association 1 ancient / modern	**Association 2** ancient / modern	**Association 3** ancient / modern	**Association 4** ancient / modern
Body size	Ancient: up to 45mm in loose-shellbeds from Porcelanite unit / up to 25mm in loose-shellbeds of lucinid from Phosphatic-Carbonate unit. Modern: up to 44mm in the shelly samples of facies 1 / up to 16mm in facies 3.			
Feeding mode (% individuals) SF=suspension feeding bivalves DF=deposit feeding bivalves	barren / 100% chemosymbiotic bivalves	58% DF, 17% SF, 20% gastropods 83% chemosymbiotic bivalves	17% DF, 57% SF, 20% gastropods / 85% SF, 4% gastropods	22% DF, 63% SF, 14% gastropods / 61% SF, 9% DF, 9% gastropods
Major Lifestyle ratio of epifauna/ infauna (individuals of pooled samples)	0 / 0	0.02 / 0.01	0.25 / 0.13	0.30 / 0.09
Taphonomic Signature AS=% of articulated shells	barren / up to 64% AS, shells sparsely distributed within the sample	up to 74% AS, sparse shells / up to 19% AS, sparse shells	up to 36% AS, loosely-packed / up to 3% AS, densely-packed, up to 17% shells rounded	up to 8% AS, densely-packed, some abraded / up to 1.5 AS, densely-packed, up to 69% shells rounded

* = richness is defined as Margalef's index d.
** = of pooled samples.
*** = the evenness index (PIE of Hurlbert, 1971) is defined logically only if a sample has more than one species. In a situation of zero or one species the interpretation is of very low evenness.

Faunal association 1, which is characterized by an absence of benthic macrofauna and microfauna (foraminifera), occurs in ancient barren porcelanite layers and laminated organic-rich carbonates, and in the modern opal and organic-rich samples. A few opal and organic-rich samples showed an extremely low richness and evenness of species with the chemosymbiotic bivalve *Lucinoma capensis* (per criteria of Taylor and Glover, 1997) comprising 99% of the pooled individuals of the assemblage (Table 4.1). Of those shells, most were articulated, which further

suggest both low bottom water energy and low oxygen conditions, supporting few or no metazoan predators at the center of the upwelling cell.

Association 2 is characterized by low species richness and moderate evenness (Table 4.1), and occurs in organic-rich carbonate and thin-bedded cherts and cherty-porcelanite in the Mishash Formation and in sediments having moderate to high organic content on the Benguela shelf. The dominant species are mostly infaunal deposit-feeding or chemosymbiotic bivalves and their shells are sparsely distributed but commonly articulated. Small fluctuations in seafloor oxygen levels are suggested by the relatively high abundance of carnivorous gastropods in the ancient example(17%), and yet dominance of infaunal deposit-feeding or chemosymbiotic bivalves. This association represents seafloor environments outside the center of the cells but nonetheless still strongly affected in terms of high organic rain and dysaerobic overlying water.

Association 3 is characterized by moderate to high species richness and evenness (Table 4.1), and occurs in samples of thin-bedded shelly chert and porcelanite from the Mishash and carbonate-rich samples from the Benguela. Intermediate abundances of the top taxon are typical, but suspension feeding, shallow burrowing bivalves dominate this facies, with both carnivorous and non-carnivorous (detritus feeding) gastropods of relatively similar abundances. Epifaunal bivalves are present but rare. Chemosymbiotic lucinid bivalves are relatively small bodied: *"Lucina"*

blankenhorni ranges up to only 25 mm in loosely-packed shell beds in the Phosphatic-Carbonate unit of the Mishash, and *Lucinoma capensis* ranges only up to 16mm in carbonate-rich sediments of Benguela. In general, molluscan shells are loosely-packed and mostly disarticulated, which may point to relatively abundant predators, scavengers and bioturbators. Situated marginal to the upwelling center, this facies characterizes an overall aerobic seafloor with reduced effects from upwelling as indicated by its diverse macrobenthic assemblage and diminished abundance and body size of chemosymbiontic lucinids. Nonetheless, the abundant chert and porcelanite layers associated with this biofacies express the proximity to the major biogenic silica source (which probably promoted silicification and formation of the shelly chert and porcelanites containing originally-carbonate shells).

In both ancient and modern systems, association 4 has the maximum species richness and high evenness, and occurs in densely-packed shell beds from the Mishash and shell- and phosphate-rich samples of Benguela. No single taxon dominates, but all samples are dominated by suspension feeding bivalves and contain the highest observed abundance of carnivorous gastropods (modern samples). Shells are densely-packed, mostly disarticulated (probably an effect of high predation), showing some abrasion and common rounding of shells in ancient and modern samples, respectively, indicating high bottom-water energy levels. Situated marginal to the upwelling center, similar to association 3, association 4

faunal assemblages indicate an aerobic seafloor with only intermittent effects from upwelling. However, it is also likely that these skeletal assemblages are the product of more prolonged time-averaging than those of other associations, thus capturing a broader range of environmental conditions at the seafloor. This greater time-averaging is inferred from the following: (1) the presence of large specimens of lucinids, usually diagnostic of upwelling centers, co-occurring with taxa that are otherwise typical of low-organic high-oxygen conditions; (2) the mixed taphonomic condition (damage levels) of shells, indicating a range in degrees of predation; (3) a relatively high frequency of rounded and abraded shells, and (4) the presence of shell stacking that is diagnostic of storm reworking (latter three are indications of water energy levels) (described in Edelman-Furstenberg, chapter 1 and chapter 3). The mixed environmental signature of these features suggest that depositional environments ranged from close to the upwelling center to environments of reduced upwelling effects during the accumulation of these shelly sediments, and is consistent with the ecologically mixed character of the faunal association itself.

Species of chemosymbiotic lucinids are also exceptionally large in these sediments: in loosely-packed shell-beds from the Porcelanite unit (inter-bedded with the barren porcelanite layers) of the Mishash Formation, *"Lucina" blankenhorni* ranges up to 45 mm in shell length (mean of 26.7 mm), and in the opal and organic-rich samples (of faunal association 1) of the Benguela *Lucinoma*

capensis ranges up to 44 mm (mean of 18.5 mm). These larger body sizes contrast to the smaller sizes (mean of 14.9 mm) of *"Lucina" blankenhorni* in loosely-packed shell-beds from the Phosphatic-Carbonate unit (inter-bedded within carbonate sediments) with t-test showing significant body size differences for *"Lucina*" between the two sets of shell beds (P-value = 0.0001), and also in body sizes of *Lucinoma* in carbonate-rich samples of the Benguela (mean of 7.7 mm), with t-test P-value of 0.0001 between opal-rich and carbonate-rich faunal associations.

DISCUSSION

In both the ancient Mishash and the modern Benguela systems, an overall increase in species richness, evenness, epifaunal-infaunal ratio, and disarticulation of shells, along with a decrease in body size of chemosymbiotic bivalves, is observed with increasing distance from the inferred (in the ancient case) upwelling center, from the siliceous facies (i.e., barren porcelanites and opal and organic-rich samples) towards the shell beds and phosphorite facies. An increase in oxygen levels along this gradient is reported for the northern Benguela (see Bailey, 1991; Shannon and Nelson, 1996). Information from the Mishash and Benguela systems on the taphonomic condition, faunal composition, and community structure of macrobenthic death/skeletal assemblages permits the widely-used biofacies scheme (of inferred levels of oxygen) of Savrda et al. (1984; Savrda and Bottjer 1987; 1991) to be improved (Table 4.2), and permits quantitative estimates of bottom-water oxygen to be applied to the ancient record. Biofacies in table 4.2 are

numbered to agree with faunal associations as recognized in this paper. The shelly samples of Benguela association 1 constitute a good modern example of Savrda and Bottjer's (1987) "exaerobic zone" (biofacies 1 below), in which large, articulated, burrowing chemosymbiotic bivalves are associated with laminated organic-rich carbonates.

Table 4.2: Bottom water oxygen levels for the biofacies from the present study compared to inferred oxygen facies of Savrda and Bottjer (e.g., 1991).

Savrda & Bottjer, (e.g., 1991)	Savrda & Bottjer, (e.g., 1991)	Present study	Present study	Present study
anaerobic 0 mlO_2/l in both OW and PW	laminated strata lacking both in-situ body fossils and microbioturbation	massive, lacking any benthic macrofauna or microfauna (benthic forams)	barren	porcelanite layers (Porcelanite unit) - Mishash / opal-rich ooze – Benguela **(biofacies 1)**
quasi-aerobic <0.1 ml/l in OW, 0 ml/l in PW	laminated strata with slight microbioturbation, containing benthic microfossils but lacking macrobenthos	laminated strata lacking any benthic macrofauna (extremely low diversity of benthic forams)	barren	organic-rich carbonates - Mishash **(biofacies 1)**
exaerobic >0.1<1 ml/l in OW, 0 ml/l in PW	laminated strata, but containing in situ macro-epibenthic body fossils	monospecific (or extremely low diversity) of infaunal, chemosymbiotic bivalves	dominant articulated shells	organic-rich ooze - Benguela **(biofacies 1)**
dysaerobic >0.1<1 ml/l in OW, some aeration of PW	bioturbated, low diversity of small macrobenthic body fossils, if any	bioturbated, dominated by infaunal deposit-feeding or chemo-symbiotic bivalves, (low diversity of benthic foraminifera	abundant articulated shells	organic-rich carbonates, chert & porcelanite – Mishash / moderate levels of opal and organic-matter – Benguela **(biofacies 2)**

Savrda & Bottjer, (e.g., 1991)	Savrda & Bottjer, (e.g., 1991)	Present study	Present study	Present study
aerobic >1.0 ml/l in OW, aeration of PW to some depth		bioturbated, (mostly *Planolites*), diverse epifaunal and shallow infaunal suspension-feeding bivalves, some gastropods (diverse benthic, foraminifera, rare planktic forams)	mixed articulation state of shells	loosely-packed shell beds, chert & porcelanite - Mishash / carbonate-rich ooze - Benguela **(biofacies 3)**
	thoroughly bioturbated, diverse assemblage of large, heavily calcified macrobenthic body fossils	bioturbated, (mostly *Thalassinoides*), very diverse epifaunal and shallow infaunal suspension-feeding bivalves, some gastropods	winnowed shell beds with abraded and abundant disarticulated and rounded shells	densely-packed shell beds - Mishash / phosphate-rich samples - Benguela **(biofacies 4)**

Figure 4.2 plots each sample's diversity measurements and indicates their environmental significance in relation to the inferred upwelling seafloor conditions, with an increasing richness and evenness associated with increasing distance from the upwelling center. The samples from the two end-member biofacies (biofacies 1 and 4) show the lowest and highest measures of richness (P-value of 0.0001) analogous to the most stressful and closest to normal marine environments, respectively. This trend is parallel in ancient and modern samples for these biofacies.

In addition, the percent of chemosymbiotic and deposit feeding bivalves are shown to increase (100% dominance in biofacies 1) towards the center of upwelling cells compared to the percent of these feeding types in biofacies 3 and 4,

which represent conditions marginal to the upwelling center (Fig. 4.4). This increase is best observed between biofacies 3 and 4 that represent aerobic conditions to biofacies 1 and 2 (P-value of 0.0001) representing dysaerobic (and even anaerobic) conditions, which in turn is associated with higher organic loads closer to the upwelling centers.

Thin-bedded chert and porcelanite samples and loosely-packed shell beds of the Mishash Fm, together with their modern correlative samples of moderate opal and organic-matter and carbonate-rich samples from the Benguela comprise the samples of the two intermediate biofacies (2 and 3, respectively). These samples of varied lithologies range between the two end members (biofacies 2 and 4) and can grouped according to their diversity measures and feeding types. Consequently, this enables an environmental reconstruction for the shelly cherts and porcelanites, which are otherwise environmentally ambiguous. It is argued here that, due to the proximity of the cherts and porcelanites to the upwelling center, these initially carbonate environments will later be most prone to diagenesis and silicification. Moreover, the community structure of the molluscan fauna from these chert and porcelanite samples are evidence of their original distance from the upwelling cell center, or in other words, of their original paleoenvironment. Once outside the upwelling cell, oxygen levels and detrital food availability are no longer a limiting factor as evidence from the richness and evenness of biofacies 2 and 3. Specifically, those samples of chert and porcelanite that cluster in biofacies 2 were

originally closer to the upwelling center, similar to the physical location of the moderate organic-rich oozes or ancient organic-rich carbonates, whereas the chert and porcelanites that cluster in biofacies 3 were originally farther from the stressful effect of the upwelling, parallel to the loosely-packed shell beds and carbonate-rich oozes (Fig. 4.2, 4.4).

Thus via a modern-ancient comparison, the facies mosaic typical of modern upwelling zones is identified fully in the Upper Cretaceous example with four biofacies distinguished by specific community characteristics. These biofacies are associated to upwelling lithotypes and depositional environments, from barren porcelanites through originally organic-rich carbonates to loosely-packed carbonate shell beds and finally to winnowed, densely-packed shell beds.

Analyzing the biogenic constituents of high-productivity settings and applying this new approach of community structure parameters thus permits a more effective teasing apart of variation in the system as well as a more complete picture of the past and present ecology of these important settings. Rather than corroborating the generally accepted characterization of these settings as consisting largely of dysaerobic seafloors (e.g., Reiss, 1962 and Almogi-Labin et al., 1993 – foraminifera evidence; Bein et al., 1990 – geochemical evidence), the macrofaunal evidence reveals a broad and dynamic gradient of oxygen levels within the upwelling zone itself, from anaerobic/exaerobic to aerobic. Sedimentological

evidence (e.g., Soudry, 1992, 2000) indicates a role for both low and high oxygen conditions for phosphate genesis and accumulation However, the emphasis of the present macrofaunal study is on the spatial mosaic of the upwelling system, which presents a range of seafloor environments concurrently. Both anaerobic, dysaerobic and aerobic conditions persist under the main upwelling zone, which consists of seafloors under the upwelling cells and also under upwelling influence but adjacent to the cell center itself. Thus, macrofaunal paleontological criteria can be used in ancient examples to recognize the paleoenvironments in spite of the high diagenesis these settings experience (as in the case of the recrystallized chert and porcelanite beds of the Mishash Formation). This may be important when using chert deposits as an indicator of the magnitude of high-productivity variations in the past (see Parrish, 1998). For example, the basal Chert Member of the Mishash Formation, which can reach a thickness of more than 40 meters in synclinal basins, is regarded as deposited under a most intense upwelling regime (e.g., Eshet and Almogi-Labin, 1996), but macrofaunal evidence from the stratigraphically higher Porcelanite unit in the Phosphate Member of the Mishash Formation argues instead that these porcelanites represents the most intense upwelling during the Upper Campanian. The Porcelanite unit ranges from completely unfossiliferous layers to loosely-packed shell beds with up to 40% abundance of large *"Lucina" blankenhorni* in a sample, typical of most intense upwelling in the modern cells (up to 100% dominance of *Lucinoma capensis* in the otherwise barren opal and organic-rich samples of Benguela). This suggests persistently high levels of organic

matter and low oxygen levels (e.g., sub-oxic in Cary et al., 1989; nearly anaerobic in Hentschel et al., 1993) during the accumulation of these sediments, and suggests that the most extreme conditions of upwelling during the Upper Campanian prevailed during the deposition of the Porcelanite unit that bears the largest specimens of these species. In contrast, the Chert Member has abundant fossiliferous layers with molluscan fauna (described by Chavan (1947), mentioned in Reiss (1962), and also personal observations): these faunas suggest that the Chert Member includes significant intervals of dysaerobic and aerobic seafloor conditions, more like that observed in the thin-bedded cherts and cherty-porcelanites and loosely-packed shell beds (i.e., biofacies 3) of the Phosphate Member.

The similarity between the community structures of macrobenthos in ancient and modern upwelling examples of this study (Figure 4.2, 4.4) is quite remarkable, especially given that oceanic configurations and global climate were so different between the Upper Cretaceous and the present and that few genera are in common. Macrofaunal evidence argues that differences in seafloor oxygen concentration along with nutrient loads (or food availability) played major roles in structuring faunal assemblages in both settings, despite their difference in geologic age, and, conversely, that these environmental variables found similar ecologic expression in evolutionarily distinct ecosystems. The ecological picture of upwelling that is provided by this integration of Cretaceous Mishash and modern Benguela evidence

constitute an improved model for upwelling systems in general, especially those of the late Mesozoic to Recent, which is the geologic interval dominated by the modern fauna of marine metazoans (sensu Sepkoski 1981) and by siliceous sediments produced by large diatom “blooms” rather than by sponge-spicules and radiolarians.

CONCLUSIONS

In conclusion, this study demonstrates the sensitivity of macrobenthos to seafloor conditions across strong gradients in bottom oxygen and organic matter supply, and especially the value of macrobenthos in differentiating and more fully understanding the seafloor mosaic under upwelling systems. The complexity of the upwelling system is further supported by the hydrodynamic behavior of the shells as grain particles, not only in terms of oxygen levels ranging from nearly anaerobic to aerobic but also in the range of bottom water energy levels that can operate.

Not only do upwelling seafloor conditions change across the shelf, but more correctly, also within a short distance of the center of the upwelling cell, and thus low diversity, "stressed" macrofaunal assemblage are present contemporaneous with high diversity, "normal-like" assemblages even within the main upwelling zone. This range of macrofaunal evidence is characteristic of and describes more accurately the patchy and wide-ranging nature of the upwelling environment of the Upper Cretaceous. More ancient/modern studies could further clarify the ongoing

discussion regarding the role of oxygen and food availability in limiting faunal distribution. Specifically, how strongly would patterns of community structure differ in macrobenthos in upwelling regions that are not oxygen-deficient, as in the case of NWAfrica?

APPENDIX 1. Major element chemical analysis

E1ement%/Samp1e	SiO2	A1203	Fe203	TiO2	CaO	MgO	MuO	Na20	K20	P205	SiO3	LOI	Total
Har Massa M-3	3.8	0.4	0.2	<0.05	53.1	0.5	<0.05	0.1	0.06	8.4	0.9	32.7	100.2
Har Massa M-3#	3.4	0.5	0.1	<0.05	53.5	0.5	<0.05	<0.05	<0.05	2.7	0.1	39.6	100.4
Har Massa M-4	79	0.9	0.3	0.05	10.3	0.5	<0.05	<0.05	<0.05	1.9	0.6	7	100.6
HarMassa M-4#	85	0.9	0.1	<0.05	7	0.2	<0.05	<0.05	<0.05	0.9	0.2	5.5	99.8
Har Massa M-5	3.3	0.4	0.1	<0.05	53.4	0.5	<0.07	<0.05	<0.05	4.8	0.3	37.5	100.4
Har Massa M-6	1.2	0.2	<0.1	<0.05	54.9	0.6	<0.05	<0.05	<0.05	1.1	0.2	41.9	100.1
YE Ashosh-6	15.2	1.4	0.4	<0.1	41	0.8		3.3	0.1	12.1	1.7	25	101
YE Ashosh-8	31	0.3	<0.1	<0.1	38	0.7		0.2	<0.1	0.2	0.2	30	100.6
YE Ashosh-9	34	1	<0.1	<0.1	33	0.7		2.5	0.1	1.1	0.7	28	101.1
YE Ashosh-11c	43	1.3	0.4	<0.1	29	0.8		1	0.2	2.3	1	22	101
98YF Ashosh-10	13	0.2	<0.1	<0.1	42	0.6		3.2	<0.1	16.5	1.4	23	99.9
98YF Ashosh-11	40	1.1	0.4	<0.1	30	1		0.9	0.2	4.2	0.3	22	100.1
98YF Ashosh-12	25	0.3	<0.1	<0.1	40	0.9		0.4	<0.1	2.5	1	30	100.1
99 YF Ashosh-5	11	0.9	0.3	<0.1	48	0.5		0.2	0.2	<0.1	0.3	24	99.7
99 YF Ashosh- 7	11.7	0.9	0.3	0.1	40.4	1.2		0.3	0.1	14.4	1.8	29	100.2
99 YF A-lOa	31	1	0.2	<0.1	35	1.1		0.9	0.2	1.3	0.5	29	100.2
99YF Ashosh-5	11	0.9	0.3	<0.1	48	0.5		0.2	<0.1	14.5	0.3	24	99.7
YE Ashosh-6	15.2	1.4	0.4	<0.1	41	0.8		3.3	0.1	12.1	1.7	25	101
99YF Ashosh- 7	11	0.8	0.3	<0.1	38	1.1		7.3	0.1	13.5	1.7	27	100.8
YE Ashosh-8	31	0.3	<0.1	<0.1	38	0.7		0.2	<0.1	0.2	0.2	30	100.6
YE Ashosh-9	34	1	<0.1	<0.1	33	0.7		2.5	0.1	1.1	0.7	28	101.1
98YF Ashosh-10	13	0.2	<0.1	<0.1	42	0.6		3.2	<0.1	16.5	1.4	23	99.9
99YF Ashosh-10a	31	1	0.2	<0.1	35	1.1		0.9	0.2	1.3	0.5	29	100.2
98 YF Ashosh-11	40	1.1	0.4	<0.1	30	1		0.9	0.2	4.2	0.3	22	100.1
YE Ashosh-11	43	1.3	0.4	<0.1	29	0.8			0.2	2.3	1	22	101
98 YF Ashosh-12	25	0.3	<0.1	<0.1	40	0.9		0.4	<0.1	2.5	1	30	100.1

APPENDIX 2.1. Macrofaunal count data for samples from the Qazra sub-basin

sample YF A-43	no. individuals
Mesosaccella perdita	87
Mesosaccella larteti	53
Mesocallista andersoni	7
Caestocorbula sp. A	7
"Lucina" blanckenhorni	2
veneroid very fine-ribbed	1
total	157

sample YF A-49	no.
Mesosaccella larteti	32
Caestocorbula sp. A	5
rounded fine-ribbed venerid	4
Gyrodes asiatica	3
Mesocallista andersoni	3
Undiscala vicina	3
total	50

sample YF O-4	no.
Mesosaccella perdita	35
Mesosaccella larteti	22
"Lucina" blanckenhorni	5
Protocardia silicea	2
Gyrodes asiatica	1
total	65

sample YF O-5A	no.
Nucula tenera	23
"Corbula" sp.	18
Mesosaccella sp.	12
Undiscala sp.	8
Gyrodes asiatica	4
Nanonavis parallelus	3
"Lucina" blanckenhorni	2
total	70

sample YF A-36A	no.
Mesosaccella larteti	54
Mesocallista andersoni	17
Caestocorbula sp. A	12
Mesosaccella perdita	11
"Lucina" blanckenhorni	10
"Corbula" sp.	5
Gyrodes farafrensis	2
Eucyclomphalus sp.	1
total	112

sample YF A-40	no.
Eucyclomphalus sp.	44
"Meretrix" sp. A	16
Mesosaccella larteti	14
Mesosaccella perdita	13
Mesocallista andersoni	7
Caestocorbula sp. A	7
Anomalofusus turris?	3
Nucula tenera	1
total	105

sample YF O-5	no. individuals
Mesosaccella perdita	24
"Meretrix" sp. A	24
Mesosaccella larteti	21
Undiscala vicina	20
Caestocorbula sp. A	3
"Lucina" blanckenhorni	3
Mesosaccella grovei	2
Nannonavis parallelus	1
Gyrodes asiatica	1
unidentified ?venerid? sp.	1
total	100

sample YF O-7A	no.
Undiscala vicina	25
"Lucina" blanckenhorni	12
Gyrodes asiatica	11
Mesocallista andersoni	9
Caestocorbula sp. A	9
"Meretrix" sp. A	8
Parmicorbula subelegans	6
Gyrodes farafrensis	4
Eucyclomphalus sp.	3
Mesosaccella larteti	3
Nuculana-like (gape, inflated)	2
Mesosaccella grovei	1
"whelk" with fine spiral ribs	1
Mesosaccella perdita	1
"whelk" - knobby	1
total	96

sample YF O-8	no.
Caestocorbula sp. A	36
Parmicorbula subelegans?	30
Nucula tenera	20
Turritella reyi	7
Undiscala vicina	4
Mesosaccella sp.	4
Mesocallista andersoni	4
Nannonavis parallelus	4
"Lucina" blanckenhorni	3
Mesosaccella larteti	3
Gyrodes farafrensis	2
"Meretrix" sp. A	2
Fasciulariid	1
total	120

sample YF A-42	no.
Mesosaccella larteti	102
"Lucina" blanckenhorni	7
Gyrodes asiatica	5
Undiscala vicina	2
"Corbula" sp.	2
Turritella reyi	2
cf. *Gegania picardi*	1
total	121

sample YF A-36	no. individuals
Mesosaccella larteti	45
Mesosaccella perdita	22
Mesocallista andersoni	14
Caestocorbula sp. A	11
"Lucina" blanckenhorni	6
Eucyclomphalus sp.	4
"Corbula" sp.	4
"Meretrix" sp. A	2
Mesocallista(?) rohlfsi?	1
Gyrodes farafrensis	1
total	110

sample YF A-43	no.
Eucyclomphalus sp.	97
Nannonavis parallelus	13
Mesosaccella larteti	7
"Lucina" blanckenhorni	4
"Corbula" sp.	4
Gyrodes farafrensis	4
Undiscala goryi	2
Caestocorbula sp. A	2
cf. *Scala* sp. (radial-rib wide-apic	1
total	134

sample YF O-6	no. individuals
"Meretrix" sp. A	20
Mesosaccella larteti	16
"Lucina" blanckenhorni	13
Mesocallista (?) *rohlfsi?*	10
Undiscala vicina	9
heterodont / venerid sp?	8
Mesocallista andersoni	7
Arcoida sp. A	6
"Corbula" sp.	3
Caestocorbula sp. A	2
Nannonavis parallelus	2
high spired =*Turritella?* sp.	1
Eucyclomphalus *sp.*	1
total	98

sample YF M-2	no.
Nannonavis parallelus	22
Turritella reyi	16
Caestocorbula sp. A	15
Eucyclomphalus sp.	14
"Corbula" sp.	10
Mesosaccella perdita	5
Nucula tenera	5
"Meretrix" sp. A	3
Gyrodes farafrensis	3
Undiscala vicina?	3
"Lucina" blanckenhorni	2
Mesocallista (?) *rohlfsi*	2
Aporrhaid sp.	2
"Lucina" sp. (wide ribbing)	1
Mesosaccella larteti	1
Bonellitia scaberrima	1
total	105

sample YF A-55	no. individuals
Caestocorbula sp. A	35
Nucula tenera	15
Mesosaccella larteti	11
Undiscala goryi	10
Nanonavis parallelus	9
Gyrodes asiatica	7
"Meretrix" sp. A	7
Mesocallista andersoni	5
Volutomorpha sp.	3
Cardium sp.	2
Mesocallista (?) *rohlfsi* ?	2
"Lucina" blanckenhorni	2
"Corbula" (Flexicorbula) vokesi	2
Mesosaccella perdita	2
Aporrhaid sp.	1
Turritella reyi	1
Crassatella rothi	1
"Mytilus" nov sp.	1
Diptygmendon elliotti	1
large venerid sp. (strong ribs)	1
Mesosaccella sp.	1
total	119

sample YF A-58	no.
Caestocorbula sp. A	32
"Meretrix" sp. A	26
Turritella reyi	14
Mesocallista andersoni	11
Crassatella rothi	8
Mesosaccella perdita	7
"Corbula" (Flexicorbula) vokesi	6
Mesocallista (?) *rohlfsi*	4
Mesosaccella larteti	4
Undiscala vicina?	3
Nanonavis parallelus	3
Aporrhaid sp.	3
Nucula tenera	2
"Lucina" blanckenhorni?	1
bivalve species with lunule	1
total	125

sample YF A-59	no.
Caestocorbula sp. A	37
Mesocallista andersoni	18
Nucula tenera	12
"Meretrix" sp. A	12
venerid sp.	4
Mesosaccella larteti	3
Pycnodonte sp.	3
Turritella sp.	3
Parmicorbula subelegans?	3
Gyrodes asiatica	2
fine-ribbed lucinid sp.	2
Nannonavis parallelus	2
Mesosaccella perdita	2
Tellinid-like sp.	1
Undiscala goryi	1
coarse-ribbed bivalve (37mm)	1
Crassatella sp.	1
cardiid sp. B	1
very inflated (not tellinid)	1
total	109

sample YF O-6A	no. individuals
Mesosaccella perdita	43
"Meretrix" sp. A	12
Caestocorbula sp. A	10
Undiscala vicina	8
Nannonavis parallelus	6
Nucula tenera	6
"Corbula" sp.	6
Mesosaccella grovei	5
Mesosaccella larteti	5
Protocardia silicea	4
Vanikoro asiatica	4
Turritella reyi	2
Gyrodes asiatica	2
Mesocallista andersoni	1
siphon-bearing gastropod	1
Cardiomya sp.	1
"Lucina" blanckenhorni	1
Turritella quadeicincta	1
Pycnodonte sp.	1
Eucyclomphalus sp.	1
Noetiidae? (Arcoid)	1
Mesocallista (?) *rohlfsi*	1
total	122

sample YF O-8C	no.
"Meretrix" sp. A	40
"Corbula" sp.	28
Caestocorbula sp. A	24
Mesocallista (?) *rohlfsi*	17
Nucula tenera	16
Nannonavis parallelus	7
Mesosaccella larteti	7
Mesosaccella perdita	6
Mesocallista andersoni	5
"Lucina" blanckenhorni	4
Turritella reyi	4
Undiscala vicina	4
whorl of smooth gastropod (*Gyrc*	4
large, lateral hinge = lucinid n. sp	3
?Plicatula sp.	1
Cardium sp. A (fine rib)	1
myoidea? straight hinge, orthogy	1
Gyrodes sp.	1
high angled gastropod with knobl	1
Fasciulariid?/buccinid?	1
small-symmetrical bivalve, no sh	1
total	176

sample YF O-7B	no. individuals
Caestocorbula sp. A	26
"Lucina" blanckenhorni	18
Crassatella rothi	13
Protocardia silicea	12
heterodont = *Crassatella?*	11
"Meretrix" sp. A	6
Parmicorbula subelegans	6
Nannonavis parallelus	4
Mesosaccella grovei?	3
venerid *(Mesocallista andersoni* ?)	3
Mesosaccella larteti	2
Pycnodonte? sp.	1
Undiscala vicina	1
arcoid - *Limopsis* ? sp.	1
?Crassatella cf. zitteli	1
cf. Tellinella sp.	1
total	109

sample YF M-1	no.
Caestocorbula sp. A	20
"Corbula" sp.	16
"Lucina" sp. (wide ribbing)	12
Gyrodes asiatica	11
large veneroid sp.	5
Turritella reyi	5
Mesocallista andersoni	5
Protocardia silicea	4
Crassatella sp.	4
Plicatula sp.	3
smooth, *?Eucyclomphalus sp.*	3
Undiscala vicina?	2
Volutomorpha sp.	2
"Lucina" blanckenhorni	2
Veniella sp.	1
long siphon gastropod -high spired	1
Nucula tenera	1
Rastellum diluvianum	1
Aporrhaid sp.?-diagonal ribbing	1
Mesosaccella sp.	1
total	100

APPENDIX 2.2 Feeding types and life styles

facies-1 (organic-rich)	life habitat-feeding mode	no.individuals
Mesosaccella perdita	dB, DF	134
Mesosaccella larteti	dB, DF	107
Mesocallista andersoni	sB, SF	10
Caestocorbula sp. A	sB, SF	12
"Lucina" blanckenhorni	dB, Ch	9
rounded fine-rib venerid	sB, SF	4
Protocardia silicea	sB, SF	2
Nucula tenera	sB, DF	23
"Corbula" sp.	sB, SF	18
Nanonavis sp.	Epi, SF	3
veneroid very fine-rib	sB, SF	1
Undiscala vicina	Car	11
Gyrodes asiatica	Car	8

bivalves = 11 species
gastropods = 2 species

LEGEND
Epi=epifauna
B=burrower
sB=shallow burrower
dB=deep burrower
SF=suspension feeder
DF=deposit feeder
Ch=chemoautotroph
Car=carnivore
NCar=non carnivore

Ecological information mainly from:

1. Moore, 1969
Treatise on invertebrate paleontology
2. Valentine et al., 2002

Taxonomic identification mainly from:

1. Z. Lewy personal collection
2. Picard, 1930; Chavan, 1947
3. Moore, 1969
Treatise on invertebrate paleontology

facies-2 (chert&porcelanite)	life habitat-feeding mode	no.individuals
Nanonavis parallelus	Epi, SF	42
Caestocorbula sp. A	sB, SF	97
"Corbula" *sp.*	sB, SF	28
Mesosaccella perdita	dB, DF	80
Nucula tenera	sB, DF	26
"Meretrix" sp. A	sB, SF	75
"Lucina" blanckenhorni	dB, Ch	60
Mesocallista (?) *rohlfsi* ?	sB, SF	13
Mesosaccella larteti	dB, DF	266
heterodont / venerid sp?	sB, SF	8
Mesocallista andersoni	sB, SF	58
Arcoida sp. A	Epi-sB, SF	6
Mesosaccella grovei	dB, DF	3
Parmicorbula subelegans	sB, SF	36
"Lucina" sp. (wide ribbing)	dB, SF	1
Turritella reyi	Ncar	26
Gyrodes asiatica	Car	17
Eucyclomphalus sp.	Ncar	164
Gyrodes farafrensis	Car	16
Undiscala vicina	Car	63
Aporrhaid sp.	Ncar	2
Undiscala goryi	Car	2
Anomalofusus turris?	Car ??	3
Bonellitia scaberrima (<1%)	Car	1
Fasciulariid (<1%)	Car	1

bivalves = 15 species
gastropods = 10 species

facies-3 (shell beds)	life habitat, feeding mode	no.individuals
"Corbula" (Flexicorbula) vokesi	sB, SF	10
Caestocorbula sp. A	sB, SF	229
Nucula tenera	sB, DF	52
Mesosaccella larteti	dB, DF	34
Nannonavis parallelus	Epi, SF	31
"Meretrix" sp. A	sB, SF	103
Mesocallista andersoni	sB, SF	48
Cardium sp.	sB, SF	2
Mesocallista (?) *rohlfsi* ?	sB, SF	24
"Lucina" blanckenhorni	dB, Ch	28
Mesosaccella perdita	dB, DF	60
Crassatella rothi	sB, SF	39
venerid sp.	sB, SF	4
Pycnodonte vesicularis	Epi, SF	4
Parmicorbula subelegans	sB, SF	12
fine-ribbed lucinid sp.	dB, SF	2
Mesosaccella grovei	dB, DF	8
Protocardia silicea	sB, SF	20
"Lucina" sp. (wide ribbing)	dB, SF	12
large veneroid sp.	sB, SF	6
Plicatula sp.	Epi, SF	4
large lateral hinge bivalve = lucinid n. sp.	dB, SF	3
Veniella sp. (less than 1%)	B, SF	1
Rastellum diluvianum (less than 1%)	Epi, SF	1
arcoid - *Limopsis?* sp. (less than 1%)	Epi-sB, SF	1
cardiid sp. B (less than 1%)	sB, SF	1
Cardiomya sp. (less than 1%)	sB, SF	1
Pycnodonte sp. (less than 1%)	Epi, SF	1
"Mytilus" nov sp. (less than 1%)	Epi, SF	1
myoidea? straight hinge-orthogyrate	sB, SF	1
Noetiidae? (Arcoid)	Epi-sB, SF	1
?Crassatella cf. zitteli	sB, SF	1
Cardium sp. A (fine rib)	sB, SF	1
Gyrodes asiatica	Car	27
Volutomorpha sp.	Car	5
Turritella reyi	Ncar	29
Aporrhaid sp.	Ncar	5
Undiscala vicina	Car	18
Vanikoro asiatica	Car	4
Undiscala goryi	Car	11
Eucyclomphalus sp.	Ncar	4
Fasciulariid?/buccinid? (less than 1%)	Car	1
Turritella sexilineata	NCar	1
bivalves = 33 sp.; gastropod = 10 sp.		

APPENDIX 2.3 Mishash species list

no. individuals in pooled samples	Species list of the Phosphate Member (Mishash Fm.)
	BIVALVES
407	*Mesosaccella larteti*
338	*Caestocorbula* sp. A
274	*Mesosaccella perdita*
178	*"Meretrix"* sp. A
116	*Mesocallista andersoni*
101	*Nucula tenera*
97	*"Lucina" blanckenhorni*
76	*Nanonavis parallelus*
74	*Parmicorbula subelegans*
39	*Crassatella rothi*
37	*Mesocallista* (?) *rohlfsi* ?
30	*"Corbula" (Flexicorbula) vokesi*
22	*Protocardia silicea*
13	*"Lucina"* sp. (wide ribbing)
12	venerid sp.
11	*Mesosaccella grovei*
8	unidentified (see list below)
6	large veneroid sp.
6	Arcoida sp. A
4	rounded fine-rib venerid
4	*Pycnodonte vesicularis*
4	*Plicatula* sp.
3	large lateral hinge bivalve = lucinid n. sp.
2	*Cardium* sp.
2	fine-ribbed lucinid sp.
1	veneroid very fine-ribbed sp.
1	*Cardium* sp. A (fine rib)
1	*Veniella* sp.
1	*Rastellum diluvianum*
1	arcoid - *Limopsis?* sp.
1	cardiid sp. B
1	*Cardiomya* sp.
1	*Pycnodonte* sp.
1	*"Mytilus"* nov sp.
1	myoidea?straight hinge-no tooth-orthogyrate
1	Noetiidae? (Arcoid)
1	*Diptygmendon elliotti*
1	*?Crassatella cf. zitteli Quass*
	UNIDENTIFIED BIVALVES:
1	small-symmetrical bivalve, no shoulders
1	Tellinid-like sp.
1	large, coarse-ribbed bivalve (37mm)
1	very inflated (so not tellinid)
1	unidentified ?venerid? Sp.
2	*Nuculana* -like but gape and inflated
1	*cf. Tellinella*

no. individuals in pooled samples	Species list of the Phosphate Member (Mishash Fm.)
	GASTROPODS
168	*Eucyclomphalus* sp.
92	*Undiscala vicina*
55	*Turritella reyi*
52	*Gyrodes asiatica*
16	*Gyrodes farafrensis*
13	*Undiscala goryi*
7	Aporrhaid sp.
7	unidentified (see list below)
5	*Volutomorpha* sp.
4	*Vanikoro asiatica*
3	*Anomalofusus turris?*
2	Fasciulariid?/buccinid?
1	*Turritella sexilineata*
1	*Bonellitia scaberrima*
	UNIDENTIFIED GASTROPODS:
1	siphon-bearing gastropod, large ribbed whorl
1	high angled gastropod with knobby ridge
1	long siphon gastropod -high spired
1	"whelk" with fine spiral ribs
1	"whelk" - knobby
1	cf. *Gegania picardi*
1	cf. *Scala* sp. (radial-rib wide-apical)

APPENDIX 3.1 Macrofaunal count data from Benguela samples

TBD-3441	no. individuals
Lucinoma capensis	68
total	68

TBD-4033	no.
Lucinoma capensis	68
gastropod sp.1	1
Lucinoma? sp.	1
total	70

TBD-3741	no.
Lucinoma capensis	8
total	8

TBD-3519	no.
Lucinoma capensis	86
Carditella similis	11
Gastropod sp.1	4
Dosinia? sp.	3
Tellina sp. (fragment-no rib?)	2
?"Mytilus"?	1
total	107

TBD-3955	no.
Lucinoma capensis	78
gastropod sp. 1	5
Dosinia lupinus	3
cf. Anodontia?	2
Nuculana sp.	1
Tellina sp. (no rib-triangular)	1
total	90

TBD-3800	no.
Carditella sp. (no lateral teeth)	117
Cardiid sp.1	5
Nassarius? sp.	4
Tellina sp. (with internal rib)	4
Tellina sp. (no rib-triangular)	4
Carditella similis	4
Lucinoma capensis	3
Veneropsis sp.	2
Pteriid - straight hinge	2
Volvarina? sp.	2
Pectinid sp. 1	1
Natica sp.	1
Trapezium sp.	1
Loripes sp.	1
total	151

TBD-3770	no. individuals
Carditella sp. (no lateral teeth)	89
Cardiid sp.1	15
Carditella similis	12
Nassarius? sp.	9
Tellina sp. (no rib-triangular)	9
subfamily Lutrariinae	7
Lucinoma capensis	4
Dosinia lupinus	3
Tellina sp. (with internal rib)	3
Mytilidae sp. cf. Modiolus sp.	2
long ribbed gastropod	2
Veneroida sp. cf. Lasaeidae? sp.	1
Loripes sp.	1
Volvarina? sp.	1
Natica sp.	1
Venerid sp. 5	1
total	160

TBD-4018	no.
Carditella sp. (no lateral teeth)	146
Carditella similis	62
Lucinoma capensis	14
Cardiid sp.1	12
Tellina sp. (no rib-triangular)	11
Tellina sp. (with internal rib)	10
Dosinia lupinus	8
gastropod cf. Alrocominella sp.	6
Nassarius? sp.	3
Trapezium? sp.	3
subfamily Lutrariinae	3
Mytilidae sp. cf. Modiolus sp.	2
Chlamys sp. cf. coruscans sp.	2
Pitar sp.	2
Pteriid - straight hinge	2
Marginella? sp.	2
Volvarina? sp.	2
long ribbed gastropod	1
long hatch-ribbed gastropod	1
Nucula nucleus	1
Pectinid sp. 1	1
total	294

TBD-CaCO3 - 4015	no. individuals
subfamily Lutrarianae	26
subfamily Mactridae	16
Lucinoma capensis	12
Tellina (no rib-triangular)	12
Anadontia sp.	11
Nassarius?	9
Arcidae sp.	3
Nucinella cf. treatise N269	3
Pectinidae, Eburmeopecten group	3
Glycimeris sp.	1
Corbula rugifera	1
Loripes sp.	1
total	98

TBD-CaCO3 - 3524	no.
Tellina no rib, elongate	6
Parvacardium sp.	5
Lasaeidae cf. Lasaea sp.	4
Lucinoma capensis	3
Pectinidae, Eburmeopecten group	2
Mactracea sp.	2
Limopsis chuni	2
Arcidae sp.	1
gastropod sp.	1
Nucinella cf. treatise N269	1
Loripes sp.	1
Cardiid cf. Fulvia	1
Pectinidae sp. (radial ribs)	1
total	30

TBD-3563	no. individuals
Lucinoma capensis	33
Tellina sp. (no rib-triangular)	27
Trapeziid sp.	22
Nassarius vinetus	21
Tellina sp. (with internal rib)	8
Limopsis chuni	6
Nucinella cf. treatise N269	5
gastropod sp. wide	3
Crassostrea? sp.	3
Turritella decliris	2
Volvarina? sp.	2
Arcid sp.2	2
Natica sp.	2
Carditella similis	2
Lutraria? sp.	1
Venerid? sp. (pronounced teeth)	1
keeled gastropod	1
Mytilidae sp. cf. Modiolus sp.	1
Nuculana sp.	1
Loripes sp.	1
Limaria sp.	1
Pectinid sp. 1	1
Anomiid sp.	1
internal ribbed gastropod	1
transparent frag (mussel?)	1
spiny Pteriid	1
Pteriid sp. straight hinge	1
total	151

TBD-3413	no. individuals
Dosinia lupinus	57
Carditella similis	45
Tellina sp. (no rib-triangular)	13
Mactra cf. glabrata	10
Cardiid sp.1	7
Turritella decliris	5
Loripes sp.	4
Mytilidae sp. cf. Modiolus sp.	3
Trapeziid sp.	3
Nuculana belcheri	2
Anomiid sp.	2
Pteriid sp. straight hinge	2
Gastropoda sp. 1	2
Nucula nucleus	2
Lucinoma capensis	2
Carditella sp. (no lateral teeth)	2
Natica? sp.	1
Gibbula? sp.	1
Whelk	1
Calyptraea?	1
Marginella? sp.	1
Pitar sp.	1
Venerid sp. 1	1
Venerid sp. 2	1
Venerid sp. 3	1
Venerid sp. 4	1
corbulid sp.	1
total	172

TBD-3710	no. individuals
Dosinia lupinus	59
Nuculana sp.	17
Pitar sp.	15
Carditella similis	11
Nucula sp.	8
Tellina sp. (no rib-triangular)	8
Lucinoma capensis	8
Malleidae sp.	5
Mallediae cf. Vulsella? sp.	3
Fasciolaria//Nucella?	3
Nassarius vinetus?	3
cardiid sp.	2
Pteriid sp. straight hinge	2
Veneropsis? sp.	2
strong beak (concentric ribs)	2
Carditella sp. (no lateral teeth)	2
Volutocorbis? sp.	1
Comitas?/Nassarius speciosus	1
Turritella decliris	1
Arcid sp.1	1
total	154

APPENDIX 3.2 Taphonomic scoring data for Benguela samples

	total #shells	score = 0	score = 1	score = 2	**TBD-3441 opal-org-rich**	score=0 %	score=1 %	score=2 %
N=	11	1	7	3	fragmentation	9	63.6	27.3
N=	11	7	4	0	EX- fine alteration	63.6	36.4	0.0
N=	11	11	0	0	EX- boring	100.0	0.0	0.0
N=	8	7	1	0	edge modification	87.5	12.5	0.0
N=	8	5	3	0	IN- fine alteration	62.5	37.5	0.0
N=	8	6	2	0	IN- boring	75.0	25.0	0.0

	total #shells	score = 0	score = 1	score = 2	**TBD-4033 Organic-rich**	score=0 %	score=1 %	score=2 %
N=	22	14	8	0	fragmentation	64	36.4	0.0
N=	22	22	0	0	EX- fine alteration	100.0	0.0	0.0
N=	22	22	0	0	EX- boring	100.0	0.0	0.0
N=	25	23	2	0	edge modification	92.0	8.0	0.0
N=	25	21	4	0	IN- fine alteration	84.0	16.0	0.0
N=	25	25	0	0	IN- boring	100.0	0.0	0.0

	total #shells	score = 0	score = 1	score = 2	**TBD-3519 marginal opal-org**	score=0 %	score=1 %	score=2 %
N=	33	3	23	7	fragmentation	9	69.7	21.2
N=	33	24	6	3	EX- fine alteration	72.7	18.2	9.1
N=	33	25	5	3	EX- boring	75.8	15.2	9.1
N=	28	22	3	3	edge modification	78.6	10.7	10.7
N=	28	24	3	1	IN- fine alteration	85.7	10.7	3.6
N=	28	25	2	1	IN- boring	89.3	7.1	3.6

	total #shells	score = 0	score = 1	score = 2	**TBD-3955 marginal opal-org**	score=0 %	score=1 %	score=2 %
N=	21	4	14	3	fragmentation	19	66.7	14.3
N=	21	20	1	0	EX- fine alteration	95.2	4.8	0.0
N=	21	16	4	1	EX- boring	76.2	19.0	4.8
N=	16	10	6	0	edge modification	62.5	37.5	0.0
N=	16	14	2	0	IN- fine alteration	87.5	12.5	0.0
N=	16	15	1	0	IN- boring	93.8	6.3	0.0

	total #shells	score = 0	score = 1	score = 2	**TBD-3770 Carbonate-rich**	score=0 %	score=1 %	score=2 %
N=	138	4	108	26	fragmentation	3	78.3	18.8
N=	138	21	94	23	EX- fine alteration	15.2	68.1	16.7
N=	138	105	15	18	EX- boring	76.1	10.9	13.0
N=	111	38	43	30	edge modification	34.2	38.7	27.0
N=	111	56	45	10	IN- fine alteration	50.5	40.5	9.0
N=	111	92	12	7	IN- boring	82.9	10.8	6.3

	total #shells	score = 0	score = 1	score = 2	**TBD-3800 Carbonate-rich**	score=0 %	score=1 %	score=2 %
N=	125	4	99	22	fragmentation	3	79.2	17.6
N=	125	45	69	11	EX- fine alteration	36.0	55.2	8.8
N=	125	94	23	8	EX- boring	75.2	18.4	6.4
N=	109	55	37	17	edge modification	50.5	33.9	15.6
N=	109	62	43	4	IN- fine alteration	56.9	39.4	3.7
N=	109	90	12	7	IN- boring	82.6	11.0	6.4

	total #shells	score = 0	score = 1	score = 2	**TBD-4018 Carbonate-rich**	score=0 %	score=1 %	score=2 %
N=	214	6	187	21	fragmentation	3	87.4	9.8
N=	214	87	104	23	EX- fine alteration	40.7	48.6	10.7
N=	214	121	44	49	EX- boring	56.5	20.6	22.9
N=	188	78	65	45	edge modification	41.5	34.6	23.9
N=	188	92	81	15	IN- fine alteration	48.9	43.1	8.0
N=	188	125	41	22	IN- boring	66.5	21.8	11.7

	total #shells	score = 0	score = 1	score = 2	**TBD-3524 Carbonate-rich**	score=0 %	score=1 %	score=2 %
N=	23	1	18	4	fragmentation	4	78.3	17.4
N=	23	18	3	2	EX- fine alteration	78.3	13.0	8.7
N=	23	22	1	0	EX- boring	95.7	4.3	0.0
N=	17	5	12	0	edge modification	29.4	70.6	0.0
N=	17	15	2	0	IN- fine alteration	88.2	11.8	0.0
N=	17	17	0	0	IN- boring	100.0	0.0	0.0

	total #shells	score = 0	score = 1	score = 2	**TBD-3413 Phosphate-rich**	score=0 %	score=1 %	score=2 %
N=	134	2	62	70	fragmentation	1.5	46.3	52.2
N=	134	4	38	92	EX- fine alteration	3.0	28.4	68.7
N=	134	28	29	77	EX- boring	20.9	21.6	57.5
N=	88	1	31	56	edge modification	1.1	35.2	63.6
N=	88	15	37	36	IN- fine alteration	17.0	42.0	40.9
N=	88	22	25	41	IN- boring	25.0	28.4	46.6

	total #shells	score = 0	score = 1	score = 2	**TBD-3563 Phosphate-rich**	score=0 %	score=1 %	score=2 %
N=	66	0	32	34	fragmentation	0	48.5	51.5
N=	66	1	31	34	EX- fine alteration	1.5	47.0	51.5
N=	66	44	10	12	EX- boring	66.7	15.2	18.2
N=	39	4	21	14	edge modification	10.3	53.8	35.9
N=	39	2	32	5	IN- fine alteration	5.1	82.1	12.8
N=	39	29	8	2	IN- boring	74.4	20.5	5.1

	total #shells	score = 0	score = 1	score = 2	**TBD-3710 Phosphate-rich**	score=0 %	score=1 %	score=2 %
N=	77	0	39	38	fragmentation	0	50.6	49.4
N=	77	2	35	40	EX- fine alteration	2.6	45.5	51.9
N=	77	16	34	27	EX- boring	20.8	44.2	35.1
N=	46	1	15	30	edge modification	2.2	32.6	65.2
N=	46	4	26	16	IN- fine alteration	8.7	56.5	34.8
N=	46	6	23	17	IN- boring	13.0	50.0	37.0

APPENDIX 3.3 feeding typed and life styles for Benguela species

life habitats / feeding strategies
Epi=epifauna
B=burrower
sB=shallow burrower
dB=deep burrower
SF=suspension feeder
DF=deposit feeder
Ch=chemoautotroph
Car=carnivore
NCar=non carnivore
MF=mixed feeding modes

Ch=chemoautotroph
=only those lucinid species that exhibit an internal shell partition mark as described by Taylor and Glover, 1997

Ecological information from:
1. Kilburn and Rippey
Sea Shells of Southern Africa
2. Valentine et al., 2002

Taxonomic identification from:
1. Kilburn and Rippey
Sea Shells of Southern Africa
2. John Pether, DeBeers Marine
personal shell collection
3. Moore, 1969
Treatise on invertebrate paleontology

BENGUELA -Bivalve species	**life habitat-feeding mode**
Dosinia lupinus	B, SF
Lucinoma capensis	dB, Ch
Tellina sp. (no rib-triangular)	dB, MF
Tellina sp. (with internal rib)	dB, MF
Carditella similis	Epi-sB, SF
Cardiid sp.1	sB, SF
Carditella sp. (no lateral tooth)	Epi-sB, SF
Trapeziid sp.	B, SF
Nuculana spp.	dB, DF
Nucula nucleus	sB, DF
Pitar sp.	B, SF
Anomiid sp.	Epi, SF
Loripes sp.	dB, SF
Limopsis chuni	sB, SF
Malleidae sp.	Epi, SF
Mallediae cf. *Vulsella* sp.	Epi, SF
Veneropsis sp.	B, SF
Mactra cf. glabrata sp.	B, DF
Mytilidae sp.	Epi, SF
Arcid sp.1	Epi-sB, SF
Pteriid - straight hinge	Epi, SF
Nucinella cf. treatise N269 (Wood, 1851)	Epi-sB, SF
Crassostrea sp.	Epi, SF
subfamily Lutrarianae	dB,SF
Pectinid (radial ribs)	Epi, SF
Anodontia sp.	dB, SF
mussel (transparent)	Epi, SF
Mytilidae sp. cf. *Modiolus* sp.	Epi, SF
Tellina sp. (no rib, elongate)	dB, MF
Parvicardium sp.	sB, SF
Cardiid cf. *Fulvia*	sB, SF
Glycymeris sp.	sB, SF
Corbula rugifera	sB, SF
subfamily Mactridae	B,SF
Pectinidae, Eburneopecten group	Epi, SF
Lasaeidae cf. *Lasaea* sp.	Epi, SF

BENGUELA -Bivalve species (continued)	**life habitat-feeding mode**
Pectinid sp. 1	Epi, SF
Pteriid sp.	Epi, SF
Limaria sp.	Epi, SF
spiny Pteriid	Epi, SF
Arcid sp.1	Epi-sB, SF
"Corbula" sp.	sB, SF
Venerid sp. 1	sB, SF
Venerid sp. 2	sB, SF
Venerid sp. 3	sB, SF
Venerid sp. 4	sB, SF
Venerid sp. 5	sB, SF
Veneroida sp. cf. *Lasaeidae*	sB, SF
Chlamys sp. Cf. coruscans	Epi, SF
UNIDENTIFIED bivalves	
strong beak (concentric ribs)	
Venerid? sp. (pronounced teeth)	

BENGUELA -Gastropod species	**life habitat-feeding mode**
Turritella decliris	Ncar
Natica sp.	Car
Volvarina sp.	Car-NCar
Nassarius vinetus	Car (primarily)
Fasciolaria/Nucella	Car
Calyptraea sp.	NCar
Gibbula sp.	NCar
Marginella sp.	Car-NCar
Comitas/Nassarius speciosus	Car
Volutocorbis sp.	Car
UNIDENTIFIED gastropods	
Gastropod sp. 1	
gastropod sp. wide	
gastropod sp.	
gastropod cf. *Alrocominella*	
long ribbed gastropod	
Whelk	
keeled gastropod	
internal ribbed gastropod?	
long hatch-ribbed gastropod	

APPENDIX 4.1 Macrofaunal count data for Mishash Fm.

BIOFACIES 2

sample YF A-43	no. individuals
Mesosaccella perdita	87
Mesosaccella larteti	53
Mesocallista andersoni	7
Caestocorbula sp. A	7
"Lucina" blanckenhorni	2
veneroid very fine-ribbed	1
total	157

sample YF A-49	no.
Mesosaccella larteti	32
Caestocorbula sp. A	5
rounded fine-ribbed venerid	4
Gyrodes asiatica	3
Mesocallista andersoni	3
Undiscala vicina	3
total	50

sample YF O-4	no.
Mesosaccella perdita	35
Mesosaccella larteti	22
"Lucina" blanckenhorni	5
Protocardia silicea	2
Gyrodes asiatica	1
total	65

sample YF A-36A	no.
Mesosaccella larteti	54
Mesocallista andersoni	17
Caestocorbula sp. A	12
Mesosaccella perdita	11
"Lucina" blanckenhorni	10
"Corbula" sp.	5
Gyrodes farafrensis	2
Eucyclomphalus sp.	1
total	112

sample YF A-42	no.
Mesosaccella larteti	102
"Lucina" blanckenhorni	7
Gyrodes asiatica	5
Undiscala vicina	2
"Corbula" sp.	2
Turritella reyi	2
cf. *Gegania picardi*	1
total	121

sample YF A-36	no. individuals
Mesosaccella larteti	45
Mesosaccella perdita	22
Mesocallista andersoni	14
Caestocorbula sp. A	11
"Lucina" blanckenhorni	6
Eucyclomphalus sp.	4
"Corbula" sp.	4
"Meretrix" sp. A	2
Mesocallista(?) rohlfsi?	1
Gyrodes farafrensis	1
total	110

sample YF A-43	no.
Eucyclomphalus sp.	97
Nannonavis parallelus	13
Mesosaccella larteti	7
"Lucina" blanckenhorni	4
"Corbula" sp.	4
Gyrodes farafrensis	4
Undiscala goryi	2
Caestocorbula sp. A	2
cf. *Scala* sp. (radial-rib wide-apical)	1
total	134

sample YF A-40	no.
Eucyclomphalus sp.	44
"Meretrix" sp. A	16
Mesosaccella larteti	14
Mesosaccella perdita	13
Mesocallista andersoni	7
Caestocorbula sp. A	7
Anomalofusus turris?	3
Nucula tenera	1
total	105

BIOFACIES 3

sample YF O-7B		no. individuals
Caestocorbula sp. A		26
"Lucina" blanckenhorni		18
Crassatella rothi		13
Protocardia silicea		12
heterodont = *Crassatella?*		11
"Meretrix" sp. A		6
Parmicorbula subelegans		6
Nannonavis parallelus		4
Mesosaccella grovei?		3
venerid *(Mesocallista andersoni* ?)		3
Mesosaccella larteti		2
Pycnodonte? sp.		1
Undiscala vicina		1
arcoid - *Limopsis*? sp.		1
?Crassatella cf. zitteli		1
cf. Tellinella sp.		1
	total	109

sample YF A-58		no.
Caestocorbula sp. A		32
"Meretrix" sp. A		26
Turritella reyi		14
Mesocallista andersoni		11
Crassatella rothi		8
Mesosaccella perdita		7
"Corbula" (Flexicorbula) vokesi		6
Mesocallista (?) *rohlfsi*		4
Mesosaccella larteti		4
Undiscala vicina?		3
Nanonavis parallelus		3
Aporrhaid sp.		3
Nucula tenera		2
"Lucina" blanckenhorni?		1
bivalve species with lunule		1
	total	125

sample YF O-5		no.
Mesosaccella perdita		24
"Meretrix" sp. A		24
Mesosaccella larteti		21
Undiscala vicina		20
Caestocorbula sp. A		3
"Lucina" blanckenhorni		3
Mesosaccella grovei		2
Nannonavis parallelus		1
Gyrodes asiatica		1
unidentified ?venerid? sp.		1
	total	100

sample YF O-7A		no.
Undiscala vicina		25
"Lucina" blanckenhorni		12
Gyrodes asiatica		11
Mesocallista andersoni		9
Caestocorbula sp. A		9
"Meretrix" sp. A		8
Parmicorbula subelegans		6
Gyrodes farafrensis		4
Eucyclomphalus sp.		3
Mesosaccella larteti		3
Nuculana-like (gape, inflated)		2
Mesosaccella grovei		1
"whelk" with fine spiral ribs		1
Mesosaccella perdita		1
"whelk" - knobby		1
	total	96

BIOFACIES 3

sample YF O-6	no. individuals
"Meretrix" sp. A	20
Mesosaccella larteti	16
"Lucina" blanckenhorni	13
Mesocallista (?) *rohlfsi?*	10
Undiscala vicina	9
heterodont / venerid sp?	8
Mesocallista andersoni	7
Arcoida sp. A	6
"Corbula" sp.	3
Caestocorbula sp. A	2
Nannonavis parallelus	2
high spired =*Turritella?* sp.	1
Eucyclomphalus *sp.*	1
total	98

sample YF O-8	no.
Caestocorbula sp. A	36
Parmicorbula subelegans?	30
Nucula tenera	20
Turritella reyi	7
Undiscala vicina	4
Mesosaccella sp.	4
Mesocallista andersoni	4
Nannonavis parallelus	4
"Lucina" blanckenhorni	3
Mesosaccella larteti	3
Gyrodes farafrensis	2
"Meretrix" sp. A	2
Fasciulariid	1
total	120

sample YF M-2	no.
Nannonavis parallelus	22
Turritella reyi	16
Caestocorbula sp. A	15
Eucyclomphalus sp.	14
"Corbula" sp.	10
Mesosaccella perdita	5
Nucula tenera	5
"Meretrix" sp. A	3
Gyrodes farafrensis	3
Undiscala vicina?	3
"Lucina" blanckenhorni	2
Mesocallista (?) *rohlfsi*	2
Aporrhaid sp.	2
"Lucina" sp. (wide ribbing)	1
Mesosaccella larteti	1
Bonellitia scaberrima	1
total	105

BIOFACIES 4

sample YF O-6A	no. individuals
Mesosaccella perdita	43
"Meretrix" sp. A	12
Caestocorbula sp. A	10
Undiscala vicina	8
Nannonavis parallelus	6
Nucula tenera	6
"Corbula" sp.	6
Mesosaccella grovei	5
Mesosaccella larteti	5
Protocardia silicea	4
Vanikoro asiatica	4
Turritella reyi	2
Gyrodes asiatica	2
Mesocallista andersoni	1
siphon-bearing gastropod	1
Cardiomya sp.	1
"Lucina" blanckenhorni	1
Turritella quadeicincta	1
Pycnodonte sp.	1
Eucyclomphalus sp.	1
Noetiidae? (Arcoid)	1
Mesocallista (?) *rohlfsi*	1
total	122

sample YF O-8C	no.
"Meretrix" sp. A	40
"Corbula" sp.	28
Caestocorbula sp. A	24
Mesocallista (?) *rohlfsi*	17
Nucula tenera	16
Nannonavis parallelus	7
Mesosaccella larteti	7
Mesosaccella perdita	6
Mesocallista andersoni	5
"Lucina" blanckenhorni	4
Turritella reyi	4
Undiscala vicina	4
whorl of smooth gastropod (*Gyrodes ?*)	4
large, lateral hinge = lucinid n. sp.	3
?Plicatula sp.	1
Cardium sp. A (fine rib)	1
myoidea? straight hinge, orthogyrate	1
Gyrodes sp.	1
high angled gastropod with knobby ridge	1
Fasciulariid?/buccinid?	1
small-symmetrical bivalve, no shoulders	1
total	176

sample YF M-1	no.
Caestocorbula sp. A	20
"Corbula" sp.	16
"Lucina" sp. (wide ribbing)	12
Gyrodes asiatica	11
large veneroid sp.	5
Turritella reyi	5
Mesocallista andersoni	5
Protocardia silicea	4
Crassatella sp.	4
Plicatula sp.	3
smooth, ?*Eucyclomphalus sp.*	3
Undiscala vicina?	2
Volutomorpha sp.	2
"Lucina" blanckenhorni	2
Veniella sp.	1
long siphon gastropod -high spired	1
Nucula tenera	1
Rastellum diluvianum	1
Aporrhaid sp.?-diagonal ribbing	1
Mesosaccella sp.	1
total	100

sample YF A-59	no.
Caestocorbula sp. A	37
Mesocallista andersoni	18
Nucula tenera	12
"Meretrix" sp. A	12
venerid sp.	4
Mesosaccella larteti	3
Pycnodonte sp.	3
Turritella sp.	3
Parmicorbula subelegans?	3
Gyrodes asiatica	2
fine-ribbed lucinid sp.	2
Nannonavis parallelus	2
Mesosaccella perdita	2
Tellinid-like sp.	1
Undiscala goryi	1
coarse-ribbed bivalve (37mm)	1
Crassatella sp.	1
cardiid sp. B	1
very inflated (not tellinid)	1
total	109

BIOFACIES 4

sample YF A-55		no. individuals
Caestocorbula sp. A		35
Nucula tenera		15
Mesosaccella larteti		11
Undiscala goryi		10
Nanonavis parallelus		9
Gyrodes asiatica		7
"Meretrix" sp. A		7
Mesocallista andersoni		5
Volutomorpha sp.		3
Cardium sp.		2
Mesocallista (?) *rohlfsi* ?		2
"Lucina" blanckenhorni		2
"Corbula" (Flexicorbula) vokesi		2
Mesosaccella perdita		2
Aporrhaid sp.		1
Turritella reyi		1
Crassatella rothi		1
"Mytilus" nov sp.		1
Diptygmendon elliotti		1
large venerid sp. (strong ribs)		1
Mesosaccella sp.		1
	total	119

APPENDIX 4.2 macrofaunal count data from Benguela samples

BIOFACIES 1

TBD-3441	no. individuals
Lucinoma capensis	68
total	68

TBD-4033	no.
Lucinoma capensis	68
gastropod sp.1	1
*Lucinoma? s*p.	1
total	70

TBD-3741	no.
Lucinoma capensis	8
total	8

BIOFACIES 2

TBD-3519	no.
Lucinoma capensis	86
Carditella similis	11
Gastropod sp.1	4
Dosinia? sp.	3
Tellina sp. *(* fragment-no rib)	2
?"Mytilus"?	1
total	107

TBD-3955	no.
Lucinoma capensis	78
gastropod sp. 1	5
Dosinia lupinus	3
cf. *Anodontia?*	2
Nuculana sp.	1
Tellina sp. (no rib-triangular)	1
total	90

BIOFACIES 3

TBD-3770	no. individuals
Carditella sp. (no lateral teeth)	89
Cardiid sp.1	15
Carditella similis	12
Nassarius? sp.	9
Tellina sp. (no rib-triangular)	9
subfamily Lutrariinae	7
Lucinoma capensis	4
Dosinia lupinus	3
Tellina sp. (with internal rib)	3
Mytilidae sp. cf. *Modiolus* sp.	2
long ribbed gastropod	2
Veneroida sp. cf. Lasaeidae? sp.	1
Loripes sp.	1
Volvarina? sp.	1
Natica sp.	1
Venerid sp. 5	1
total	160

TBD-3800	no. individuals
Carditella sp. (no lateral teeth)	117
Cardiid sp.1	5
Nassarius? s p.	4
Tellina sp. (with internal rib)	4
Tellina sp. (no rib-triangular)	4
Carditella similis	4
Lucinoma capensis	3
Veneropsis sp.	2
Pteriid - straight hinge	2
Volvarina? sp.	2
Pectinid sp. 1	1
Natica sp.	1
Trapezium sp.	1
Loripes sp.	1
total	151

TBD-4018	no. individuals
Carditella sp. (no lateral teeth)	146
Carditella similis	62
Lucinoma capensis	14
Cardiid sp.1	12
Tellina sp. (no rib-triangular)	11
Tellina sp. (with internal rib)	10
Dosinia lupinus	8
gastropod cf. *Alrocominella* sp.	6
Nassarius? sp.	3
Trapezium? *s* p.	3
subfamily Lutrariinae	3
Mytilidae sp. cf. *Modiolus* sp.	2
Chlamys sp. cf. *coruscans* sp.	2
Pitar sp.	2
Pteriid - straight hinge	2
Marginella? sp.	2
Volvarina? sp.	2
long ribbed gastropod	1
long hatch-ribbed gastropod	1
Nucula nucleus	1
Pectinid sp. 1	1
total	294

BIOFACIES 4

TBD-3413	no. individuals
Dosinia lupinus	57
Carditella similis	45
Tellina sp. (no rib-triangular)	13
Mactra cf. glabrata	10
Cardiid sp.1	7
Turritella decliris	5
Loripes sp.	4
Mytilidae sp. cf. *Modiolus* sp.	3
Trapeziid sp.	3
Nuculana belcheri	2
Anomiid sp.	2
Pteriid sp. straight hinge	2
Gastropoda sp. 1	2
Nucula nucleus	2
Lucinoma capensis	2
Carditella sp. (no lateral teeth)	2
Natica? sp.	1
Gibbula? sp.	1
Whelk	1
Calyptraea?	1
Marginella? sp.	1
Pitar sp.	1
Venerid sp. 1	1
Venerid sp. 2	1
Venerid sp. 3	1
Venerid sp. 4	1
corbulid sp.	1
total	172

TBD-3710	no. individuals
Dosinia lupinus	59
Nuculana sp.	17
Pitar sp.	15
Carditella similis	11
Nucula sp.	8
Tellina sp. (no rib-triangular)	8
Lucinoma capensis	8
Malleidae sp.	5
Mallediae cf. Vulsella? sp.	3
Fasciolaria//Nucella?	3
Nassarius vinetus?	3
cardiid sp.	2
Pteriid sp. straight hinge	2
Veneropsis? sp.	2
strong beak (concentric ribs)	2
Carditella sp. (no lateral teeth)	2
Volutocorbis? sp.	1
Comitas?/Nassarius speciosus	1
Turritella decliris	1
Arcid sp.1	1
total	154

BIOFACIES 4

TBD-3563	no. individuals
Lucinoma capensis	33
Tellina sp. (no rib-triangular)	27
Trapeziid sp.	22
Nassarius vinetus	21
Tellina sp. (with internal rib)	8
Limopsis chuni	6
Nucinella cf. treatise N269	5
gastropod sp. wide	3
Crassostrea? sp.	3
Turritella decliris	2
Volvarina? sp.	2
Arcid sp.2	2
Natica sp.	2
Carditella similis	2
Lutraria? sp.	1
Venerid? sp. (pronounced teeth)	1
keeled gastropod	1
Mytilidae sp. cf. *Modiolus* sp.	1
Nuculana sp.	1
Loripes sp.	1
Limaria sp.	1
Pectinid sp. 1	1
Anomiid sp.	1
internal ribbed gastropod	1
transparent frag (mussel?)	1
spiny Pteriid	1
Pteriid sp. straight hinge	1
total	151

APPENDIX 5. FIGURES

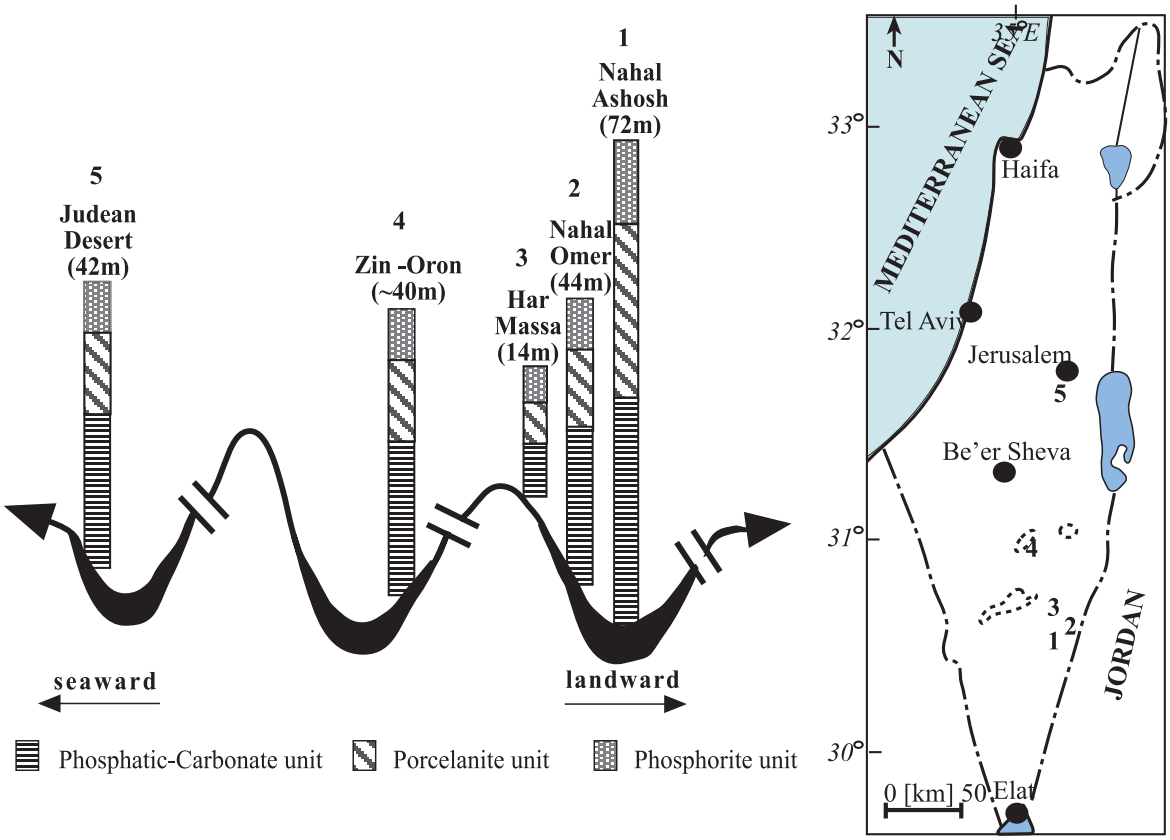

Figure 1.1: Location map of five measured sections of Upper Campanian Mishash Fm in Israel and NW-SE section across the folded ramp-shelf. Schematic bathymetry during the deposition of the Phosphate Member and its three sub-units. Maktesh-"crater" structures are sketched in dotted line. Thickness of the Phosphate Member is given in meters "(40m)".

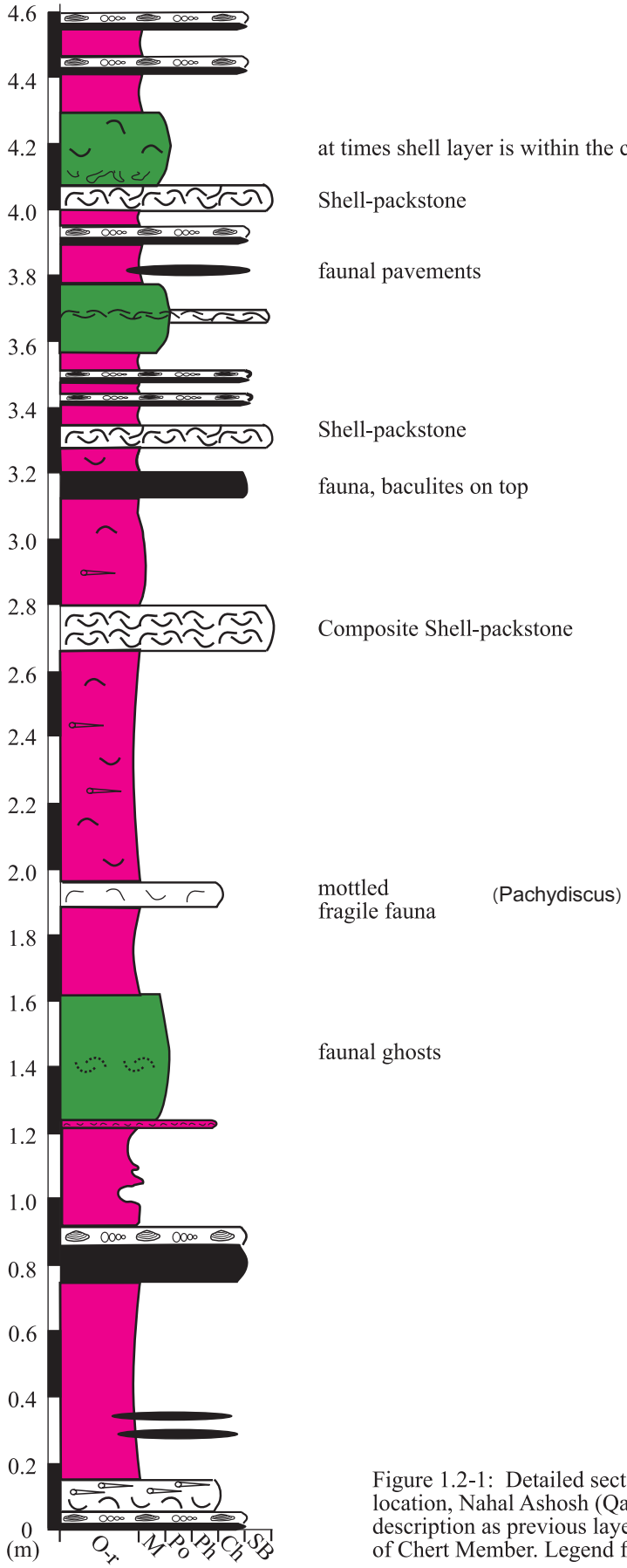

Figure 1.2-1: Detailed section description of paleolow location, Nahal Ashosh (Qazra sub-basin). (same)=same description as previous layer. Description starts from top of Chert Member. Legend for figures 1.2-1.3

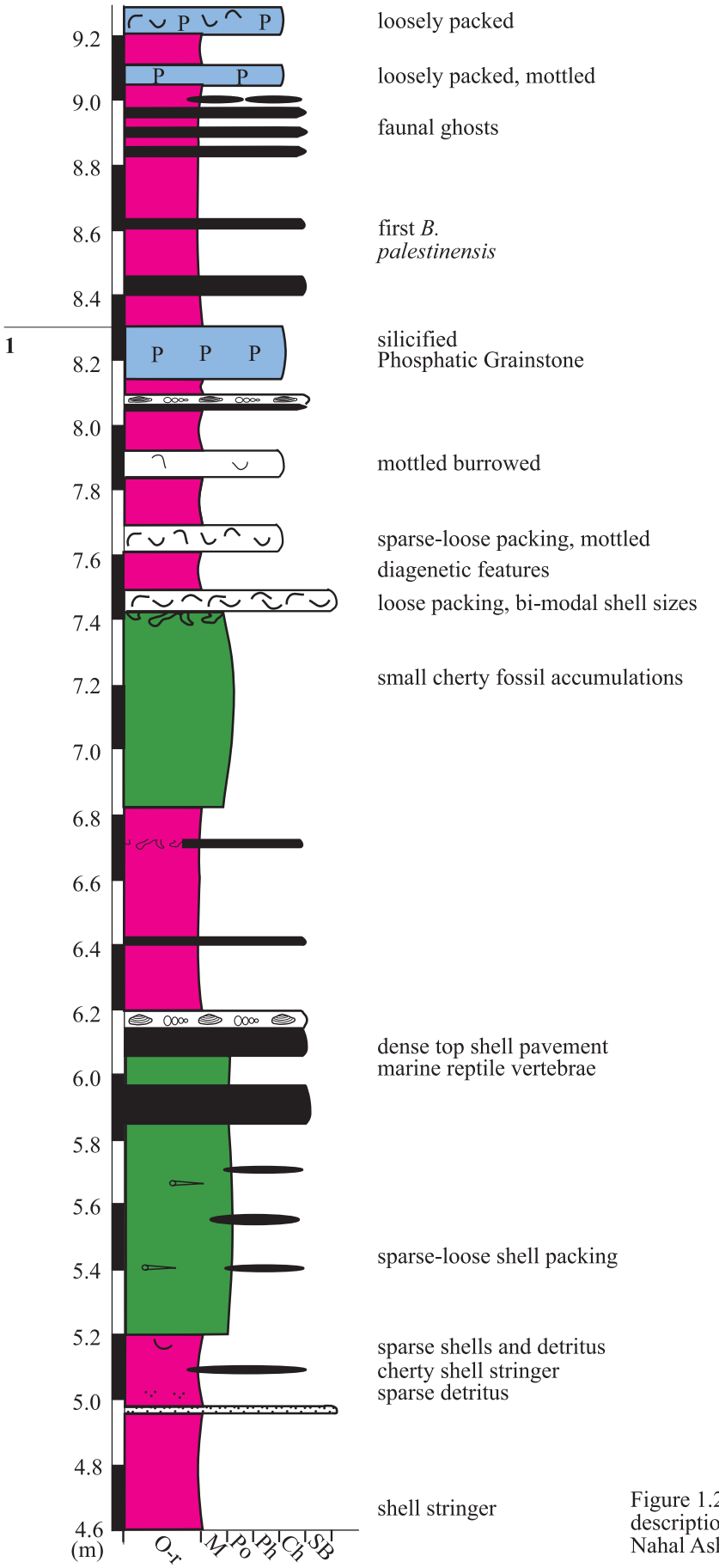

Figure 1.2-2: Detailed section description of paleolow location, Nahal Ashosh (Qazra sub-basin).

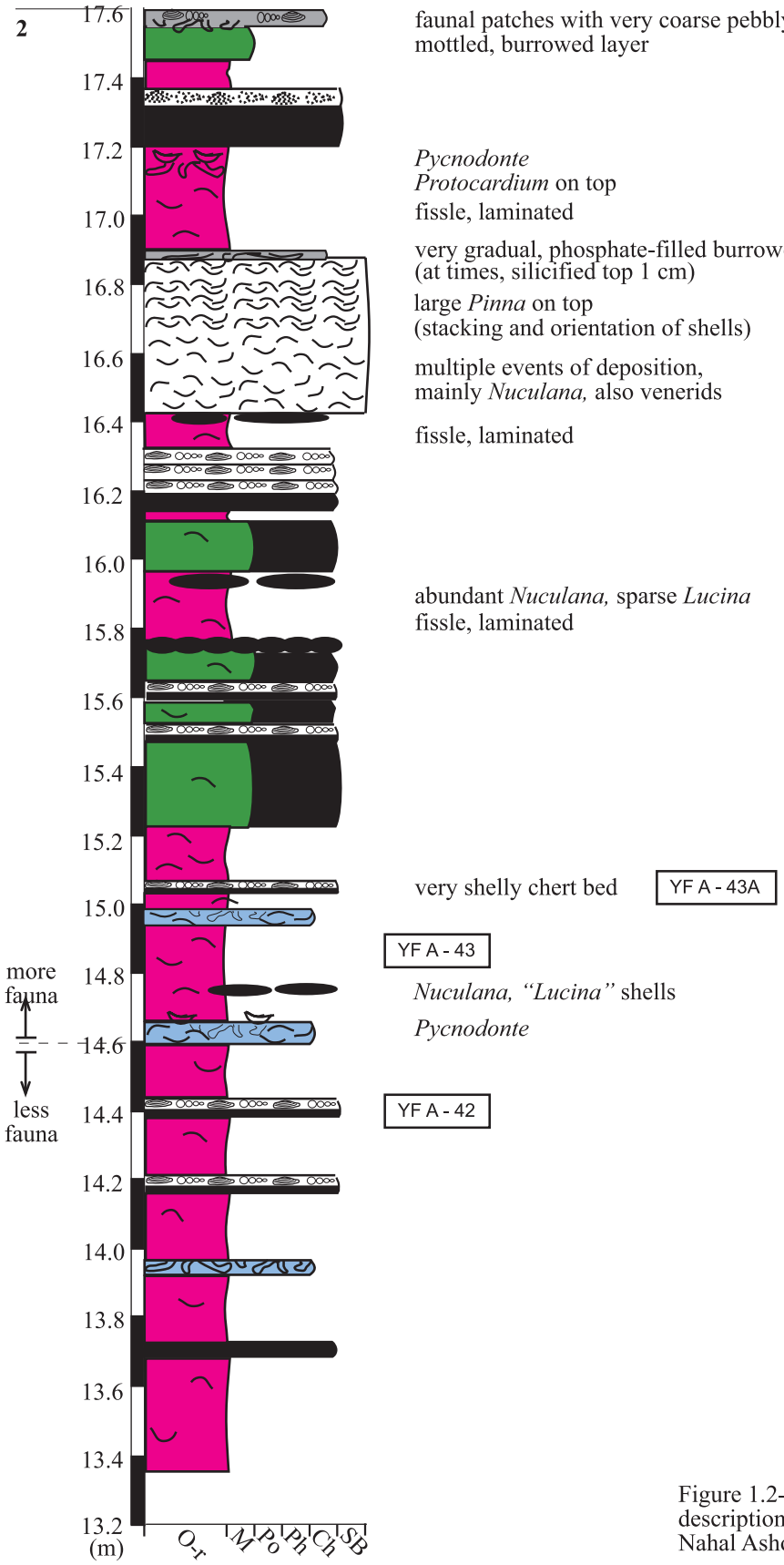

Figure 1.2-4: Detailed section description of paleolow location, Nahal Ashosh (Qazra sub-basin).

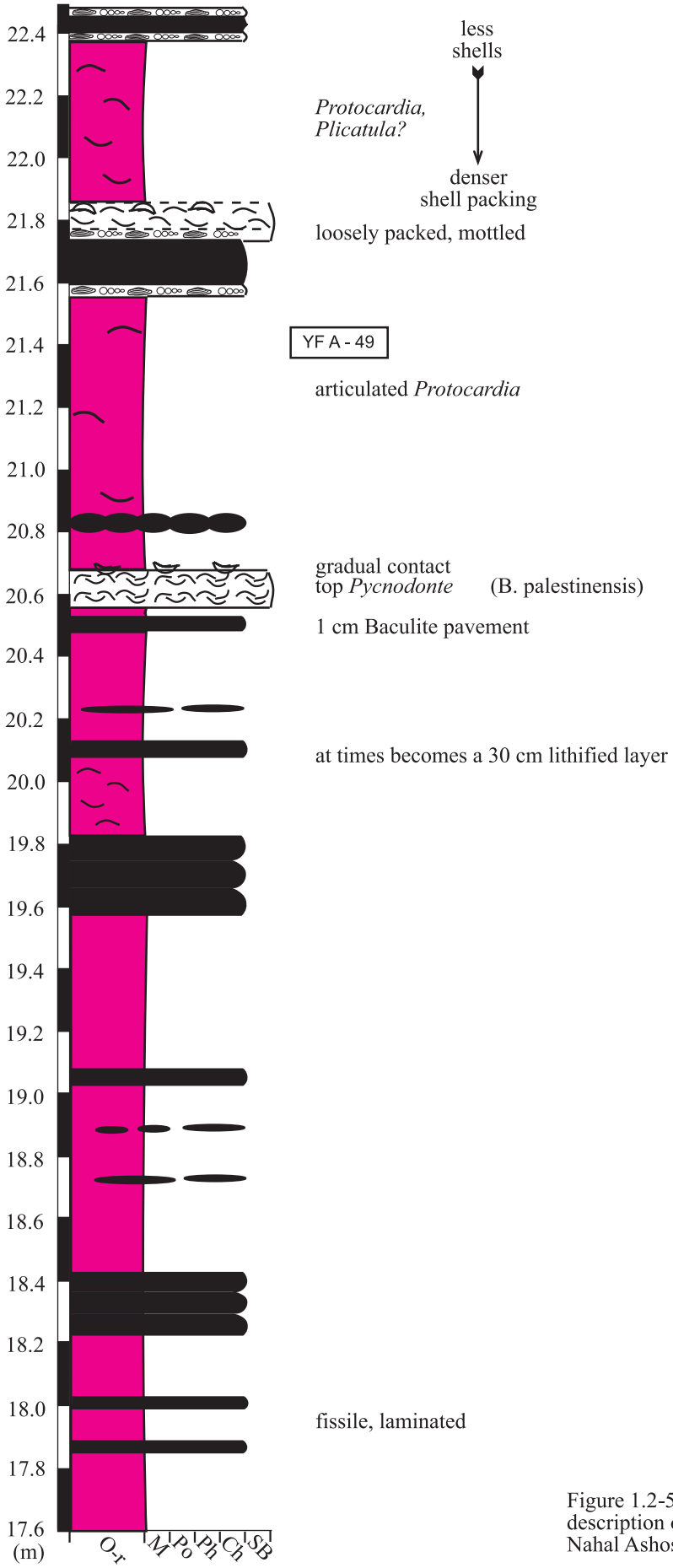

Figure 1.2-5: Detailed section description of paleolow location, Nahal Ashosh (Qazra sub-basin).

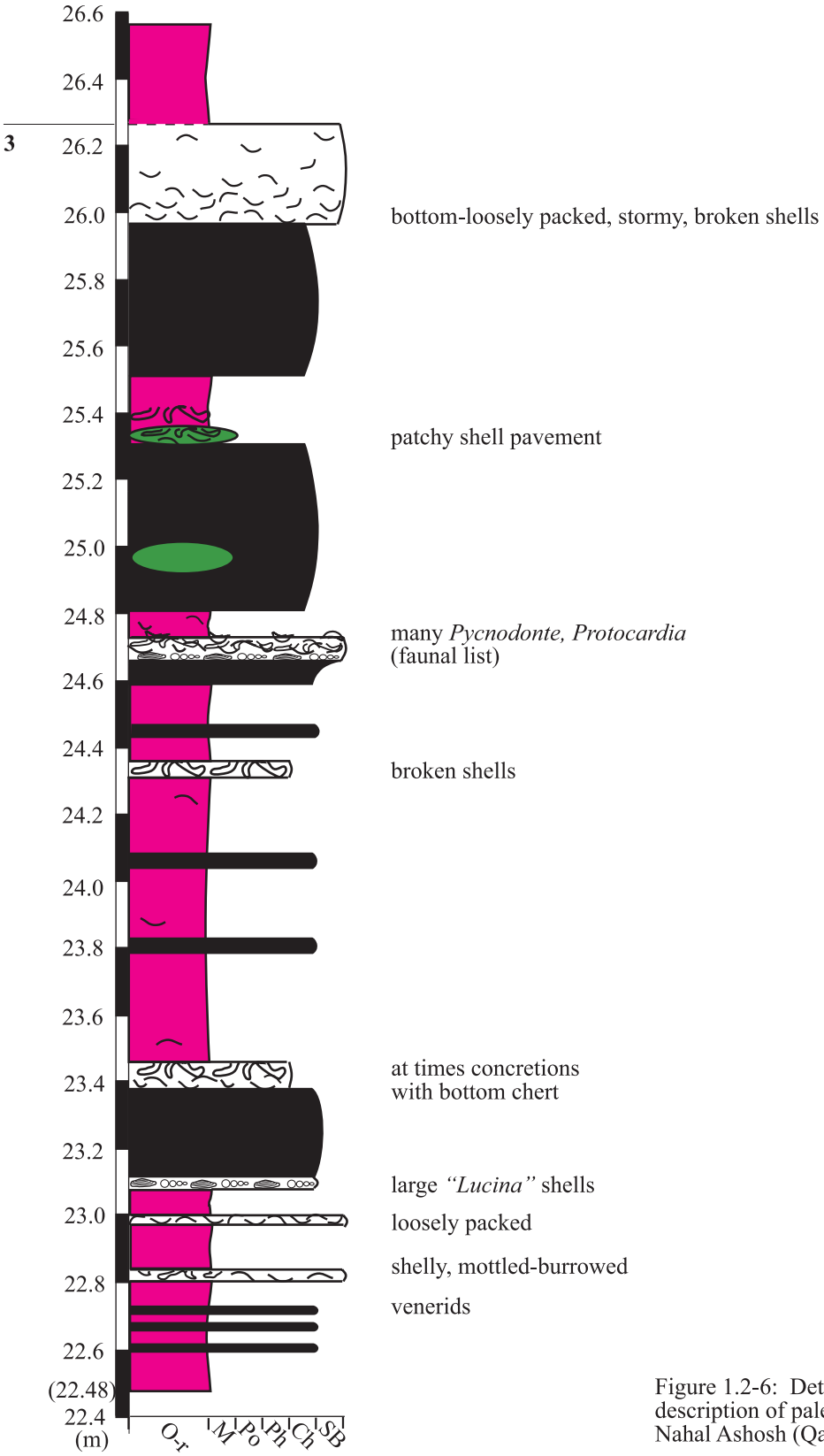

Figure 1.2-6: Detailed section description of paleolow location, Nahal Ashosh (Qazra sub-basin).

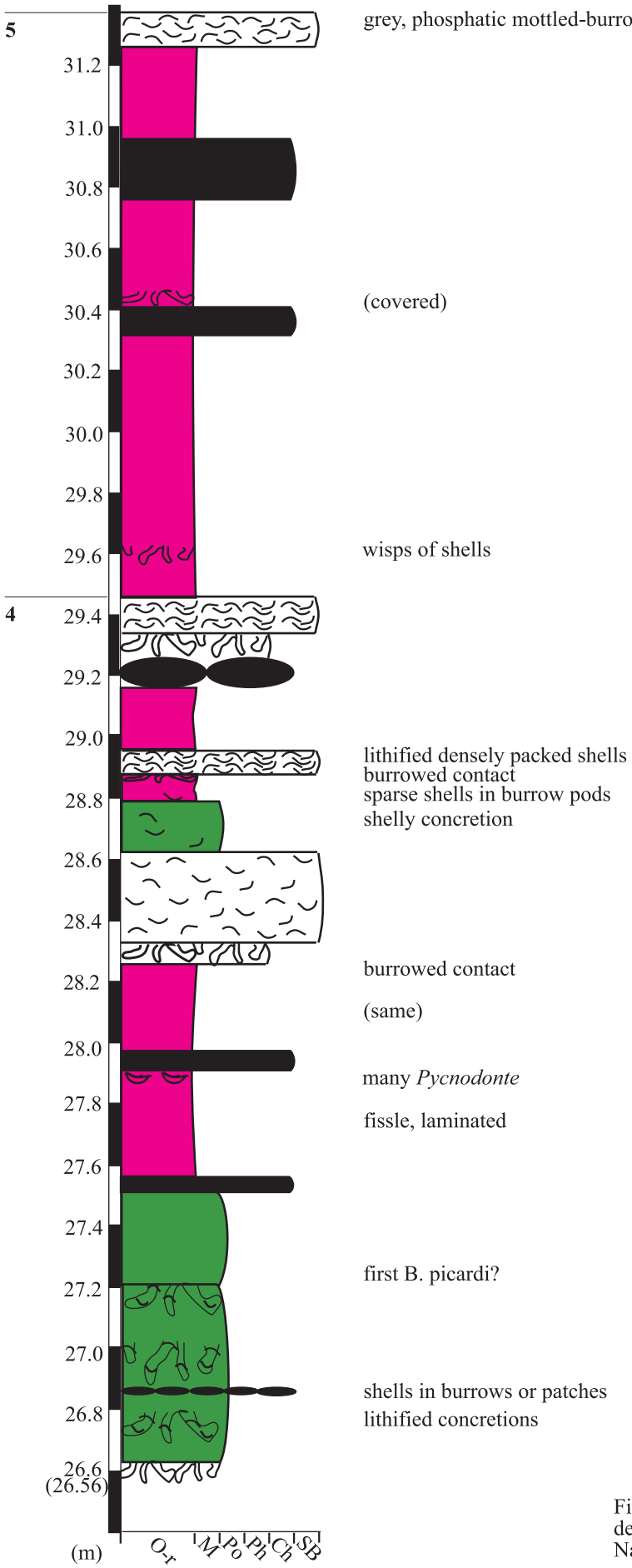

Figure 1.2-7: Detailed section description of paleolow location, Nahal Ashosh (Qazra sub-basin).

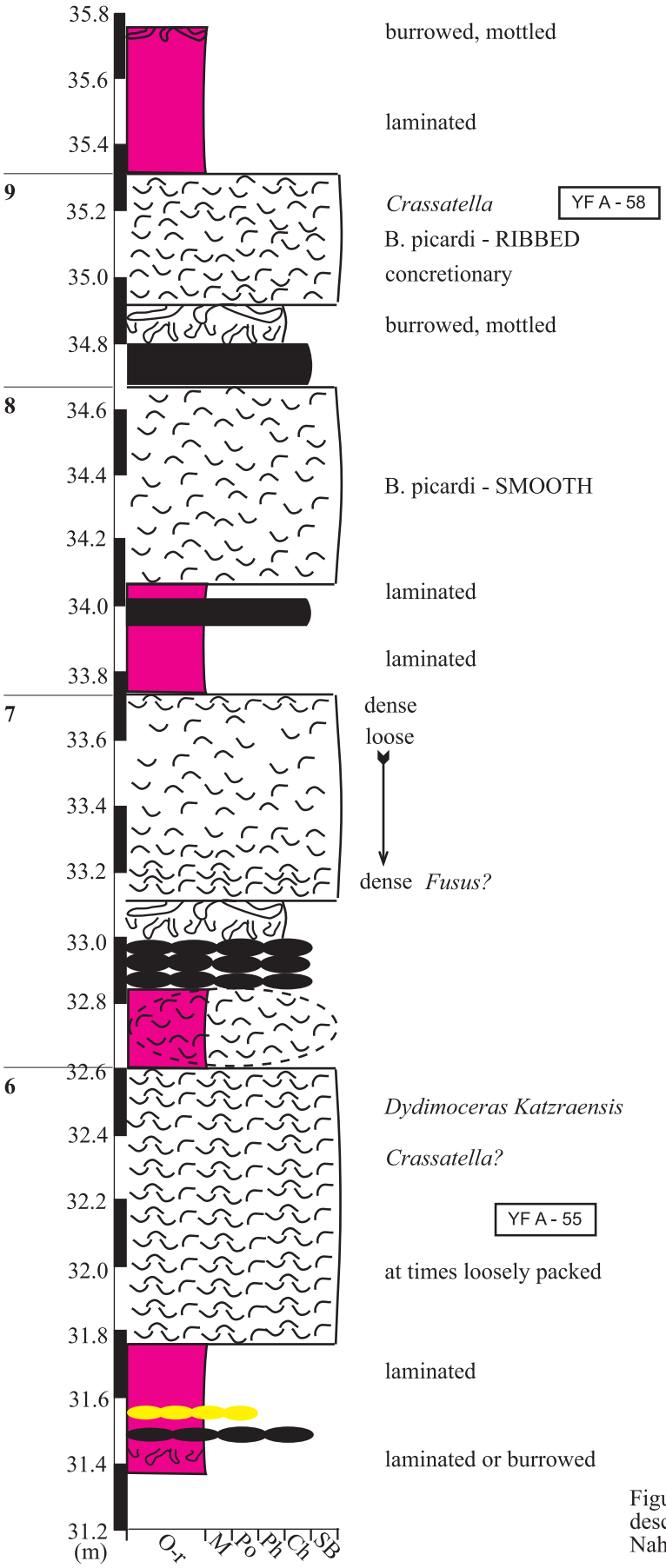

Figure 1.2-8: Detailed section description of paleolow location, Nahal Ashosh (Qazra sub-basin).

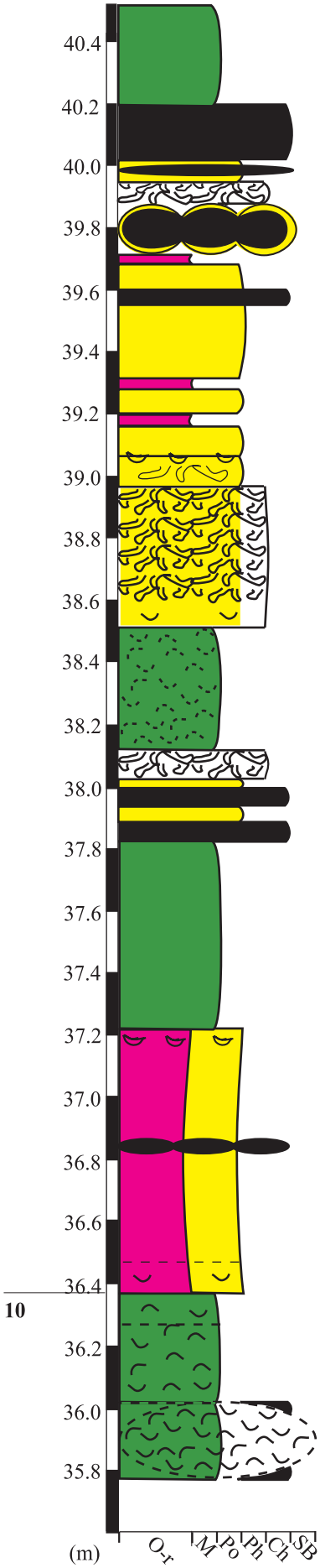

Figure 1.2-9: Detailed section description of paleolow location, Nahal Ashosh (Qazra sub-basin).

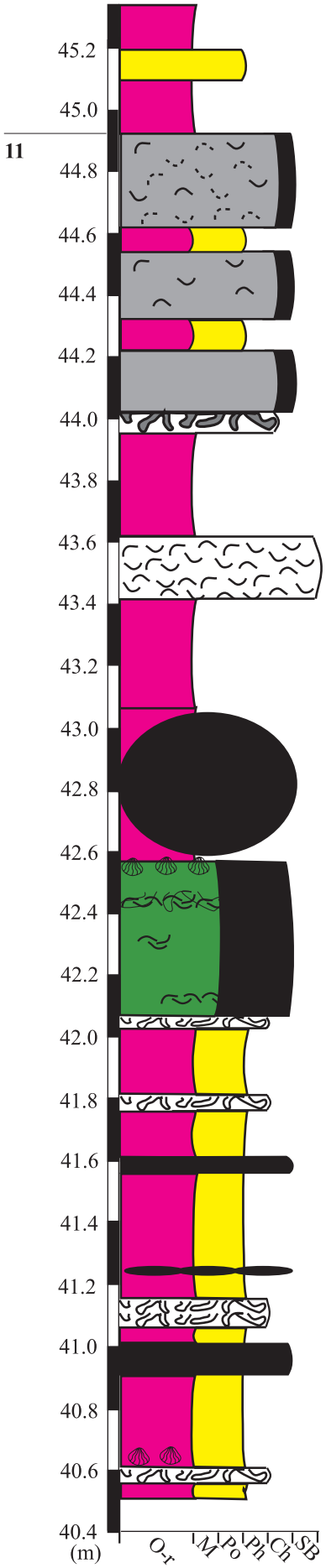

(same)

(medium bedding)

laminated, fine grained

top of phosphatic-carbonate Unit

shelly fragments/ghosts

sparse shells

burrowed contact
coarse, dark-grey silicified phosphate

white-grey, fine grained

hard, lithified

concretionary chert

many *Plicatula*
densely shell-filled burrows

dense-shelled stringers
mottled

many *Plicatula*

Figure 1.2-10: Detailed section description of paleolow location, Nahal Ashosh (Qazra sub-basin).

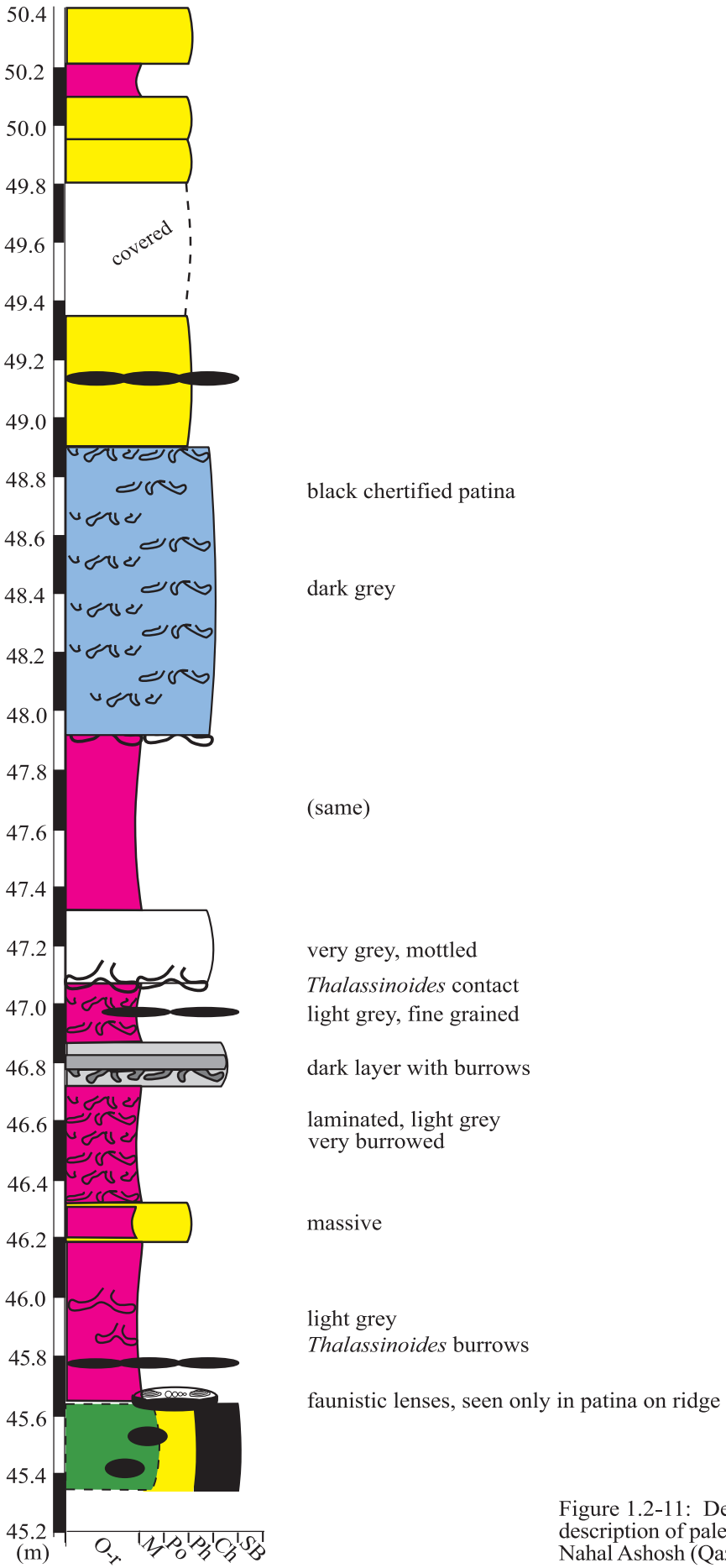

Figure 1.2-11: Detailed section description of paleolow location, Nahal Ashosh (Qazra sub-basin).

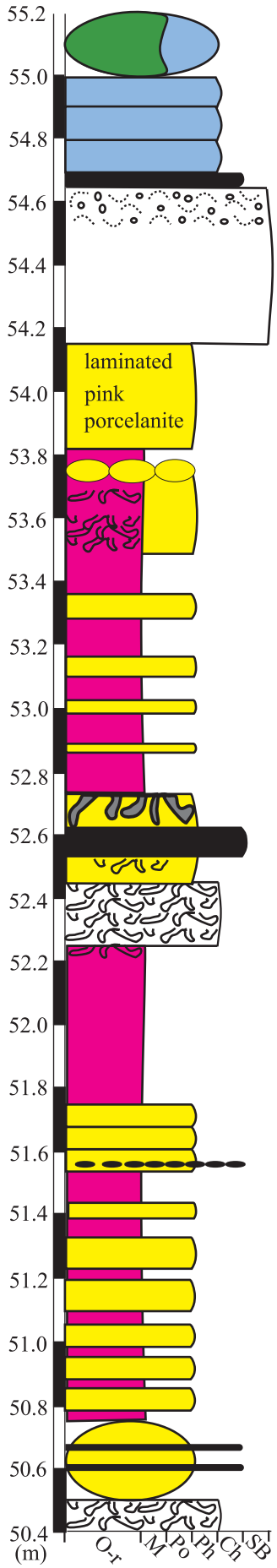

Inoceramus and bivalve ghosts
lithified concretions

grey, fine grained

white, fine grained

grey, coarse grained

top pebbly fragments, shell ghosts
boring in shells

hard lithified, grey layer

(same), grey, fine grained

burrowed/mottled

(same), pink-grey-orange

(same), pink-grey

laminated / mottled, medium grained

(same)
pink porcelanite
laminated / mottled
gradual contact
burrows filled with coarse phosphate

burrows

burrowed/mottled

grey-pink, mottled

laminated

(same)

(same)

(same)

(same)

(same)

laminated

concretionary

Figure 1.2-12: Detailed section description of paleolow location, Nahal Ashosh (Qazra sub-basin).

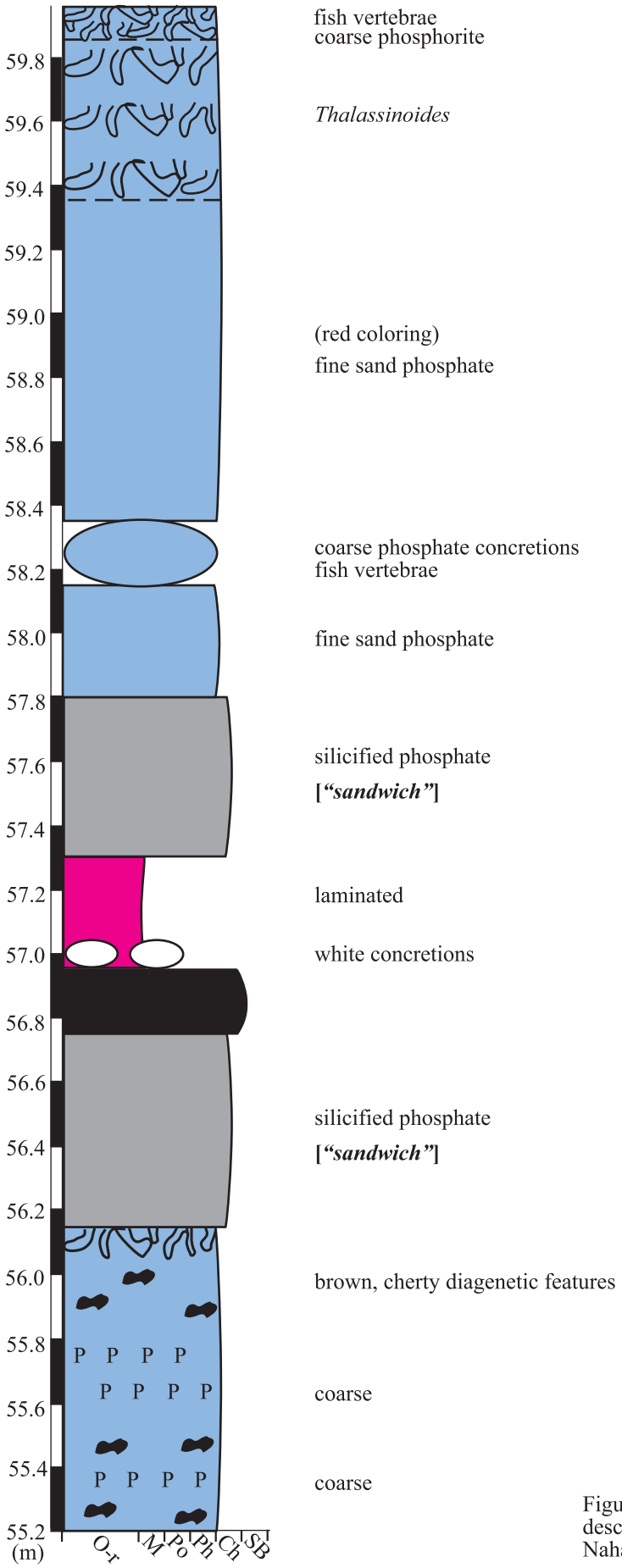

Figure 1.2-13: Detailed section description of paleolow location, Nahal Ashosh (Qazra sub-basin).

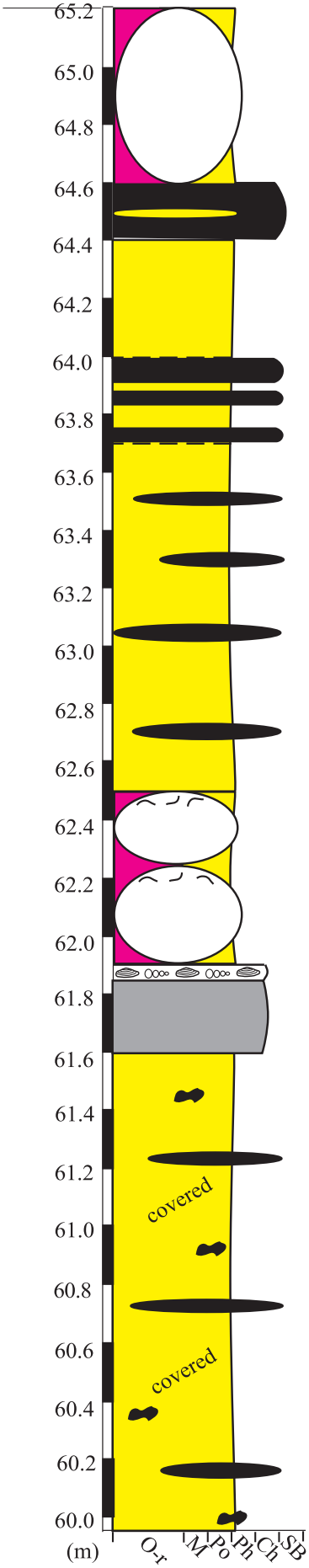

top of Porcelanite Unit

large concretions or 10cm of background

(same)

secondary gypsum on top

fossil ghosts?

(same) secondary gypsum within

shells on top of concretions

large *Lucina*
loosely packed silicified shell layer
mottled, coarse phosphate

brittle, laminated

Figure 1.2-14: Detailed section description of paleolow location, Nahal Ashosh (Qazra sub-basin).

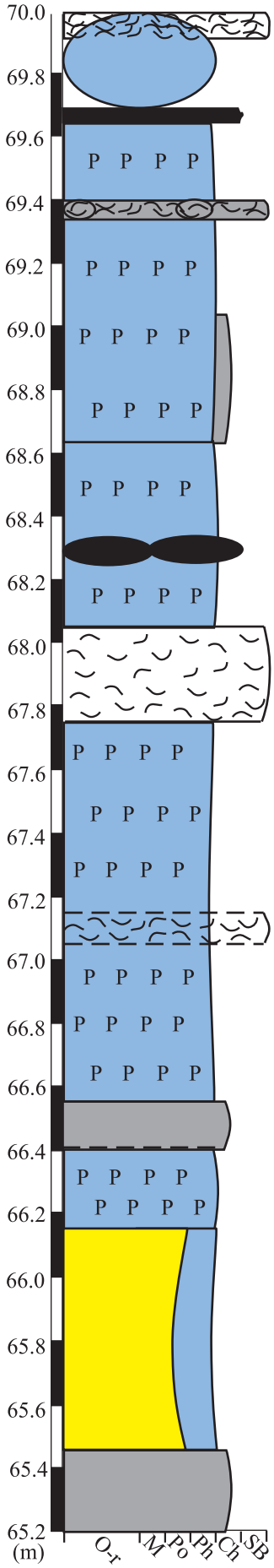

mainly *Nuculana*

coarse phosphate

(same) coarse, dark phosphate

(same) coarse, **silicified** phosphate
baculites and bivalve ghosts

(same)

(same) coarse, dark phosphate
white bone pebbles

Solenoceras humei

many fish remains

(same)
Libycoceras

Solenoceras humei

(same) coarse, dark phosphate
Libycoceras

many fish remains and vertebrae

very coarse, dark phosphate
white bone pebbles

silicified phosphate

Figure 1.2-15: Detailed section description of paleolow location, Nahal Ashosh (Qazra sub-basin).

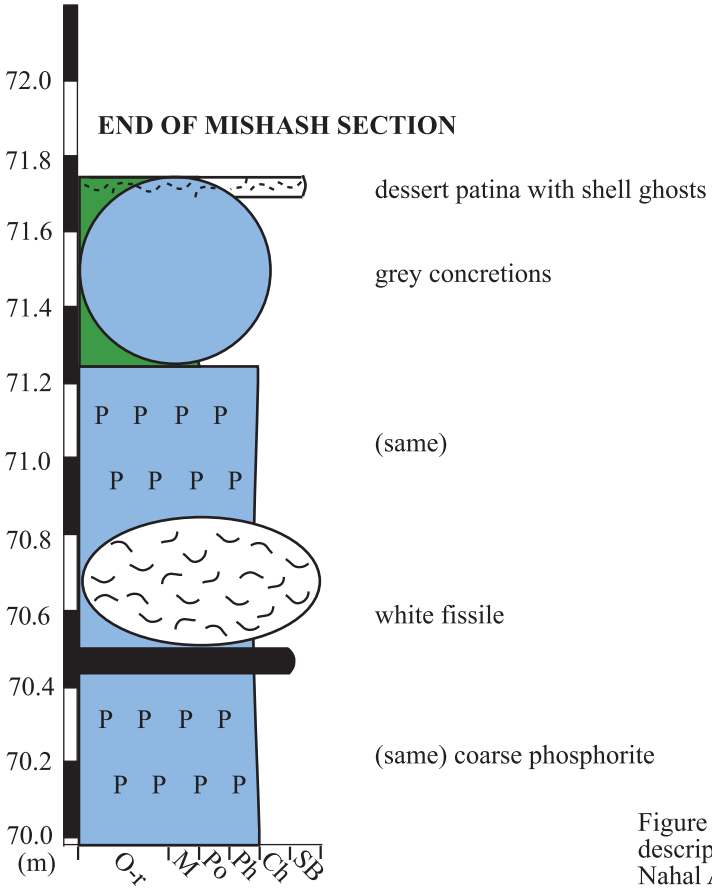

Figure 1.2-16: Detailed section description of paleolow location, Nahal Ashosh (Qazra sub-basin).

LEGEND

O-r = organic-rich
M = massive micrite
Po = porcelanite
Ph =phosphorite
Ch = chert
SB = shell bed

Figure 1.3-1: Detailed section description of paleointermediate location, Nahal Omer (Qazra sub-basin).

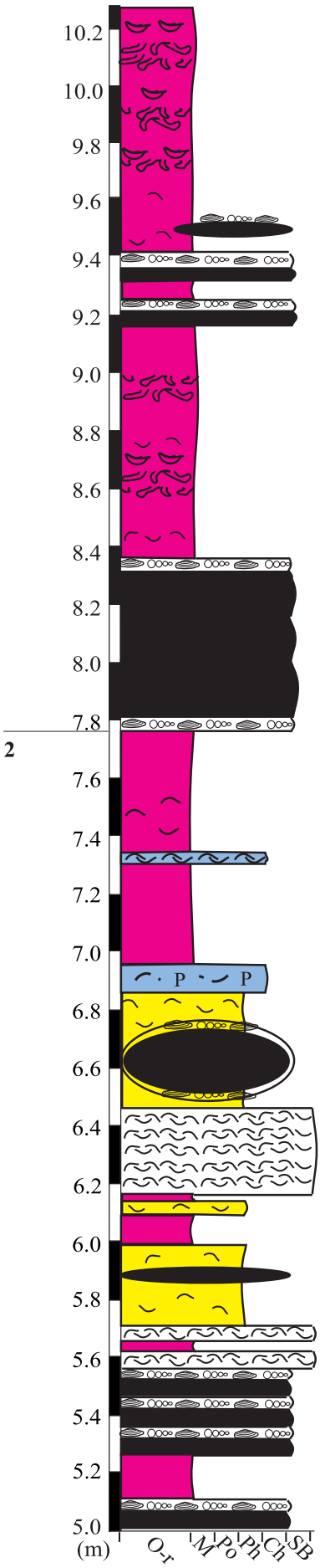

loosely packed *Pycnodonte*

laminated
patches of *Pycnodonte*

sparsely packed *Pycnodonte*

Protocardia, Venerids

laminated

YF O - 5A

laminated (whitish)

sparsely packed *Pycnodonte* and Corbulids

patchy fauna

fissle YF O - 4

sparse fauna, at times shell pits
coarse phosphate with loose fauna

shell fragments, *Pycnodonte, Plicatula,* shell debris

lensy, mostly densely packed

laminated
laminated

Figure 1.3-2: Detailed section description of paleointermediate location, Nahal Omer (Qazra sub-basin).

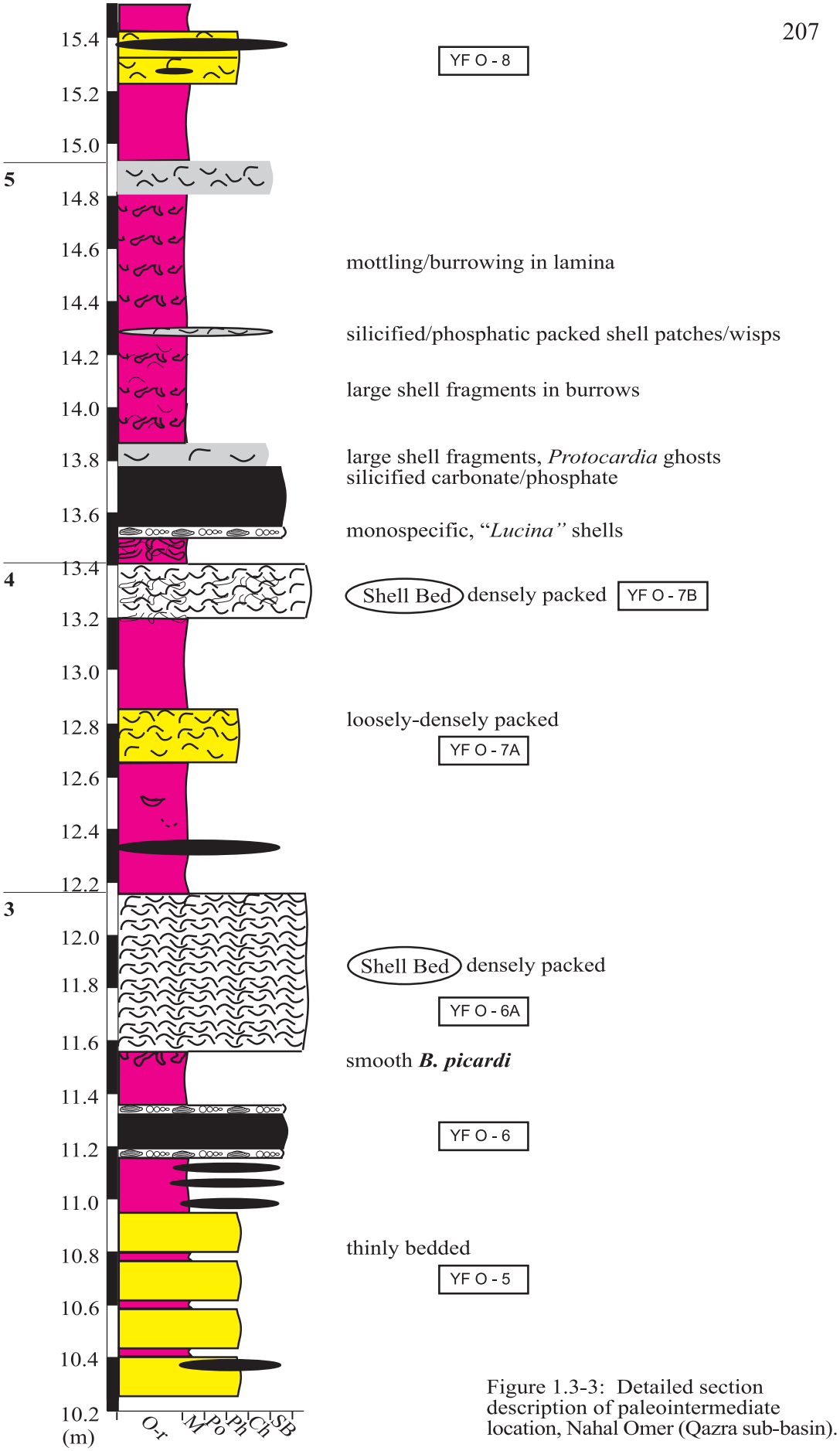

Figure 1.3-3: Detailed section description of paleointermediate location, Nahal Omer (Qazra sub-basin).

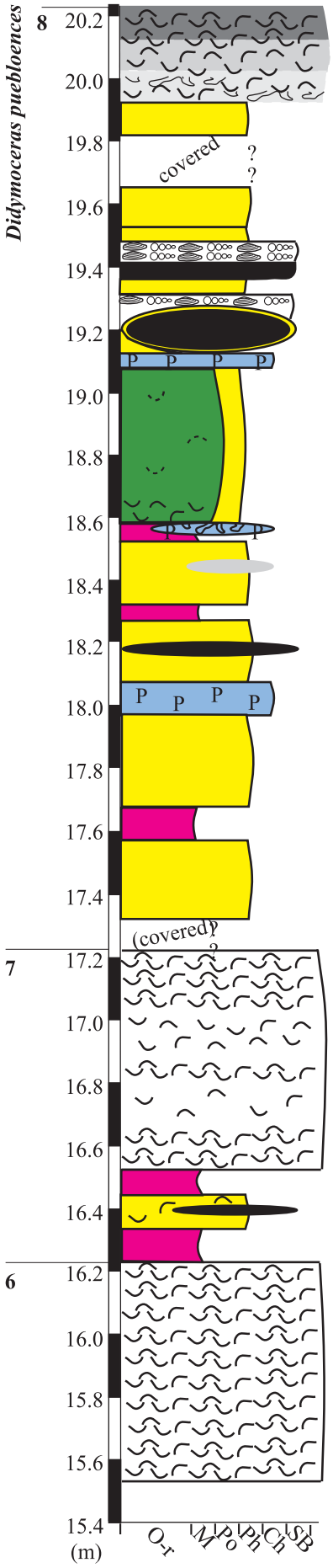

(desert varnish)

silicified *Crassatella* (coarser ribs, larger)

Shell Bed loose-dense packing, a composite shell bed
silicifies carbonate/phosphate

huge shell pavement

patchy, loose packing

coarse phosphorite, mottled contact

faunal ghosts
hard concretions within

loose packing
coarse phosphorite, lenses *Plicatula* on top

laminated

also many *Crassatella, Plicatula*

Shell Bed densely packed, a composite shell bed

also silicified *Plicatula*

Shell Bed densely packed

YF O - 8C

Figure 1.3-4: Detailed section description of paleointermediate location, Nahal Omer (Qazra sub-basin).

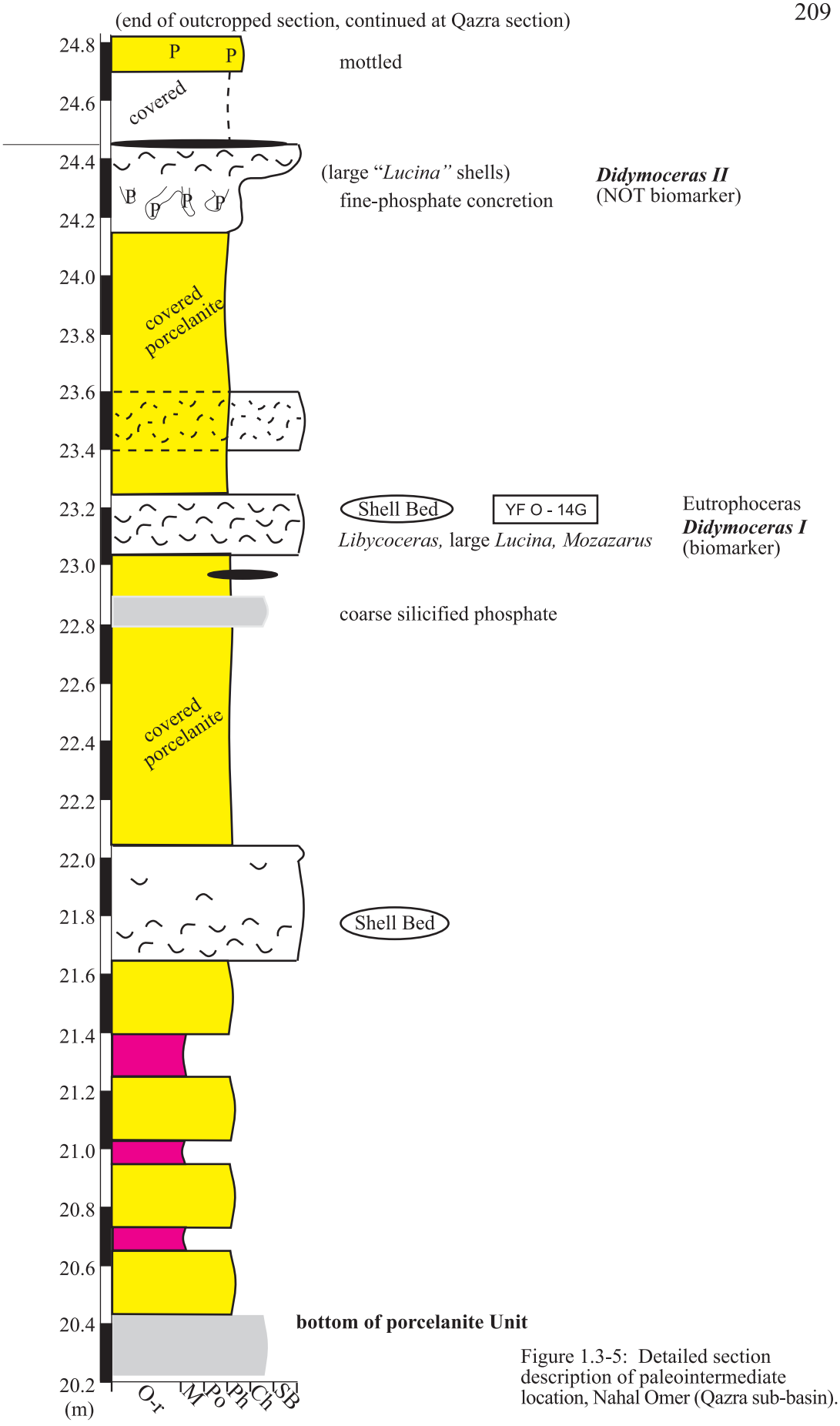

Figure 1.3-5: Detailed section description of paleointermediate location, Nahal Omer (Qazra sub-basin).

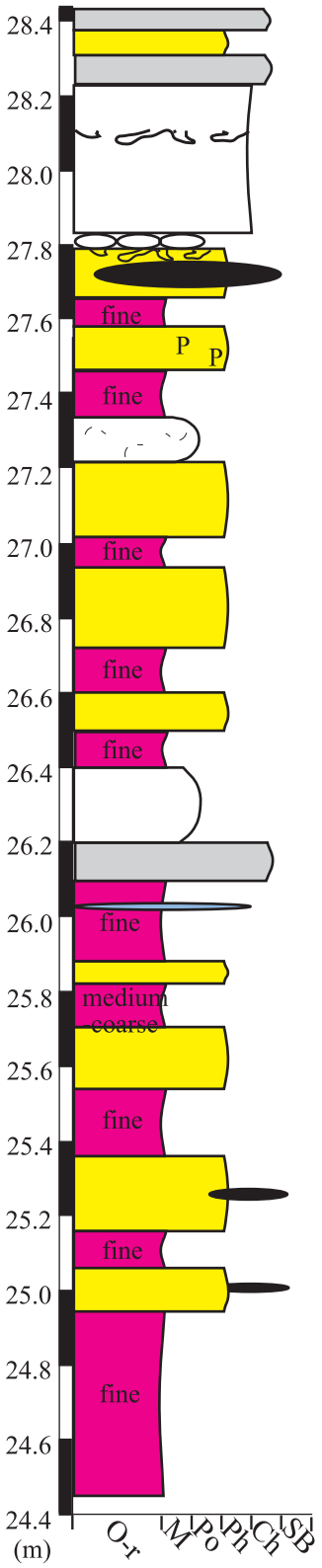

dark, mostly silicified, coarse phosphorite

dark, mostly silicified, coarse phosphorite (darker)

mottled, medium phosphorite with coarse fragments (lighter)

coarse-phosphorite filled burrows

mottled, at timed silicified

top root-like digenetic features

laminated

laminated

laminated

fish vertebrae

(1cm) coarse material

gradual contact

very mottled

Figure 1.3-6: Detailed section description of paleointermediate location, Nahal Qazra (Qazra sub-basin).

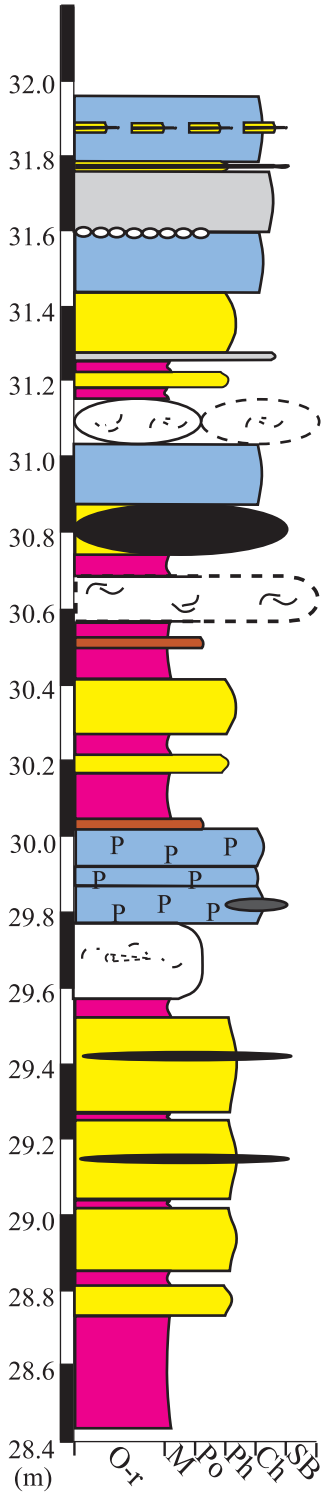

same coarse phosphorite, brown

same coarse phosphorite, only silicified
limy, 3cm concretions
coarse phosphorite

medium grained
medium grained
lithified fish debris, 5cm concretions 80cm apart throughout

very coarse white phosphoritic fragments

dark cherty/limy concretions with bottom porcelanite

coarse grained
lithified shell patches

red/brown diagenetic layer

same as below

very fine grey phosphorite with 2cm cherty concretions
red/brown diagenetic layer
grey coarse phosphorite, white fragments
brown lithified phosphorite, medium
black silicified patches in coarse grey phosphorite

fish vertebrae, organic debris

YF O - barren

fissile

Figure 1.3-7: Detailed section description of paleointermediate location, Nahal Qazra (Qazra sub-basin).

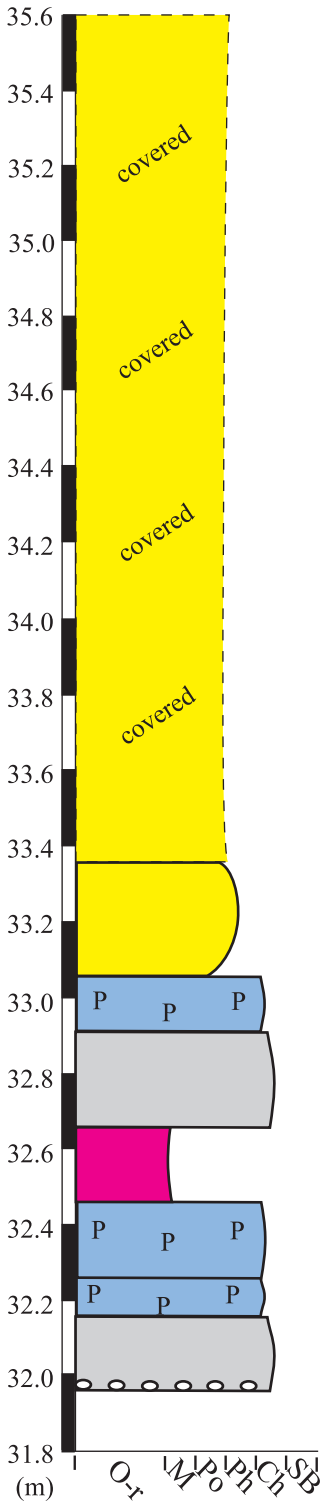

concretions

grey phosphorite

coarse grained

sharp contact

white, fine, laminated

same coarse, brown-grey mottled phosphorite

very gradual contact

coarse, brown-grey mottled phosphorite

gradual, undulatory contact

dark, silicified coarse phosphorite

white limy-looking phosphate “rip ups”

Figure 1.3-8: Detailed section description of paleointermediate location, Nahal Qazra (Qazra sub-basin).

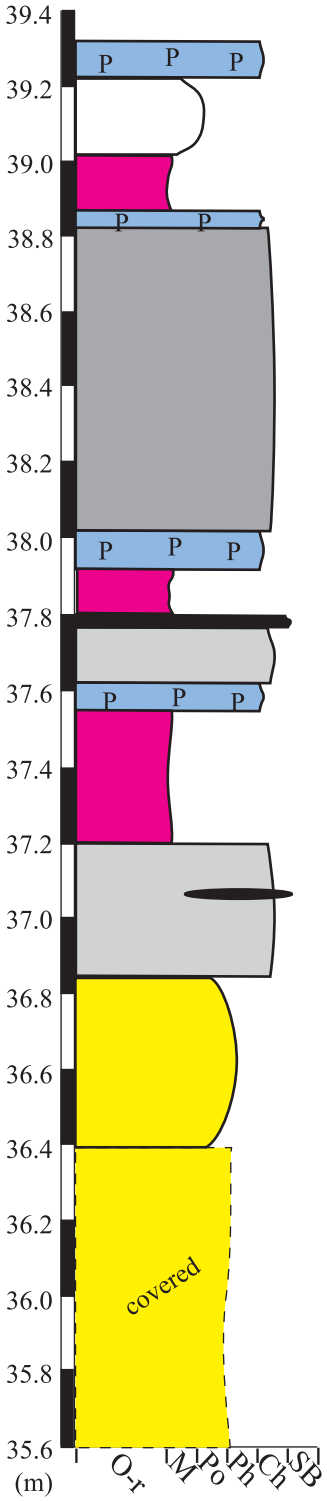

coarse brown phosphorite with white bone fragments, oriented

concretions

fine grained, laminated, coarse material within

coarse

very dark , cherty looking with blue/white fragments
seen throughout section (mostly top of section)

very coarse brown phosphorite, mottled looking

dark brown, medium laminated phosphorite with coarse fragments

very coarse dark brown phosphorite

white concretionary layer

Figure 1.3-9: Detailed section description of paleointermediate location, Nahal Qazra (Qazra sub-basin).

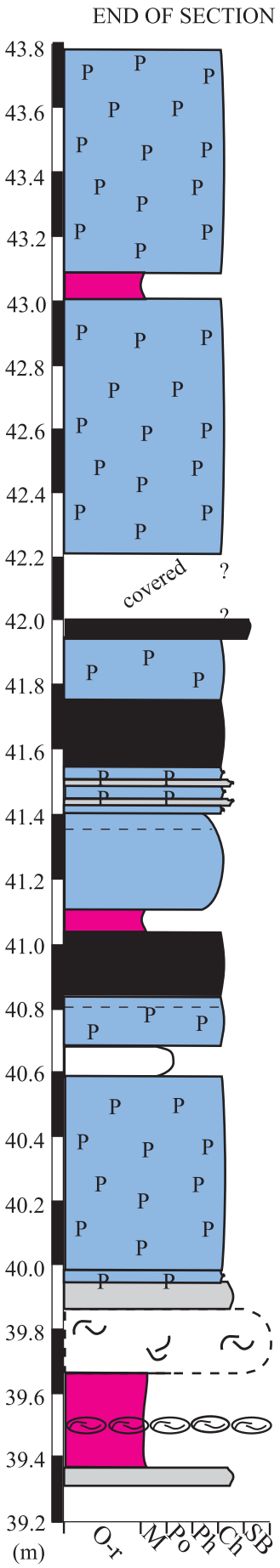

top *Pycnodonte* (?)

coarse phosphorite, 3cm white bone fragments, no orientation
shark teeth, fish vertebrae

fine grained laminated phosphorite

shell fragments within

white-grey medium grained

medium grained
medium grained

top fish debris

fine grained, lithified, grey phosphatic concretions

laminated, with 1cm long white bones

fine grained
medium grained
concretions
coarse
fine

coarse

fine
coarse
bones and fish debris layer

fine, laminated, shark teeth

5cm shelly concretions with coarse material, within

Figure 1.3-10: Detailed section description of paleointermediate location, Nahal Qazra (Qazra sub-basin).

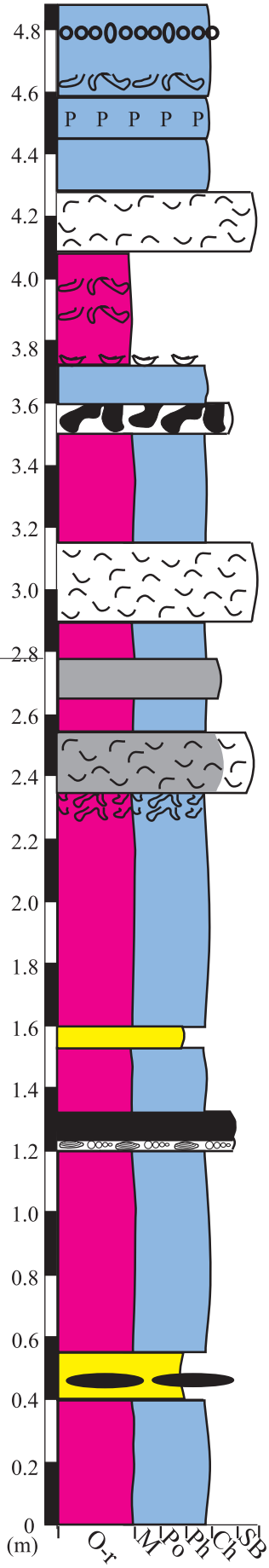

1

very coarse
rip-ups of micritic phosphate,
large bones, angular pebbles, shark teeth

finer

very coarse mottled, large pebbles and frags

finer

patchy, OR very coarse rounded phosphate pebbles
many large *"Lucina"*, loosely-packed
Hauericeras fayoli ***Exiteloceras*** (Omeroceras)

YF M - 3

fine
↑ sand size, mottled
Pycnodonte
coarse

burrowed chert with dark fills of silicified phosphate

coarse
↑ mottled sandy
fine bottom laminated

loosely packed ***Didymoceras I***
burrowed-mottled coarse grainstone.

fine grained **bottom of Porcelanite unit**

silicified coarse

medium sand silicified phos (mottled)
sparsely-loosely packed
Crassatella, Plicatula

YF M - 1

burrows

shark teeth,
baculites,
frags

phosphate bearing
(wispy) coarse sand
with pebbly frags

same, with
fish debris

chert shell pavement

YF M - 2

same, with rock frags strewn through

massive porcelanite and chert in porcelanite

(top laminated)

fine grained light grey phosphate-bearing layer

Figure 1.4-1: Detailed section description of paleohigh location, HarAMassaQazra sub-basin).

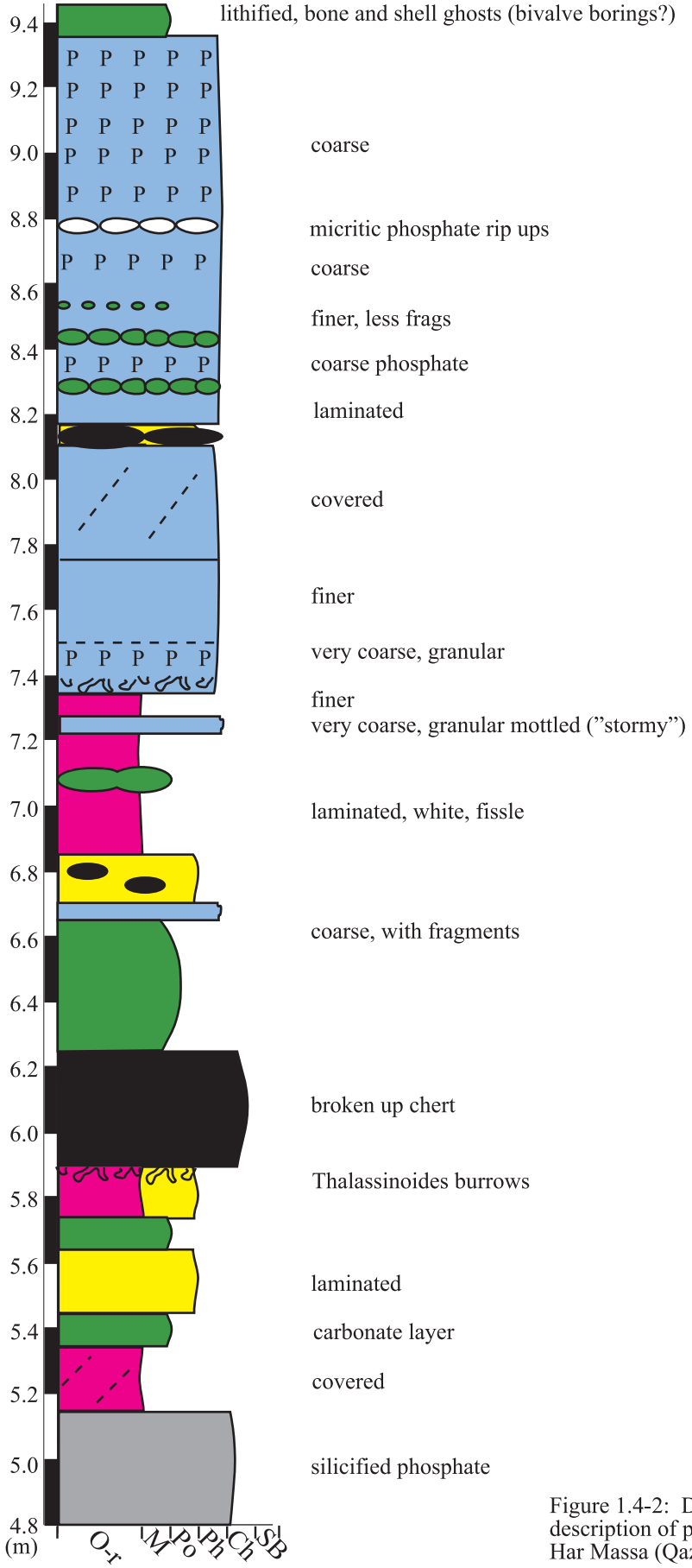

Figure 1.4-2: Detailed section description of paleohigh location, Har Massa (Qazra sub-basin).

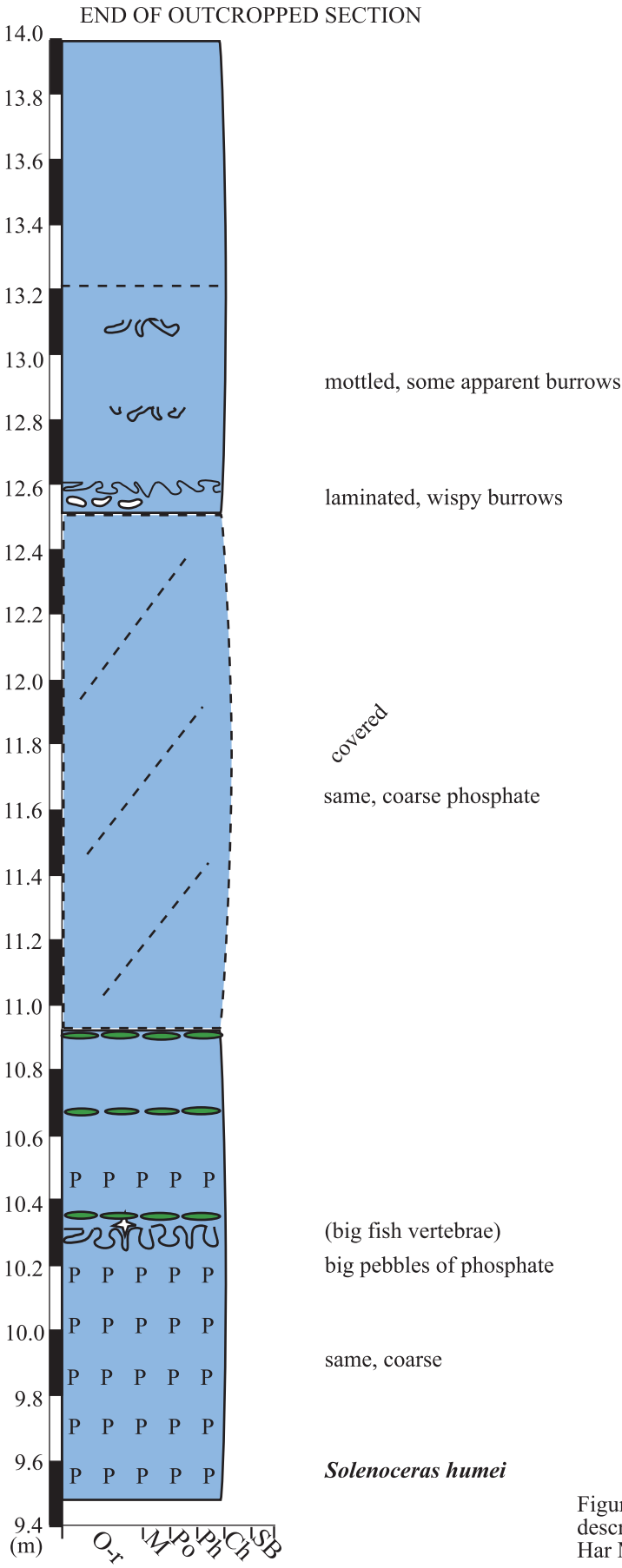

Figure 1.4-3: Detailed section description of paleohigh location, Har Massa (Qazra sub-basin).

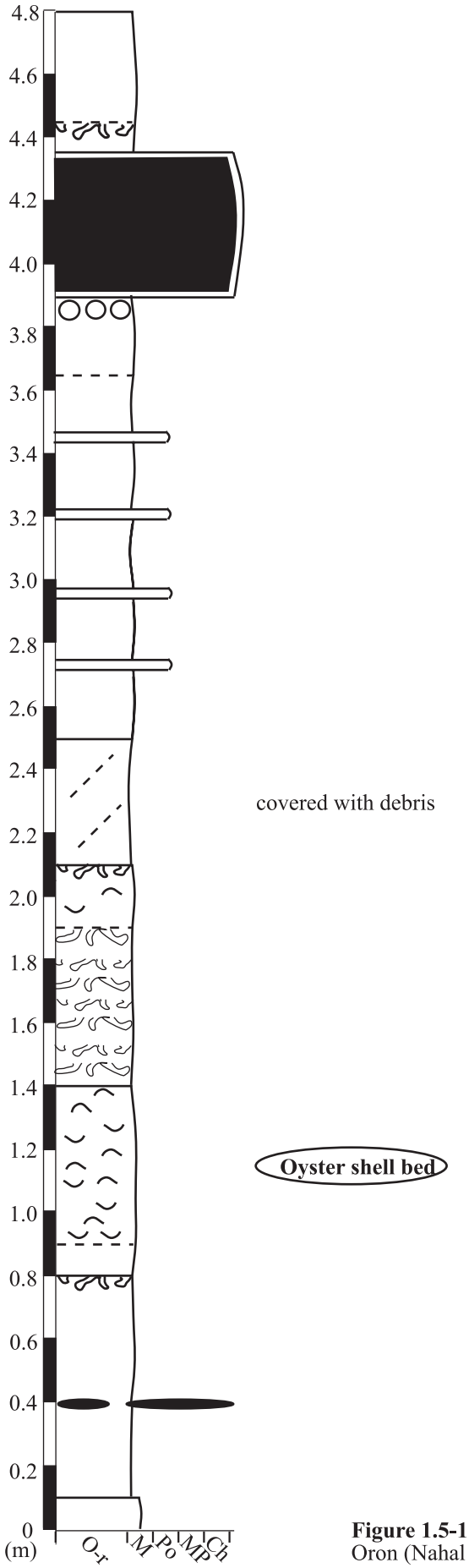

Figure 1.5-1: Section description of paleointermediate, Oron (Nahal Talul) in the Zin sub-basin

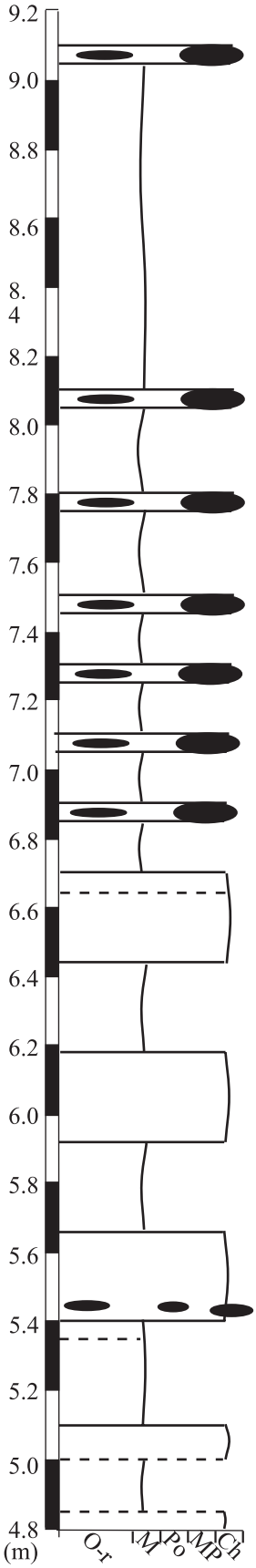

Figure 1.5-2: Section description of paleointermediate, Oron (Nahal Talul) in the Zin sub-basin

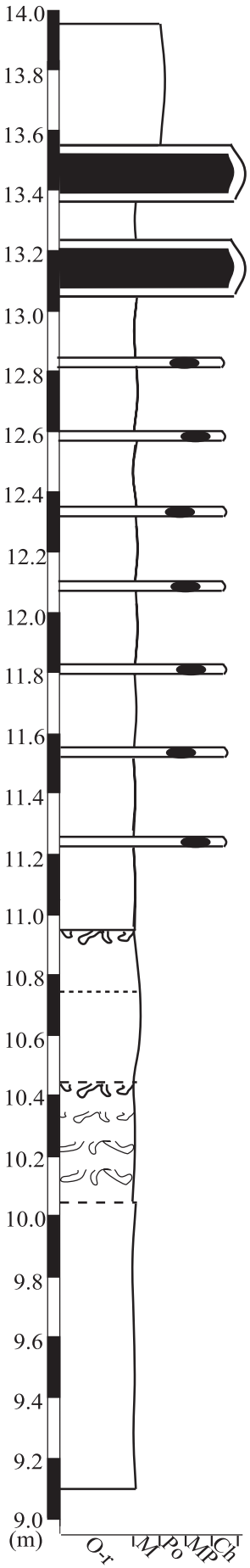

Figure 1.5-3: Section description of paleointermediate, Oron (Nahal Talul) in the Zin sub-basin

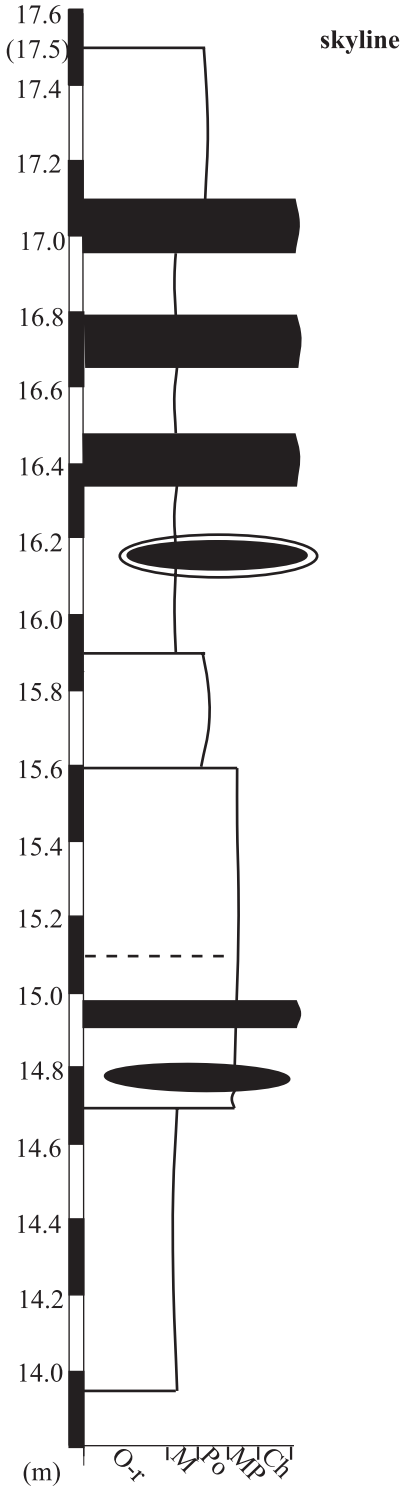

Figure 1.5-4: Section description of paleointermediate, Oron (Nahal Talul) in the Zin sub-basin

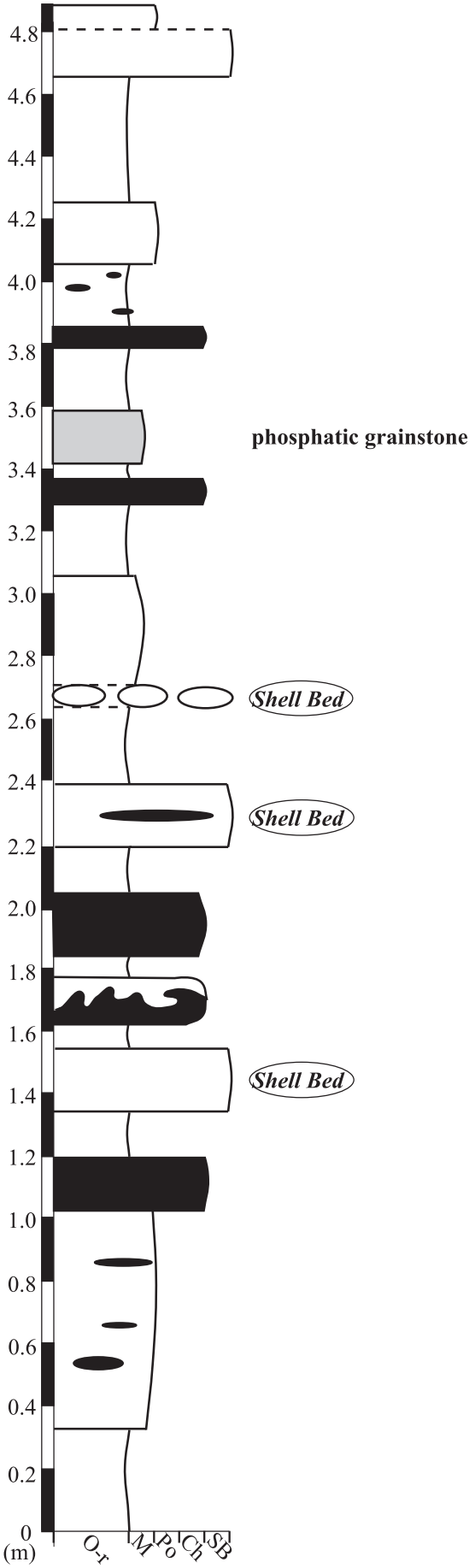

LEGEND

O-r = organic-rich
M = massive micrite
Po = porcelanite
Ch = chert
SB = shell bed

Figure 1.6-1: Section description of paleointermediate, Wadi El Qilt

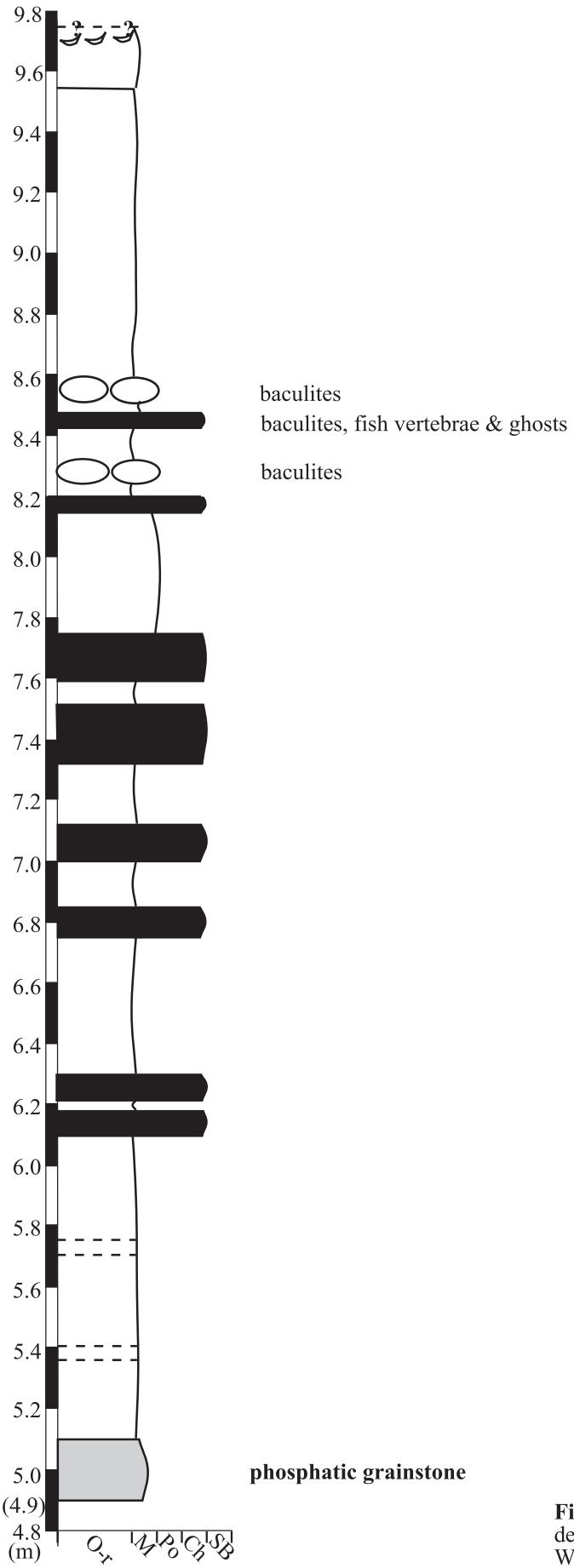

Figure 1.6-2: Section description of paleointermediate, Wadi El Qilt

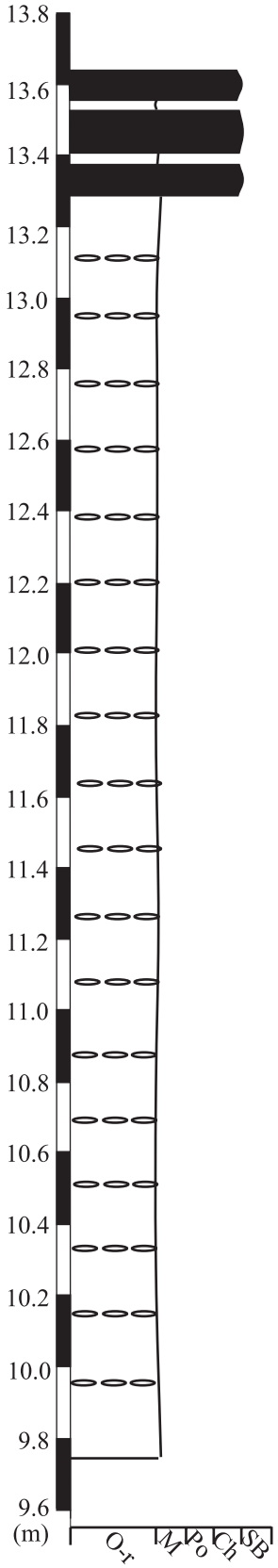

Figure 1.6-3: Section description of paleointermediate, Wadi El Qilt

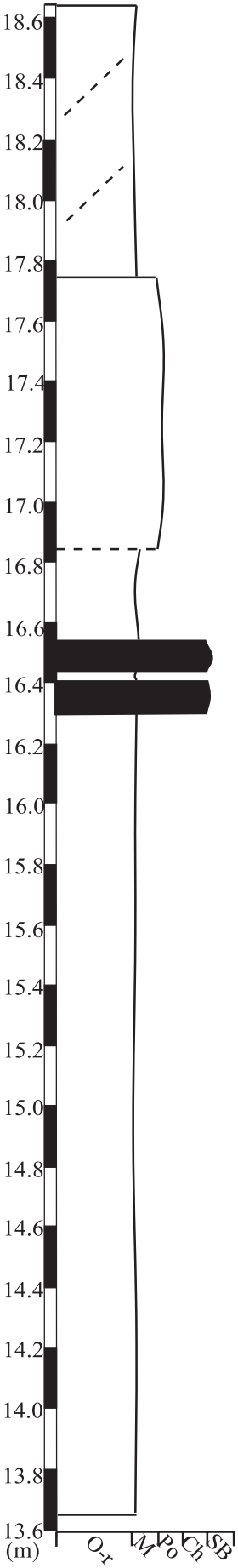

Figure 1.6-4: Section description of paleointermediate, Wadi El Qilt

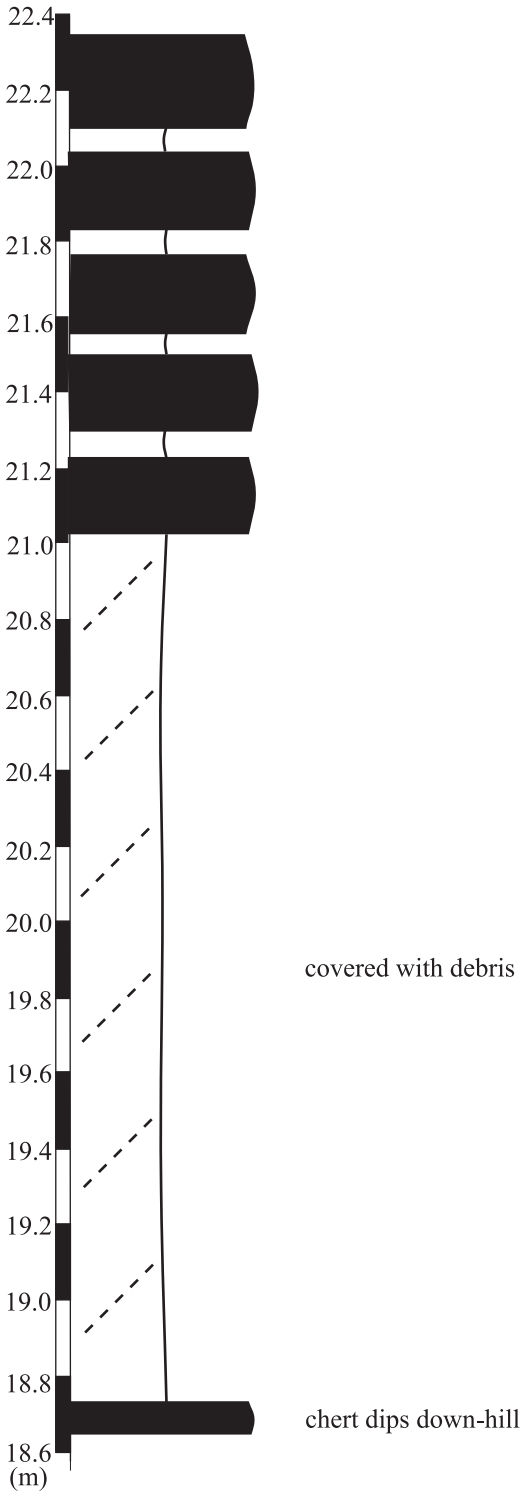

Figure 1.6-5: Section description of paleointermediate, Wadi El Qilt

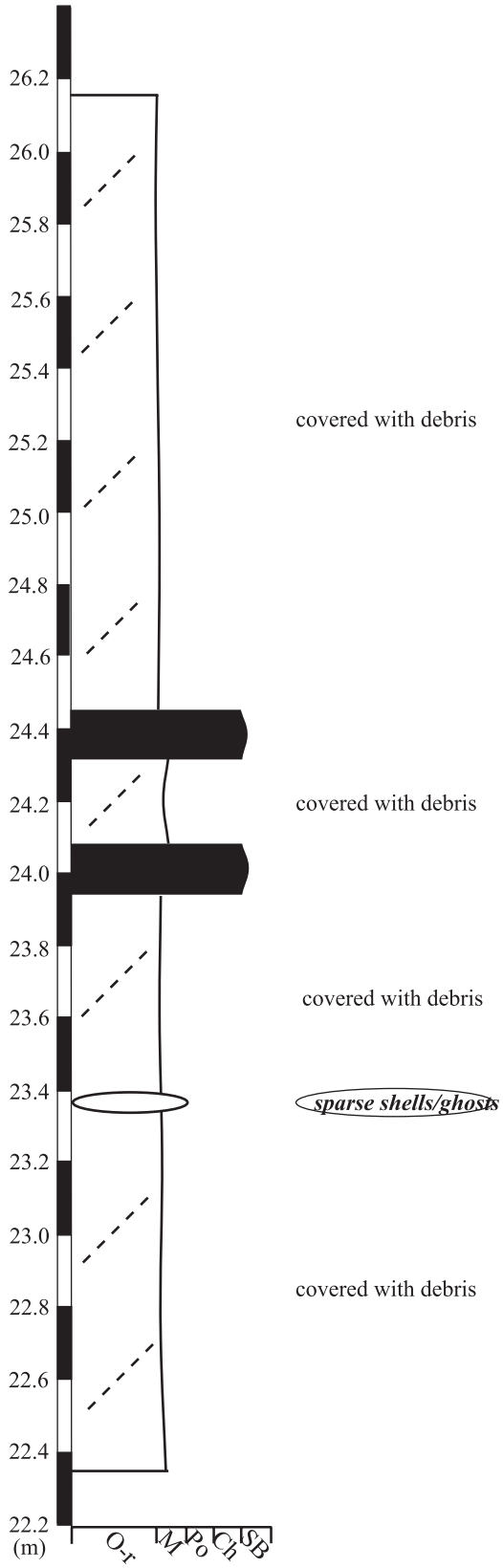

Figure 1.6-6: Section description of paleointermediate, Wadi El Qilt

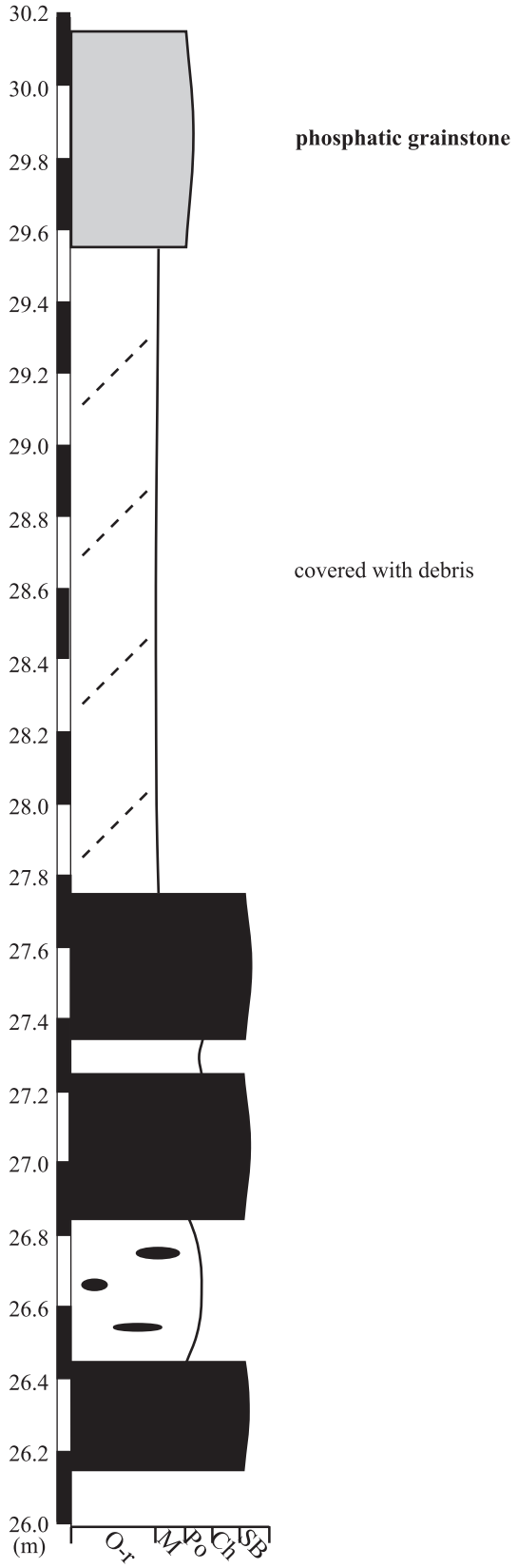

Figure 1.6-7: Section description of paleointermediate, Wadi El Qilt

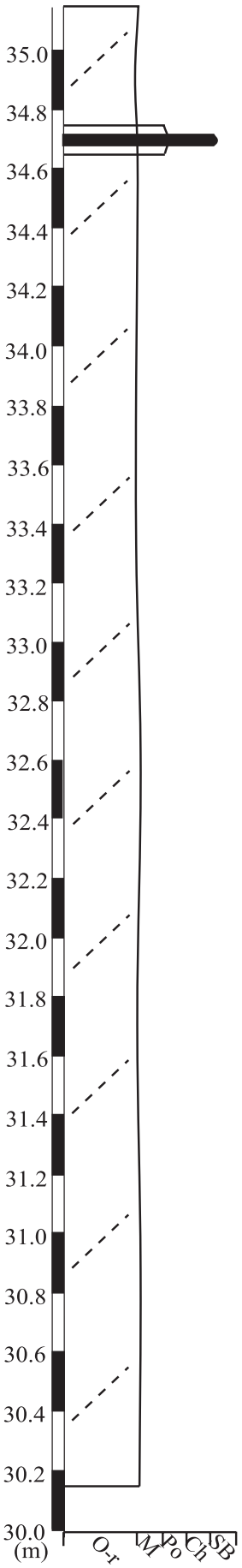

Figure 1.6-8: Section description of paleointermediate, Wadi El Qilt

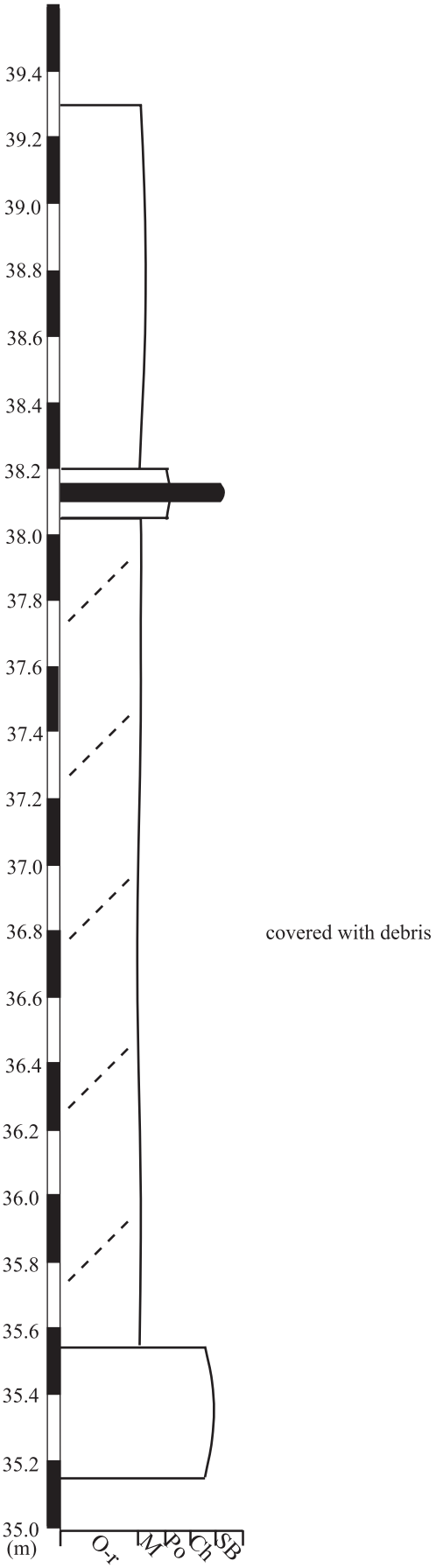

Figure 1.6-9: Section description of paleointermediate, Wadi El Qilt

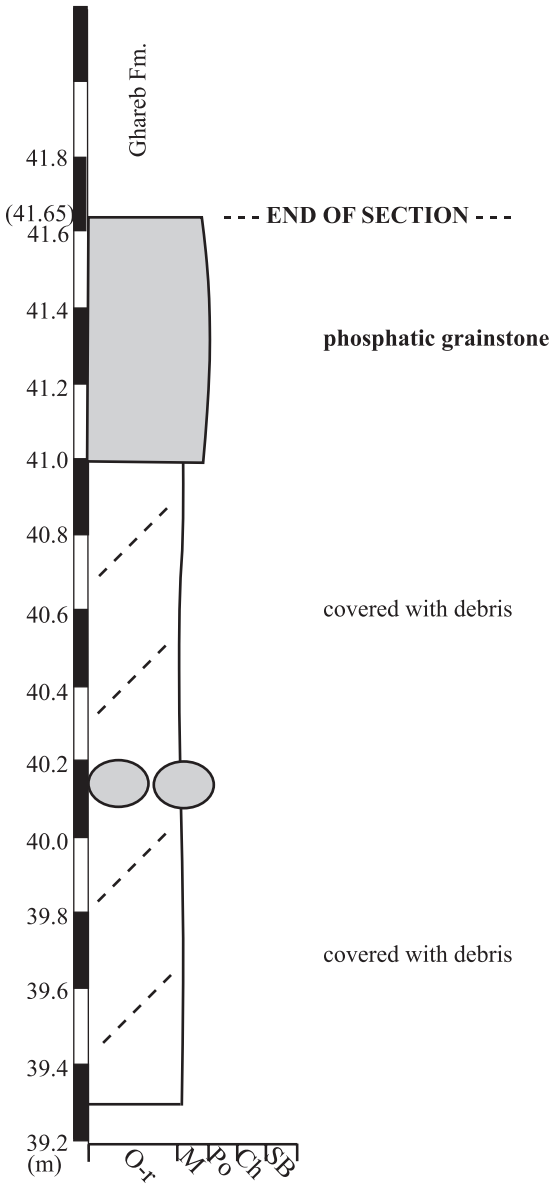

Figure 1.6-10: Section description of paleointermediate, Wadi El Qilt

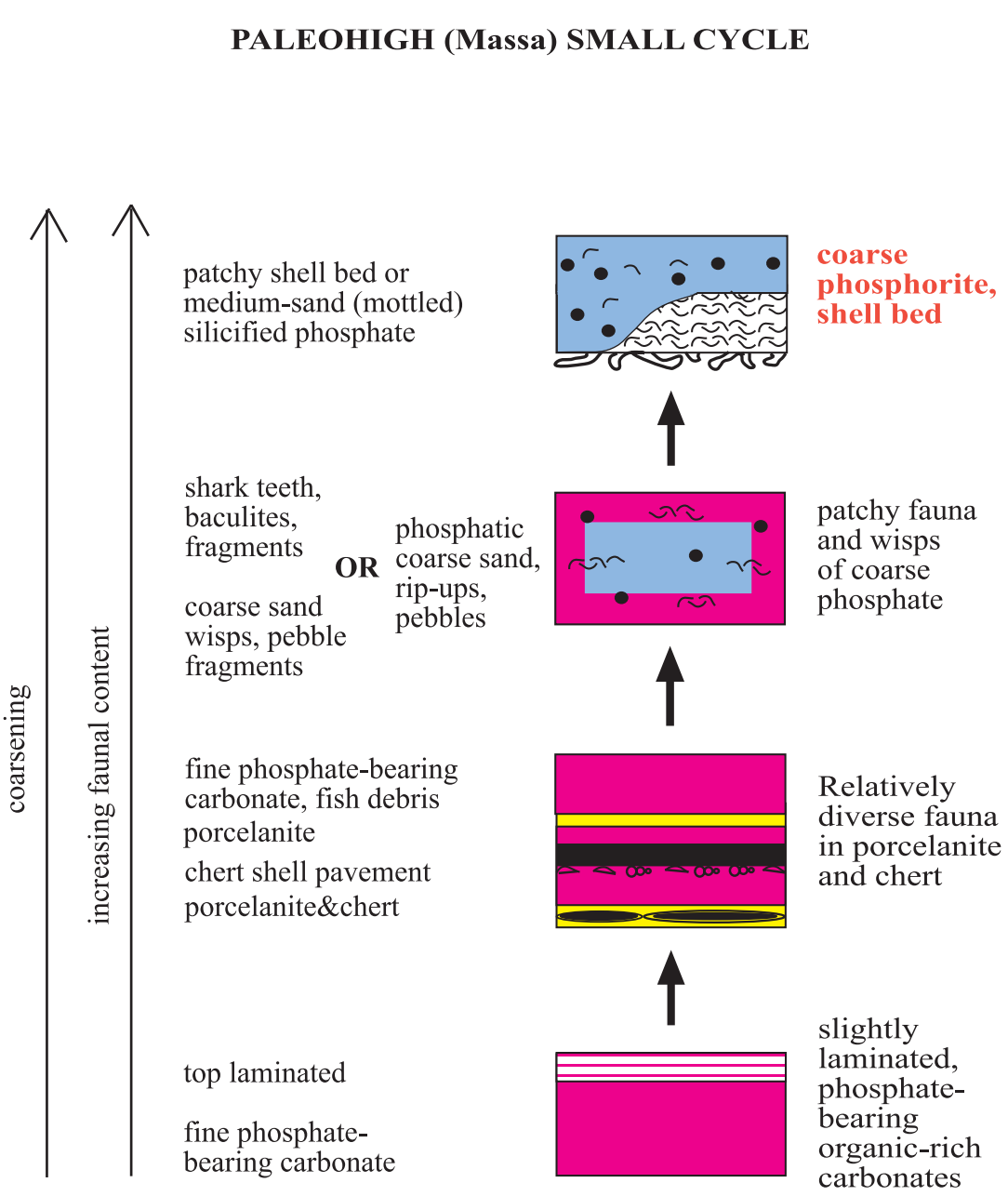

Figure 1.7: Paracycle of the paleohigh location, Har Massa from the bottom unit of the Phosphate Member. Note in particulat the higher concentration of the coarse phosphatic material.

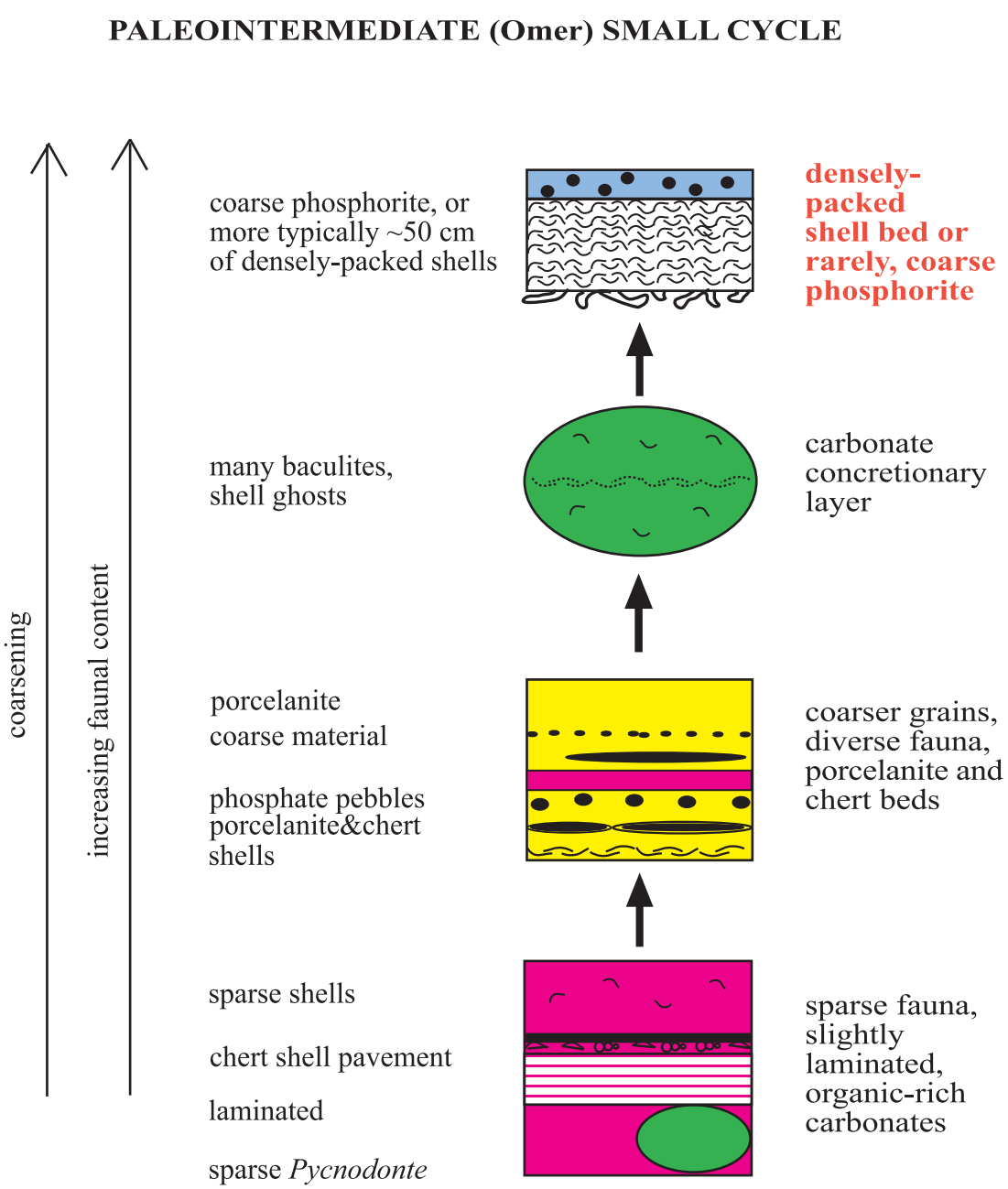

Figure 1.8: Paracycle of the paleointermediate location, Nahal Omer from the bottom unit of the Phosphate Member. Note in particular the increasing component of the shell material on the expense of the coarse phosphorite.

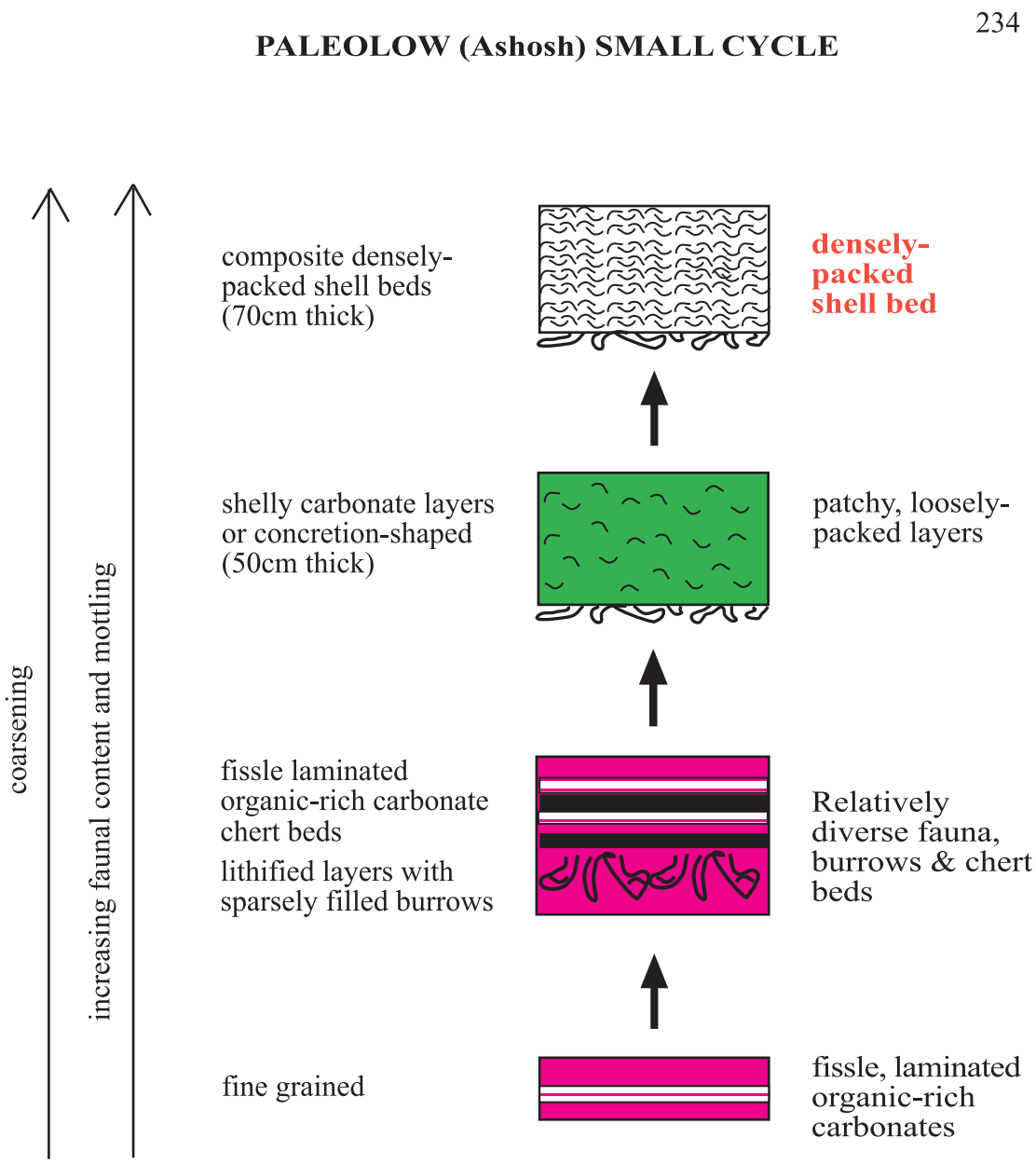

Figure 1.9: Paracycle of the paleolow location, Nahal Ashosh from the bottom unit of the Phosphate Member. Note in particular the increase in shell component and great decrease in coarse phosphatic material.

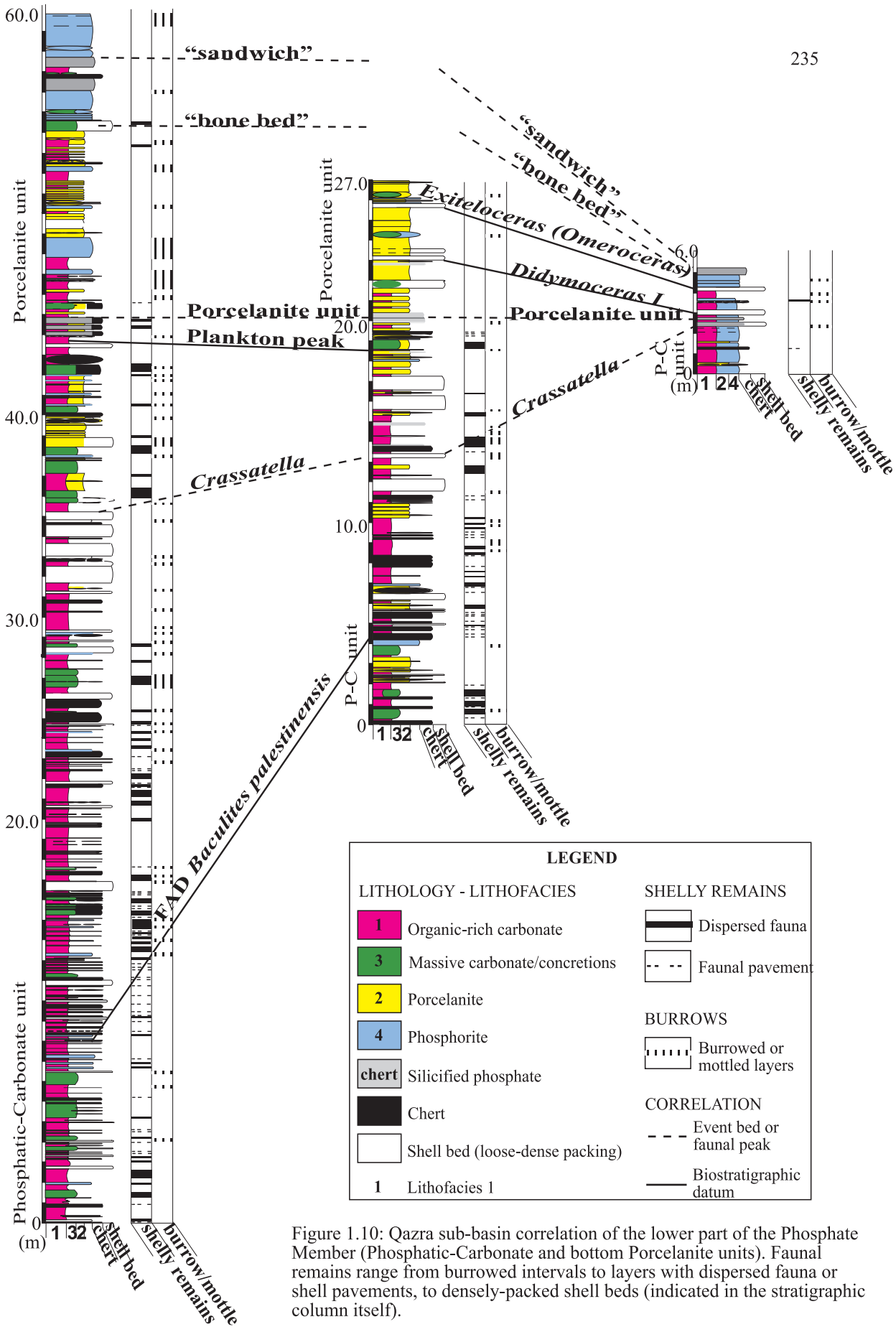

Figure 1.10: Qazra sub-basin correlation of the lower part of the Phosphate Member (Phosphatic-Carbonate and bottom Porcelanite units). Faunal remains range from burrowed intervals to layers with dispersed fauna or shell pavements, to densely-packed shell beds (indicated in the stratigraphic column itself).

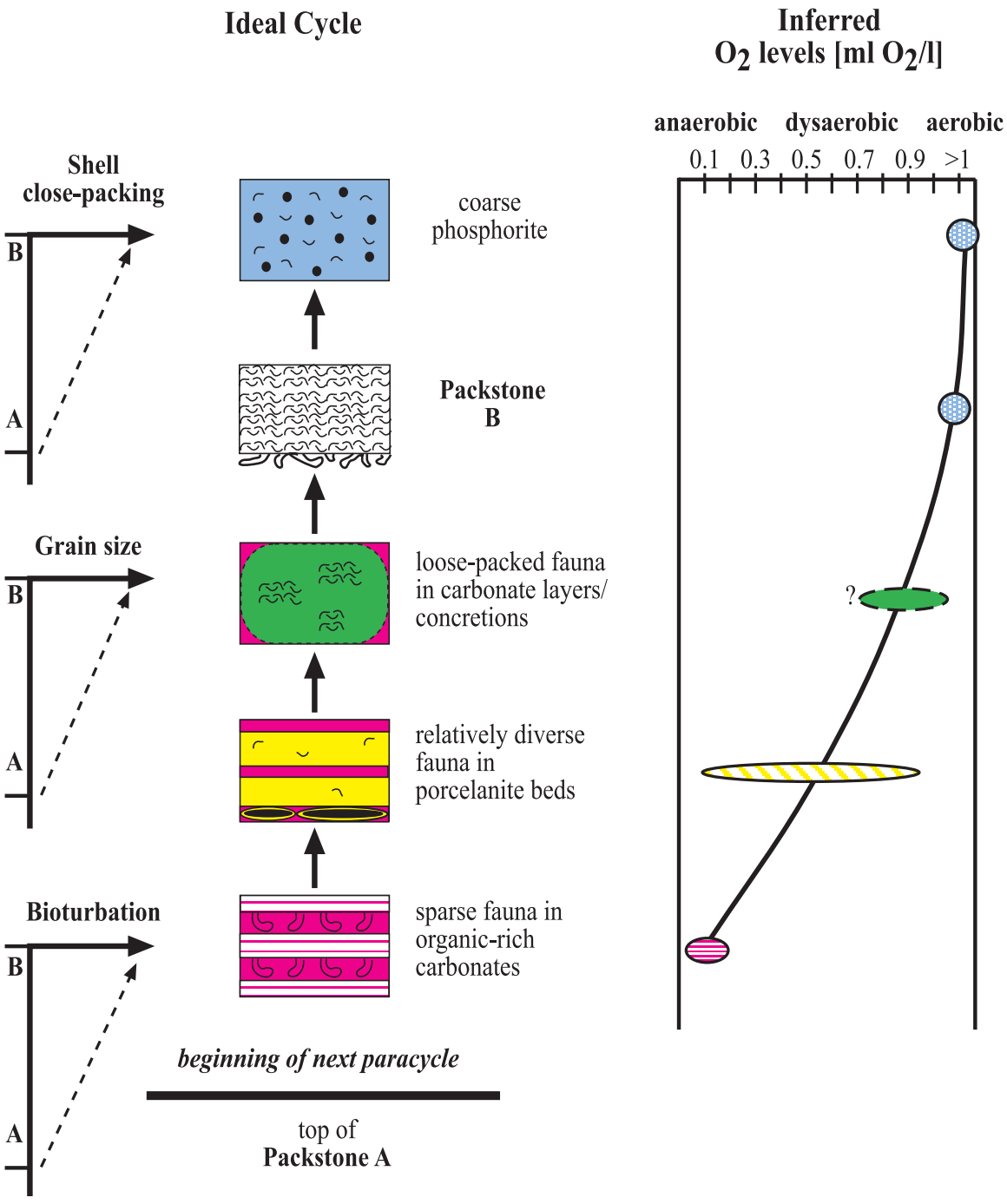

Figure 1.11: Inferred dissolved oxygen levels for the Mishash high-productivity facies following an "Ideal paracycle" for Qazra sub-basin. A full succession of lithologies from top of packstone-A to the end of cycle at packstone-B / phosphorite.

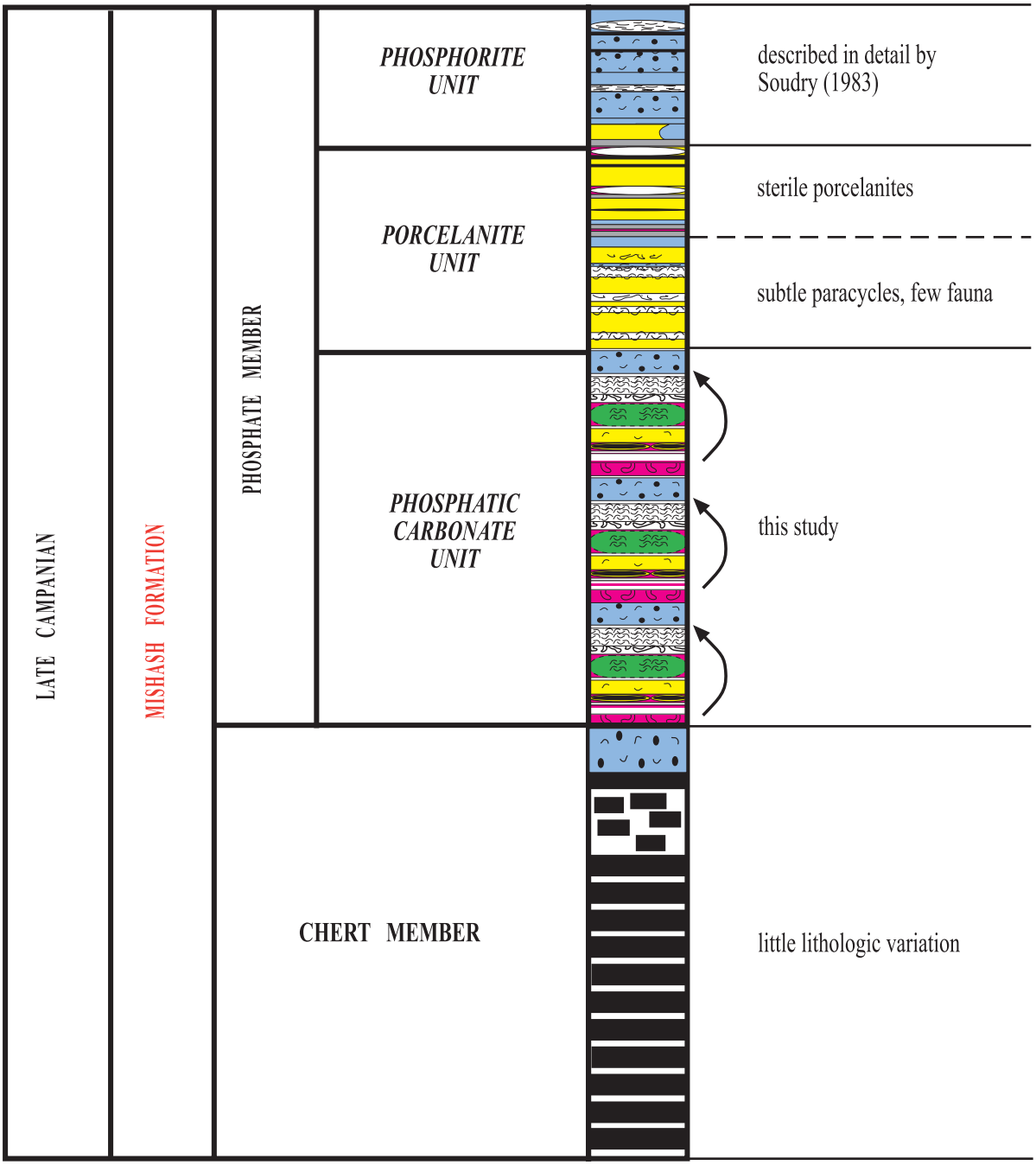

KEY TO SYMBOLS

- Organic-rich carbonate
- Massive carbonate/concretions
- Porcelanite
- Phosphorite
- Chert
- Brecciated chert
- densely packed shell bed
- Shells
- Burrows

Figure 1.12: Mishash section with reference to this study and Soudry's work.

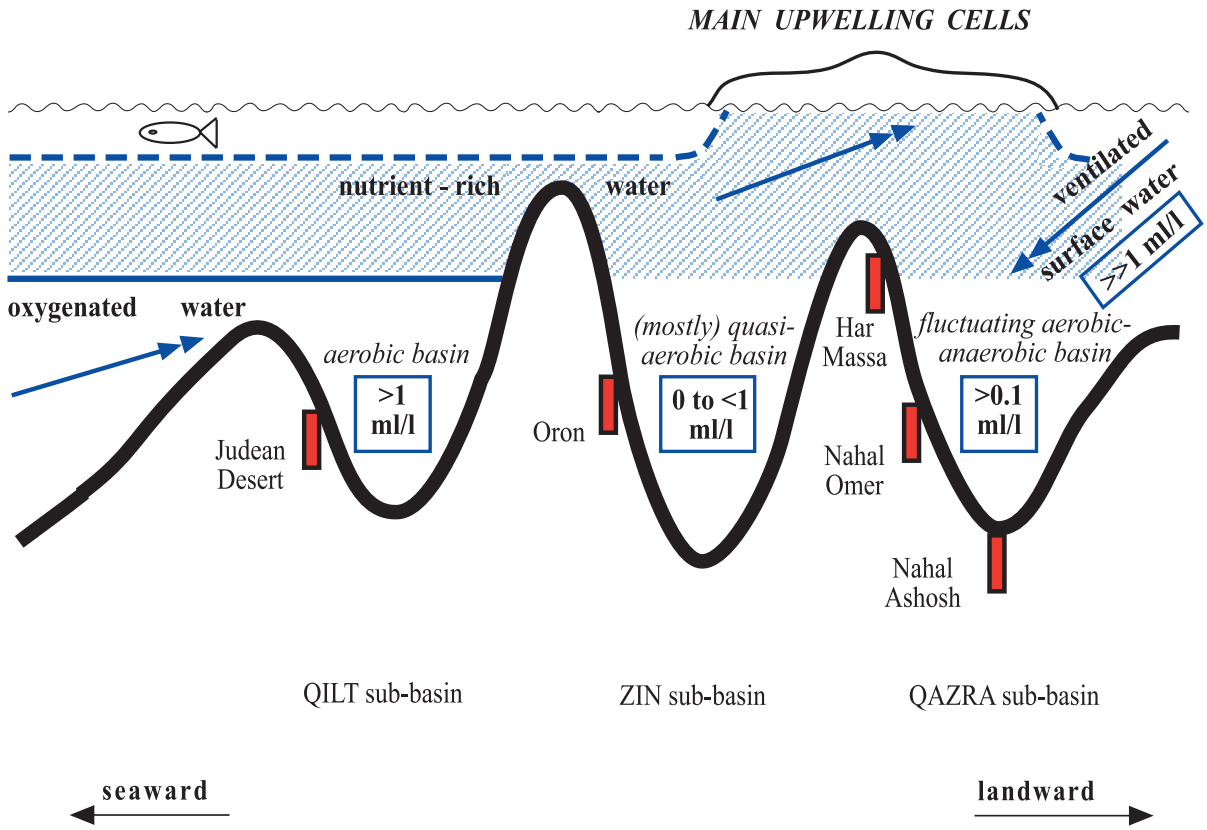

Figure 1.13: Regional paleoceanographic reconstruction during the Upper Campanian of the Mishash high-productivity tract. Schematic ocean circulation, main water bodies, basin seafloor oxygen levels and exaggerated bathymetry with relative position of sections shown within the basin. Basins are positioned at relative distance from paleoshore to the southeast. Arrows indicate water flow direction within the different water masses. Main upwelling cell indicated by abundance of biogenic silica.

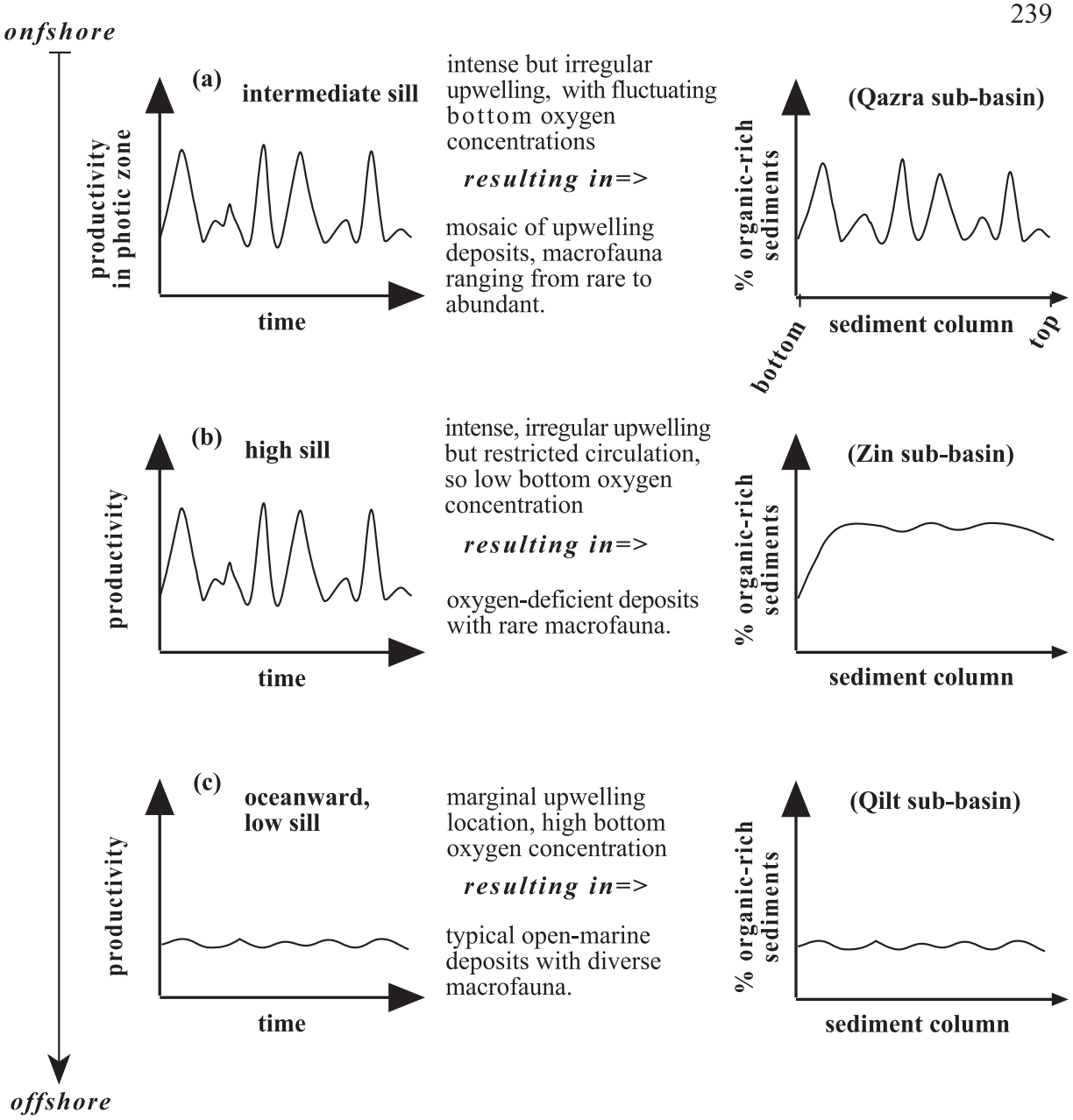

Figure 1.14: Shifts in upwelling intensity, or increasing frequency of upwelling pulses, across the region as indicated by schematic productivity levels in the photic zone. **(a)** Under irregular but intense winds oxygen replenishment is periodic and levels fluctuate. A mosaic of upwelling deposits are expected under these environemnts. These deposits show a range of macrofaunal abundance from rare to dominant. **(b)** Under the same conditions but with restricted water circulation due to different bottom tophography (a high barrier), oxygen-deficient deposits are characteristic. These deposits are high in organic matter content and low in macrofaunal abundance. **(c)** A decrease in photic-zone productivity related to a subdued effect of upwelling results in marine deposits with moderate upwelling imprints. Marginal upwelling environments are characteristic of close to normal-marine assemblages of macrofauna.

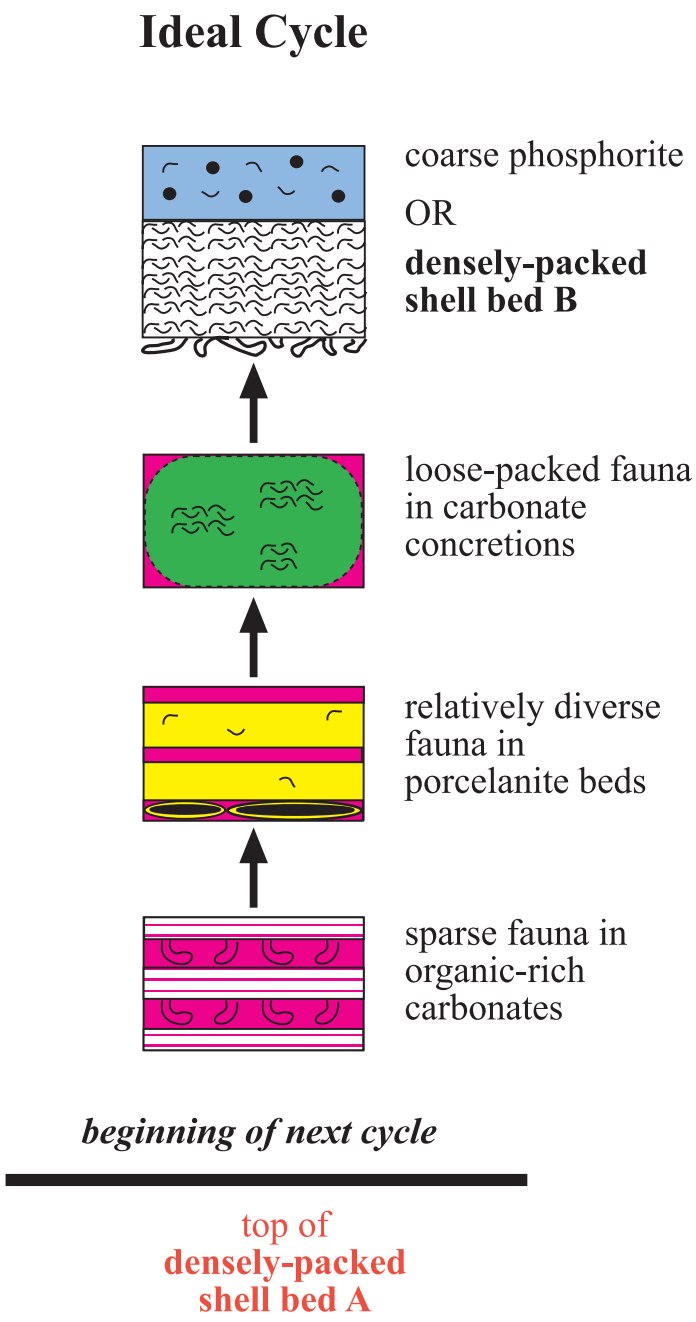

Figure 2.1: An "ideal small cycle" for the Qazra sub-basin in the Mishash Formation, southern Israel. A full succession of lithologies from top of packstone-A to the end of cycle at packstone-B / phosphorite constitute the four main lithotypes that charaterize the Mishash seafloor.

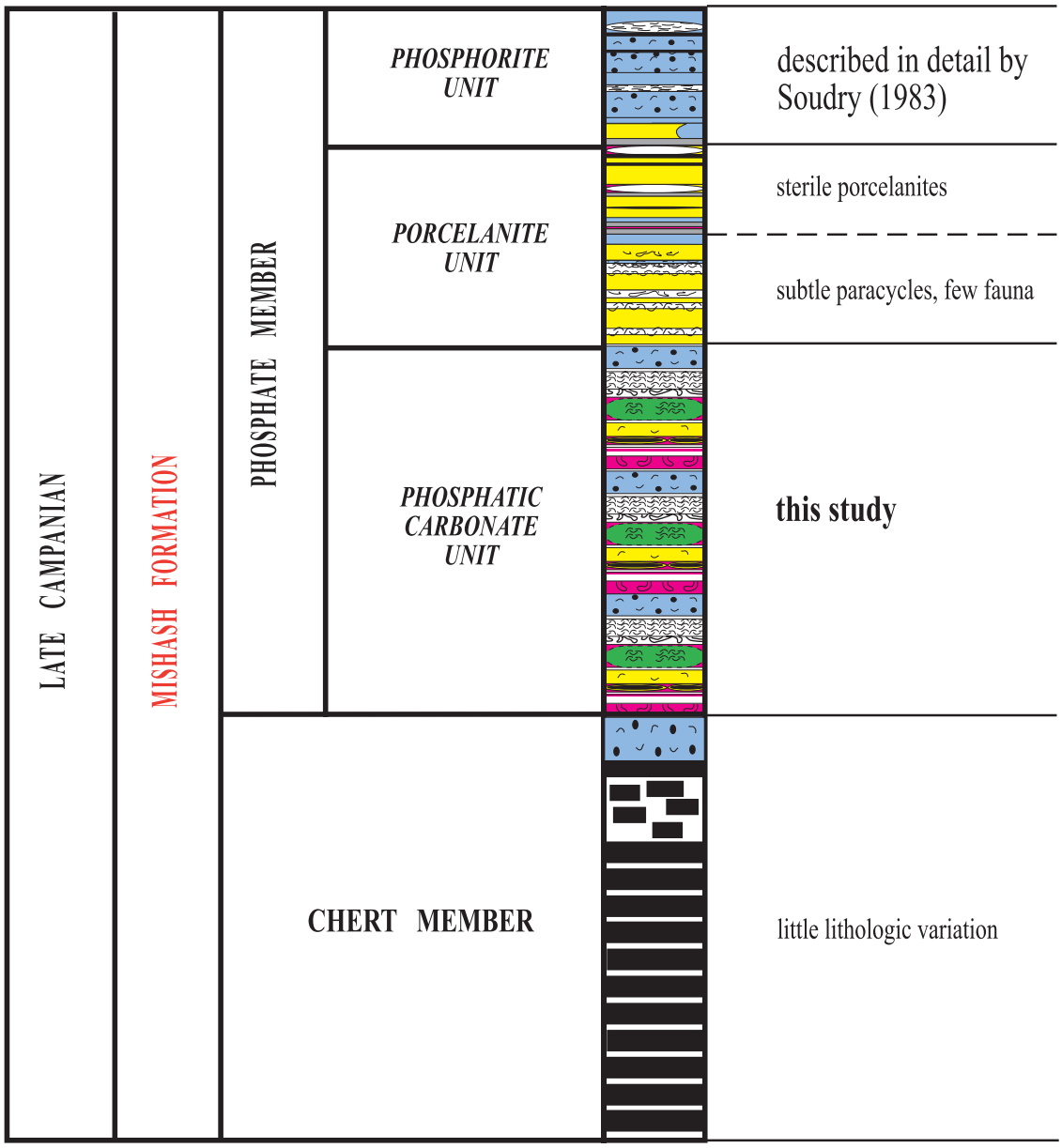

KEY TO SYMBOLS

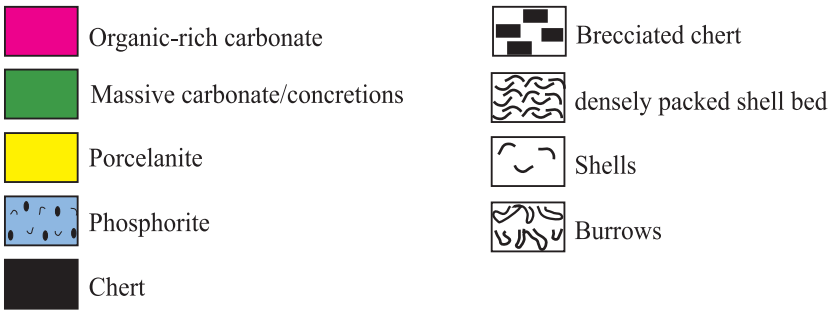

Figure 2.2: Mishash section with reference to this study and Soudry's work.

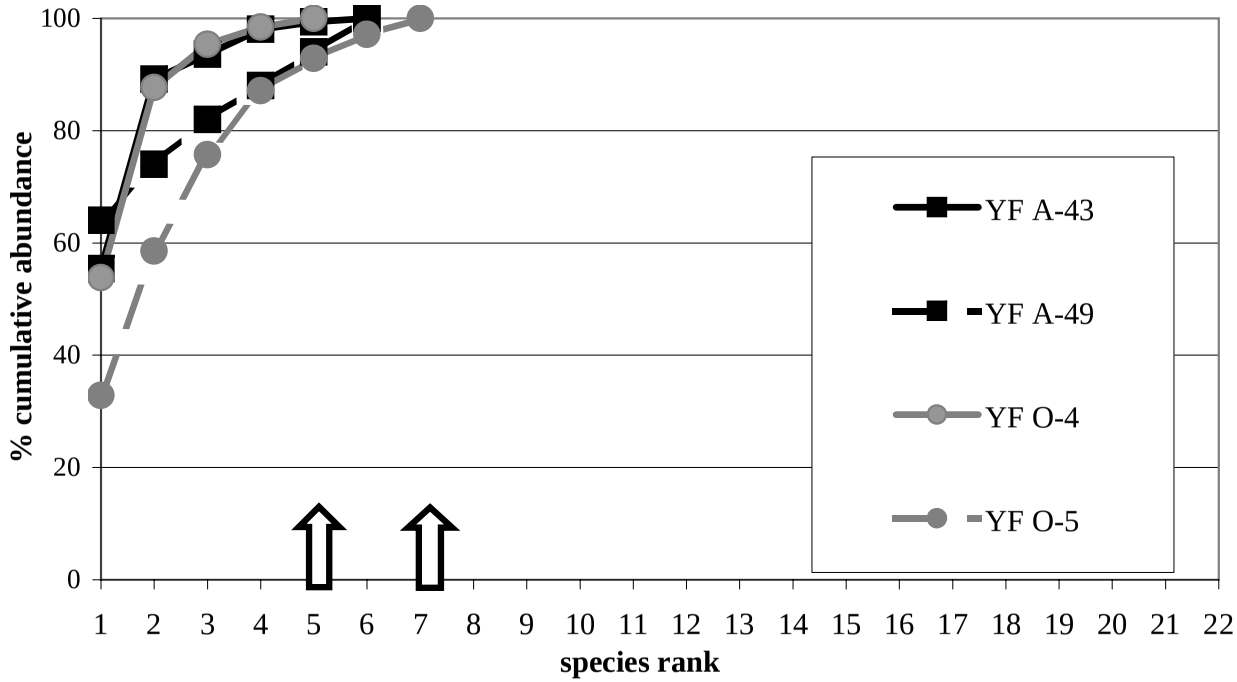

Figure 2.3: Ranking of species in decreasing order of abundance is plotted in relation to the cumulative abundance of the species for the organic-rich carbonate samples of the Mishash high-productivity region. Arrows indicate the range of species richness for facies 1. Sample labels indicate sampling from location YF A or YF O.

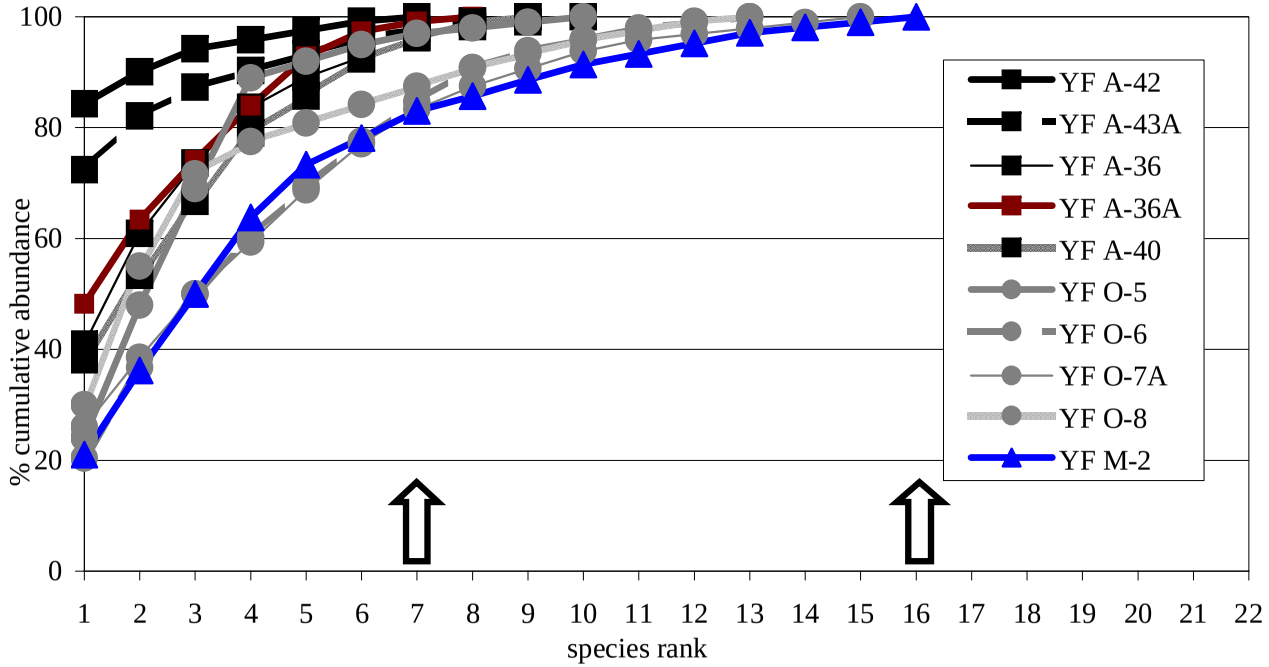

Figure 2.4: Ranking of species in decreasing order of abundance is plotted in relation to the cumulative abundance of the species for the chert and porcelanite samples of the Mishash high-productivity region. Arrows indicate the range of species richness for facies 2. Sample labels indicate sampling from locations YF A, YF O or YF M.

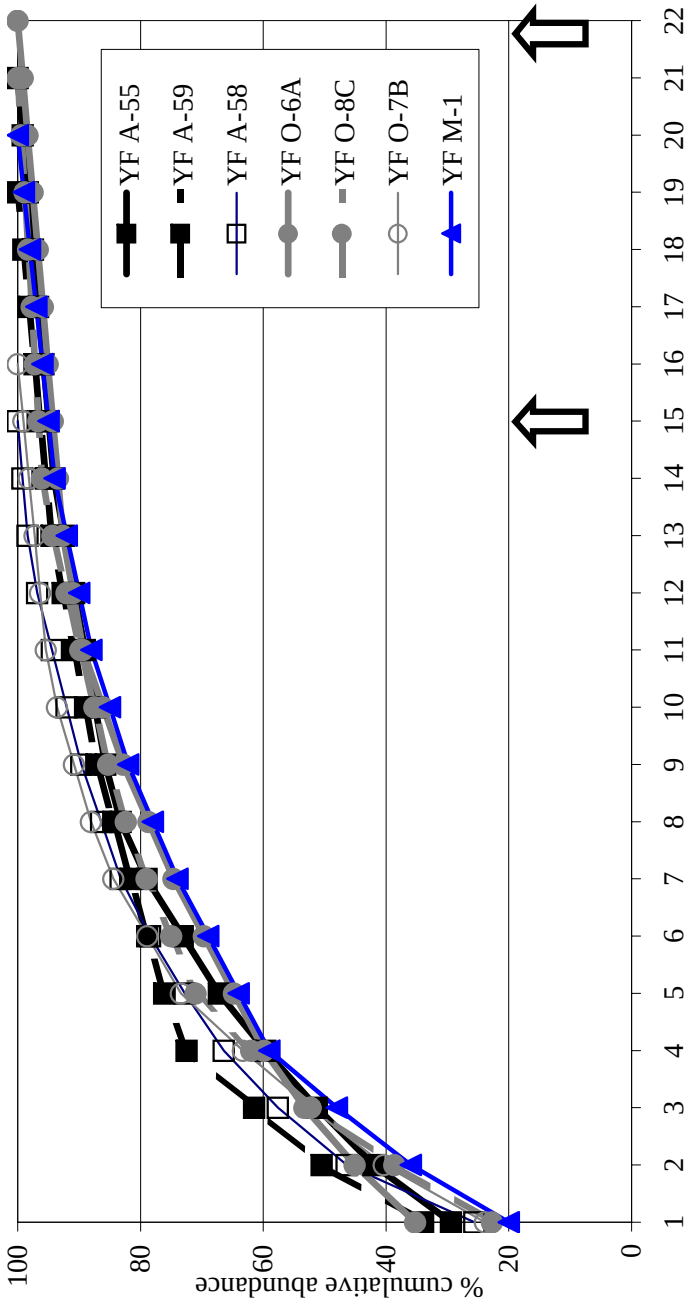

Figure 2.5: Ranking of species in decreasing order of abundance is plotted in relation to the cumulative abundance of the species for the shell bed samples of the Mishash high-productivity region. Arrows indicate the range of species richness for facies 3. Sample labels indicate sampling from locations YF A, YF O or YF M.

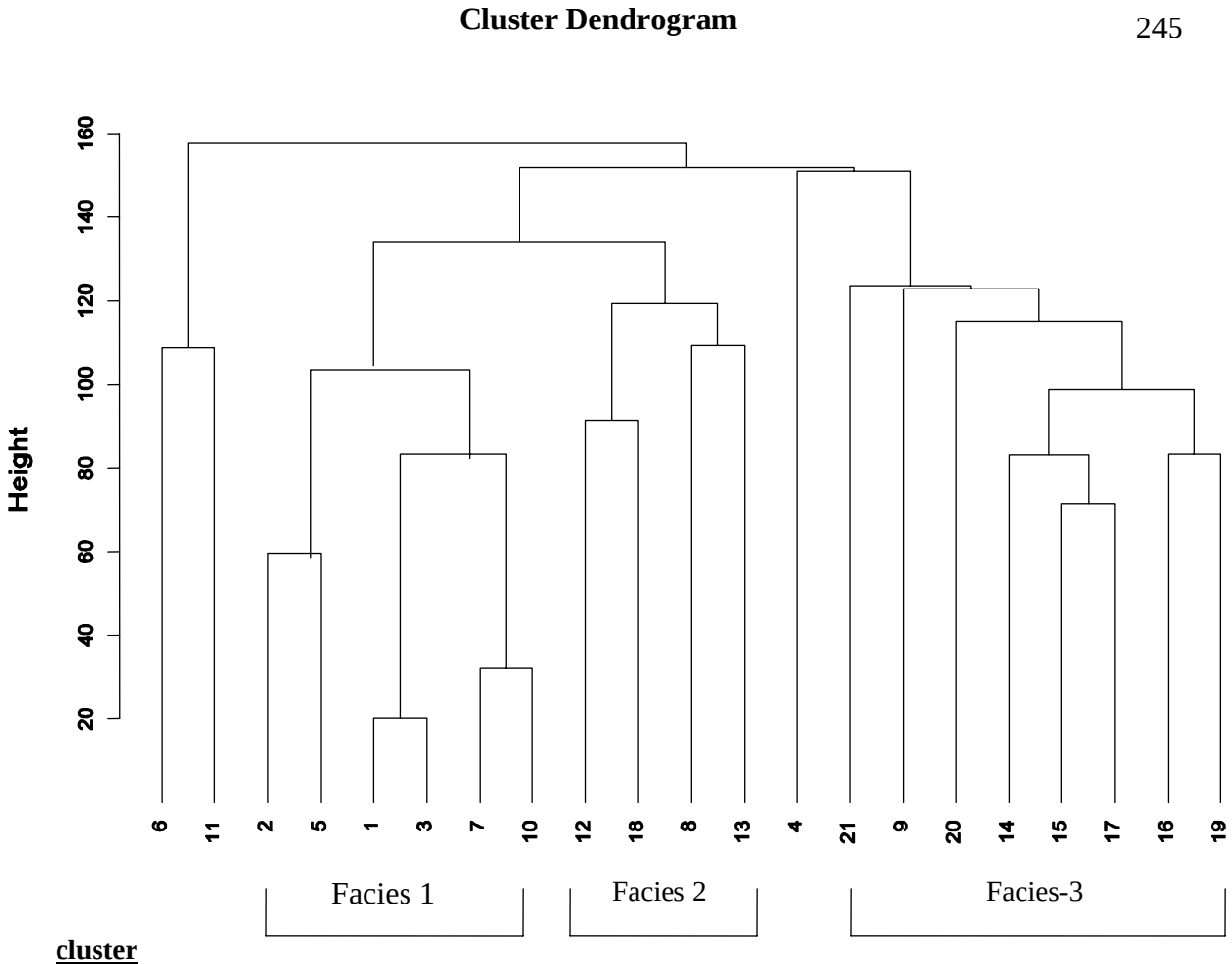

cluster number index -

organic-rich carbonates:	cherts:	porcelanites	shell beds:
	5 = YF A 42	10 = YF A 36A	15 = YF A 55
1 = YF A 43	6 = YF A 43A	11 = YF A 40	16 = YF A 58
2 = YF A 49	7 = YF A 36	12 = YF O 5	17 = YF A59
3 = YF O 4	8 = YF O 6	13 = YF O 7A	18 = YF O 6A
4 = YF O 5A	9 = YF M2	14 = YF O 8	19 = YF O 8C
			20 = YF O 7B
			21 = YF M 1

Figure 2.6: Cluster analysis of associations between the different samples examined. Three main associations were found correlating to lithologic dominance of the different samples. Association 1 (facies 1) corresponds to the area influenced most intensely by the ancient upwelling and is characterized by organic-rich carbonate samples. Association 2 (facies 2) corresponds to the chert and porcelanite samples, which comprise a mixture of variables that range from facies 1 to facies 3, and finally association 3 corresponds to facies 3 with phosphate-rich shell beds. The two samples with extremely high abundances of gastropods (numbers 6 and 11) cluster separately from the rest. Sample number 4 (organic-rich sample) was taken from right below a densely-packed shell bed and may represent a mixture of environments rather than the carbonate-rich environments itself.

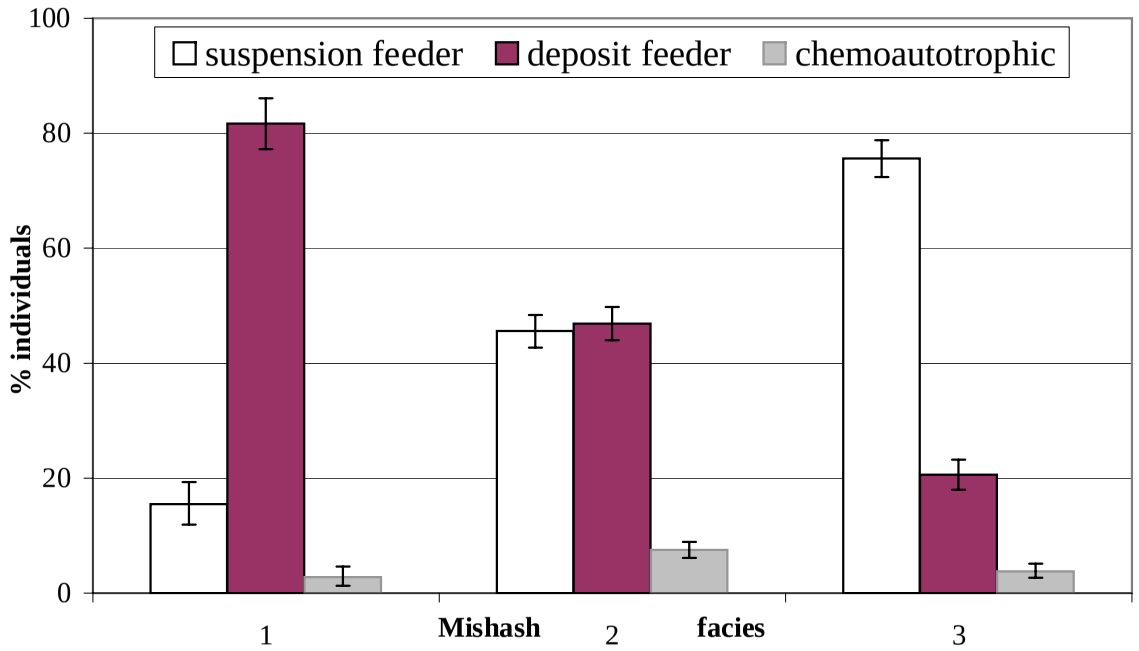

Figure 2.7: Feeding types for Upper Campanian bivalves. Percent of individuals of bivalves for pooled samples from each of the high-productivity facies are given with 95% binomial confidence intervals. Facies-1 characterizes the area closest to the ancient upwelling center, facies-2 represents a mixed facies ranging from facies 1 to 3, and facies-3 characterizes the area marginal to the ancient upwelling.

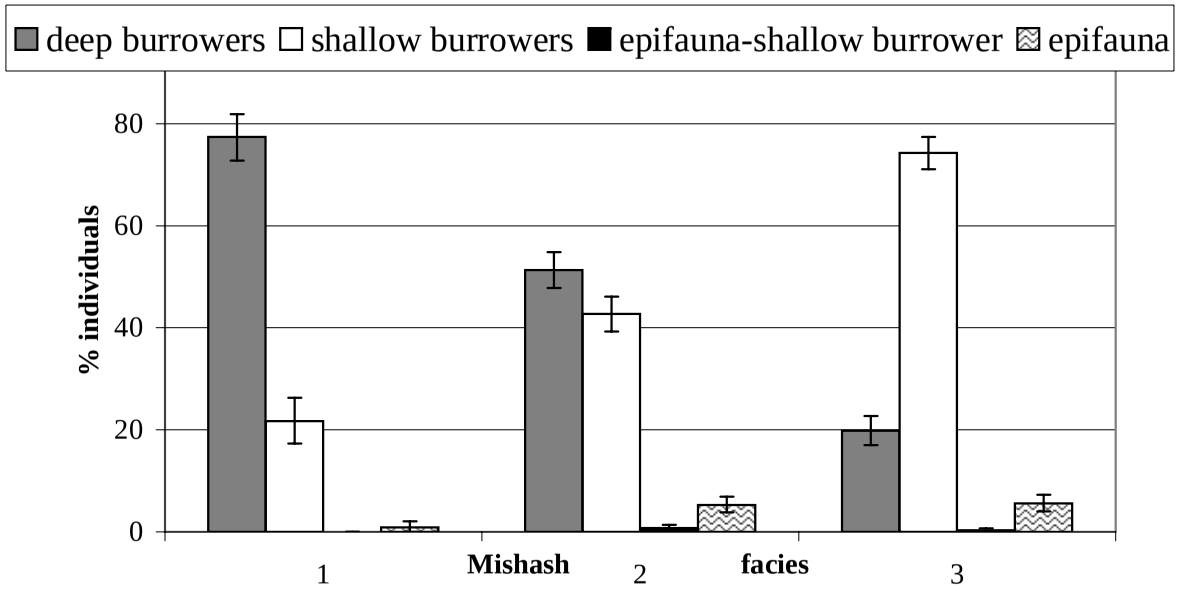

Figure 2.8: Life habitats for Upper Campanian Bivalves. Percent individualds of bivalves for pooled samples from each of the high-productivity facies are given with 95% binomial confidence intervals. Facies-1 characterizes the area closest to the ancient upwelling center, facies-2 represents a mixed facies ranging from facies 1 to 3, and facies-3 characterizes the area marginal to the ancient upwelling.

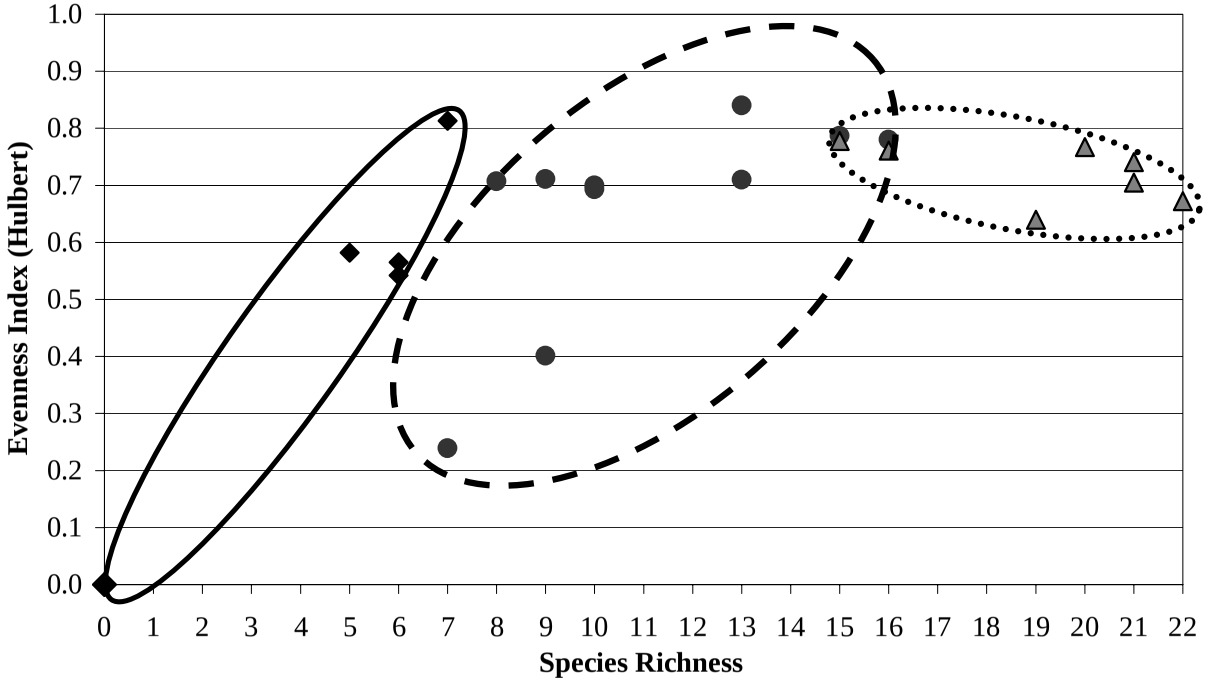

Figure 2.9: Species richness vs. species evenness from each key lithofacies; organic-rich carbonates, chert & porcelanites and phosphorite-rich shell beds.

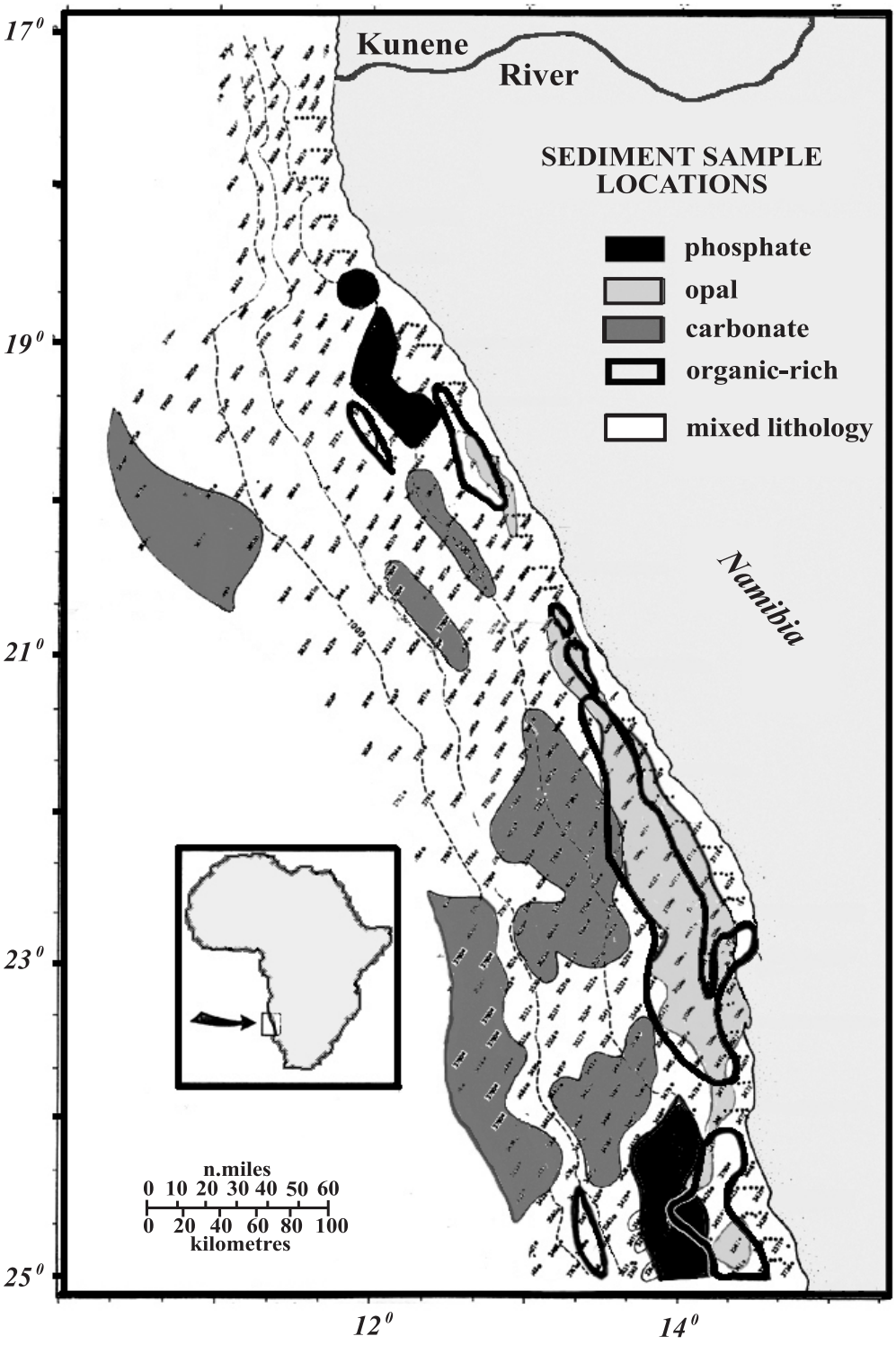

Fig. 3.1: Sediment sample location map of the Benguela upwelling region, Walvis Shelf, between 17^{O}-25^{O} S. Key lithofacies of the upwelling area are based on Bremner, 1978 data regarding highest weight percentages of opal, organic-matter, $CaCO_3$ and phosphate (50-88%, 19-24%, >75% and >20%, respectively).

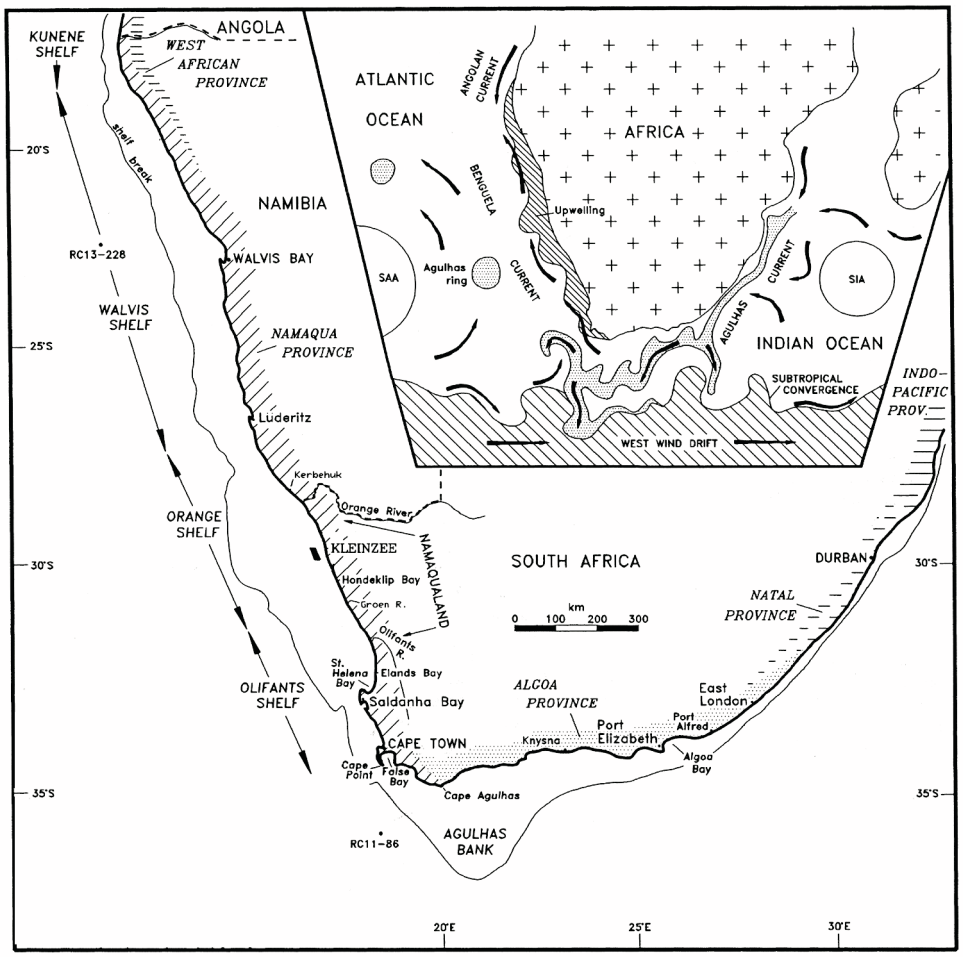

Fig. 3.2: Map of the Benguela current system, SW Africa. Taken from Pether, 1994.

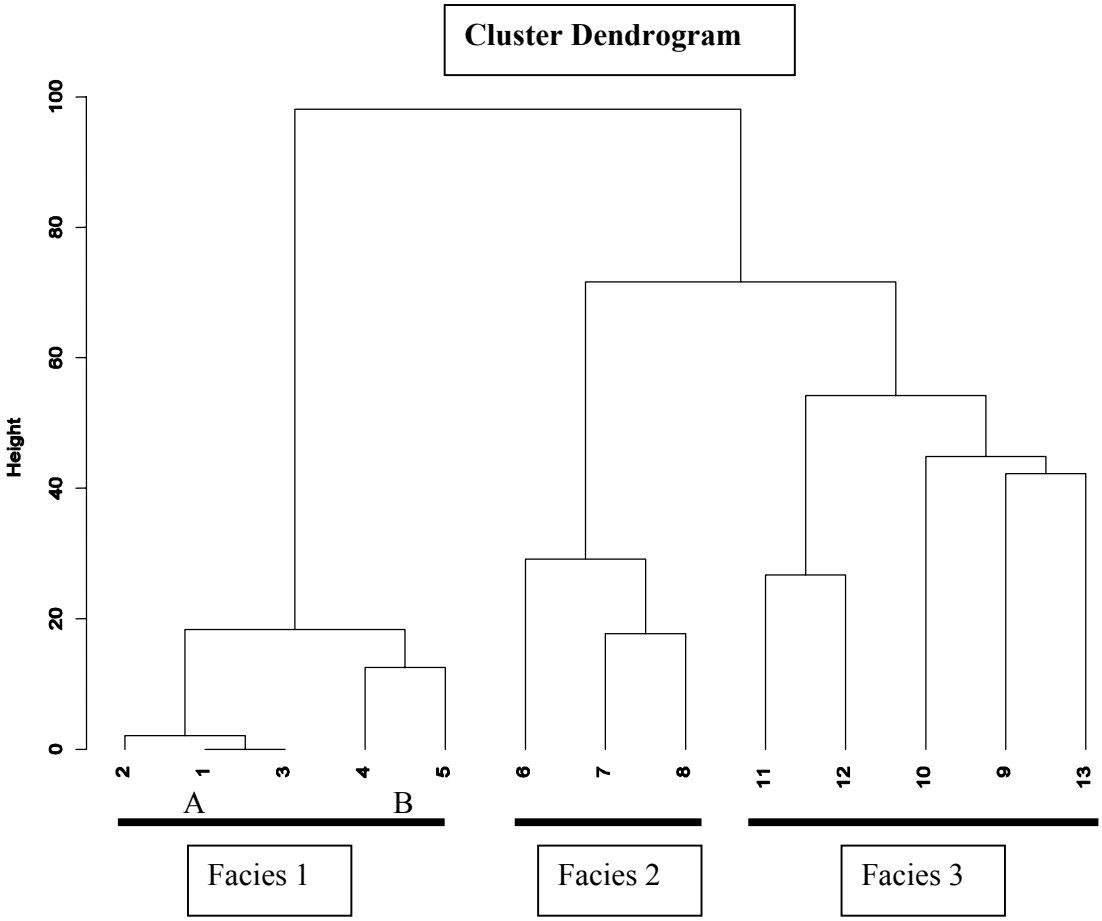

samples in facies 1	samples in facies 2	deep carbonates	samples in facies 3
1 = TBD 3441	6 = TBD 3800	9 = TBD 4015	11 = TBD 3413
2 = TBD 40336	7 = TBD 3770	10 = TBD 3524	12 = TBD 3710
3 = TBD 3741	8 = TBD 4018		13 = TBD 3563
4 = TBD 3519			
5 = TBD 3955			

Figure 3.3: Cluster analysis of associations between the different samples examined. Three main association were found correlating to lithologic dominance of the different samples. Association 1 corresponds to the center of the upwelling and is characterized by samples with a high opal and organic-matter content. Association 2 corresponds to facies 2, which comprises the shallow carbonate-rich samples, and finally association 3 corresponds to facies 3 with samples rich in phosphate. Two deeper carbonate-rich samples (numbers 9, 10) cluster with samples rich in phosphate, but they are regarded as "outliers" to the system as a whole since they are marginal to the main upwelling system.

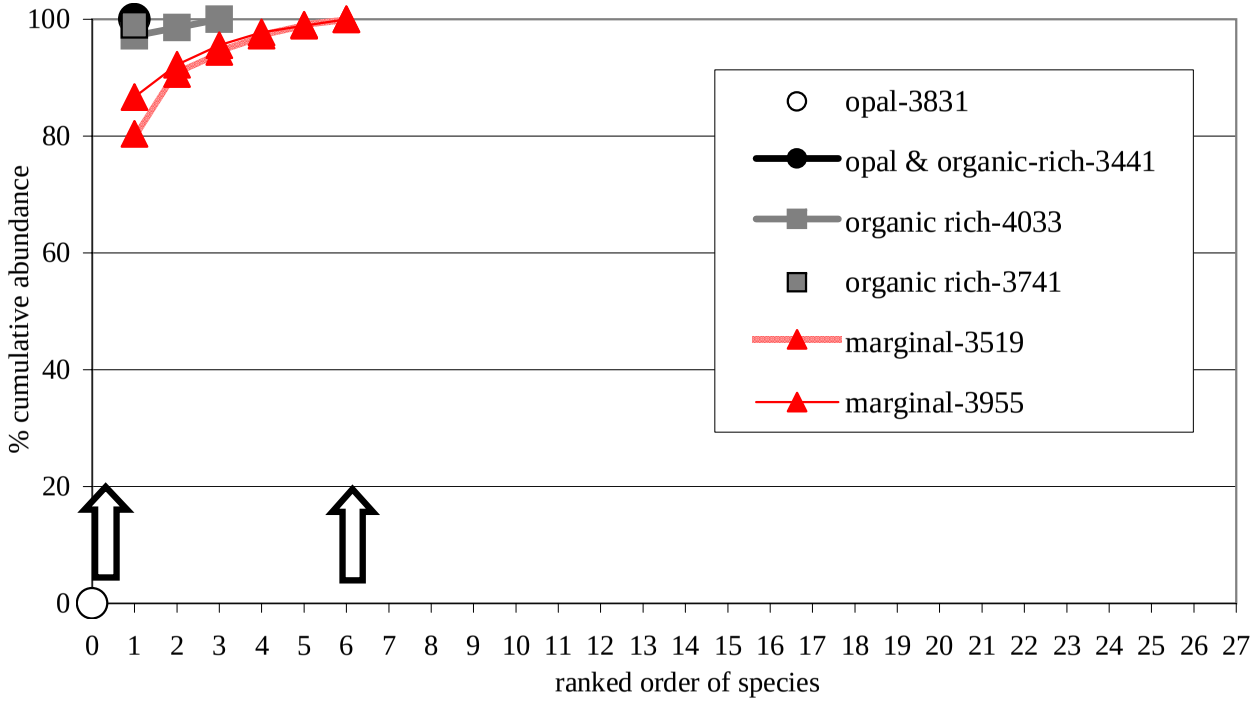

Figure 3.4: Ranking of species in decreasing order of abundance is plotted in relation to the cumulative abundance of the species for the diatomaceous/opal and organic rich ooze samples of the Benguela upwelling region. Arrows indicate range of species richness for facies 1.

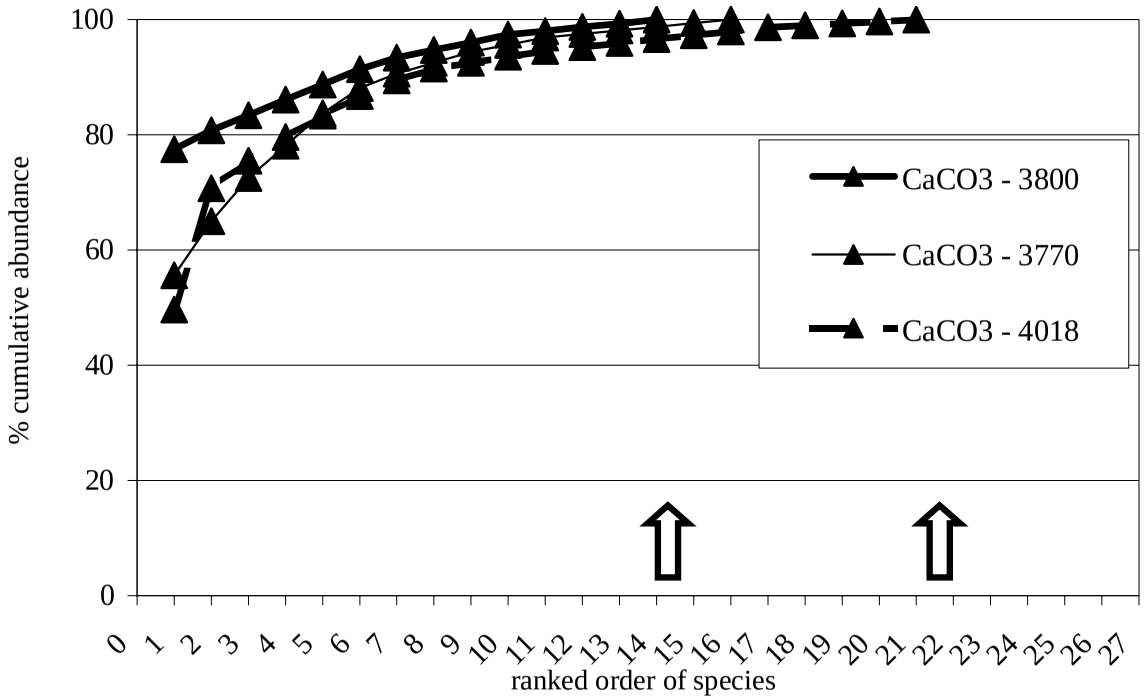

Figure 3.5: Ranking of species in decreasing order of abundance is plotted in relation to the cumulative abundance of the species for the shallow carbonate ooze samples of the Benguela upwelling region. Arrows indicate range of species richness for facies 2.

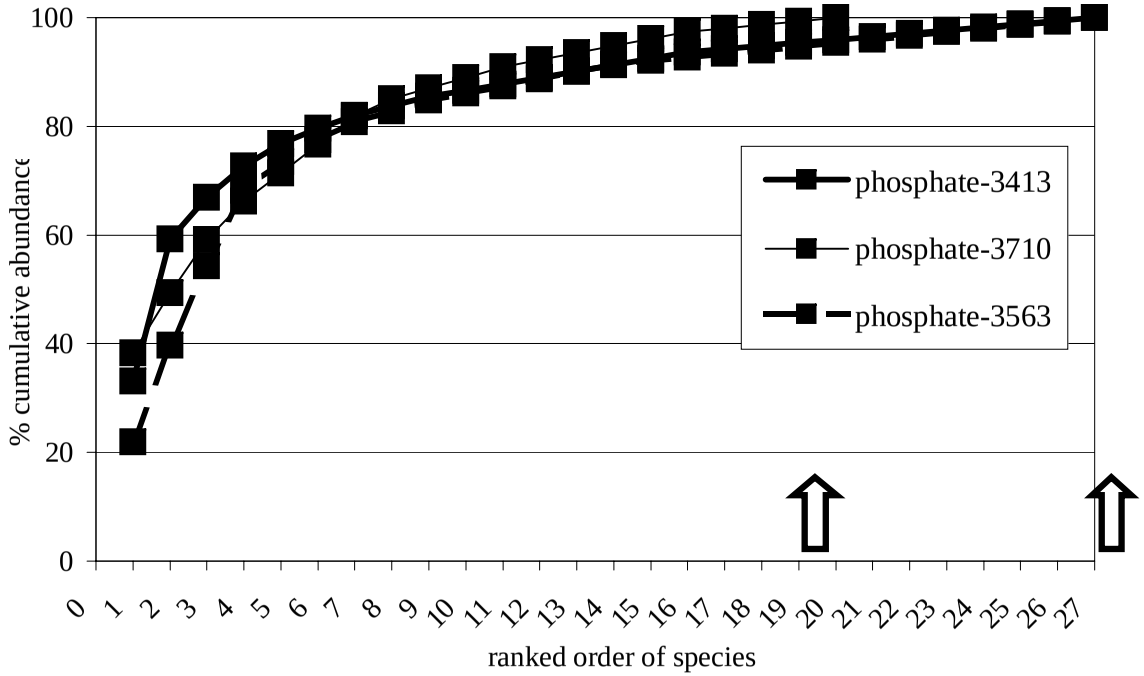

Figure 3.6: Ranking of species in decreasing order of abundance is plotted in relation to the cumulative abundance of the species for the phosphate-rich samples of the Benguela upwelling region. Arrows indicate range of species richness for facies 3.

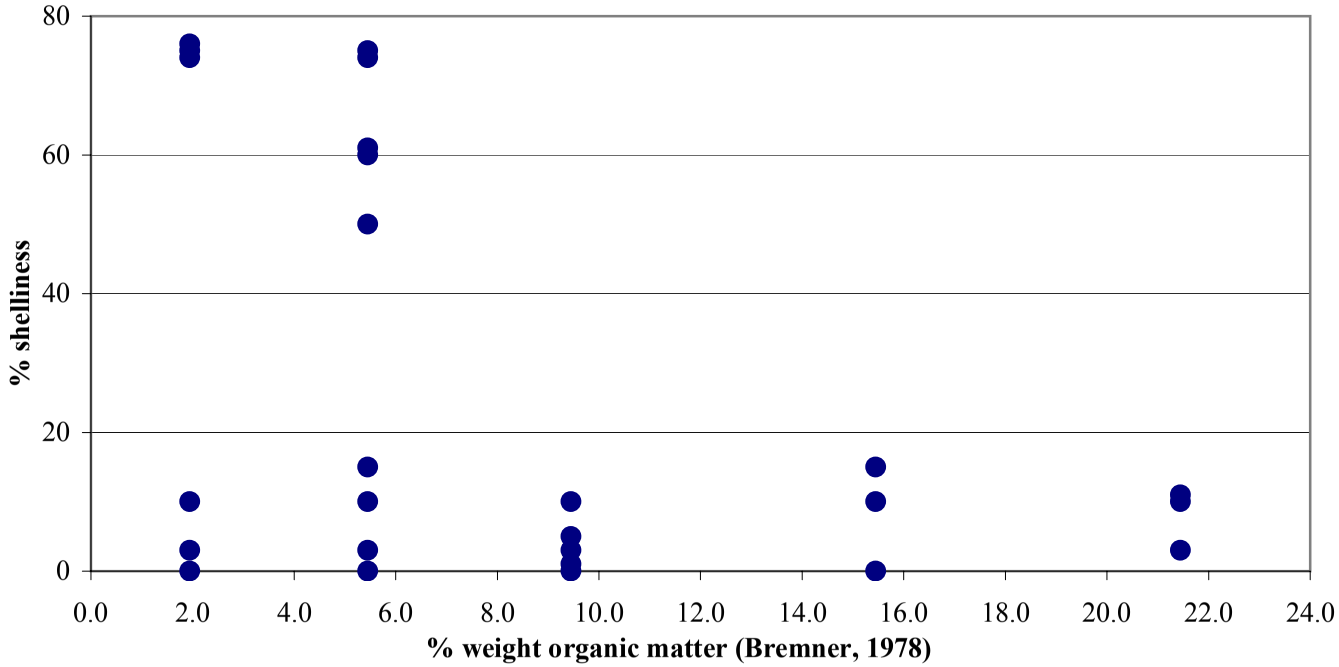

Figure 3.7: Degree of shelliness plotted aginst binned weight percentages of organic matter for each of the 26 samples from the Namibian shelf. A negative correlation (r = -0.44) is shown. Note that above levels of 7% organic matter shelliness does not exceed 15%.

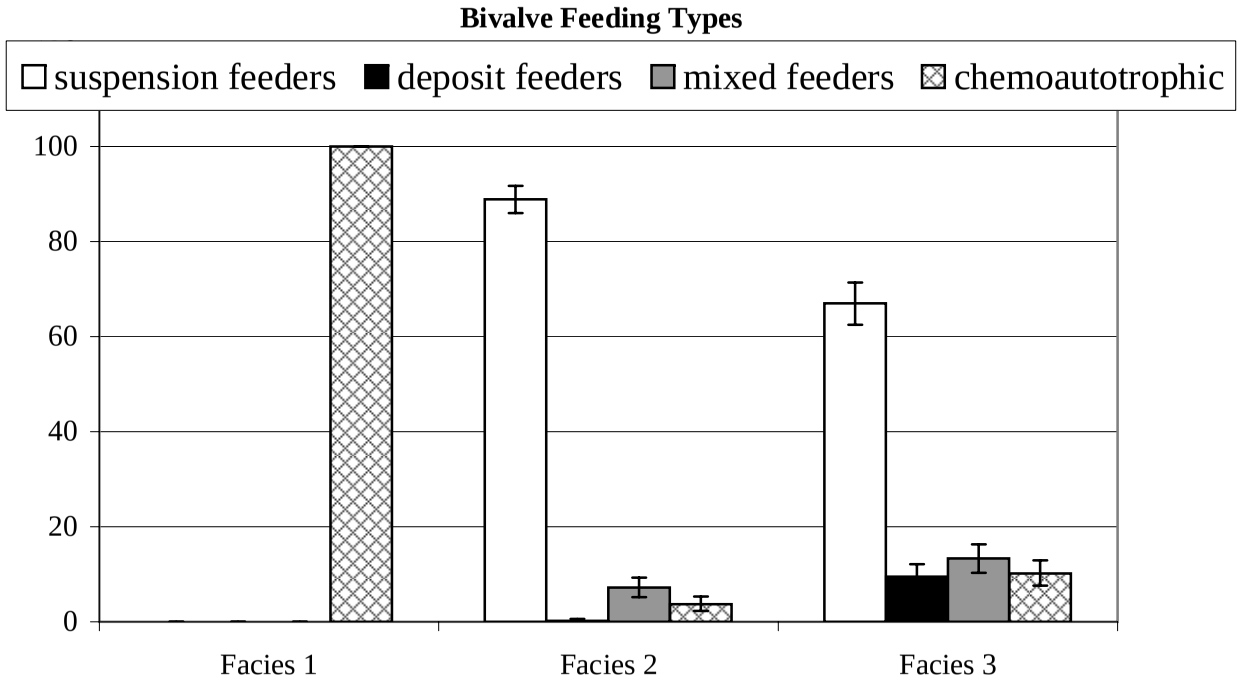

Figure 3.8: Feeding types for Benguela upwelling mollusks. Percent of individuals of bivalves and gastropods for pooled samples from each of the upwelling facies are given with 95% binomial confidence intervals. Facies-1 characterizes the area closest to the upwelling center, facies-2 represents a mixed facies ranging from facies 1 to 3, and facies-3 characterizes the area marginal to the upwelling.

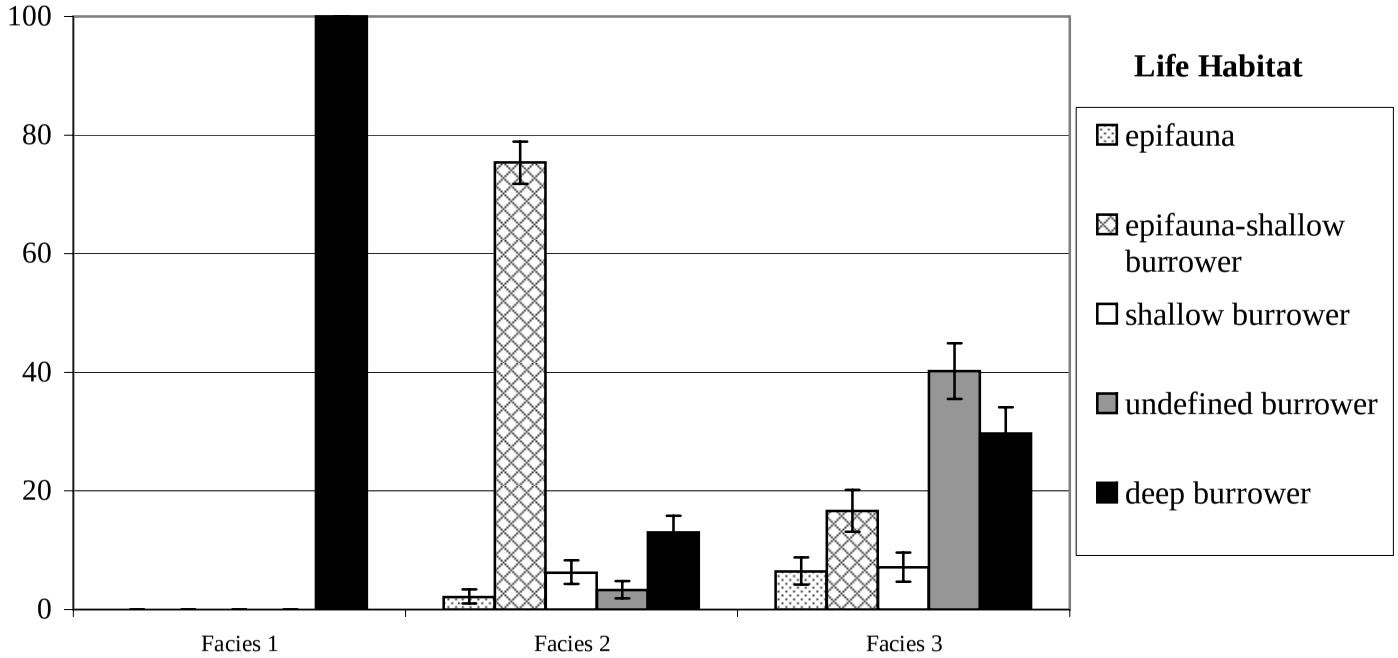

Figure 3.9: Life habitats for Benguela upwelling mollusks. Percent of individuals of bivalves and gastropods for pooled samples from each of the upwelling facies are given with 95% binomial confidence intervals. Facies-1 characterizes the area closest to the upwelling center, facies-2 represents a mixed facies ranging from facies 1 to 3, and facies-3 characterizes the area marginal to the upwelling.

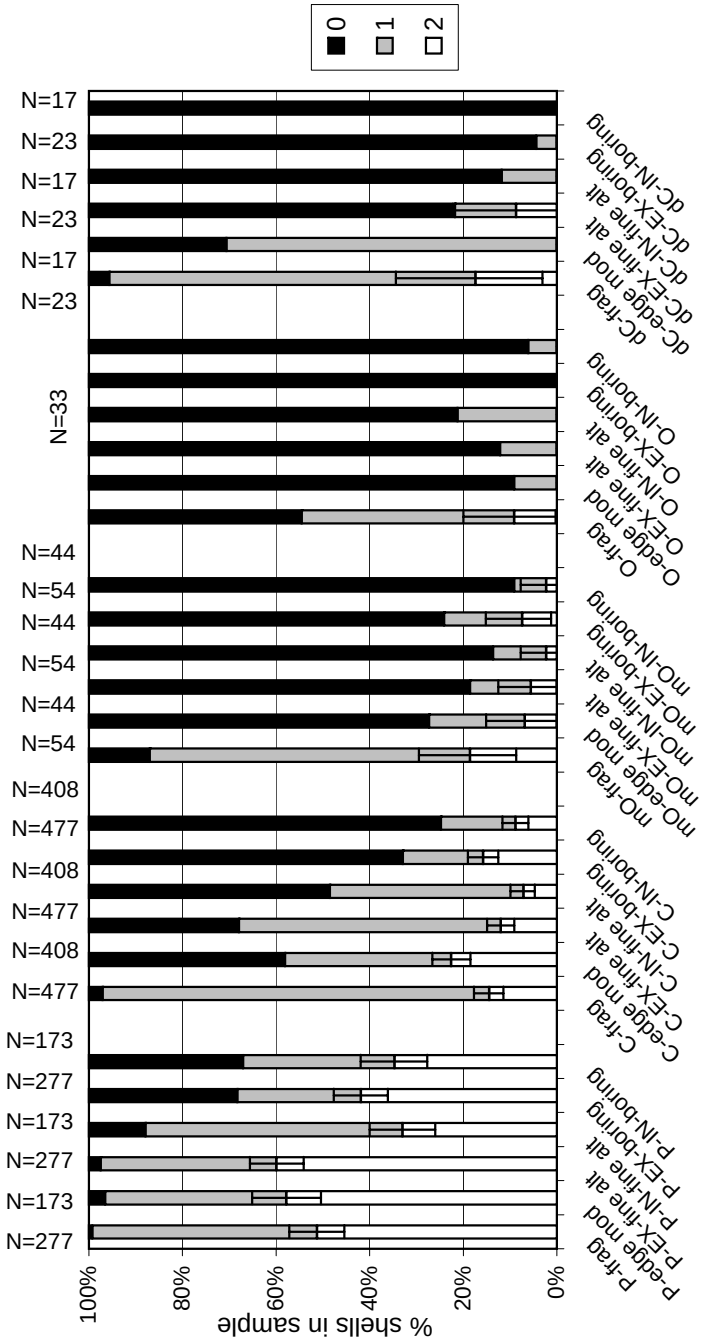

Figure 3.10: Damage profile for exterior and interior of shells from the three main facies of the Benguela system plus samples examined in moderate opal and organic matter concentrations and also offshore carbonate samples. Damage states are scored into three categories: 0=no damage, 1=moderate damage, 2=high damage. The highest degree of damage, score 2, is given with 95% binomial confidence intervals. P=phosphate facies, C=carbonate facies, mO=moderate opal-organic, O=opal-organic rich facies, dC=deep carbonate. frag = fragmentation, edge mod = edge modification, fine alt = fine alteration, EX= shell exterior, IN=shell interior.

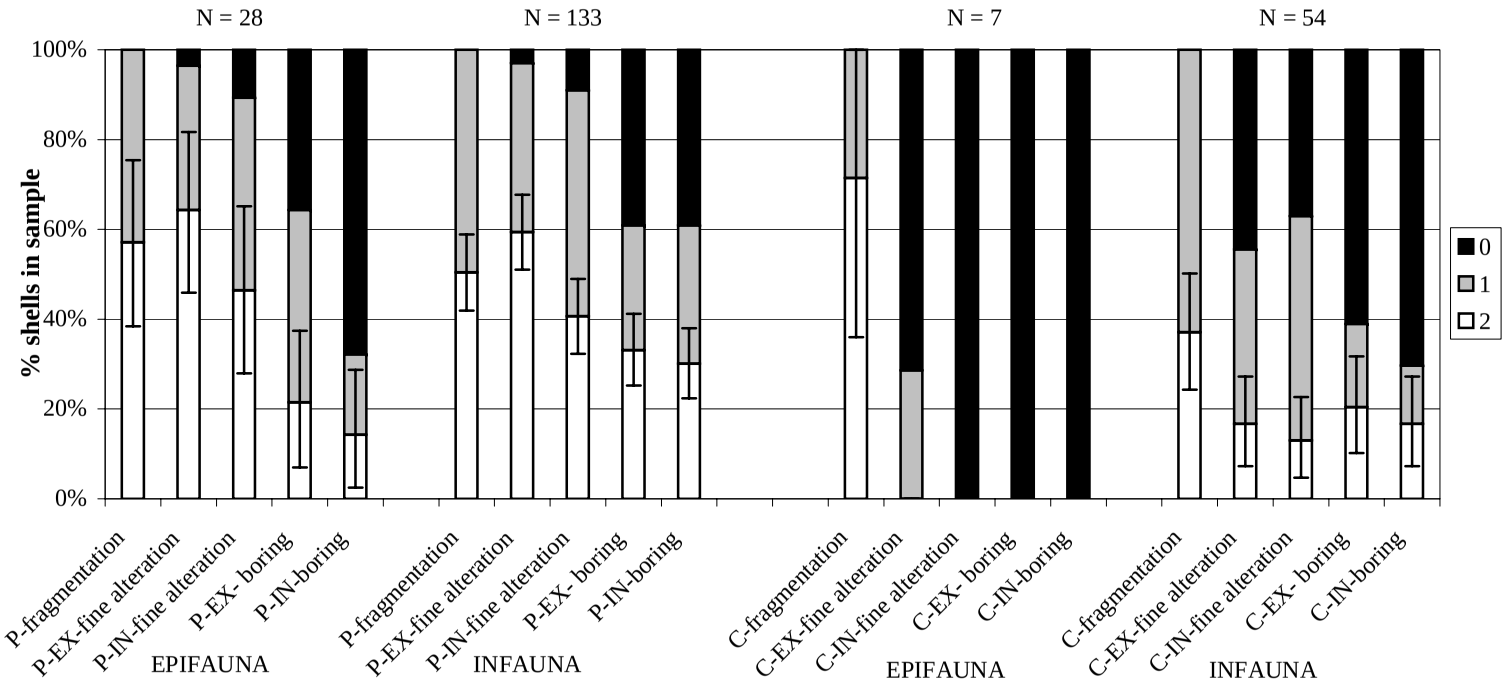

Figure 3.11: Damage profiles comparing exterior and interior of shells of epifaunal and infaunal species from the phosphate-rich and carbonate-rich facies of the Benguela upwelling system. The damage states are scored into three categories. Score 0=no damage, 1=moderate damage, 2=high damage. The highest degree of damage, score 2, is given with 95% binomial confidence intervals. P=phosphate facies, C=carbonate facies, EX= shell exterior, IN=shell interior. Note the low number of individual shells scored for the epifaunal carbonate facies (N=7).

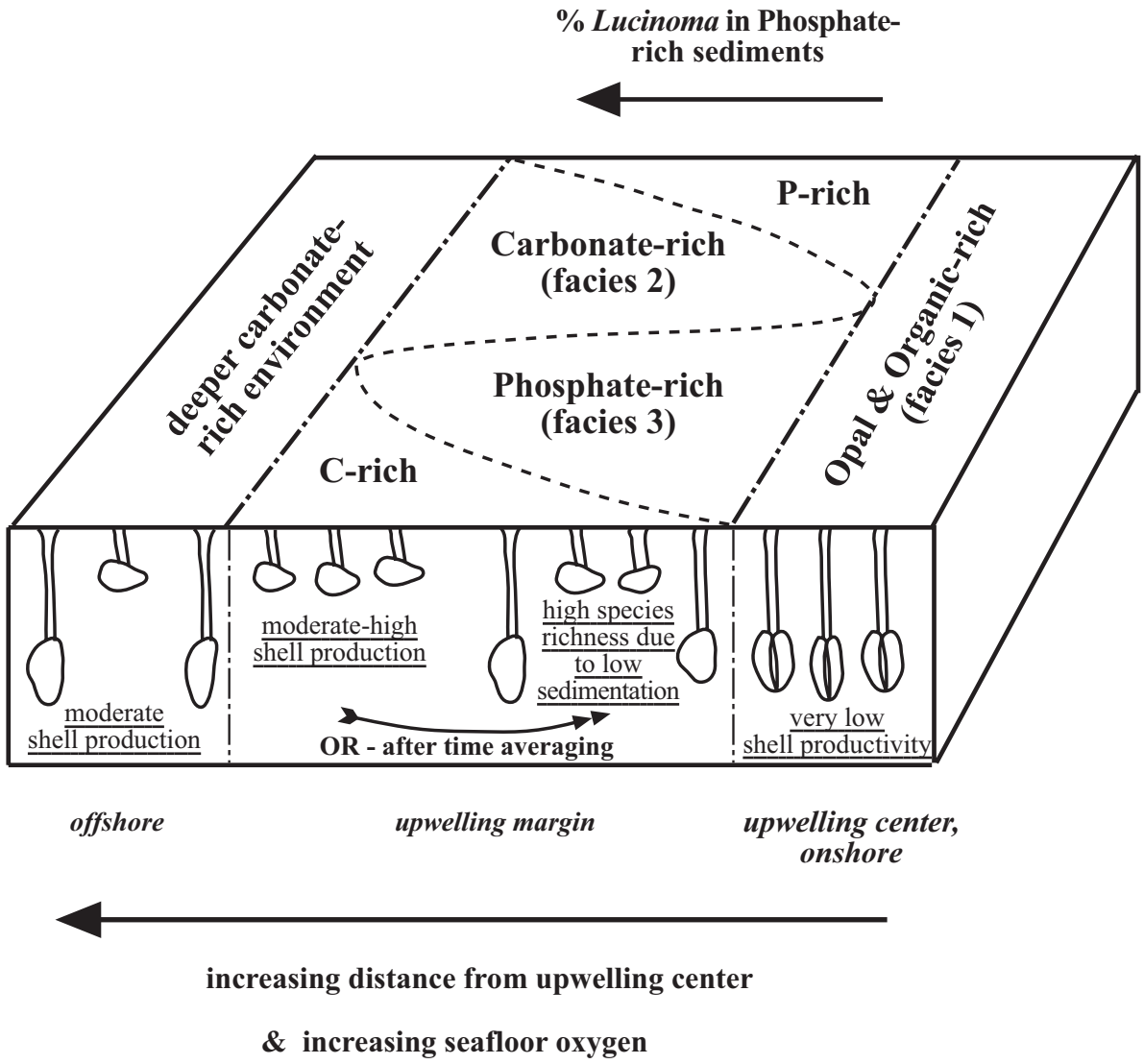

Figure 3.12: Schematic diagram showing the different facies across the Benguela upwelling region, along an increasing distance from the upwelling center. Key molluscan life habitat are schematically shown. Note the patchy nature of the Carbonate and Phosphate facies along a S-N transect. Increasing abundance of the upwelling-characteristic bivalve *Lucinoma* is shown by arrow and given for the Phosphate facies. This indicates initial habitat location of death assemblages prior to taphonomic processess. This means that the death assemblages that originated in close proximity to the upwelling center will show higher relative abundances than samples that were originally populated with species in a more distal location.

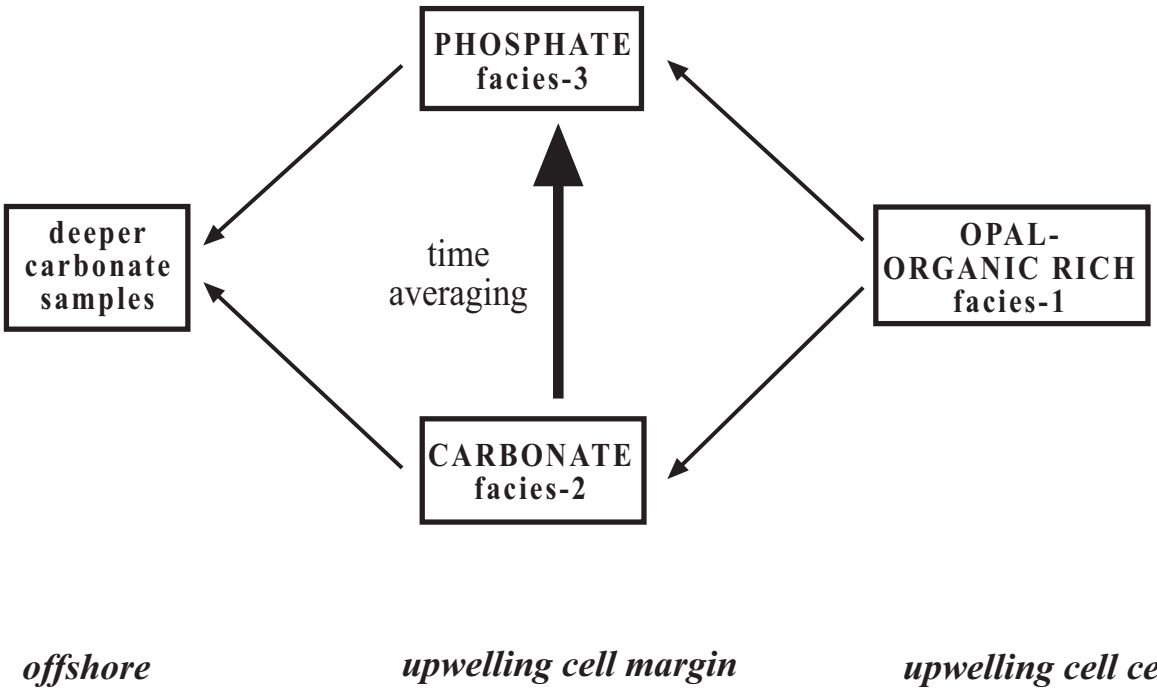

Figure 3.13: Degree of time averaging in molluscan death assemblages across the region of the Benguela upwelling system. From the center of the upwelling cells (facies 1), through the marginal cell facies (either facies 2 OR 3) and offshore, towards the deeper carbonate-rich samples.

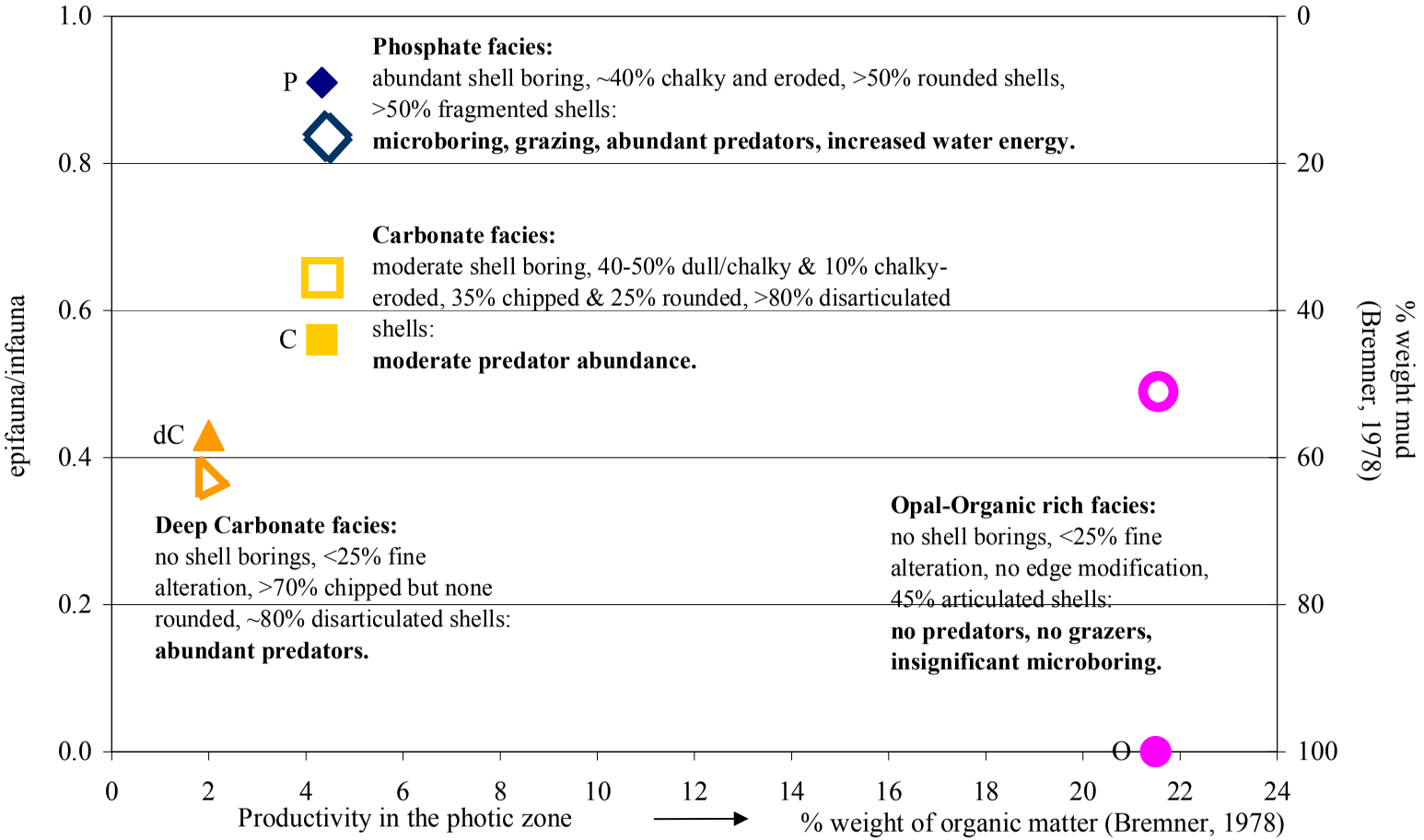

Figure 3.14: Taphofacies of the Benguella upwelling system. Epifaunal-infaunal ratio and % weight of the mud fraction in the sediment is plotted against %weight of organic matter for the main upwelling facies. P=phosphate facies, C=carbonate facies, O=opal-organic rich facies. The open symbols = mud frequencies. Note greater shell damage further from the main upwelling (facies O towards facies C & P, respectively). Also note greater shell damage along a trend of increasing substrate hardening that is linked to increased time averaging.

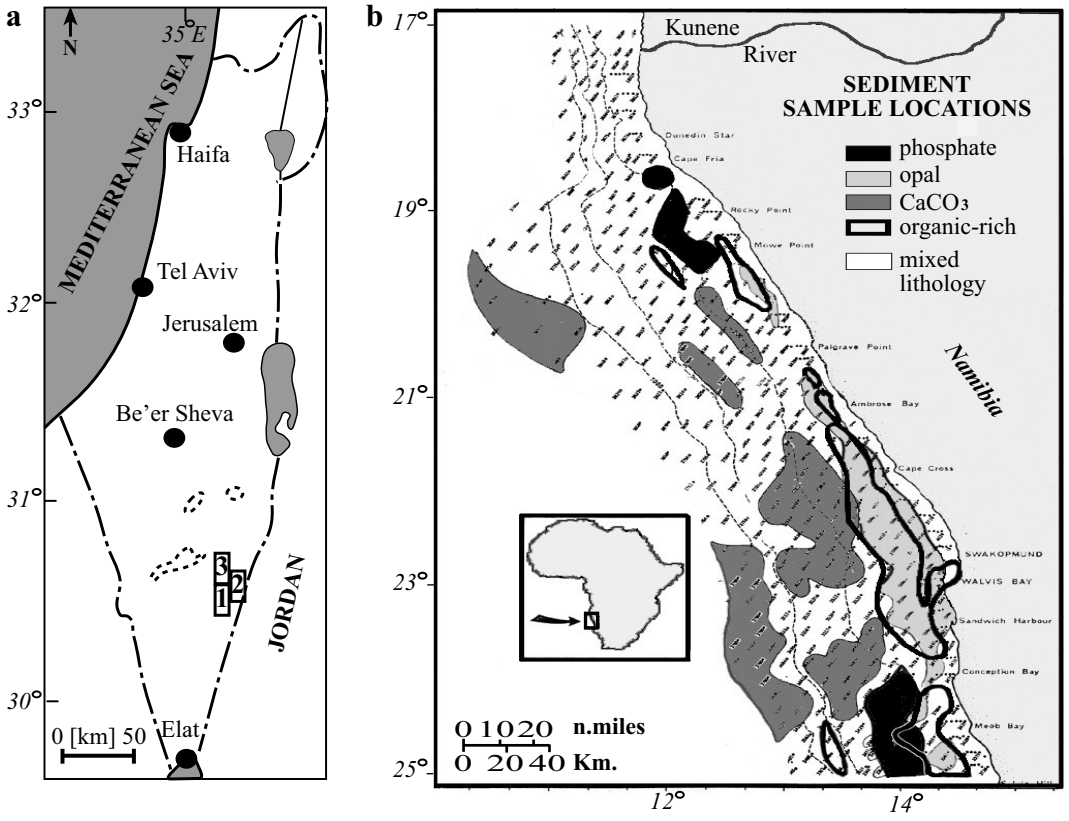

Fig. 4.1: (a) Location map of three measured sections of Upper Campanian Phosphate Member of the Mishash Fm in southern Israel. Sampling was done from major key lithologies that comprise the ancient upwelling facies: organic-rich carbonates, thin, fossiliferous cherts & porcelanites and loosely to densely packed shell beds were collected from the lower Phosphatic-Carbonate unit of the Phosphate Member, while barren porcelanite layers and loosely-packed shell beds intermittent within these massive porcelanites were collected from the higher Porcelanite unit of the Phosphate Member. Locations are sketched as squares. Maktesh-"crater" structures are sketched in dotted line. **(b)** Sediment sample location map of the Benguela upwelling region, Walvis Shelf, between 17^{O}-25^{O} S. Sub-sampling was dome from the key biofacies of the upwelling area, which are based on Bremner, 1978 data regarding highest weight percentages of opal, organic-matter, CaCO3 and phosphate (50-88%, 19-24%, >75% and >20%, respectively).

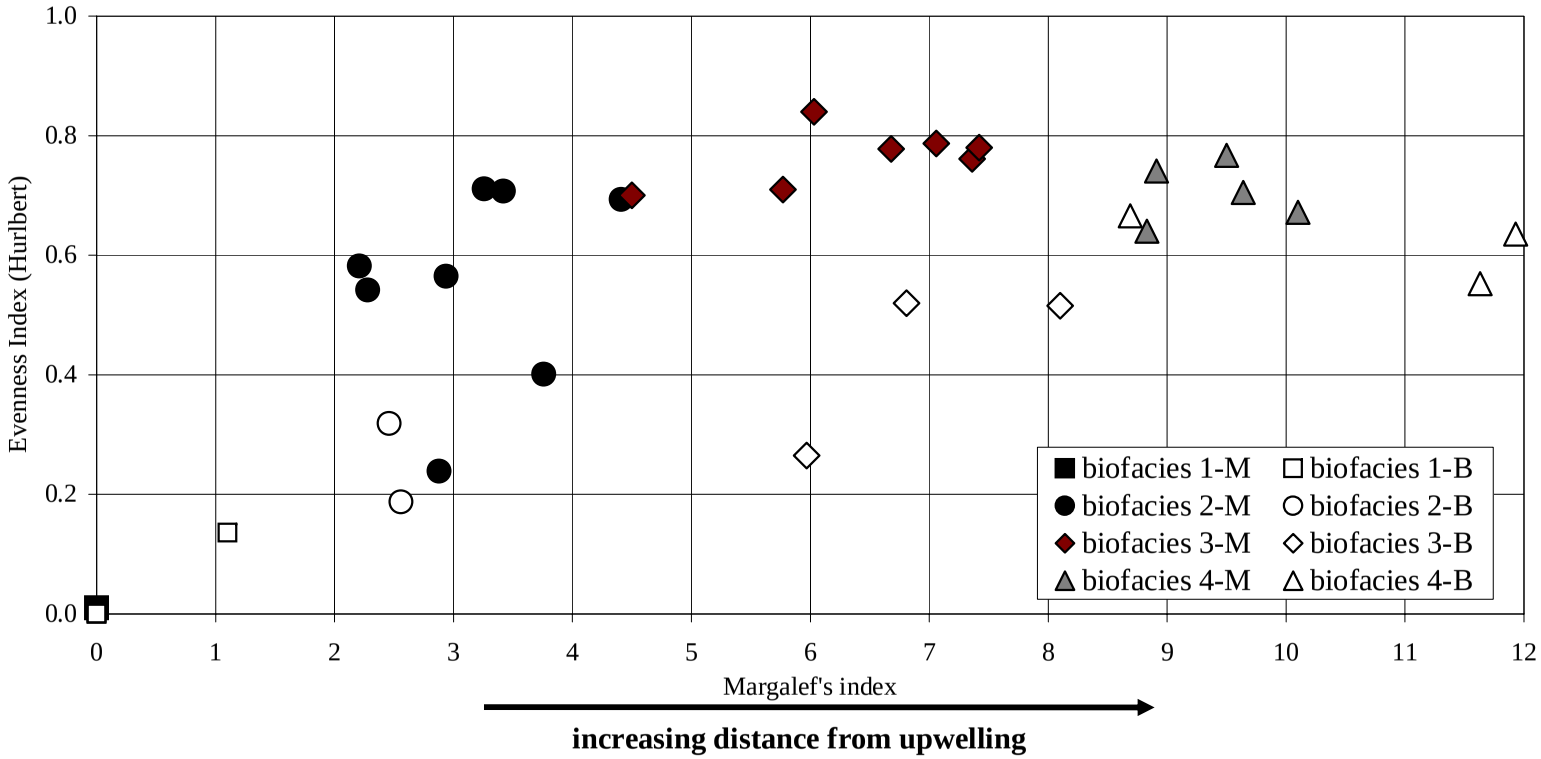

Figure 4.2: Margalef's index vs. Hulbert's PIE for ancient and modern upwelling samples. The samples divide according to their species richness and evenness into four main biofacies typical of the mosaic of seafloor conditions under the main upwelling zone. Biofacies 1-4 follow a gradient of increasing distance from the upwelling center parallel to an inferred increase in seafloor oxygen. Biofacies 1-M=samples from Mishash Fm. that group under facies 1, biofacies 1-B=samples from the Benguela upwelling.

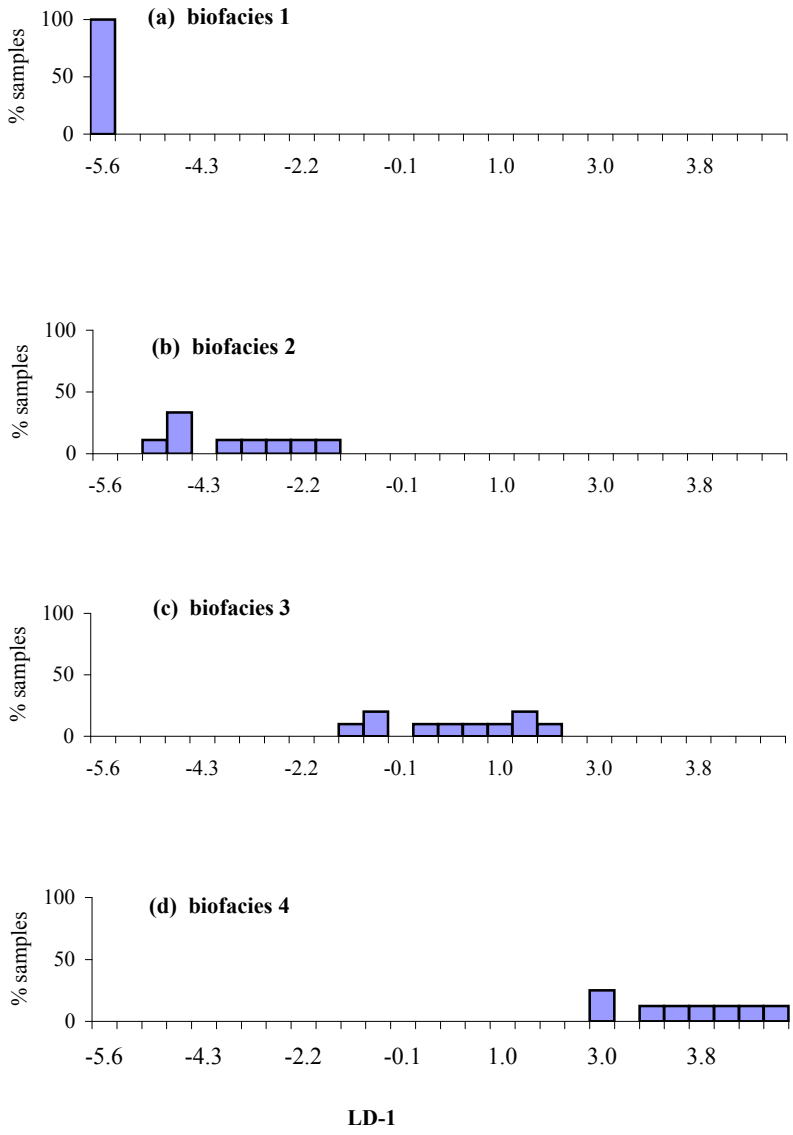

Figure 4.3 (a-d): Discmininant analysis scores for ancient and modern upwelling samples. The percent of samples is plotted against linear discriminant function 1 (LD-1), which represents 90% of the variance. Each panel (a-d) represents the four biofacies that characterize the upwelling regions.

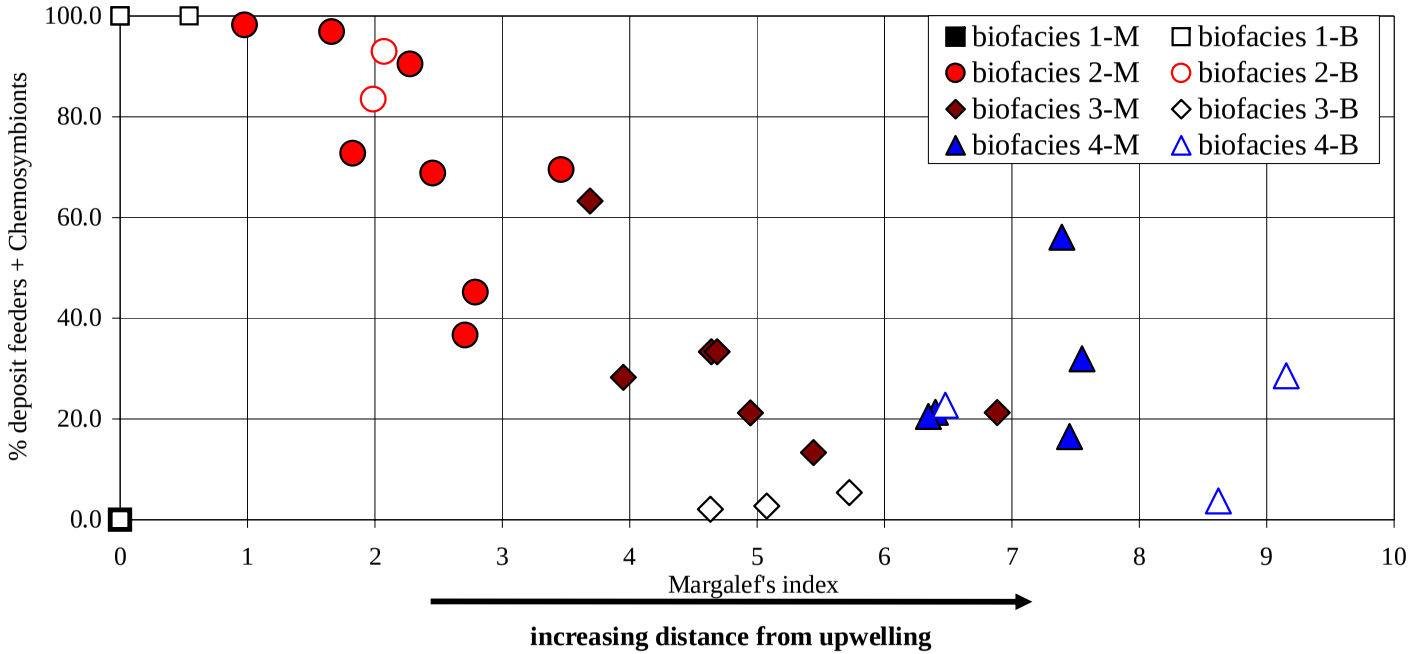

Figure 4.4: Margalef's index vs. % chemosymbionts+depodit feeding bivalves for ancient and modern upwelling samples. The samples divide according to their species richness and feeding types into four main biofacies typical of the mosaic of seafloor conditions under the main upwelling zone. Biofacies 1-4 follow a gradient of increasing distance from the upwelling center parallel to an inferred decrease in organic matter in seafloor oxygen. Biofacies 1-M=samples from Mishash Fm. that group under facies 1, biofacies 1-B=samples from the Benguela upwelling.

REFERENCES

Abed, A.M. and Sadaqah, R., 1998. Role of Upper Cretaceous oyster bioherms in the deposition and accumulation of high-grade phosphorites in central Jordan. *J. Sed. Res.*, 68(5) part A: 1009-1020.

Aller, J.Y., 1995. Molluscan death assemblages on the Amazon Shelf: implication for physical and biological controls on benthic populations. *Palaeogeogr., Palaeoclimatol., Palaeoecol*., 118: 181-212.

Allmon, W.D., Spizuco, M.P. and Jones, D.S., 1995. Taphonomy and paleoenvironment of two turritellid-gastropod-rich beds, Pliocene of Florida. *Lethaia*, 28: 75-83.

Almogi-Labin, A., Luz, B. and Duplessy J-C., 1986. Quaternary paleo-oceanography, pteropod preservation and stable-isotope record of the Red Sea. *Palaeogeogr., Palaeoclimatol., Palaeoecol*., 57: 195-211.

Almogi-Labin, A., Reiss, Z. and Caron, M., 1986. Senonian Globotruncanidae from Israel. *Eclogae Geol. Helv.*, 79: 849-895.

Almogi-Labin, A., Bein, A. and Sass, E., 1990. Agglutinated foraminifera in organic-rich neritic carbonates (Upper Cretaceous, Israel) and their use in identifying oxygen levels in oxygen-poor environments. In: *Paleoecology, Biostratigraphy, Paleoceanography and Taxonomy of Agglutinated Foraminifera.* Hemleben C., et al. (eds.), Dordrecht, Kluwer Academic Publishers, pp. 565-585.

Almogi-Labin, A., Bein, A. and Sass, E., 1993. Late Cretaceous upwelling system along the southern Tethys margin (Israel): Interrelationship between productivity, bottom water environments and organic matter preservation. *Paleoceanography*, 8: 671-690.

Aqrabawi, M., 1993. Oysters (Bivalvia-Pteriomorphia) of the Upper Cretaceous rocks of Jordan. Palaeontology, stratigraphy and comparison with the Upper Cretaceous oysters of northwest Europe. *Mitt. Geol.-Paläont. Inst. Univ. Hamburg,* 75: 1-135.

Arntz, W.E., Tarazona, J., Gallardo, V.A., Flores, L.A. and Salzwedel, H., 1991. Benthos communities in oxygen deficient shelf and upper slope areas of the Peruvian and Chilean Pacific coast, and changes caused by El Niño. In: *Modern and Ancient Continental Shelf Anoxia*. Tyson R.V. and Pearson T.H. (eds.), Geological Society of London Publication No. 58, pp. 131-154.

Bailey, G.W., 1991. Organic carbon flux and development of oxygen deficiency on the modern Benguela continental shelf south of 22°S: spatial and temporal variability. In: *Modern and Ancient Continental Shelf Anoxia*. Tyson R.V. and Pearson T.H. (eds.), Geological Society Publication No. 58, pp. 171-183.

Bandel., K, Shinaq, R. and Nazzal, J., 1999. Palaeoecological and diagenetical significance of a silicified soft bottom fauna of Campanian age (Qatrana Unit, Jordan). *Mitt. Geol.-Paläont. Inst. Univ. Hamburg,* 83: 203-218.

Baturin, G.N., 1982. *Phosphorites on the Sea Floor: Origin, composition, and Distribution*. Dev. Sedimentology, 33: 1-343. Amsterdam, Elsevier.

Behrensmeyer, A.K., Kidwell, S.M., Gastaldo, R.A., 2000. Taphonomy and paleobiology. In: *Deep time: Paleobiology's perspective*. Erwin D.H. and Wing S.L. (eds.), Lawrence, Kansas, Paleontol. Soc., pp. 103-147.

Beisel, J.-N., Usseglio-Polatera, P., Bachmann, V. and Moreteau, J.-C., 2003. A comparative analysis of evenness index sensitivity. *Internat. Rev. Hydrobiol.*, 88: 3-15.

Bernhard, J.M., 1992. Benthic foraminiferal distribution and biomas related to pore-water oxygen-content – central California continental-slope and rise. *Deep-Sea Research Part A*, 39: 585-605.

Bernhard, J.M., and Reimers, C.E., 1991. Benthic foraminiferal population fluctuations related to anoxia: Santa Barbara Basin. *Biogeochemistry*, 15: 127-149.

Best, M.M.R., 2000. Fates of skeletal carbonate in tropical marine siliciclastic and carbonate sediments, Panama. *Unpublished PhD Dissertation, University of Chicago,* 309 pp.

Birch, G.F., 1975. Sediments on the continental margin off the west coast of South Africa. *PhD Thesis, Geology Department, University of Cape Town*, 210 pp.

Bonsdorff, E., Diaz, R.J., Rosenberg, R., Norkko, A. and Cutter, G.R., Jr., 1996. Characterization of soft-bottom benthic habitats of the Aland Islands, northern Baltic Sea. *Marine Ecology Progress Series*, 142: 235-245.

Boyd, A.J., 1987. The oceanography of the Namibian shelf. *PhD Thesis, Geology Department, University of Cape Town*, 295 pp.

Bremner, J.M., 1978. Sediments on the continental margin off South West Africa between latitudes 17º and 25ºS. *PhD Thesis, Geol. Dept. Univ. Cape Town*, 300 pp.

Bremner, J.M., 1980. Concretionary phosphorite from SW Africa. *J. Geol. Soc. London*, 137: 773-786.

Bremner, J.M., 1981. Shelf morphology and surficial sediment off central and northern South West Africa (Namibia). *Geo-Marine Letters*, 1:91-96.

Bremner, J.M., 1983. Biogenic sediments on the South West African (Namibian) continental margin. In: *Coastal Upwelling, Its Sediment Record, Part B: In Sedimentary Record of Ancient Coastal Upwelling.* Theide J. and Suess E. (eds.), NATO Conference Series, IV, Marine Sciences, 10(b): 73-104.

Brett, C.E. and Baird, G.C., 1986. Comparative taphonomy: a key to paleoenvironmental interpretation based on fossil preservation. *Palaios*, 1: 207-227.

Brongersma-Sander, M., 1957. Mass mortality in the sea. *Mem. Geol. Soc. Am*., 67: 941-1010.

Brown, A.C. and Jarman, N., 1978. Coastal marine habitats. In: Werger, M.J.A., (ed.), Biogeography and ecology of Southern Africa, Part 2. Hague: Junk. *Monographiae Biologicae*, 31: 1239-1277.

Bruchert, V., Pérez, M.E. and Lange, C.B., 2000. Coupled primary production, benthic foraminiferal assemblage, and sulfur diagenesis in organic-rich sediments of the Benguela upwelling system. *Mar. Geol.*, 163: 27-40.Bein, A., Almogi-Labin, A. and Sass, E., 1990. Sulfur sinks and organic carbon relationships in Cretaceous organic-rich carbonates: Implications for evaluation of oxygen-poor depositional environments. *Am. J. Sci.*, 290: 882-911.

Calvert, S.E. and Price, N.B., 1983. Geochemistry of Namibian shelf sediments. In: *Coastal upwelling: Its sediment record, Part B: Sedimentary records of ancient coastal upwelling*. Thiede J. and Suess E. (eds), Plenum Press, New York, 337-375 pp.

Cary, S.C., Vetter, R.D. and Felbeck, H., 1989. Habitat characterization and nutritional strategies of the endosymbiont-bearing bivalve *Lucinoma aequizonata*. *Marine Ecology Progress Series*, 55: 31-45.

Chapman, P. and Shannon, L.V., 1985. The Benguela ecosystem. Part II. Chemistry and related processes. *Oceanogr. Mar. Biol. Annu. Rev*., 23:183-251.

Chavan, A., 1947. La faune Campanienne du Mont des Oliviers d'après les matériaux Vignal-Massé. *J. Conchyliol*., 87:125-197.

Clarke, K.R. and Warwick, R.M., 1994. Change in marine community: an approach to statistical analysis and interpretation. Natural Environment Research Council, UK, 144pp.

Compton, J.S., Hodell, D.A., Garrido, J.R. and Mallinson, D.J., 1993. Origin and age of phosphorite from the south-central Florida Platform: relation of phosphogenesis to sea-level fluctuations and $\delta^{13}C$ excursions. *Geochim. Cosmochim. Acta*, 57: 131-146.

Compton, J.S., Mulabisana, J. and McMillan, I.K., 2002. Origin and age of phosphorite from Last Glacial Maximum to Holocene transgressive succession of the Orange River, South Africa. *Mar. Geol*., 186: 243-261.

Dauer, D.M., Rodi Jr., A.J. and Ranasinghe, J.A., 1992. Effects of low dissolved oxygen events on the macrobenthos of the lower Chesapeake Bay. *Estuaries*, 15: 384-391.

Davies, D.J., Powell, E.N. and Stanton Jr., R.J., 1989. Taphonomic signature as a function of environmental process: Shells and shell beds in a hurricane-influenced inlet on the Texas coast. *Palaeogeogr., Palaeoclimatol., Palaeoecol*., 72: 317-356.

De Stigter, H.C., 1996, Recent and fossil benthic foraminifera in the Adriatic Sea: distribution patterns in relation to organic carbon flux and oxygen concentration at the sea bed. Geologica Ultraiectina, 254 pp.

Diaz, R.J., Rosenberg, R., 1995. Marine benthic hypoxia: A review of its ecological effects and the behavioural responses of benthic macrofauna. *Oceanogr. Mar. Biol*., 33: 245-303.

Diester-Haass, L., Meyers, P.A., and Rothe, P., 1992. The Benguela Current and associated upwelling on the southwest African Margin: a synthesis of the Neogene-Quaternary sedimentary record at DSDP sites 362 and 532. In Summerhayes, C.P., Prell, W.L., and Emeis, K.C., eds., Upwelling systems: Evolution Since the Early Miocene. *Geol. Soc. London Spec. Publ*., 64, 331-342.

Dingle, R.V., 1995. Continental shelf upwelling and benthic Ostracoda in the Bengueal system (southeastern Atlantic Ocean). *Mar. Geol*., 122: 207-225.

Dingle, R.V., Lord, A.R. and Boomer, I.D., 1989. Ostracod faunas and water masses across the continental margin off southwestern Africa. *Mar. Geol*., 87: 323-328.

Dingle, R.V., Bremner, J.M., Giradeau, J. and Buhmann, D., 1996. Modern and palaeo-oceanographic environments under Benguela upwelling cells off southern Namibia. *Palaeogeogr., Palaeoclimatol., Palaeoecol*., 123: 85-105.Clarke, K.R. and Warwick, R.M., 1994. Change in marine community: an approach to statistical analysis and interpretation. *Natural Environment Research Council*, UK, 144pp.

Donn, T.E. and Cockcroft, A.C., 1989. Macrofaunal community structure and zonation of two sandy beaches on the central Namib coast, South West Africa/Namibia. *Madoqua*, 16: 129-135.

Dodd, J.R. and Stanton, R.J, 1990. Paleoecology, concepts and applications (second addition): Wiley-Intersciences, New York, 400 pp.

Droser, M. and Bottjer, D.J., 1986. A semiquantitative field classification of ichnofabric. *J. Sed. Pet*., 56: 558-559.

Edelman-Furstenberg, Y., 2004. Cyclic upwelling facies along the Late Cretaceous southern Tethys: benthic ecological evidence of a high-productivity mosaic, Israel. Unpublished Ph.D. Dissertation, University of Chicago, Chapter 1.

Edelman-Furstenberg, Y., 2004. Taphonomy and ecology of molluscan skeletal remains along an upwelling tract: Benguela system, SW Africa. Unpublished Ph.D. Dissertation, University of Chicago, Chapter 3.

Edelman-Furstenberg, Y, Scherbacher, M., Hemleben, Ch. and Almogi-Labin, A., 2001. Deep-sea benthic foraminifera from the central Red Sea. *J. Foraminifer. Res*., 31: 48-59.

Eshet, Y. and Almogi-Labin, A., 1996. Calcareous nannofossils as paleoproductivity indicators in Upper Cretaceous organic-rich sequences in Israel. *Mar. Micropaleontol.*, 29: 37-61.

Eshet, Y., Almogi-Labin, A. and Bein, A., 1994. Dinoflagellate cysts, paleoproductivity and upwelling systems: A Late Cretaceous example from Israel. *Mar. micropaleontol.*, 23: 231-240.

Fenner, J., 2001. Middle and Late Albian geography, oceanography, and climate and the setting of the Kirchrode I and II borehole sites. *Palaeogeogr., Palaeoclimatol., Palaeoecol*., 174: 5-32.

Flexer, A., 1968. Stratigraphy and facies development of Mount Scopus group (Senonian-Paleocene) in Israel and adjacent countries. *Isr. J. Earth-Sci.*, 17: 85-114.

Fürsich, F.T., 1978. The influence of faunal condensation and mixing on the preservation of fossil benthic communities. *Lethaia*, 11:243-250.

Giraudeau, J., 1993. Planktic foraminiferal assemblages in surface sediments from the southwest African continental margin. *Mar. Geol*., 110: 47-62.

Glenn, C.R. and Arthur, M.A., 1990. Anatomy and origin of a Cretaceous phosphorite-greensand giant, Egypt. *Sedimentology,* 37: 123-154.

Gray, J.S., Ashcan, M., Carr, M.R., Clark, K.R., Green, R.H., Pearson, T.H., Rosenberg, R., Warwick, R.M. and Bayne, B.L., 1988. Analysis of community attributes of the benthic macrofauna of Frierfjord/Langesundfjord and in a mesocosm experiment. *Marine Ecology Progress Series*, 46: 151-165.

Gray, J.S., Clarke, K.R., Warwick, R.M. and Hobbs, G., 1990. Detection of initial effects of pollution on marine benthos: an example from the Ekofisk and Eldfisk oilfields, North Sea. *Marine Ecology Progress Series*, 66: 285-299.

Gvirtzman, G., Almogi-Labin, A., Moshkovitz, S., Lewy, Z., Honigstein, A. and Reiss, Z., 1989. Upper Cretaceous high-resolution multiple stratigraphy, northern margin of the Arabian platform, central Israel. *Cretaceous Res*., 10: 107-135.

Hentschel, U., Cary, S.C. and Felbeck, H., 1993. Nitrate respiration in chemoautotrophic symbionts of the bivalve *Lucinoma aequizonata*. *Marine Ecology Progress Series*, 94: 35-41.

Hoek, R.P., Eshet, Y. and Almogi-Labin, A., 1996. Dinoflagellate cyst zonation of Campanian-Maastrichtian sequences in Israel. *Micropaleontology,* 42: 125-150.

Hulbert, S.H., 1971. The nonconcept of species diversity: A critique and alternative parameters. *Ecology*, 52: 577-586.

Jorrisen, F.J., De Stigter, H.C., and Widmark, J.G.V., 1995. A conceptual model explaining benthic foraminiferal microhabitats. *Marine Micropalontology*, 26: 3-15.

Johnson, T.C., Hamilton, E.L. and Berger, W.H., 1977. Physical properties of calcareous ooze; Control by dissolution at depth. *Marine Geology*, 24:259-277.

Kaiho, K., 1999. Effect of organic carbon flux and dissolved oxygen on the benthic foraminiferal oxygen index (BFOI). *Marine Micropalontology*, 37: 67-76.

Kidwell, S.M., 1997. Time-averaging in the marine fossil record: overview of strategies and uncertainties. *Geobios*, 30: 977-995.

Kidwell, S.M., 1991. The stratigraphy of shell concentrations. In: *Taphonomy, Releasing the Data Locked in the Fossil Record.* Allison P.A. and Briggs D.E.G. (eds.), New York, Plenum Press, pp. 211-290.

Kidwell, S.M., 2001. Preservation of species abundance in marine death assemblages. *Science*, 294: 1091-1094.

Kidwell, S.M. 2002a. Mesh-size effect on the ecological fidelity of death assemblages: a meta-analysis of molluscan live-dead studies. *Geobios mémoire spécial n. 24*, 107-119.

Kidwell, S.M., 2002b. Time-averaged molluscan death assemblages: palimpsests of richness, snapshots of abundance. *Geology*, 30: 803-806.

Kidwell, S.M., 2003. Developing biologically realistic null models to evaluate bias in death assemblages. *Geol. Soc. Amer. Abstr. Program*, 34(7): 84.

Kidwell, S.M., Fürsich, F.T. and Aigner, T., 1986. Conceptual framework for the analysis and classification of fossil concentrations. *Palaios*, 1: 228-238.

Kidwell, S.M. and Bosence, D.W.J., 1991. Taphonomy and time-averaging of marine shelly faunas. In Allison, P.A., and Briggs., eds. *Taphonomy, Releasing the Data Locked in the Fossil Record.* New York: Plenum Press, p. 115-209.

Kidwell, S.M. and Holland, S.M., 1991. Field description of coarse bioclastic fabrics. *Palaios*, 6: 426-434.

Kidwell, S.M., Rothfus, T.A. and Best, M.M.R., 2001. Sensitivity of taphonomic signatures to sample size, sieve size, damage scoring system, and target taxa. *Palaios*, 16: 26-52.

Kolodny, Y., 1980. Carbon isotopes and depositional environment of a high productivity sedimentary sequence – the case of the Mishash-Ghareb Formations, Israel. *Isr. J. Earth Sci.*, 29: 147-156.

Kolodny, Y., Nathan, Y. and Sass, E., 1965. Porcellanite in the Mishash Formation, Negev, southern Israel. *J. Sed. Pet*., 35: 454-463.

Kolodny, Y. and Garrison, R.E., 1994. Sedimentation and diagenesis in paleo-upwelling zones of epeiric sea and basinal settings: A comparison of the Cretaceous Mishash Formation of Israel and the Miocene Monterey Formation of California. *Proc. 29th International Geol. Congr., Part C*, pp. 133-158.

Krenkel, E., 1924. Der Syrische Bogen. *Cent. Miner. Geol. Paleontol. Abh. B.*,9 and 10: 274-281, 301-313.

Kilburn, R. and Rippey, E., 1982. Sea shells of Southern Africa. Johannesburg: MacMillan, 249 pp.

Levin, A.L., Gage, J.D., Martin, C. and Lamont, P.A., 2000. Macrobenthic community structure within and beneath the oxygen minimum zone, NW Arabian Sea. *Deep-Sea Research part II*, 47: 189-226.

Levin, L., Gutierrez, D., Rathburn, A., Neira, C., Sellanes, J., Munoz, P., Gallardo, V. and Salamanca, M., 2002. Benthic processes on the Peru margin: a transect across the oxygen minimum zone during the 1997-98 El Nino. *Progress in Oceanography*, 53 (1): 1-27.

Lescinsky, H.L., Edinger, E. and Risk, M.J., 2002. Mollusc shell encrustation and bioerosion rates in a modern epeiric sea: Taphonomy experiments in the Java Sea, Indonesia. *Palaios*, 17: 171-191.

Lewy, Z., 1990. Transgressions, regressions and relative sea level changes on the Cretaceous shelf of Israel and adjacent countries. A critical evaluation of Cretaceous global sea level correlations. *Paleoceanography*, 5: 619-637.

Lewy, Z., 2001. Campanian ammonites from the Mishash Formation (southern Israel) and their implication on ammonoid mode of life and functional morphology. *Geol. Survey Israel Report/38/01*, 28 pp.

Lewy, Z. and Odin, G.S., 2001. Magnetostratigraphy across the Campanian-Maastrichtian boundart at Teris les Bains in comparison with northern Germany, the Apennines (central Italy) and North America; biostratigraphical and geochronological constraints. In: *The Campanian-Maastrichtian boundary*. Odin G.S. (ed.), Amsterdam, Elsevier Science B.V., pp. 175-183.

Lewy, Z. and Edelman-Furstenberg, Y., 2003. Taxonomy and paleoecology of marine benthic macrofossils of high-productivity settings, Upper Campanian Phosphate Member of Mishash Formation. *Geol. Survey Israel Report/20/03*, 32 pp, 5 plates.

Little, M.G., Schneider, R.R., Kroon, D., Price, B., Bickert, T. and Wefer, G., 1997. Rapid palaeoceanographic changes in the Benguela Upwelling System for the last 160,000 years as indicated by abundances of planktonic foraminifera. *Palaeogeogr., Palaeoclimatol., Palaeoecol*., 130: 135-161.

Longhurst, A. (ed.), 1998. Ecological geography of the sea, San Diego, Academic Press, 398 pp.

Loubere, P., 1997. Benthic foraminiferal assemblage formation, organic carbon flux and oxygen concentrations on the outer continental shelf and slope: *J. Foraminifer. Res*., 27: 93-100.

Martinez, P., Bertrand, P., Calvert, S.E., Pedersen, T.F., Shimmield, G.B., Lallier-Verges, E. and Fontugne, M.R., 2000. Spatial variations in nutrient utilization, production and diagenesis in the sediments of a coastal upwelling regime (NW Africa): Implications for the paleoceanographic record. *J. Marine Research,* 58: 809-835.

McLachlan, A., 1985. The ecology of two sandy beaches near Walvis Bay. *Madoqua*, 14: 155-163.

McLachlan, A., Cockcroft, A.C. and Malan, D.E., 1984. Benthic faunal response to a high energy gradient. *Mar. Ecol. Prog. Ser.,* 16: 51-63.

Meldahl, K.H. and Flessa, K.W., 1990. Taphonomic pathways and comparative biofacies and taphofacies in a Recent intertidal/shallow shelf environment. *Lethaia*, 23: 43-60.

Moore, R.C. (ed.), 1969. Treatise on Invertebrate Paleontology, Part N, Mollusca 6, Bivalvia, Vol. 1-3. Kassab, A.S. and Mohamed, A.S., 1996. Upper Cretaceous macrofossils from the Duwi Formation of the Nile Valley, southern Egypt. *N. Jb. Geol. Paläont. Abh.,* 200 (3): 259-284.

Moskovitz, S., Ehrlich, A. and Soudry, D., 1983. Siliceous microfossils of the Upper Cretaceous Mishash Formation, central Negev, Israel. *Cretaceous Research*, 4: 173-194.

Natan, Y., Shilino, Y., Roded, R., Gal, I. and Deutsch, Y., 1979. The geochemistry of the northern and central Negev phosphorites (Southern Israel). *Isr. Geol. Surv. Bull*., 73: 43 pp.

Niermann, U., Bauerfeind, E., Hickel, W. and Westernhagen, H.V., 1990. The recovery of benthos following the impact of low oxygen content in the German Bight. *Netherlands Journal of Sea Research*, 25: 215-226.

Notholt, A.J.G., Sheldon, R.P. and Davidson, D.F. eds., 1989. *Phosphate deposits of the world, volume 2, Phosphate rock resources*. Cambridge University Press, 566 pp.

Parrish, J.T. and Curtis, R.L., 1982. Atmospheric circulation, upwelling, and organic-rich rocks in the Mesozoic and Cenozoic eras. *Palaeogeogr., Palaeoclimatol., Palaeoecol*., 40: 31-66.

Parrish, J.T., (ed.) 1998. Marine lithologic indicators of paleoclimate. In: *Interpreting Pre-Quaternary climate from the geologic record.* Columbia University Press, New York, pp. 91-132.

Parrish, J.T., Droser, M.L. and Bottjer D.J., 2001. A Triassic upwelling zone: the Shublik Formation, arctic Alaska, USA. *J. Sed. Res.*, 71(2) part B: 272-285.

Pearson, T.H. and Rosenberg, R., 1978. Macrobenthic succession in relation to organic enrichment and pollution of the marine environment. *Oceanogr. Mar. Biol*. Annu., Rev., 16: 229-311.Pearson, T.H, and Rosenberg, R., 1978. Macrobenthic succession in relation to organic enrichment and pollution of the marine environment. *Oceanogr. Mar. Biol. Annu. Rev.,* 16: 229-311.

Peterson, C.H., 1977. The paleoecological significance of undetected short-term temporal variability. *J. Paleontol.*, 51: 976-981.

Pether, J., 1993. Relict shells of subantarctic mollusca from the Orange Shelf, Benguela region, off southwestern Africa. *The Veliger*, 36: 276-284.

Pether, J., 1994. Molluscan evidence for enhanced deglacial advection of Aghulhas water in the Benguela current, off southwestern Africa. *Palaeogeogr., Palaeoclimatol., Palaeoecol*., 111: 99-117.

Picard, L. 1930. Upper Cretaceous (chiefly Campanian and Maastrichtian) Gastropoda and Pelecypods from Palestine. *Ann. Mag. Nat. Hist*., Ser. 10, 5: 513-543.

Pufahl, P.K., Grimm, K.A, Abed, A.M. and Sadaqah, R.M.Y., 2003. Upper Cretaceous (Campanian) phosphorites in Jordon: implications for the formation of a south Tethyan phosphorite giant. *Sedimentary Geology*, 161: 175-205.

Rabalais, N.N., Turner, R.E. and Wiseman Jr., W.J., 2002. Gulf of Mexico hypoxia, a.k.a. "the dead zone". *Annu. Rev. Ecol. Syst*., 33: 235-263.

Raup, D.M., 1991. The future of analytical paleobiology. In: *Analytical Paleobiology: Short course notes, Paleontological Society*. Gilinsky N.L. and Signor P.W., (eds.), Knoxville, p. 207-216.

Reiss, Z., 1962. Stratigraphy of phosphate deposits in Israel. *Isr. Geol. Surv. Bull*., 34: 1-23.

Reiss, Z., 1988. Assemblages from a Senonian high-productivity sea. *Rev. Paleobiologie,* Spec. vol. 2: 323-332.

Reiss, Z., Almogi-Labin, A., Honigstein, A., Lewy, Z., Lipson-Benitah, S., Moshkovitz, S. and Zak, Y., 1985. Late Cretaceous multiple stratigraphic framework of Israel. *Isr. J. Earth Sci.*, 34: 147-166.

Rhoads, D.C., and Morse, J.W., 1971. The Benguela Ecosystem. Part VII. Marine-geological aspects. *Lethaia*, 4: 413-428.

Rhoads, D.C., and Boyer, L.F., 1982. The effects of marine benthos on physical properties of sediments-a successional perspective. In: *Animal-sediment relations: the biogenic alteration of sediments.* McCall P.L. (ed.), New York, Plenum Press, p. 3-52.

Rogers, J., 1977. Sediments on the continental margin off the Orange River and the Namib Desert. *PhD Thesis, Geology Department, University of Cape Town*, 212 pp.

Rogers, J. and Bremner, J.M., 1991. Evolutionary and ecologic significance of oxygen-deficient basins. *Oceanogr. Mar. Biol. Annu. Rev.,* 29: 1-85.

Rosenberg, R, 1976. Benthic faunal dynamics during succession following pollution abatement in a Swedish estuary. OIKOS 27: 414-427.

Sakko, A.L., 1998. The influence of the Benguela upwelling system on Namibia's marine biodiversity. *Biodiversity and Conservation*, 7: 419-433.

Sass, E. and Kolodny, Y., 1972. Stable isotopes, chemistry and petrology of carbonate concretions (Mishash Formation, Israel). *Chem. Geol.,* 10: 261-286.

Savrda, C.E., Bottjer, D.J. and Gorsline, D.S., 1984. Development of a comprehensive oxygen-deficient marine biofacies model: evidence from Santa Monica, San Pedro, and Santa Barbara Basins, California continental borderland. *Amer. Assoc. Petroleum Geologists Bull*., 68: 1179-1192.

Savrda, C.E. and Bottjer, D.J., 1986. Trace fossil model for reconstruction of paleo-oxygenation in bottom waters. *Geology*, 14: 3-6.

Savrda, C.E. and Bottjer, D.J., 1987. The exaerobic zone, a new oxygen-deficient marine biofacies. *Nature*, 327: 54-56.

Savrda, C.E. and Bottjer, D.J., 1991. Oxygen-related biofacies in marine strata: an overview and update. In; Tyson R.V. & Pearson T.H. (eds.), *Modern and ancient continental shelf anoxia*, Geol. Soc. Spec. Publ., 58: 201-219.

Schneider, R. and Wefer, G., 1990. Shell horizons in Cenozoic upwelling-facies sediments off Peru: distribution and mollusk fauna in cores from Leg 112. *Proceedings of the Ocean Drilling Program, Scientific Result*s, V. 112, 335-352.

Schuette, G. and Schrader, H., 1981. Diatom taphocoenoses in the coastal upwelling area off South West Africa. *Marine Micropaleontoly*, 6: 131-155.

Schweimanns, M. and Felbeck, H., 1985. Significance of the occurrence of chemoautotrophic bacterial endosymbionts in lucinid clams from Bermuda. *Marine Ecology Progress Series*, 24: 113-120.

Sen Gupta, B.K., and Machain-Castillo, M.L., 1993. Benthic foraminifera in oxygen-poor habitats. *Marine Micropaleontology*, 20: 183-201.

Sepkoski, J.J. Jr., 1981. A factor analytic description of the Phanerozoic marine fossil record. *Paleobiology*, 7: 36-53.

Shannon, L.V., 1985. The Benguela Ecosystem part I. Evolution of the Benguela, physical features and processes. *Oceanogr. Mar. Biol. Ann. Rev.*, 23:105-182.

Shannon, L.V. and Nelson, G., 1996. The Benguela: large scale features and processes and system variability. In: *The south Atlantic: present and past circulation.* Wefer, G., Berger, W.H., Siedler, G. and Webb, D.J. (eds.), Springer-Verlag, Berlin Heidelberg, p. 163-210.

Shemesh, A. and Kolodny, Y., 1988. Oxygen isotopes variations in phosphorites from the southeastern Tethys. *Isr. J. Earth Sci.*, 37: 1-15.

Smith, B. and Wilson, J.B., 1996. A consumer's guide to evenness indices. *Oikos*, 76: 70-82.

Soudry, D., 1983. Étude de la série phosphatée de la région d'Ein Yahav (Néguev central Israel) - Logique séquentielle, pétrologie, approche de la phosphatogénèse. *Unpublished Thèse Doctorat d'État: Institut National Polytechnique de Lorraine, Nancy,* 177 pp.

Soudry, D., 1987. Ultra-fine structures and genesis of the Campanian Negev high-grade phosphorites (southern Israel). *Sedimentology*, 34: 641-660.

Soudry, D., 1992. Primary bedded phosphorites in the Campanian Mishash Formation, Negev, southern Israel. *Sedimentary geology*, 80: 77-88.

Soudry, D., 1994. Bottom-dwelling microphytes and phosphate sediment accretion: The case of the Campanian phosphorites, Negev, southern Israel. *Kaupia – Darmstädter Beiträge zur Naturgeschichte*, 4: 61-70.

Soudry, D., 2000. Carbonate-phosphate competition in the Negev phosphorites (southern Israel): a microstructural study. In: *Marine authigenesis: from global to microbial*. Geological Society of London Special Publication, No. 66, pp. 415-426.

Soudry, D. and Champetier, Y., 1983. Microbial processes in the Negev phosphorites (southern Israel). *Sedimentology*, 30: 411-423.

Soudry, D., Nathan, Y. and Roded R., 1985. The Ashosh-Haroz facies and their significance for the Mishash palaeogeography and phosphorite accumulation in the northern and central Negev, southern Israel. *Isr. J. Earth Sci.*, 34: 211-220.

Soudry, D. and Lewy, Z., 1988. Microbially influenced formation of phosphate nodules and megafossil moulds (Negev, southern Israel). *Palaeogeogr., Palaeoclimatol., Palaeoecol*., 64: 15-34.

Soudry, D. and Nathan, Y., 2001. Diagenetic trends of fluorine concentration in Negev phosphorites, Israel: implications for carbonate fluorapatite composition during phosphogenesis. *Sedimentology*, 48: 723-743.

Soudry, D., Ehrlich, S., Yoffe O. and Nathan, Y., 2002. Uranium oxidation state and related variations in geochemistry of phosphorites from the Negev (southern Israel). *Chemical Geology*, 189:213-230.

Sousa, W.P., 2001. Natural disturbances and the dynamics of marine benthic communities. In: *Marine community ecology*. Bertness M.D., Gaines S.D and Hay M.E. (eds.), Sinauer Associates, Sunderland, MA, pp. 85-130.

Stachowitsch, M., 1991. Anoxia in the Northern Adriatic Sea: rapid death, slow recovery. In: *Modern and Ancient Continental Shelf Anoxia*. Tyson R.V. and Pearson T.H. (eds.), Geological Society Publication of London, No. 58, pp. 119-129.

Steyn, D.G. and Lussi, M. (eds.), 1998. Marine shells of South Africa. Ekogilde Publishers, 264 pp.

Suess, E. and J. Thiede, (Eds.), 1983. *Coastal Upwelling: Its Sediment Record, Part A: Responses of the Sedimentary Regime to Present Coastal Upwelling*, NATO Conference Series IV, Marine Sciences 10a, 604 pp.

Summerhayes C. P., Prell W. L. and Emeis K-C., 1992. Evolution of upwelling systems since the Early Miocene. In: *Upwelling systems: Evolution of upwelling systems since the Early Miocene*. Summerhayes C.P., Prell W.L. and Emeis K-C. (eds.), Geological Society of London Special Publication, No. 64, pp. 1-5.

Tayler, J.D. and Glover, E.A., 1997. The lucinid bivalve genus *Cardiolucina* (Mollusca, Bivalvia, Lucinidae): systematics, anatomy and relationships. *Bulletin of the Natural History Museum London (Zoology),* 63: 93-122.

Thiede, J. and E. Suess (eds.), 1983. *Coastal Upwelling, Its Sediment Record, Part B: Sedimentary Records of Ancient Coastal Upwelling*, NATO Conference Series IV, Marine Sciences, 10b, 610 pp.

Tyson, R.V. and Pearson, T.H., 1991. Modern and ancient continental shelf anoxia: an overview. In: *Modern and Ancient Continental Shelf Anoxia*.

Tyson R.V. and Pearson T.H. (eds.), Geological Society of London Publication No. 58, pp. 1-24.

Vengosh, A., Kolodny, Y. and Tepperberg, M., 1987. Multi-phase oxygen isotopic analysis as a tracer of diagenesis: the example of the Mishash Formation, Cretaceous of Israel. *Chemical Geology*, 65: 235-253.

Wilkerson, F.P., Dugdale, R.C., Kudela, R.M. and Chavez, F.P., 2000. Biomass and productivity in Monterey Bay, California: contribution of the large phytoplankton. *Deep-Sea Research part II*, 47: 1003-1022.

Valentine, J.W., Roy, K. and Jablonski, D., 2002. Carnivore/non-carnivore ratios in northeastern Pacific marine gastropods. *Mar, Ecol. Prog. Ser*., 228: 153-163.

Verheye, H.M., 2000. Decadal-scale trends across several marine trophic levels in the Southern Benguela upwelling system off South Africa. *Ambio*, 29: 30-34.

Warwick, R.M., 1988. Effects on community structure of a pollutant gradient – summary. *Marine Ecology Progress Series*, 46: 207-211.

Zuschin, M, Stachowitsch, M. and Stanton Jr. R.J., 2003. Patterns and processes of shell ragmentaion in modern and ancient environments. *Earth-Science Reviews*, 63: 33-82.

מאספי המאקרובנטוס של מערכת הזרימעלה של הבנגואלה משתנים הדרגתית בניצב למדף היבשת במקביל לירידה בעוצמת ה- upwelling ועליה בריכוזי החמצן בקרקעית הים (כפי שנמדד בעבודות של חוקרים אחרים). האנליזה הפאוניסטית הראתה עליה בעושר מינים, ביחס בין מינים אפיפאונליים למינים אינפאונליים, במספר הקשוות הלא מחוברות, וכן ירידה בגודל גוף הצדפות הכימוסימביוטיות ובנפיצות הצדפות אוכלות הרקב במקביל להתרחקות מאזור מרכז הזרימעלה, כלומר, מהבוץ הדיאטומטי העשיר בחומר אורגני לכוון החול הפוספטי.

הנפיצות והגוון המקומי של מאקרובנטוס בסביבות זרימעלה וכן רגישותם הרבה לתנאי קרקעית הים מוצגים בעבודה זו. כתמיות (patchiness) ודינמיות מאפיינות הן את המערכת המודרנית של הבנגואלה וכן את המערכת הקרתיקונית של המישאש, בעיקר המצאות בו-זמנית של תנאים אירוביים ואנאירוביים גם באזור מרכז הזרימעלה עצמו.

תקציר

סדימנטים עשירים בסיליקה, חומר אורגני ופוספט מאפיינים סביבות ימיות בעלות פוריות גבוהה. מערכות אילו מורכבות מאוד ושאלות הנוגעות לתנאי הקרקעית בזמן השקעת סדימנטים אילו עדיין אינן ברורות. החומר האורגני הרב המגיע לקרקעית הים ותנאי חוסר החמצן הקשורים לכך גורמים לתמותה המונית של חיות ואכן הקרקעיות של אזורים אלו ידועים כ״אזורי מוות״. בניגוד לסטריאוטיפ זה, בתצורת מישאש מהקרתיקון העליון בדרום הארץ ישנו מגוון רב ונפיצות גבוהה של מאקרופאונה בנטונית. תצורה זו מייצגת את אחת המערכות הימיות הפוריות ביותר בחתך הסטרטיגרפי והיא משתרעת על פני שטח גיאוגרפי נרחב. בעבודה זו בחנתי רקורד עתיק זה וכן מאספים מתים של מאקרובנטוס מהמערכת המודרנית של מערכת הזרימעלה של הבנגואלה (מול חופי דרום מערב אפריקה) כדי לחקור את מבנה החברה של המאקרובנטוס ושינויים בתנאים הטפונומיים על פני קרקעיות של אזורי זרימעלה כדי להשתמש במידע זה לשחזור תנאי הקרקעית, בעיקר ריכוז החמצן.

עבודת השדה כללה תיאור של חמישה חתכים של תצורת מישאש בדרום הארץ. לאורך החלק התחתון של התצורה, ביחידה הפוספטית-קרבונטית, נמצאו מחזורים סדימנטריים קטנים בעובי 1-9 מטר המתארים את רוב הגוון הליתולוגי וביולוגי בתצורה. מחזורים אלה מורכבים מקרבונטים מיקריטיים עשירים בחומר אורגני, צור ופורצלניט, שכבות קרבונטיות שעברו דיאגנזה, כאשר המחזור מסתיים בשכבה עשירת-צדפות המכילה חלקיקים פוספטיים. עליה כללית בגודל הגרגר, בנפיצות המאובנים ובצפיפות האריזה של הצדפות לאורך מחזור סדימנטרי מייצגים עליה בריכוזי החמצן ובאנרגית המים על קרקעית הים, מסביבות דלות חמצן (מתחת לבסיס הגלים של סערות storm wave base-) לסביבות אירוביות לחלוטין (מעל לבסיס הגלים הרגיל - fair-weather wave base). אנליזה פאוניסטית של המאקרובנטוס הראתה ירידה בעושר מינים, בגודל גוף המאובנים ובנפיצות הצדפות אוכלות הרקב במקביל לירידה בריכוזי החמצן המומס (הלמוד) על קרקעית הים, ובמקביל לקירבה היחסית למרכז הזרימעלה.

משרד התשתיות הלאומיות
המכון הגיאולוגי

פלאואקולוגיה וטפונומיה על-פי מאקרובנתוס של סביבות ימיות בעלות פוריות גבוהה: תצורת מישאש של הקרטיקון העליון ואנלוג מודרני

***יעל אדלמן-פורסטנברג**

*המחלקה למדעי הגיאופיסיקה, אוניברסיטת שיקגו, ארה״ב
והמכון הגיאולוגי, רח׳ מלכי ישראל 30, ירושלים

עבודה זו הוגשה כחיבור לקבלת תואר ״דוקטור לפילוסופיה״
לסנאט אוניברסיטת שיקגו, ארה״ב

העבודה נעשתה בהדרכתם של:
פרופ׳ סוזן מ. קידוול , המחלקה למדעי הגיאופיסיקה, אוניברסיטת שיקגו, ארה״ב
דר׳ אהובה אלמוגי-לבין ודר׳ זאב לוי, המכון הגאולוגי, ירושלים

דוח מס׳ GSI/10/04
ירושלים, אוקטובר 2004